Modelling of the microglial response to neuronal α-synuclein aggregation

Antigoni Katsikoudi

St Cross College
University of Oxford



Supervised by Prof. George Tofaris

This dissertation is submitted for the degree of Doctor of Philosophy

June 2022

Abstract

Parkinson's disease is the second most common neurodegenerative disease, characterised by α-synuclein aggregation and loss of dopaminergic and other types of neurons. Inflammation, the activation of microglial and other immune cells in response to pathology, is a well-documented feature of the neurodegenerative process. Yet, it remains unresolved whether inflammation prevents or promotes the degeneration of dopaminergic neurons in Parkinson's disease. One reason for this knowledge gap is the lack of relevant human experimental models to study the interaction between neurons and microglia in response to pathological α-synuclein. In this study, I sought to establish human *ex vivo* and *in vitro* models to decipher the microglial response to neuronal α-synuclein aggregation that was triggered by the addition of *de novo* generated fibrils. Using mouse organotypic cultures, I showed that microglia are activated in response to aggregation. In a novel iPSC-based dopaminergic neuron-microglial co-culture model, I found that α-synuclein aggregation and aggregate-induced neuronal loss were mitigated by the presence of microglia. Gene expression studies and whole transcriptome analyses revealed an association between this beneficial phenotype and a transition from a homeostatic to a disease-related microglial gene expression profile. Further, pilot single cell RNA sequencing data revealed treatment specific clusters and biological pathways. Altogether my data showed that under certain conditions, microglia exert a beneficial effect in response to neuronal α-synuclein aggregation and identified morphological changes, cytokine secretion and disease-specific pathways that underpin this process. Further validation of these findings could offer immunological targets for disease modifying therapies in Parkinson's disease.

Declaration of Originality

The work presented in this study is the result of my own work and not a collaborative result, unless declared and specified within this thesis.

The present study has not been submitted before or is planned to be submitted for any other degree or diploma or other qualification at the University of Oxford or any other University or similar institution unless stated in the present thesis. I further state that no substantial part of my thesis has already been submitted or is due to be submitted for any other degree or diploma or other qualification at the University of Oxford or any other University or similar institution unless stated in the present thesis.

The present thesis does not exceed the prescribed word limit as indicated by the relevant Degree Committee.

Acknowledgments

First and foremost, I would like to express my sincere gratitude to my academic supervisor, George Tofaris, who entrusted myself to establish the work on neuroinflammation in his laboratory and I could not be more honoured by this. I am indebted by his unwavering devotion in completing this piece of work. Further, I am grateful to my industrial supervisor Suchira Bose and Eli Lilly, who further supported me through my academic journey.

The present thesis could not have been completed without the untiring support of my colleagues and dear friends, Dr Samiha Sheikh, Dr Benedict Tanudjojo, Dr Cheng Jiang, Dr Jade Marsh and Dr Rahel Lewin. Special acknowledgements ought to be given to Dr Dmitry Zenko. I will never forget our endless conversations over coffee and how that motivated me to the finishing line. Further, I am grateful to Dr Bjorn Vahsen with whom I shared discussions and exciting findings over wine at the High Tables of the University of Oxford. Finally, I would like to thank the Motor Neuron Disease Group and its members that I now call my friends.

I am also grateful to our collaborators and their contributions to my work that enabled me to explore my project on a multidisciplinary level.

Lastly, I would like to dedicate this dissertation to my parents, grandparents and partner. I would never have made it where I am if it was not for their support when times were mostly arduous.

‘’There is no happiness when there is no wisdom’’

-Sophocles, Antigone

Glossary of Abbreviations

α-Syn	α-synuclein
AA	Ascorbic acid
Aβ	Amyloid beta peptide
AD	Alzheimer's disease
ALS	Amyotrophic lateral sclerosis
ATM	Axonal tract microglia
BCA	Bicinchoninic acid
BDNF	Brain-derived neurotrophic factor
BMP4	Bone morphogenetic protein
CHI3L1	Chitinase 3-like
CNS	Central nervous system
Co-pMGL	Induced pluripotent-derived microglia co-cultured with neurons
CRISPR	Clustered regularly interspaced short palindromic repeats
Cryo-EM	Cryogenic electron microscopy
CSF	Cerebrospinal fluid
CSF1R	Colony stimulating factor 1
CX3CL1	Fractalkine
CX3CR1	Fractalkine receptor
DAM	Disease associated microglia
DAMP	Damage-associated molecular patterns
db-cAMP	Dibutyryl cyclic adenosine monophosphate

DDC	Dopa decarboxylase
DG	Dentate gyrus
DGE	Differential gene expression
DIV	Days *in vitro*
DLB	Dementia with Lewy bodies
DN	Dopaminergic neurons
DPPIV	Dipeptidyl peptidase IV
EB	Embryoid body
EM	Electron microscopy
exAM	*Ex vivo* activated microglia
FBS	Fetal bovine serum
FGF8a	Fibroblast growth factor 8a
Fib	*De novo* generated α-synuclein preformed fibrils
FISH	Fluorescence *in situ* hybridisation
FRET	Fluorescence resonance energy transfer
GBA1	Gene encoding β-glucocerebrosidase
GDNF	Glia-derived neurotrophic factor
GO	Gene ontology
GSEA	Gene set enrichment analysis
GWAS	Genome-wide association studies
HC	Healthy control
HTRF	Homology time resolved fluorescence
IBA1	Ionised calcium binding adaptor molecule 1

ICC	Immunocytochemistry
IFN-γ	Interferon-γ
IL-	Interleukin-
iPSC	Induced pluripotent stem cell
KSR	Knockout serum replacement medium
LB	Lewy bodies
LDH	Lactate dehydrogenase
LN	Lewy neurites
LPS	Lipopolysaccharides
LRRK2	Leucine-rich repeat kinase 2
MAP2	Microtubule associated protein 2
MAPT	Microtubule associated protein 2
M-CSF	Macrophage colony-stimulating factor
MG	Microglia
MIF	Macrophage migration inhibitory factor
MMC	Mitomycin-C
MPTP	1-methyl-4-phenyl-1,2,3,6-tetrahydropyridine
mRNA	Messenger RNA
MSA	Multiple system atrophy
MSD	Meso scale discovery
mTOR	Mechanistic target of rapamycin
NAC	Non-amyloidogenic component
NAMP	Neurodegeneration-associated molecular patterns

NO	Nitric oxide
NSC	Non-seeded control
OHS	Organotypic hippocampal slices
PAMP	Pathogen-associated molecular pattern
PCA	Principal component analysis
PD	Parkinson's disease
PFA	Paraformaldehyde
PET	Positron emission tomography
PI3K-	Phosphoinositide 3-kinase
pMacpre	Induced pluripotent derived macrophage/microglia precursors
PMCA	Protein misfolding cyclic amplification
pMGL	Induced pluripotent derived microglia-like cells
PonS	Ponceau stain
pSYN	α-synuclein phosphorylated on serine 129
RBD	Rapid eye movement behaviour disorder
RIPA	Radioimmunoprecipitation assay (buffer)
RNA	Ribonucleic acid
ROCKi	Y-27632
ROS	Reactive oxygen species
S129A	α-synuclein with the serine 129 to alanine mutation
SEC	Size exclusion chromatography
SCF	Stem cell factor

SDS	Sodium dodecyl sulphate
SHH	Sonic hedgehog
siRNA	Small-interfering RNA
SMURF1	SMAD ubiquitin regulatory factor 1
SNCA	Gene encoding α-synuclein
SNCA^{TRIP}	iPSC line from *SNCA* triplication patient
SNc	Substantia nigra pars compacta
TEM	Transmission electron microscopy
TGFβ3	Transforming growth factor β3
TH	Tyrosine-hydroxylase
ThT	Thioflavin-T
TLR	Toll-like receptor
TMEM119	Transmembrane protein 119
TNFα	Tumour necrosis factor α
TREM2	Triggering receptor expressed on myeloid cells 2
TREM2^{ISO}	iPSC line from healthy control patient with CRISPR/Cas9-mediated knockout of *TREM2*
TUJ1	β-3 tubulin
VEGF	Vascular endothelial growth factor
VTA	Ventral tegmental area
WB	Western blotting, immunoblotting

Table of Contents

Abstract 3

Declaration of Originality 4

Acknowledgments 5

Glossary of Abbreviations 6

List of Figures 14

List of Tables 17

Chapter 1: General introduction 18

1.1 Parkinson's disease 18

1.1.1 Epidemiology & diagnosis of Parkinson's disease 18

1.1.2 Current therapeutic strategies 20

1.1.3 Genetics of Parkinson's disease 21

1.1.4 Neuropathology of Parkinson's disease 25

1.2 α-synuclein 30

1.2.1 Synucleinopathies 30

1.2.2 Structure, function & pathobiology of α-synuclein 30

1.2.3 Lewy pathology in Parkinson's disease 34

1.2.4 Prion-like propagation and aggregation of α-synuclein 36

1.3 Microglia 40

1.3.1 The origins of microglia 40

1.3.2 The functions of microglia 43

1.3.3 Microglia phenotypes 47

1.3.4 Human and murine microglia 52

1.3.5 Modelling microglia phenotypes with induced pluripotent stem cells 53

1.3.6 Aims and objectives 55

Chapter 2: Materials and Methods 56

2.1 Cell Culture 56

2.1.1 Stem cell culture 56

2.1.2 Differentiation of human iPSCs into midbrain dopaminergic neurons 58

2.1.3 Differentiation of human iPSCs into macrophage/microglia precursors via Embryoid Body formation using AggreWells 61

2.1.4 Co-cultures of human iPSC-derived midbrain dopaminergic neurons and microglia (co-pMGL) 64

2.1.5 Microglia-like monocultures (pMGL) 65

2.1.6 Addition of *de novo* α-synuclein fibrils in iPSC-derived dopaminergic neurons and microglia 66

2.1.7 Measurement of Cell Viability using lactate dehydrogenase (LDH) assay 67

2.2 Organotypic Slice Cultures 68

2.2.1 *Ex vivo* mice hippocampal slices 68

2.2.2 *Ex vivo* live human cortical slices 70

2.3 70

2.3 Generation of α-synuclein fibrils 71

2.4 Molecular biology techniques 73

2.4.1 qRT-PCR 73

2.4.2 Transcriptome analysis 75

2.5 Biochemical Techniques 84

2.5.1 Estimation of protein concentration 84

2.5.2 Immunoblotting 85
2.5.3 Immunofluorescence 89
2.5.4 Time-resolved FRET 91
2.5.5 Proteome Profiler Array: Human XL cytokine array 93
2.5.6 Immunoassay-Quanterix Simoa 95

2.6 Statistical Analysis 96

2.7 Ethical approval 96

Chapter 3: Set up of organotypic slices to study recombinant fibrils induced neuronal α-synuclein aggregation and microglia phenotypes 97

3.1 Introduction 97
3.1.1 Organotypic slices as *ex vivo* models of Parkinson's disease 97
3.1.2 Organotypic slices as an *ex vivo* tool to model neuroinflammation in Parkinson's disease 100
3.1.3 α-synuclein *de novo* fibrils generation, seeded aggregation and phosphorylation on serine 129 101
3.1.4 Human organotypic slices as a novel *ex vivo* tool to study neurodegeneration 104
3.1.5 Experimental workflow: α-synuclein seeded aggregation on mouse transgenic hippocampal organotypic slices 105
3.1.6 Aims and objectives 106

3.2 Results 107
3.2.1 *De novo* generation of α-synuclein fibrils 107
3.2.2 *Ex vivo* TgA53T mouse hippocampal organotypic slices 113
3.2.3 Pilot studies with human organotypic cultures 122

3.3 Discussion 124

Chapter 4: A microglia-neuronal co-culture system to decipher the microglial response to intraneuronal α-synuclein aggregation 131

4.1 Introduction 131
4.1.1 Modelling the cellular pathology of Parkinson's disease using human stem cells 131
4.1.2 Differentiation of dopaminergic neurons 134
4.1.3 Microglia differentiation 136
4.1.4 Microglia and neurodegeneration 140
4.1.5 Parkinson's disease related mutations, LRRK2 and GBA: is there a link to microglial responses? 143
4.1.6 Co-culture assay workflow: α-synuclein seeded aggregation of patient derived dopaminergic neurons followed by addition of microglia precursors 146
4.1.7 Aims and Objectives 148

4.2 Results 149
4.2.1 Dopaminergic neurons express neuronal and dopaminergic specific markers 149
4.2.2 Generation of human iPSC derived microglia 154
4.2.3 *De novo* generated α-synuclein fibrils induce neurotoxic, pSYN positive inclusions in $SNCA^{TRIP}$ dopaminergic neurons 162
4.2.4 Microglia reduced pSYN levels when co-cultured with dopaminergic neurons containing α-synuclein aggregates 164
4.2.5 Physical contact between microglia and dopaminergic neurons was required for reduction of pSYN levels. 169
4.2.6 Effect of microglial LRRK2 and GBA mutations on neuronal α-synuclein aggregation. 171
4.2.7 Phagocytosis may be relevant to the clearance of aggregates 172

4.3 Discussion 174

Chapter 5: Microglial phenotypes in response to neuronal α-synuclein aggregation ... 183

5.1 Introduction 183

5.1.1 Homeostatic microglia 183
5.1.2 Disease-associated microglia 185
5.1.3 Disease-associated microglia: universal sensors of neurodegeneration and their molecular patterns 187
5.1.4 TREM2 function and role in Parkinson's disease 189
5.1.5 Disease associated microglia phenotype is initiated by a TREM2 independent mechanism 192
5.1.6 Cytokine levels in Parkinson's disease 193
5.1.7 Uptake and clearance of α-synuclein by microglia 194
5.1.8 Aims and Objectives 195

5.2 Results 196

5.2.1 Whole transcriptome analysis of iPSC-derived microglial-dopaminergic neuronal co-cultures following neuronal α-synuclein seeded aggregation 196
5.2.2 Microglia express homeostatic and disease-associated genetic markers 200
5.2.3 Assessment of TREM2 function on the uptake or degradation of α-synuclein fibrils 202
5.2.4 Pilot single-cell RNA sequencing analysis identifies distinct microglia and neuronal clusters in iPSC-derived co-cultures with neuronal α-synuclein aggregation 207
5.2.5 Secreted cytokine profile in seeded iPSC-derived co-cultures 213

5.3 Discussion 215

Chapter 6: General Discussion 229

REFERENCES 235

List of Figures

Figure 1.1 Main diagnostic neuropathological features of Parkinson's disease. 26

Figure 1.2 The six stages of Parkinson's disease pathology. 29

Figure 1.3 The conformational landscapes of α-synuclein. 31

Figure 1.4 The prion-like paradigm of α-synuclein seeded aggregation and intraneuronal propagation. 37

Figure 1.5 Developmental origins of microglia and macrophages. 42

Figure 1.6 Neuronal regulation and maturation achieved by microglia. 44

Figure 1.7 Microglia phenotypes. 51

Figure 1.8 Basic and comprehensive phenotypic characterisation of human iPSC-derived microglia. 54

Figure 2.1 BCA Standard curve 84

Figure 2.2 The homology time resolved fluorescence assay, Cisbio. 92

Figure 2.3 Principle of cytokine profiler array. 94

Figure 3.1 Assay workflow of modelling α-synuclein aggregation in organotypic hippocampal slices from A53T transgenic mice pups. 105

Figure 3.2 Expression and purification of recombinant α-synuclein monomer. 108

Figure 3.3 α-synuclein de novo fibrils and relative ThT fluorescence intensity signal signifying binding on amyloid β-sheet structures. 110

Figure 3.4 HEK295T α-synuclein-Venus cells were seeded with *de novo* generated fibrils. 112

Figure 3.5 Workflow for acquiring organotypic hippocampal slices from transgenic A53T mice. 114

Figure 3.6 Long term organotypic hippocampal slices maintained their structural and cellular composition. 115

Figure 3.7 α-synuclein fibrils induced pSYN positive neuronal inclusions. 117

Figure 3.8 Microglia in organotypic hippocampal slices were activated in response to seeded intraneuronal α-synuclein aggregation. 119

Figure 3.9 Secretion of pro-inflammatory cytokine IL-6 in the conditioned media of α-synuclein fibril treated A53T OHS. 121

Figure 3.10 Workflow of human cortical slices as an organotypic culture model. 123

Figure 4.1 Generation, differentiation and applications of human iPSC-derived cells. 133

Figure 4.2 Ontological origin of macrophage subpopulations in the central nervous system (CNS). 137

Figure 4.3 Suggested positive feedback loop for microglia's involvement in neurodegeneration of Parkinson's disease. 142

Figure 4.4 Chronic iPSC-derived co-culture system to study microglia effects on neurons containing α-synuclein aggregates. 147

Figure 4.5 Floor plate differentiation protocol for generation of dopaminergic neurons from human iPSCs. 150

Figure 4.6 Time-course photo journal of differentiating cells to dopaminergic neurons from DIV0 to DIV45. 151

Figure 4.7 Characterisation of human iPSC-derived dopaminergic neurons by immunocytochemistry (ICC). 153

Figure 4.8 Timeline of microglia differentiation via Embryonic Bodies formation that recapitulated *in vivo* embryonic development. 155

Figure 4.9 pMGL (monocultures) and co-pMGL (co-cultures) acquired ramified morphology and expressed the microglial specific marker, IBA1. 157

Figure 4.10 iPSC-derived mono and co-cultured microglia express consensus microglia markers. 159

Figure 4.11 Dopaminergic neuron identity and microglia identified by bulk RNA-Sequencing. 161

Figure 4.12 α-Synuclein seeded aggregation in $SNCA^{TRIP}$ iPSC-derived dopaminergic neurons resulted in increased pSYN levels and neurotoxicity. 163

Figure 4.13 Progressive morphological maturation of pMacpre into co-cultured microglia (co-pMGL). 165

Figure 4.14 Microglial transition to morphologically activated phenotypes, reduces levels of pSYN and rescue neuronal loss when co-cultured with α-synuclein seeded dopaminergic neurons. 167

Figure 4.15 pSYN inclusions decreased when microglia were cultured in direct contact with dopaminergic neurons. 170

Figure 4.16 pSYN levels are not affected by microglial LRRK2 or GBA mutations. 171

Figure 4.17 HC iPSC-derived microglia uptake exogenous α-synuclein fibrils via phagocytosis. 173

Figure 5.1 Disease Associated Microglia phenotype: a universal phenotype across neurodegeneration. 188

Figure 5.2 TREM2 and downstream pathways upon receptor activation. 191

Figure 5.3 Principal component analysis on the 1000 most variable protein-coding genes by bulk RNA-Seq in seeded co-cultures versus non-seeded co-cultures. 197

Figure 5.4 Differential gene expression by bulk RNA-Seq in co-cultures of microglia with either fibril seeded (Fib) or non-seeded control (NSC) neurons. 199

Figure 5.5 Co-cultured microglia express key homeostatic and DAM genes. 201

Figure 5.6 Uptake of fibrillar α-synuclein in HC iPSC-derived microglia was not modified by addition of TREM2-specific antibodies. 203

Figure 5.7 Generation of the TREM2 KO iPSC line. 204

Figure 5.8 TREM2 does not influence the uptake of α-synuclein fibrils in iPSC-derived microglia cells. 205

Figure 5.9 TREM2 KO does not modify the microglial effect on neuronal pSYN levels. 206

Figure 5.10 Single cell RNA-Seq analysis revealed microglial and neuronal specific clusters. 209

Figure 5.12 Single cell RNA-Seq analysis identified differentially expressed genes and their pathways within microglial and neuronal subpopulations under fibril-treated conditions. 211

Figure 5.13 Gene Set Enrichment Analysis identified the microglial pathways that were differentially regulated under seeding conditions. 212

Figure 5.14 Secretome analysis of microglia co-cultured with α-synuclein seeded dopaminergic neurons. 214

List of Tables

Table 1.1 Summary of monogenic variants associated with Parkinson's disease. 21
Table 2.1 List of stem cell lines used in the present study 58
Table 2.2 List of components for the Embryoid bodies (EB) medium (1X)..... 62
Table 2.3. List of components for the Factory Medium 63
Table 2.4 List of components for microglia co-culture and monoculture medium 64
Table 2.5 List of components for mice organotypic hippocampal slices medium..... 69
Table 2.6 List of primers used in the present study 74
Table 2.7 Composition of buffers used for the present study..... 86
Table 2.8 List of the primary and secondary antibodies used in the present study..... 88

Chapter 1: General introduction

1.1 Parkinson's disease

1.1.1 Epidemiology & diagnosis of Parkinson's disease

Parkinson's disease is the second most common neurodegenerative disorder and a leading cause of chronic disability globally (Collaborators, 2019). Parkinson's disease prevalence increases with age and affects approximately 1% of the population over 60 years, rising to almost 3% in individuals aged 80 years and older (Nussbaum and Ellis, 2003, Pringsheim et al., 2014). Additionally, Parkinson's disease is considered the fastest growing neurological disorder globally with its prevalence estimated to increase up to 12 million people by 2040 (Dorsey et al., 2018) fuelled by increased longevity and ageing populations. The high prevalence of Parkinson's disease is also accompanied by increased economic burden; for example in the United States of America the economic burden from Parkinson's disease was estimated at 51.9$ billion (Yang et al., 2020). Parkinson's disease is twice as common in males compared to females, suggesting a gender-related risk factor (Cerri et al., 2019).

The movement disorder was first described by James Parkinson (1783-1824) in his seminal essay on the ''*paralysis agitans*''. The afflicted patients were described as exhibiting '' involuntary tremulous motion, with lessened muscular power in parts and not in action and even when supported''. The same disease was further described by the Scottish pathologist William Rutherford Sanders (1828-1881) and French neurologist Jean-Martin Charcot (1825-1893) who suggested the disease's eponym (Charcot & Sigerson, 1879). The cardinal clinical features of Parkinson's

disease include bradykinesia, resting tremor, rigidity and postural instability. The early motor symptoms are typically asymmetrical and respond to levodopa treatment, which can differentiate Parkinson's from other forms of atypical Parkinsonism.

The prodromal phase of the disease may start 12-14 years before the clinical diagnosis (Postuma et al., 2012). Parkinson's disease patients manifest a plethora of non-motor symptoms that affect multiple bodily systems, such as hyposmia, constipation, depression, anxiety, dementia, fatigue and urinary dysfunction (Ansari and Johnson, 1975, Braak et al., 2004, Edwards et al., 1993, Cummings, 1992). Rapid Eye Movement (REM) sleep behaviour disorder (RBD) is most strongly associated with Parkinson's disease, as almost 90% of individuals with RBD develop some form of parkinsonism (Schenck et al., 1986). As the disease progresses so do the non-motor symptoms, which have a severe impact on the quality of life of the patients (Martinez-Martin et al., 2011).

1.1.2 Current therapeutic strategies

Most Parkinson's disease brains exhibit depigmentation of the substantia nigra pars compacta (SNc) and locus coeruleus due to extensive loss of neuromelanin-containing dopaminergic neurons in the SNc and noradrenergic neurons in the locus coeruleus (Dickson, 2012). The gold-standard treatment for Parkinson's disease remains the administration of dopamine precursor, 3,4-dihydroxyphenylalanine L-DOPA which promotes synthesis of dopamine in the midbrain (Tan, 2001, Lees et al., 2009, Salat and Tolosa, 2013). However, the clinical benefits from L-DOPA administration are limited to symptomatic control and its efficacy declines with time due to the progressive loss of dopaminergic neurons (Castrioto et al., 2013). Deep brain stimulation (DBS) a neurosurgical procedure has also been introduced as a widely used therapeutic approach for Parkinson's (Lozano and Snyder, 2008, Lozano et al., 2010) but its effectiveness is not higher than what can be achieved with maximal medical therapy. Even though DBS alleviates the motor symptoms and improves the quality of life of the patients it can also lead to adverse effects, such as verbal impairment and aggravated freezing gait (Carlson et al., 2014, Foley et al., 2017, Højlund et al., 2017). Another promising approach involves transplantation of embryonic midbrain nigral cells to restore dopaminergic neurons (Stoker et al., 2017, Kupsch et al., 1995). All the current therapeutic approaches involve symptomatic treatment and do not halt the disease's progression. Therefore, there is a huge and urgent need for disease-modifying therapies.

1.1.3 Genetics of Parkinson's disease

Parkinson's disease is predominantly a sporadic disease. However, family history has been observed in about 15% of the reported cases with 5-10% of them following a Mendelian pattern of inheritance (Lesage and Brice, 2009). To date, several causal genes have been linked to Parkinson's (Table 1.1) and only a small percentage of apparently sporadic cases harbour mutations in Parkinson's-related genes (Bandres-Ciga et al., 2020).

	Gene (HGNC Approved Name)	Alternative Gene Names	Inheritance	Pathogenicity	PD Phenotype	Function
High penetrance	*SNCA*	*PARK1, PARK4, NCAP*	AD	Pathogenic	Early-onset	Uncertain (encodes α-synuclein)
	VPS35	*PARK17, MEM3*	AD	Pathogenic	Typical	Retromer and endosomal trafficking
	PINK1	*PARK6*	AR	Pathogenic	Early-onset	Mitochondrial
	PARK7	*DJ-1*	AR	Pathogenic	Early-onset	
	PRKN	*PARK2, PARKIN*	AR	Pathogenic	Early-onset	
	PLA2G6	*PARK14, IPLA2*	AR	Pathogenic	Early-onset, atypical	Cell membrane
	ATP13A2	*PARK9*	AR	Pathogenic	Early-onset, atypical	Lysosomal
	FBXO7	*PARK15, FBX7*	AR	Pathogenic	Early-onset, atypical	Mitochondrial
	POLG	*POLG1, POLGA*	AD	Pathogenic	Early-onset, atypical	Mitochondrial DNA maintenance
	DNAJC6	*PARK19, DJC6*	AR	Likely pathogenic	Early-onset	Synaptic vesicle formation and trafficking
	DNAJC13	*PARK21, RME8*	AD	Conflicting reports	Typical	
	TMEM230	*C20ORF30*	AD	Conflicting reports	Typical	
	SYNJ1	*PARK20*	AR	Pathogenic	Early-onset, atypical	
	VPS13C	*PARK23*	AR	Pathogenic	Early-onset	Mitochondrial
	CHCHD2	-	AD	Pathogenic	Typical	Uncertain
	DCTN1	-	AD	Pathogenic	Atypical	Microtubule
Variable penetrance	*LRRK2*	*PARK8, DARDARIN*	AD	Pathogenic	Typical	Lysosomal, mitochondrial, microtubule
	GBA	*GBA1*	AD	Pathogenic	Typical	Lysosomal
Associated with PD but unlikely to be pathogenic	*HTRA2*	-	AD	Uncertain/likely benign	-	Mitochondrial
	UCHL1	*PARK5*	AD	Uncertain/likely benign	-	Ubiquitin-proteasome
	GIGYF2	*PARK11*	AD	Uncertain/likely benign	-	Uncertain
	EIF4G1	-	AD	Benign	-	mRNA translation
	LRP10	*LRP9*	AD [1]	Uncertain	-	Uncertain

[1] AD = autosomal dominant, AR = autosomal recessive, HNGC = HUGO Gene Nomenclature Committee.

Table 1.1 Summary of monogenic variants associated with Parkinson's disease. Table adapted from (Day and Mullin, 2021).

The first gene was identified in the late nineties when a dominantly inherited missense mutation (p.A53T) in the *SNCA* gene that encodes the α-synuclein protein was reported in a large Greek-Italian kindred (Polymeropoulos et al., 1997). Several other *SNCA* point mutations (p.A30P, p.E46K, p.H50Q, p.G51D, p.A53E, p.A53V) were subsequently discovered in separate families (Appel-Cresswell et al., 2013, Kiely et al., 2013, Krüger et al., 1998, Lesage et al., 2013, Pasanen et al., 2014, Proukakis et al., 2013, Zarranz et al., 2004). Duplications and triplications of the chromosomal region of the *SNCA* gene also cause Parkinson's disease exhibiting a dose-dependent effect (Chartier-Harlin et al., 2004, Ibáñez et al., 2004, Singleton et al., 2003). Duplication of the *SNCA* cause a clinical phenotype that is similar to sporadic disease but with earlier age of onset, whereas *SNCA* triplication causes aggressive forms of the disease with earlier onset and severe cognitive impairment.

Mutations in *LRRK2*, *GBA1*, *DJ-1* (PARK-7), *VPS35*, *PRKN* (Parkin) and *PINK1* have also been associated with Parkinson's disease. *LRRK2* encodes leucine-rich zipper kinase 2, which regulates endosomal-lysosomal trafficking and mutations in this gene are the most common cause of familial Parkinson's disease. To date, several *LRRK2* mutations have been reported as pathogenic (Paisán-Ruíz et al., 2004, Zimprich et al., 2004, Tolosa et al., 2020). Particularly, the p.G2019S mutation accounts for approximately 4% of familial Parkinson's and 1% of sporadic cases (Li et al., 2014a). Additionally, mutations in the *GBA1* gene encoding β-glucocerebrosidase constitute the highest genetic risk factor for sporadic Parkinson's disease (Neudorfer et al., 1996, Aflaki et al., 2016). *GBA1* mutations have also been linked to Gaucher's disease, which is a lysosomal storage disorder. Mutations in mitochondrial-related genes, *PINK1* (PTEN-induced kinase 1), *PRKN* (Parkin) and *DJ-*

1 (PARK7) have been associated with early onset recessive Parkinson's disease (Valente et al., 2004, Bonifati et al., 2003, Kitada et al., 1998). PINK1 and Parkin initiates mitophagy in a process by which PINK1 is stabilised on the outer membrane of damaged mitochondria and phosphorylates Parkin and ubiquitin, and both these modifications stimulate Parkin's E3 ubiquitin ligase (Pickrell et al., 2015). Lastly, DJ-1 has been involved in multiple functions including an antioxidant and a deglycase function (Richarme et al., 2015, Biosa et al., 2017).

1.1.3.1 Role of Parkinson's disease genes in immune function

In addition to the neurodegenerative phenotype, local CNS and peripheral inflammation has also been confirmed in Parkinson's disease patients. Interestingly, some of the monogenic mutations exhibit key roles in inflammatory responses. For example, *LRRK2* is expressed by microglia, the brain's resident macrophages and it is induced by pro-inflammatory stimuli (Moehle et al., 2012). *LRRK2* is also expressed by peripheral immune cells and some of its variants have been correlated with increased risk of Crohn's disease (Barrett et al., 2008). Additionally, immune dysregulation has been associated with *GBA1* mutations, such as multisystem inflammation, increased levels of pro-inflammatory cytokines, microglia activation and astrogliosis (Barak et al., 1999, Farfel-Becker et al., 2011). It has been shown that microglia exhibit increased *SNCA* expression following stimulation with lipopolysaccharides (LPS) (Tanji et al., 2002) and pathogenic forms of α-synuclein bind to the microglia toll-like receptors 2 and 4 (TLR 2, 4) (Kim et al., 2013). In addition, α-synuclein induces T-cell specific responses early in the disease process (Lindestam Arlehamn et al., 2020).

Out of the multiple identified loci by genomic wide association studies (GWAS) associated with Parkinson's disease (Chang et al., 2017, Nalls et al., 2014), several have been implicated in immunological mechanisms and pathways. For example, two of these loci are found within the human leukocyte antigen (HLA) region. Additionally, other loci are implicated in the development of B-and T-lymphocytes. Four of the identified loci are variants of the *NFκB*, which encodes the homonymous transcription factor regulating expression of a plethora of immune-related genes.

1.1.4 Neuropathology of Parkinson's disease

The cardinal neuropathologies of idiopathic Parkinson's disease are the dramatic loss of dopaminergic neurons in the SNc and the abnormal accumulation of α-synuclein in the cell bodies and neurites, which form inclusions termed Lewy bodies and Lewy neurites, respectively. These structures were firstly identified in the brain by Fritz Jacob Heinrich Lewy (Lewy, 1912) and were termed later as 'corps de Lewy' in the SNc of Parkinson's patients by Constantin Tretiakoff (Tretiakoff, 1919). Following the discovery of a point mutation (p.A53T) in *SNCA* in familial Parkinson's (Polymeropoulos et al., 1997) it was shown that α-synuclein protein is the main component of the Lewy bodies and neurites in sporadic Parkinson's disease (Spillantini et al., 1997).

Neither the loss of pigmented dopaminergic neurons in the SNc nor the neuronal deposition of α-synuclein are specific to Parkinson's disease (Dickson et al., 2009, Halliday et al., 2011). However, when the two are combined they are definitive for diagnosis of idiopathic Parkinson's disease (Figure 1.1) (Poewe et al., 2017).

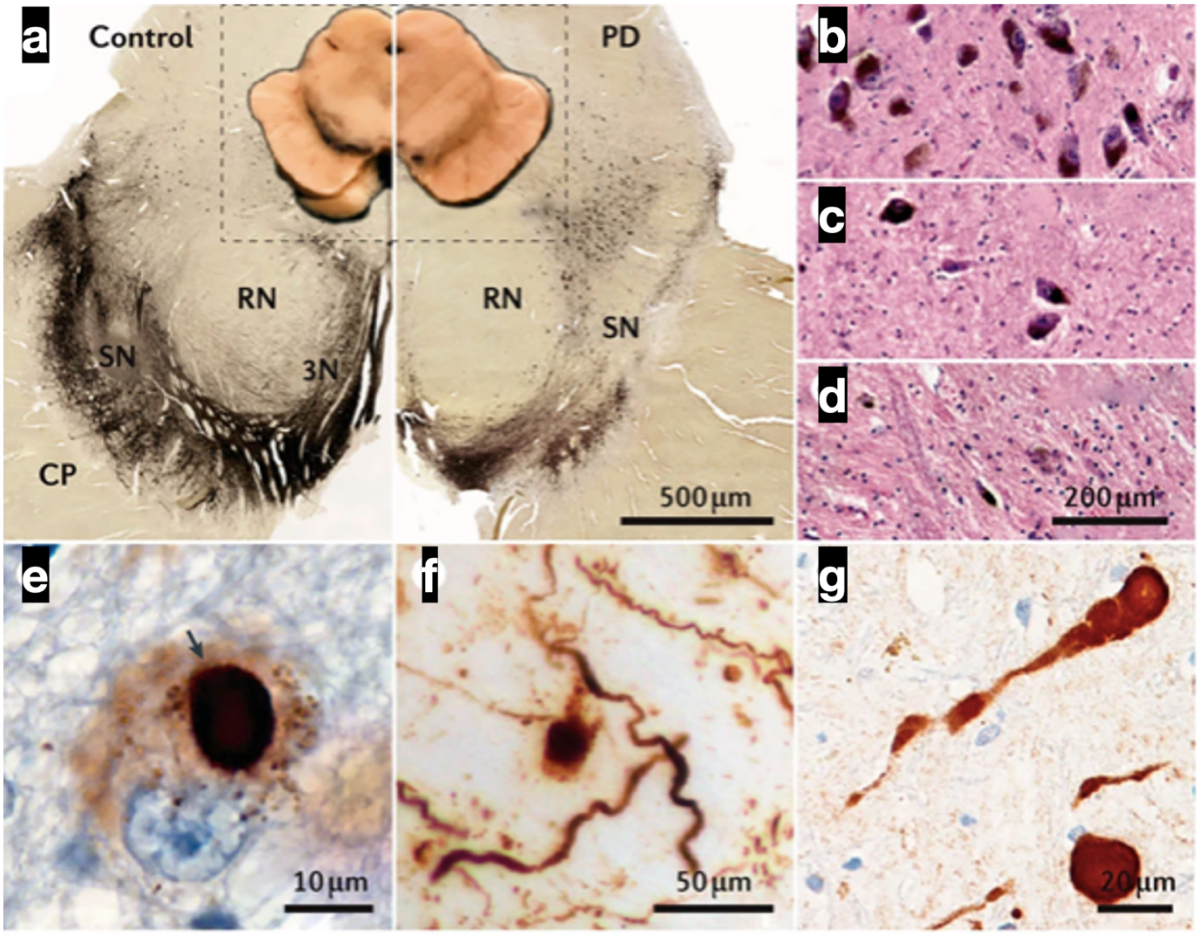

Figure 1.1 Main diagnostic neuropathological features of Parkinson's disease. **a.** Parkinson's disease is characterised by loss of pigmented neurons in the substantia nigra (SN) (right panel) compared to a healthy control individual (left panel). Macroscopical (inset) and transverse sections of midbrain immunohistochemically stained for tyrosine hydroxylase (TH), the rate limiting enzyme for the synthesis of dopamine. The Parkinson's disease histological section also depicts the selective loss of ventrolateral parts of the SN. **b, c, d.** Ventrolateral region of the SN stained with haematoxylin and eosin shows a normal distribution of pigmented dopaminergic neurons in a healthy control individual (**b**) and diagnostically mild (**c**) and severe (**d**) dopaminergic loss in Parkinson's brains. **e, f, g.** Immunohistochemical staining of α-synuclein indicates the round deposits known as Lewy bodies (e, black arrow), more diffused, granular deposits (e, f), deposits in neuronal processes (f), dot-like α-synuclein structures (f) and α-synuclein spheroids in neuronal axons (g). 3N, 3rd nerve fibres, CP, cerebral peduncle, RN, red nucleus. Image is adapted from (Halliday and McCann, 2010) & (Poewe et al., 2017).

A thorough investigation of brain post-mortem samples at various stages of the disease by Braak and colleagues led to the “Braak staging of disease progression’’, which has been widely adopted when describing patterns of α-synuclein pathology progression in Parkinson’s and tau pathology in Alzheimer’s disease (Figure 1.2) (Braak et al., 2003a, Braak and Del Tredici, 2008). In Parkinson’s disease, stage 1 and stage 2 exhibit pathology in the olfactory structures or lower brainstem (Del Tredici et al., 2002) and could explain the non-motor symptoms observed in Parkinson’s patients at the prodromal phase. The degeneration of neurons in the SNc follows in stages 3 and 4 and the heterogeneity in SNc involvement may reflect the differential susceptibilities of the dopaminergic neurons in developing Lewy bodies and Lewy neurites (Braak et al., 2003a). At this stage motor symptoms, such as bradykinesia, tremor, and rigidity occur. According to the staging classification, the hallmark of stage 4 is the involvement of the anteromedial temporal mesocortex, a transition zone between the allocortex and the neocortex. Finally, involvement of key areas of the neocortex allows for distinction between stages 5 and 6. At stage 5 the pathology progresses from the mesocortex to the sensory areas of the neocortex and at stage 6 it reaches the first order sensory association areas. These late stages correlate with cognitive involvement, which is a hallmark of the late stages of Parkinson’s and is detected in up to 80% of patients who have the disease for 20 or more years.

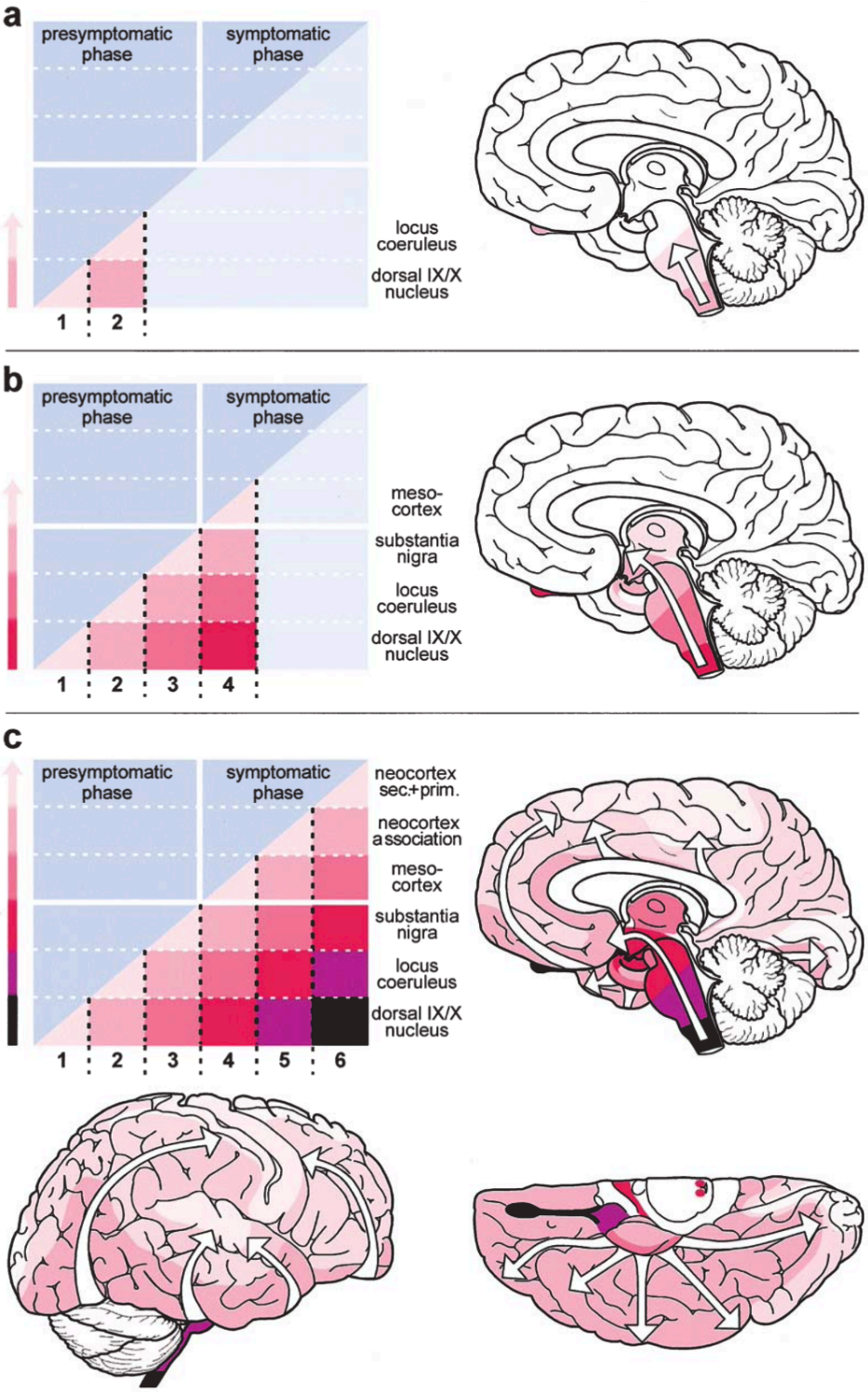
a
presymptomatic phase
symptomatic phase
locus coeruleus
dorsal IX/X nucleus
1
2
b
presymptomatic phase
symptomatic phase
meso-cortex
substantia nigra
locus coeruleus
dorsal IX/X nucleus
1
2
3
4
c
presymptomatic phase
symptomatic phase
neocortex sec.+prim.
neocortex association
meso-cortex
substantia nigra
locus coeruleus
dorsal IX/X nucleus
1
2
3
4
5
6

Figure 1.2 The six stages of Parkinson's disease pathology.
a. α-synuclein positive inclusions occur in the dorsal IX/X (vagus nerve) motor and anterior olfactory nuclei. The pathology spreads to the brainstem and from that point follows an upward trajectory (white arrow). In stage 2, lesions within the locus coeruleus occur. **b.** Stages 3-4 include the cortical involvement commencing in the mesocortex. Stage 3 marks the appearance of inclusions within the substantia nigra and the cholinergic nuclei of the basal forebrain. Stage 4 includes the involvement of the anteromedial temporal mesocortex. At this point the typical motor symptoms of Parkinson's start. **c.** In stages 5-6 the neocortex succumbs to the pathology's progression. Stage 5 progression includes prefrontal cortical areas and during the final stage 6 the disease has reached the highest order sensory association areas, which marks the advanced phase of Parkinson's disease (Dubois and Pillon, 1997). Image is adapted from (Braak et al., 2003a).

α-synuclein immunoreactive inclusions have been observed in the gastric myenteric and submucosal plexuses within the enteric nervous system (ENS)(Braak et al., 2006) at the early stages of the disease. This observation suggested that the occurrence of pathology in the submucosal plexus of Meissner may spread via the vagus nerve: it either starts with ENS involvement with spread of α-synuclein pathology to the brainstem (Braak et al., 2003b) or in the brainstem with subsequent ENS involvement (Braak et al., 2006).

1.2 α-synuclein

1.2.1 Synucleinopathies

Synucleinopathies are a group of disorders that are characterised by progressive aggregation and accumulation of insoluble fibrillary α-synuclein within neurons or glia resulting in neurodegeneration with a spectrum of clinical manifestations (Jellinger, 2010).

1.2.2 Structure, function & pathobiology of α-synuclein

α- and β-synuclein were discovered by immunoblotting studies where an antibody against phosphorylated tau protein recognised two extra protein bands with an approximate observed molecular weight of 14 kDa (Jakes et al., 1994). Later, it was discovered that α-synuclein was the main component of Lewy bodies and Lewy neurites (Spillantini et al., 1997). Antibodies that were raised against β- and γ-synuclein failed to stain Lewy bodies and neurites demonstrating that out of the three mammalian synucleins only α-synuclein accumulates in the Lewy neuropathological structures (Spillantini et al., 1998).

The *SNCA* gene that encodes α-synuclein is located at position 21 on chromosome 4 (Shibasaki et al., 1995). The protein, which is abundantly expressed in neurons is 140 amino acids (aa) long and its structure is divided in three domains (Figure 1.3): a) the N-terminal domain (1-60 aa) with α-helical proclivity b) the main central hydrophobic domain (60-91 aa), also known as the non-amyloid component (NAC) and involved in misfolding processes when acquiring β-sheet structure and c) the negatively charged C-terminal domain (91-140 aa). α-synuclein is considered as intrinsically disordered protein, lacking a well-defined conformation in solution yet

acquiring a partial α-helical structure at the N-terminus (Villar-Piqué et al., 2016), in the presence of membrane lipids (Vamvaca et al., 2009). Interestingly, α-synuclein has been described as a chameleon protein due to the protein's high conformational plasticity, which range from distinct secondary structure elements to high-molecular weight insoluble assemblies (Uversky, 2003).

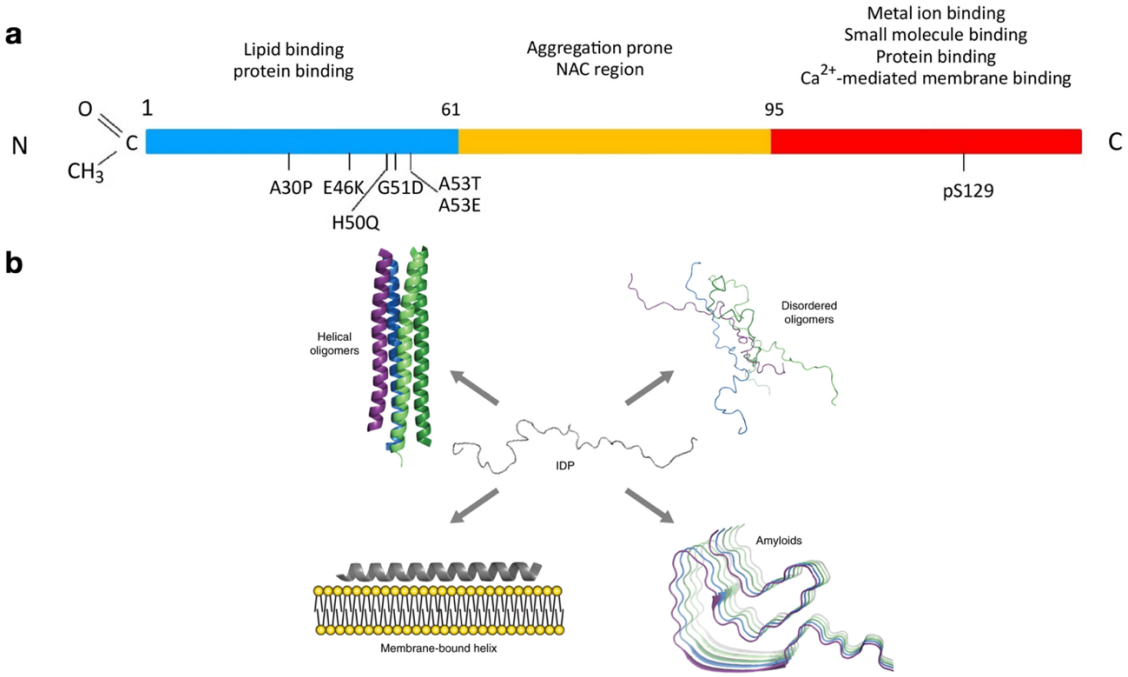

Figure 1.3 The conformational landscapes of α-synuclein.

a. The native monomeric α-synuclein consist of three well-defined regions. The N-terminus region (in blue) (1-60 aa) is an amphipathic domain responsible for the membrane binding properties of the protein. All the identified familial point mutations related to early onset Parkinson's disease are located in this domain. Quite characteristically, the N-terminus contains seven distinct eleven residue repeats (KTKEGV), which are highly conserved and estimated to form an amphipathic α-helical structure (Bendor et al., 2013). The central region (in yellow) (61-95 aa) encompasses the non-amyloid component (NAC) domain, which is hydrophobic and highly prone to aggregation by forming cylindrical and amyloid β-sheets (Deleersnijder et al., 2013). The C-terminus region (in red) (96-140 aa) is enriched with acidic residues and post-translational modifications occur in this domain, including phosphorylation at serine 129 (pSer129) **b.** Schematic illustration of the intrinsically disordered conformations that α-synuclein may acquire: helix-rich oligomers, membrane-bound helical states and amyloid-like conformers with distinct β-sheet structures, as well as disordered regions. Image adapted from (Newberry et al., 2020).

α-synuclein undergoes post-translational modifications, such as phosphorylation (Anderson et al., 2006), ubiquitination (Tofaris et al., 2003), sumoylation (Krumova et al., 2011) and nitration (Giasson et al., 2000), which have been implicated in its propensity to aggregate. Furthermore, truncations at the C- and N-terminus of the protein have also been isolated from Lewy body extracts (Tofaris et al., 2003, Baba et al., 1998). Phosphorylation of pSer129 is the most abundant post-translational modification (>90%) of α-synuclein in Lewy pathology in sporadic and familial Parkinson's disease (Anderson et al., 2006, Fujiwara et al., 2002, Saito et al., 2003). Under healthy conditions there is little α-synuclein phosphorylated at Ser129, reportedly less than 4% (Fujiwara et al., 2002). The kinases involved in this modification belong to the G-protein coupled receptor family, as well as polo-like kinases and casein kinases (Mbefo et al., 2010, Pronin et al., 2000, Lee et al., 2004). Due to the significance of pSer129 and Lewy pathology the aforementioned modification is widely used as an indicator of pathological α-synuclein in model systems and diagnostic studies.

Although it has been more than two decades since the discovery of α-synuclein as prominent feature of the Lewy pathology, its function is not fully understood. α-Synuclein localises mainly in the pre-synaptic terminals of neurons and exerts subtle effects in the regulation of synaptic transmission. Specifically, α-synuclein localises in the pre-synaptic terminal (Maroteaux et al., 1988, Withers et al., 1997) and co-localises with synaptic vesicles (Lee et al., 2011a, Zhang et al., 2008). α-synuclein may recycle the vesicular synaptic pool by modulating the number released, their mobilisation and endocytosis (Bendor et al., 2013, Vargas et al., 2014). α-synuclein may also enhance vesicular clustering (Diao et al., 2013), which was

suggested to involve multimerization of the protein upon membrane binding (Wang et al., 2014). In mouse models, the C-terminus of α-synuclein interacts with synaptobrevin-2 (VAMP2), which is an essential component of exocytosis (Burré et al., 2010).

1.2.3 Lewy pathology in Parkinson's disease

Staining of Lewy bodies and Lewy neurites with antibodies specific to the C- and N-terminus of α-synuclein revealed identical immunoreactivity patterns suggesting that full length α-synuclein is present in these inclusions (Spillantini et al., 1998). Filaments of α-synuclein isolated from Lewy body extracts are between 50 to 700 nm in length and 5 to 10 nm in diameter. It is widely accepted that Lewy bodies and neurites are highly heterogeneous structures comprised of lipids, membranous organelles, cytoskeleton proteins suggesting that the interactions of α-synuclein with these components is critical for the formation and heterogeneity of these inclusions, as well as the neurodegeneration events that follow (Duffy and Tennyson, 1965). The structural diversity also reflects the heterogeneity of the Lewy pathology across the different brain regions, as well as patient subpopulations (Forno, 1969, Forno and Norville, 1976, Gibb et al., 1991, Kuusisto et al., 2003). For example, inclusions in the brainstem have an eosinophilic core and a clear surrounding halo. Regarding their structure, they consist of a dense core full of filamentous and granular material (Duffy and Tennyson, 1965, Roy and Wolman, 1969). In contrast, the abundant Lewy bodies in the cortex, which are a hallmark of the late stages of Parkinson's disease and of dementia with Lewy bodies (DLB), lack a distinctive halo and core.

Electron microscopy studies have revealed the nature of the Lewy structures in high resolution. In detail, it has been reported that the membranous structures that are part of the Lewy structures originate from vesicles and fragmented organelles, such as mitochondria and lysosomes (Duffy and Tennyson, 1965, Shahmoradian et al., 2019). Selective antibodies used in combination with STED microscopy also revealed that Lewy bodies exhibit a three-dimensional onion-like skin architecture

with a backbone enriched in pSer129 α-synuclein and neurofilaments engulfing truncated C-terminus, as well as membrane related α-synuclein epitopes (Moors et al., 2018). The fact that α-synuclein associates with membranous lipids correlates with the hypothesis that α-synuclein and membranes interactions may be nucleation events that ultimately endorse aggregation (Fanning et al., 2021, Galvagnion et al., 2015). Quite interestingly, a recent cryo-EM study on insoluble sarkosyl extracts from PD, PDD and DLB patients' brains revealed that α-synuclein filaments from these synucleinopathies are identical and comprise of a single protofilament, termed as ''Lewy fold'' (Yang et al., 2022). In contrast to tau where distinct conformers define different diseases (Shi et al., 2021), this observation reveals that PD, PDD and DLB are closely related suggesting an involvement of these diseases in a continuum of brain disorders.

The above observations have shifted the field's attention from protein-related toxicity to glycolipid insults. Additionally, they have paved the way towards establishing appropriate experimental conditions that will allow the formation of *de novo* seeded aggregates that recapitulate the *in vivo* α-synuclein folds. Quite noteworthy, the exact relationship between neuroinflammation and lipid disturbances remains to be fully deciphered, particularly since the appreciation that neurodegeneration is not purely neuron-centric has been cemented.

1.2.4 Prion-like propagation and aggregation of α-synuclein

Parkinson's disease and other neurodegenerative diseases such as Alzheimer's, amyotrophic lateral sclerosis (ALS) and frontotemporal dementia (FTD) share common fundamental pathological mechanisms which involve the seeded aggregation of different proteins (Guo and Lee, 2014, Jucker and Walker, 2013). The driving mechanism behind seeded aggregation is the prion-like paradigm (Prusiner, 2012, Prusiner, 2013) (Figure 1.4). According to this, ''prion'', a proteinaceous infectious particle consists of a β-sheet protein assembly that can template the conversion of the soluble form of the protein into the misfolded form, causing toxicity as observed in prion-diseases, such as Creutzfeldt-Jakob disease, Gerstmann Straussler-Scheinker disease, bovine spongiform encephalopathy (BSE) and others (Prusiner, 1982, Prusiner, 1987).

According to the Braak staging, Lewy pathology evolves across anatomically interconnected areas (Braak et al., 2003a) (Figure 1.2), suggesting that pathological α-synuclein may spread from neuron-to-neuron via seeding-competent assemblies which template the monomeric protein into a misfolded form (Brundin and Melki, 2017). Multiple mechanisms of propagation are involved, such as endocytosis, extracellular vesicles release (Emmanouilidou et al., 2010), tunnelling nanotubes as well as via non-neuronal cells such as microglia (Guo et al., 2020, Gallardo, 2019).

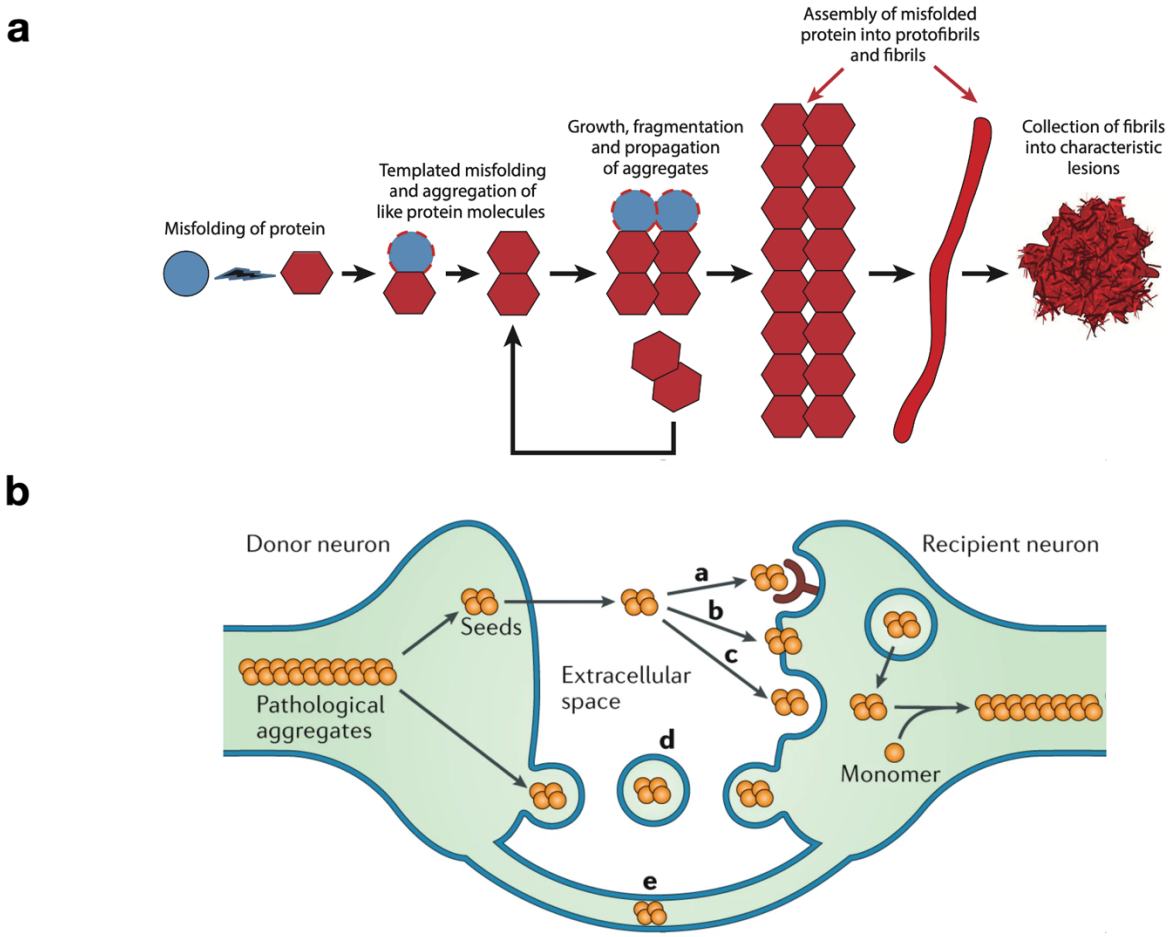

Figure 1.4 The prion-like paradigm of α-synuclein seeded aggregation and intraneuronal propagation.

a. Schematic diagram illustrates the suggested series of events from initial misfolding of α-synuclein to accumulation of filamentous protein species in pathological inclusions. Self-aggregation of monomeric protein leads to higher molecular weight species that range in size, from oligomers to large polymers that can act as ‘’seeds’’ which template endogenous monomeric α-synuclein and promote fibrilization. The endpoint of the seeded aggregation cascade is the assembly of misfolded proteins into insoluble protofibrils and fibrils, which then deposit intracellularly (Lewy bodies and neurites) or extracellularly (Aβ plaques in Alzheimer’s disease). Image adapted from (Jucker and Walker, 2013). **b.** The prion-like paradigm has been widely accepted in the field of neurodegeneration and it has been proposed that pathological aggregates, termed as ‘’seeds’’ are released in the extracellular space from a donor neuron either as naked proteins or enclosed in vesicles, such as exosomes. Sequentially, a recipient neuron may uptake these aggregates via (a) receptor-mediated endocytosis, (b) direct penetration of the plasma membrane or (c) fluid phase endocytosis. (d) The vesicle enclosed seeds may cross to the recipient cell via fusion with the cell membrane. (e) Nanotubes connecting the two cells may also enable the transfer of the aggregates. Image adapted from (Peng et al., 2020a).

The seeded aggregation model of α-synuclein has emerged from several *in vitro* and *in vivo* lines of investigation. Recombinant α-synuclein fibrils can template intracellular monomeric protein initiating aggregation in cell lines and neurons (Luk et al., 2009, Volpicelli-Daley et al., 2011). Similarly, injection of purified fibrils or brain homogenates from mice exhibiting α-synuclein pathology in wild type and transgenic mice has also shown to seed and accelerate formation of Lewy inclusions (Luk et al., 2012c, Luk et al., 2012a). Injection of sarkosyl-extract from DLB patients has also resulted in inclusion formation in wild type mice (Masuda-Suzukake et al., 2013). Stereotypical and topographical transmission of Lewy pathology is suggestively a critical component in Parkinson's disease pathology (Braak et al., 2003a). Remarkably, grafted dopaminergic neurons in Parkinson's disease patients following the subjects' death were also shown to contain Lewy-like inclusions and were immunohistochemically positive to phosphorylated α-synuclein at Ser129. (Li et al., 2008). Interestingly, activated microglia have also been reported around inclusions of grafted neurons, strengthening the hypothesis that they might also contribute to propagation of misfolded species of α-synuclein (Sigurdsson et al., 2002). Although the prion-like hypothesis for seeded aggregation and propagation of pathological α-synuclein has been cemented, there is no evidence to support transmission between individuals (Aguzzi and Lakkaraju, 2016, Tamgüney and Korczyn, 2018).

α-synuclein is prone to aggregate through its hydrophobic core (NAC) and checkpoint mechanisms are in place to ensure its physiological trafficking. It has been demonstrated that α-synuclein is re-cycled within the cells by degradation pathways that include molecular chaperones (Burmann et al., 2020), the ubiquitin proteosome and lysosome system (Vogiatzi et al., 2008, Webb et al., 2003) and autophagy (Vilchez

et al., 2014). Another physiochemical property of α-synuclein that enables its accumulation and binding on membranous structures is located on the amphipathic domain of the N-terminus (Pranke et al., 2011). Toxicity may be initiated by membrane interactions acting as a focal point of high concentration. Another hypothesis in the field is that when α-synuclein interacts with lipid membranous structures that can lead to misfolding through the brief exposure to the hydrophobic residues (Jao et al., 2004, Trexler and Rhoades, 2009, Ulmer et al., 2005). Evidently, ablation of key central NAC domain residues eradicated the aggregation prone potential of α-synuclein (Giasson et al., 2001). Changes in the physiological pH conditions in organelles, such as the lysosomes have been also reported to harbour a permissive environment for the formation of aggregated α-synuclein assemblies (Breydo et al., 2012, Buell et al., 2014, Galvagnion et al., 2015).

1.3 Microglia

1.3.1 The origins of microglia

Microglia were first described and characterised almost a century ago by Pio del Rio Hortega as a small population of phagocytotic and migratory cells of mesodermal origin (del Rio Hortega, 1932). A couple of years later he assigned those cells the name ‘’microglia cells’’ due to their size being the smallest of all glia and further characterised them as non-neuronal, non-astrocytic elements highly distinguished from the ectodermal-originated oligodendrocytes (del Rio Hortega, 1939). The origin of microglia has been controversial, with some studies reporting their ectoderm origin (Rezaie and Male, 2002). However, several lines of evidence supported Hortega’s findings regarding their mesodermal origin by using a combination of immunohistochemistry and light/electron microscopy confirming morphological similarities of microglia and macrophages over various developmental stages (Murabe and Sano, 1982, Murabe and Sano, 1983). Additionally, the fact that microglia cells were recognised by antisera raised against macrophages established the mesodermal lineage between both microglia and CNS macrophages (Hume et al., 1983, Perry et al., 1985). The controversy around the developmental lineage of microglia impacted on methodologies to generate human microglia. The overwhelming phenotypic similarities between microglia and macrophages led researchers to believe that both share myeloid origins (Lawson et al., 1990). Additionally, the scientific community believed that microglia could potentially originate from blood monocytes, the circulating precursors of macrophages. According to those studies performed on chimeric animal models, the increased number of recruited microglia to the CNS following an injury involved expansion of

the resident pool, as well as active recruitment of bone marrow derived microglia from the bloodstream (Simard and Rivest, 2004, Priller et al., 2001, Kennedy and Abkowitz, 1997, Flügel et al., 2001). Nevertheless, other studies reported that microgliosis in the CNS was the result of the expansion of a local pool supporting the notion that the CNS is a closed microenvironment and not accessible to cells from the bloodstream (Hickey et al., 1992, Hickey and Kimura, 1988, Massengale et al., 2005). The studies on chimeric animals obtained by parabiosis from the Rossi and Prinz laboratories were a milestone in our understanding of the microglia origins and cemented the fact that there was no microglia recruitment from the bloodstream contributing to enhanced CNS microgliosis (Ajami et al., 2007, Mildner et al., 2007).

The difficulty in separating the lineage of microglia from blood monocytes was the complication of the dual source of blood cells during development (Ginhoux et al., 2013). There are two areas that contribute to this: the embryonic yolk-sac and the foetal liver (Tavian and Péault, 2005) (Figure 1.5). Using murine models, it was first shown that microglia progenitors are present in the yolk-sac and their numbers increase after E9-E9.5 until 2 weeks following birth (Alliot et al., 1991). Similar developmental events occur in the human embryo as well, with amoeboid microglia progenitors entering the cerebral wall from the ventricular lumen at 4.5 weeks of gestation (Rezaie et al., 2005). Thus, microglia arise from embryonic yolk sac precursors (YS) and colonise the neuroepithelium during the early days of embryogenesis differentiating into microglia (Palis et al., 1999, Ginhoux et al., 2010, Gomez Perdiguero et al., 2015b, Hoeffel et al., 2015). These YS-derived macrophages are dependent on transcription factors IRF8 and PU.1 but independent of MYB (Kierdorf et al., 2013a, Schulz et al., 2012). However, hematopoietic cells

derive from the aorto-gonado-mesonephros region and colonise the bone marrow producing therefore, blood monocyte cells, which depend on MYB for their renewal. As a result, MYB dependence is what distinguishes YS-derived brain-resident microglia from peripheral macrophages that originate from their blood monocyte counterparts.

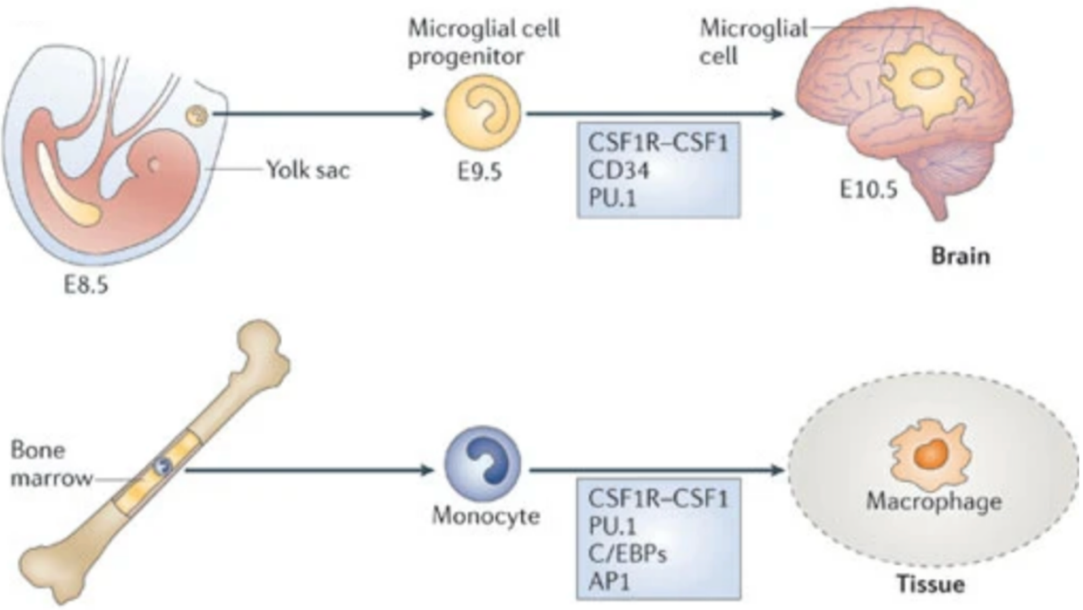

Figure 1.5 Developmental origins of microglia and macrophages.

Microglia originate from primitive haematopoiesis in the foetal yolk-sac and migrate to the brain during early stages of development, in both human and mice embryos. Microglia migration and proliferation requires colony stimulating factor 1 (CSF1) and its receptor (CSF1R), CD34 and transcription factor PU.1. Tissue macrophages derive from bone marrow hematopoietic stem cells through definitive haematopoiesis processes that takes place in the foetal liver, and they also require CSF1/CSF1R, PU.1, CCAAT/enhancer-binding proteins (C/EBPs) and activator protein 1 (AP1). Image adapted from (Saijo and Glass, 2011).

1.3.2 The functions of microglia

1.3.2.1 Microglia foster the CNS development

Microglia are the resident macrophages of the CNS and have key roles in maintaining the homeostasis of the brain's microenvironment, as well as contributing to neuronal development, maturation and plasticity (Figure 1.6). During development, microglia prune neuronal synapses via complement components, such as C1q or C3 that act by tagging unnecessary neuronal synapses for phagocytosis (Stevens et al., 2007). The complement components, among others are termed as ''eat me'' signals as they actively promote phagocytosis by marking unwanted materials in the brain's millieu (Lauber et al., 2004). Precise synaptic connectivity is secured by the phagocytic activity of microglia that perform the imperative function of synapse elimination (Purves and Lichtman, 1980) by removing synaptic spines that do not form connections (Tremblay et al., 2011). Synaptic pruning is also achieved by interaction of microglial CX3CR1 and neuronal CX3CL1 (fractalkine), a glycoprotein that is secreted after proteolytic cleavage. Additional receptor proteins on microglia also recognise "don't-eat-me'' signals from ligands expressed on neurons, which counterbalance the ''eat me'' signals. Those signals include the CD47 immunoglobulin protein that is expressed on the neuronal surface and binds to its microglial ligand SIRPα (Okazawa et al., 2005), as well as polysialylated proteins that interact with microglial sialic acid binding Ig-like lectins (SIGLECs) (Arcuri et al., 2017).

Microglia produce a plethora of trophic factors that enable the correct developmental lineage of various cell types, from neurons to oligodendrocytes. Some of the critical pathways for neuronal survival include the TGF-β signalling (Zöller et al., 2018, Butovsky et al., 2014b), and the insulin growth factor-1 (IGF-1) signalling

that promotes development of neuronal progenitors (Zhang et al., 2014, Butovsky et al., 2006, Aberg et al., 2003), as well as oligodendrocytes (McKinnon et al., 1993). Under homeostatic conditions, microglia also regulate neuronal survival and apoptosis (Oppenheim et al., 1990) by secreting neurotrophins (Figure 1.6) (Miller and Kaplan, 2001).

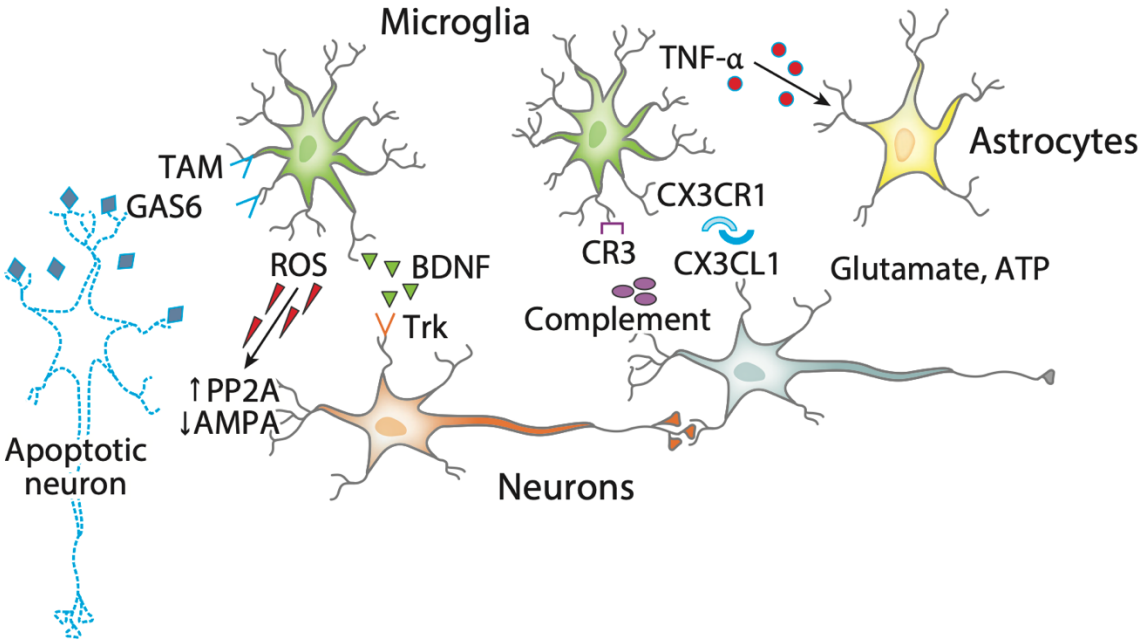

Figure 1.6 Neuronal regulation and maturation achieved by microglia.

Microglia perform synaptic elimination by tagging unnecessary synapses with complement proteins (CR3), as well as through the CX3CR1-CX3CL1 interaction. Microglia contribute to neuronal plasticity by secreting brain derived neurotrophic factor (BDNF) which in turn activates Trk, a key component in regulating neuronal plasticity. Additionally, secretion of reactive oxygen species (ROS) leads to downregulation of neuronal AMPA receptors. Neuronal apoptosis during development is regulated by TAM receptors that enable engulfment of apoptotic neurons that have been opsonised by the Gas6 protein. Neuronal activity may be also modulated indirectly via astrocytic involvement. Astrocytes can release glutamate and ATP in response to microglial secreted tumour necrosis factor-α (TNF-α). Image adapted from (Colonna and Butovsky, 2017).

1.3.2.2 Microglia and neuronal crosstalk

Multiple lines of evidence indicate that there is a bidirectional interaction between microglia and neurons, with neurons actively contributing to microglial regulation (Biber et al., 2007). Irrespective of neurons being healthy or damaged, they send “on” and “off’’ signals to microglia influencing their activity. Through these signals the brain’s local milieu is maintained under immunosuppression to prevent excessive neuroinflammation, which occurs under conditions of chronic, persisting damage, such as in neurodegeneration. These “off’’ signals are constitutively expressed in the healthy brain regulating homeostatic conditions whereas the “on’’ signals are expressed on demand to initiate microglia activation.

The CD200-CD200R ligand-receptor interaction is among those that attenuate microglia activation. CD200 belongs to the immunoglobulin superfamily and is expressed on the neuronal surface membrane (Hoek et al., 2000, Wright et al., 2001) whilst its receptor is primarily expressed on microglia (Hoek et al., 2000). Transgenic mice with genetic ablation of CD200 exhibited uncontrolled microglia infiltration under conditions of neurological injury (Wright et al., 2000). Additionally, CD45 is expressed by microglia in low levels under homeostatic conditions. However, when there is enhanced expression of its neuronal ligand, CD22 as seen in the response to neuronal damage, microglial activity is inhibited (Tan et al., 2000). Recently, it was shown that inhibiting neuronal CD22 using antibodies improved the microglial phagocytosis of protein aggregates in animal models (Pluvinage et al., 2019).

Purinergic signalling between neurons and microglia is another important bridge of communication between the two cell types (Agostinho et al., 2020). Microglia express a plethora of purinergic receptors, such as *ADORA3*, *P2RX7*,

P2RY12, *P2RY13* and *NT5E*. Neurons and microglia reside near one another, which is highly important for the synaptic maintenance and the purinergic interactions rely heavily on the ATP/adenosine release, ectonucleotidase release and receptor stimulation. *P2RY12* is exclusively expressed by microglia (Haynes et al., 2006) and is possibly the most studied microglial purinergic receptor.

In addition to the role of CX3CL1-CX3CR1 in synaptic plasticity, this interaction also mediates microglia neurotoxicity (Biber et al., 2007). *In vitro* studies revealed that exposure of neuron-microglia co-cultures to CX3CL1 (fractalkine) ameliorate microglia-meditated neurotoxicity (Zujovic et al., 2000, Mizuno et al., 2003). *In vivo*, absence of CX3CR1 in mice led to enhanced microglial pro-inflammatory activation and increased neuronal death (Cardona et al., 2006).

Microglia are the professional phagocytotic cells of the CNS and through their signalling interactions with neurons and other cell types, such as astrocytes, they are maintained in homeostatic conditions to minimise exacerbated inflammatory activities whereas excessive activation contributes to neurodegeneration. Therefore, signals that mediate the microglia-neuronal crosstalk may be potential therapeutic targets.

1.3.3 Microglia phenotypes

1.3.3.1 Microglia and brain region heterogeneity

Microglia population numbers are estimated to range between 5 and 20% across the brain (Lawson et al., 1990). Studies in mice have revealed that microglia populate all brain regions, but their distribution is unequal across regions. It was also observed that among the most heavily microglial-populated areas are the hippocampus, the olfactory telencephalon and the SNc, as well as the basal ganglia with some studies even reporting higher numbers in the SNc compared to the hippocampus and cortex (Kim et al., 2000) These findings were also confirmed in healthy human brain tissues (Mittelbronn et al., 2001). Other murine studies reported that the number of microglia in the SNc and striatum dramatically decrease with ageing (Sharaf et al., 2013). Additionally, general microglia features have been reported to differ within the basal ganglia nuclei compared to other areas (De Biase et al., 2017). Specifically, following pharmacological ablation of microglia by CSF1R specific antagonist, PLEX5622 it was shown that they can re-populate and re-establish their regional heterogeneity. This suggests that microglia establish their regional heterogeneity depending on local cues specific to different brain regions.

The concept of microglial regional heterogeneity is multidimensional, and it involves aspects, such as temporospatial variations, gender-specific distributions, colonisation, morphological plasticity with gene expression heterogeneity being the most studied one (Tan et al., 2020). One of the first studies that revealed the phenotypic regional heterogeneity of microglia was performed in the Biber laboratory (de Haas et al., 2008). The authors investigated an array of microglial markers across brain regions. For example, they reported lower numbers of CD45 positive microglia

within the hippocampus. A more recent study reported that microglia in the SNc express significantly higher levels of TNFα compared to other brain regions (Doorn et al., 2015). More recently, the regional heterogeneity of microglia was also confirmed by a large comprehensive genetic and transcriptomic study performed on human isolated microglia from healthy individuals, as well as samples from Parkinson's and Alzheimer's disease post-mortem samples (Lopes et al., 2022). The study confirmed downregulation of microglial genes in ageing brain samples particularly of purinergic receptor *P2RY12*, a major component in neuronal-microglial interactions (Badimon et al., 2020). Additionally, the authors suggested a possible implication of *P2RY12* in Parkinson's disease as it was significantly downregulated across samples (Lopes et al., 2022). Microglia subpopulations have also been confirmed in samples isolated from live patients' tissues and they have also been compared to genetic loci, such as *BIN1* correlated with high risk of Alzheimer's disease (Young et al., 2021).

1.3.3.2 Unique microglia subpopulations associated with neurodegeneration

Once microglia have infiltrated the brain during development, they sustain their population pool throughout life with local clonal expansion and self-renewal (Tay et al., 2017). They also have an extremely versatile range of phenotypes both in a healthy and diseased brain microenvironment. Before the introduction of advanced technologies, such as RNA-sequencing, quantitative proteomics and epigenetic studies, microglia phenotypes were categorised based on their surface receptors profiles and secreted cytokines into “M1, classically activated’’ or “M2, alternatively activated’’, a concept that was firstly introduced to describe activated macrophages (Mackaness, 1962). The original observation was further expanded by the ability of macrophages to differentially respond to widely used inflammatory stimuli, such as bacterial lipopolysaccharides (LPS) or interferon-γ (IFN-γ) by following distinct metabolic pathways (Mills et al., 2000). The two stimuli were categorised into two phenotypic polarising states, M1 (IFN-γ combined with LPS or TNF-α) and M2 (IL-4, IL-10 and GC) (Mantovani et al., 2004). According to this phenotypic classification, M1 macrophages and microglia release proinflammatory mediators that result in neurotoxicity, whereas M2 activated macrophages and microglia release neurotrophic factors and clear pathogenic stimuli and debris through phagocytosis (Figure 1.7a) (Mosser and Edwards, 2008, David and Kroner, 2011).

In the current era of genomics and single cell transcriptomics, the M1/M2 phenotypic dichotomy is outdated. It is now widely accepted that microglia exist in highly dynamic states *in vivo*. To begin with, the M1/M2 was conceived on isolated cells (Ransohoff, 2016). Further, the stimuli that invoke the M1/M2 states do not exist in isolation *in vivo*. Additionally, there is no evidence to support any clonal

propagation of microglia *in vivo* maintaining these two phenotypes. Finally, the concept of M1/M2 polarisation was conceived using bone marrow-derived macrophages and as mentioned earlier, brain resident microglia originate from yolk-sac progenitors.

The novel applications of single cell RNA sequencing have led to a better understanding of the regional brain heterogeneity of microglia (Zeisel et al., 2015, Matcovitch-Natan et al., 2016, Tasic et al., 2016). Transcriptomic studies on the single-cell level have identified unique subpopulations of microglia in the context of neurodegeneration termed as disease-associated microglia (DAM), which bear the potential to restrict neurodegeneration (Figure 1.7 b) (Keren-Shaul et al., 2017). It was also suggested that DAM is a universal phenotype in neurodegeneration with shared molecular patterns and pathways (Deczkowska et al., 2018). The transcriptomic studies also revealed that the transition from homeostatic microglia to DAM is regulated by a two-step mechanism with the second step being dependent on the microglia specific triggering expressed myeloid receptor 2 (TREM2). DAM were first identified with single cell RNA sequencing on an Alzheimer's disease mouse model and were correlated with neuroprotective effects against Aβ pathology. Ever since, it has become apparent that as the disease progress microglia-specific genes correlated with phagocytosis and lipid metabolism exhibit increased expression leading to a detrimental switch of microglia phenotypes from beneficial to detrimental.

Collectively, brain region heterogeneity and disease-specific subpopulations of microglia should be taken into consideration when investigating their role in neurodegeneration in general, and Parkinson's disease in particular.

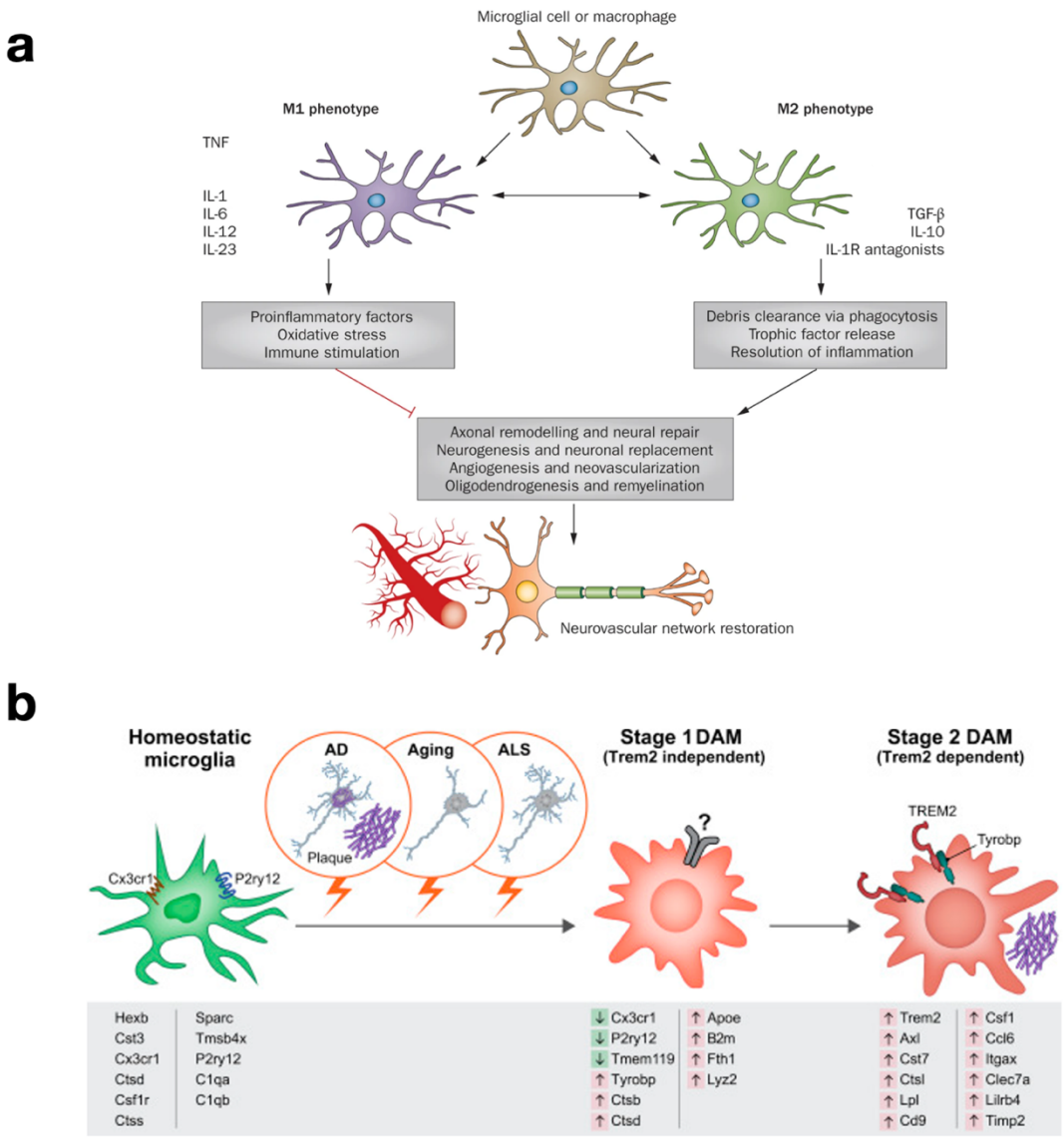

Figure 1.7 Microglia phenotypes.

a. Suggestively, the M1/M2 phenotypes are acquired by microglia and macrophages following pathogenic stimuli or injury within the CNS. The signature proteins of the M1 phenotype are typically TNF, and interleukins 1, 6, 22 and 23 (IL-6, IL-1, IL-22 and IL-23). The aim of these pro-inflammatory markers, as well as free radicals is to impair brain repair. On the contrary, the signature proteins of the M2 phenotype are among others IL-10 and TGF-β that promote neuronal regeneration. Image adapted from (Hu et al., 2015). **b.** Homeostatic microglia express an array of genes as identified by RNA sequencing, which are downregulated in neurodegeneration. Activated microglia transitions to a DAM phenotype via a two-step mechanism with the second stage being TREM2-dependent. The homeostatic gene downregulation is accompanied by upregulation of an array of DAM-related genes. Image adapted from (Keren-Shaul et al., 2017).

1.3.4 Human and murine microglia

Animal studies using wild type and transgenic rodent models have benefited the field of neurodegeneration particularly in investigating molecular mechanisms of proteotoxicity. However, recent advances in sequencing techniques have revealed that the animal models cannot faithfully recapitulate the wide genetic variability and polymorphisms of the neurological polygenic disorders (Dawson et al., 2018, Friedman et al., 2018b, Ueda et al., 2016). One possibility of addressing this challenge is the development of chimeric models where human microglia is transplanted in mice brains (Hasselmann et al., 2019, Fattorelli et al., 2021). Additionally, recent advances in the field of stem cell technology have enabled the development of protocols that mimic the developmental ontogeny of human microglia (Muffat et al., 2016, Haenseler et al., 2017a, Abud et al., 2017). Therefore, research on the relationship between microglia and neurodegeneration is only at its infancy.

Comparative analyses between human and mouse microglial transcriptomes have revealed an extensive overlap between the two species, particularly in core microglial signatures (Gosselin et al., 2017b). However, there are numerous genetic signatures that follow differential expression patterns in ageing between the two species (Galatro et al., 2017a). Interestingly, a large-scale analysis across species from the Prinz laboratory revealed a high conservational homology of microglia in mammals (Geirsdottir et al., 2019). However, in humans microglia exhibited more subtypes across individuals, with some subtypes being similar across individuals.

1.3.5 Modelling microglia phenotypes with induced pluripotent stem cells

The advances in induced pluripotent stem cell (iPSC) methodologies have been used to generate human macrophages and microglia, which can recapitulate an adult phenotype that can be validated with various assays and markers (Figure 1.8) (Pocock and Piers, 2018). This is extremely helpful to model rare genetic mutations linked to neurodegenerative diseases, such as the *SNCA* triplication and variants of *TREM2*. Currently, most of the protocols for microglia generation mimic their developmental ontogeny by including factors that induce mesodermal specification (Haenseler et al., 2017a). The differentiation of microglial cells from blood monocytes has been under scrutiny since it became evident that microglia originate from erythromyeloid precursors of the yolk-sac. It has been shown that microglia-like cells can be generated by combining factors, such as macrophage colony stimulating factor-1 (m-CSF1) and interleukin-34 (IL-34) (Muffat et al., 2016), IL-34 and granulocyte-macrophage colony stimulating factor (GM-CSF) (Douvaras et al., 2017), IL-3, IL-34 and GM-CSF (Pandya et al., 2017), IL-34, TGF-β1, CX3CL1 and CD200 (Abud et al., 2017). Although the generated cells express key microglia markers and perform microglia-related functions, such as phagocytosis, it is widely accepted that co-culture with neurons is required for full phenotypic maturation (Haenseler et al., 2017a, Muffat et al., 2016, Takata et al., 2017). Co-cultured microglia require IL-34, an alternative ligand to CSF1R and low levels of GM-CSF that promote survival through the interactions with neurons. Although, a good model for studying human microglial-neuronal interactions, these co-cultures lack the cellular complexity of the living brain. This may be bypassed by the transplantation of human iPSC-derived microglia into mouse models of disease (Chen et al., 2010, Biju et al., 2013).

Another issue that remains unresolved is how the newly generated iPSC-derived microglia compare to the microglial phenotypes in the ageing brain. One study used RNA sequencing to compare iPSC-derived microglia with human foetal and adult microglia and demonstrated significant differences (Abud et al., 2017).

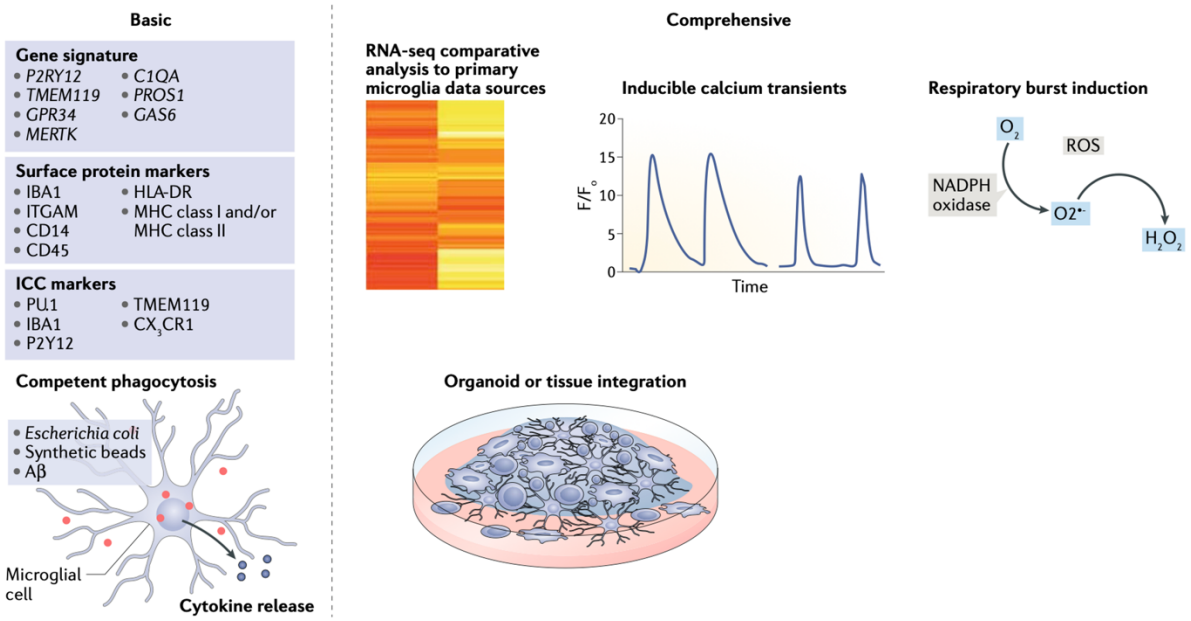

Figure 1.8 Basic and comprehensive phenotypic characterisation of human iPSC-derived microglia.

The protocols for generation of iPSC-derived microglia use an array of assays to assess and demonstrate the dynamic range of microglia phenotypes. Basic characterisation includes microglial-specific gene expression, as well as surface protein markers. Additionally, microglia are assessed for key functions, such as phagocytosis by exposure to bacteria stimuli, synthetic beads or misfolded proteins (Aβ peptide for example) and release of cytokines. More comprehensive analyses include RNA sequencing, particularly for comparison with *in vivo* microglia, evaluating their ability to produce calcium transients and respiratory bursts. Additionally, co-culturing of microglia with organoids, or transplantation in animals may be required for their full maturation. Image adapted from (Pocock and Piers, 2018).

1.3.6 Aims and objectives

The study of microglia in Parkinson's disease has so far focused on reductionist models that mainly model human microglia-like monocultures, chimeric neuronal and microglial co-cultures and primary murine microglia. The absence of human disease-relevant co-cultures between microglia and dopaminergic neurons is a limiting factor in delineating the role of α-synuclein proteotoxicity in neuron-microglial interactions. Therefore, the aim of my doctoral studies was to develop human *ex vivo* and iPSC-derived *in vitro* models to investigate the relationship between pathological α-synuclein aggregation and microglia activation with a view to identify potential targets for therapeutic approaches.

My hypothesis was that microglia exhibit activated phenotypes around α-synuclein aggregated neurons. These phenotypes involve morphological activation, as well as transcriptomic signatures related to the disease associated subpopulations as identified by the literature.

The objectives of this dissertation were to:

1. Generate *ex vivo* slices to investigate microglia activation following endogenous α-synuclein aggregation.
2. Develop a human iPSC-derived co-culture of microglia and dopaminergic neurons to assess the microglial response to neuronal seeded aggregation.
3. Define the transcriptomic signature and determine the potential function of disease-relevant genes in microglia exposed to neurons with aggregates.

Chapter 2: Materials and Methods

2.1 Cell Culture

2.1.1 Stem cell culture

Thawing and plating

6-well plates were pre-coated with 1 mL of Geltrex (Life Technologies) in basal medium [Knockout (KO)-DMEM)] (Life Technologies) at 37°C in a humidified atmosphere containing 5% CO_2. Stem cells were thawed by immersing the cryovials in 37°C water, followed by centrifugation in pre-warmed Dulbecco's phosphate-buffered saline (DPBS) (Life Technologies) for 5 mins at 400 x g. Cells were re-suspended in 2 mL mTeSR1 (StemCell Technologies) supplemented with 10 μM apoptotic ROCK inhibitor (Y27632) (Bio-Techne), plated in two densities (30 and 70%) at the pre-coated plate and incubated at 37°C and 5% CO_2. The medium was changed daily. For passaging, TryplE (Life Technologies) was pre-warmed and added at 1mL on the cells for at least 5 mins at at 37°C in a humidified atmosphere containing 5% CO_2. Cells were transferred in pre-warmed DPBS, centrifuged for 5 mins at 400 x g and plated in Geltrex pre-coated 6-well plates at a $5x10^5$ cells/well density optimised for differentiation.

Cryopreservation

Induced Pluripotent Stem Cell (iPSC) stocks were cryopreserved in 2x freeze medium, composed of 60% ES-qualified fetal bovine serum (FBS) (Life Technologies), 20% KO-DMEM, 20% DMSO (Sigma). Cells were dissociated using TryplE, as described above, centrifuged at 500 x g for 4 mins and re-suspended in

mTeSR1. Equal volume of the 2x freeze medium was added and the cell suspension was aliquoted in 1 mL in cryovial tubes (Nunc, Thermo Scientific) before storage in a pre-refrigerated freezing container (Mr. Frosty, Nalgene) at -80 °C. After 24 h, the cryovials were moved to liquid nitrogen storage. Each cryovial contained $1x10^6$ cells/mL.

2.1.2 Differentiation of human iPSCs into midbrain dopaminergic neurons

Using a floor plate-based strategy first described by (Kriks et al., 2011) iPSC-derived stem cells were differentiated into mid brain dopaminergic precursors (Tanudjojo et al., 2021). All stem cell lines used in this study have been previously characterised (Haenseler et al., 2017a, Dafinca et al., 2016, Fernandes et al., 2016, Sandor et al., 2017, Lang et al., 2019) and are summarised in Table 2.1. Reprogramming of the patient cells to iPSCs was performed by Dr. Sally Cowley (Dunn School of Pathology, University of Oxford).

ID	Diagnosis	Genotype	Sex	Biopsy age (years)	Original ID	Re-programming method	Source	Passage no	Publication
HC-1	HC	WT/WT	F	78	SFC856-03-04	Cytotune II	StemBancII	P22	(Haenseler et al., 2017a)
HC-2	HC	WT/WT	M	49	OX3-6	Sendai Virus	StemBancII	P27	(Dafinca et al., 2016)
HC-3	HC	WT/WT	M	67	SFC840-03-03	Cytotune II	StemBancII	P17	(Fernandes et al., 2016)
SNCA^{TRIP}-3	PD	SNCA triplication	F	55	SFC831-03-03	Cytotune II	StemBancII	P19	(Haenseler et al., 2017c)
LRRK2-1	PD	LRRK2 (G2019S)	F	57	MK144	Retroviruses	StemBancII	P12	(Sandor et al., 2017)
LRRK2-2	PD	LRRK2 (G2019S)	M	57	SFC855-03-01	Cytotune II	StemBancII	P15	(Sandor et al., 2017)
GBA-1	PD	GBA (N370S)	M	72	SFC834-03-01	Cytotune II	StemBancII	P11	(Lang et al., 2019)
GBA-2	PD	GBA (N370S)	M	72	SFC834-03-03	Cytotune II	StemBancII	P11	(Lang et al., 2019)
TREM2-ISO	HC	WT/WT	M	19	BIONi010-C	Cytotune II	Bioneer	P6	(Rasmussen et al., 2014)
TREM2-KO	HC	TREM2^{-}/TREM2^{-}	M	19	BIONi010-C-17	Cytotune II	Bioneer	P6	(Rasmussen et al., 2014)

Table 2.1 List of stem cell lines used in the present study

Each line and their clones were diifferentiated at least three times.

The protocol used does not require any differentiation passages and therefore, the differentiated cells received daily media changes supplemented with an array of small molecules (detailed schematic diagram included in results Chapter 4, Figure 4.5). On day 0, when cells acquired a >90% confluency and a characteristic tadpole-like morphology they were exposed to dual SMAD inhibitors, 2 μM A83-01 (Biotechne) and 100 nM LDN (Sigma). These were added in KSR media, which involves KO-DMEM supplemented with 15% knockout serum replacement (KSR), 2 mM L-glutamine (Gibco), non-essential amino-acids (Gibco) and 10 μM β-mercaptoethanol (Gibco). Cells received KSR media with 2 μM A83-01, 100 nM LDN, 300 ng/mL sonic hedgehog (SHH) (Biotechne), 2 μM purmorphamine, 200 ng/mL fibroblast growth factor 8a (FGF-8a) from day 1-4 when floor-plate induction occurred. Then, on day 5 there was a gradual shift to Neurobasal medium (NB) without phenol red (Life Technologies) enriched with N2 supplement (Life Technologies) [N (N2) B] and B-27 without vitamin A (Life technologies) until day 10, because this is the time point when the cells transition to a neuronal fate (Kriks et al., 2011). Day 7-10 media contained 100 nM LDN and 3 μM CHIR-99021 (Biotechne). From day 10 onwards generation of mid brain dopaminergic neurons commences (Kriks et al., 2011) and the media used is NB enriched with B27 and Gluta-Max (Life Technologies) (NBE+). NBE+ media contains 20 ng/mL brain derived neurotrophic factor (BDNF) (Peprotech), 20 ng/mL growth derived neurotrophic factor (GDNF) (Peprotech), 1 ng/mL transforming growth factor beta 3 (TGFβ3), 10 μM DAPT (Biotechne), 200 μM ascorbic acid (AA) (Sigma), 500 μM dibutyryl cyclic adenosine monophosphate (db-cAMP, Sigma). On days 17-25 1 μg/mL laminin (Sigma) was

added in the media. By day 25 mid brain dopaminergic neurons (DNs) have occurred with apparent axonal projections forming within the neuronal monolayer and are re-plated in different plate formats, pre-coated with 1% Geltrex such as 12-, 24- and 96-well plates. For the 24-well plates coverslips were additionally pre-coated with 0.1% poly-L-ornithine. Mature DNs were maintained until day 73 in culture with weekly medium changes with NBE+ supplemented with previously mentioned growth factors.

2.1.3 Differentiation of human iPSCs into macrophage/microglia precursors via Embryoid Body formation using AggreWells

Human microglia-specific cells were generated from iPSC following a previously published and characterised protocol (Haenseler et al., 2017a, Karlsson et al., 2008, van Wilgenburg et al., 2013). A 6-well plate was pre-coated with 1 mL of Geltrex added into basal medium Advanced DMEM/F12 (Gibco) for 30 mins at 37°C, 5% CO_2. Stem cells from healthy control (HC), LRRK2 (G2019S) and GBA (N370S) donors were thawed. Subsequently, cells were centrifuged in sterile DPBS (Sigma) for 5 mins at 400 x g. Cells were resuspended in mTeSR1, supplemented, 10 μM Y27632 and added to the pre-coated 6-well plate and incubated at 37°C and 5% CO_2.

Stem cell medium was changed daily, and cells were passaged once. Cells were washed once with sterile DPBS and incubated with 0.5 mL of pre-warmed TryplE (Life Technologies) for 5 mins at 37°C and 5% CO_2. Then cells were centrifuged in sterile DPBS for 5 mins at 400 x g and plated at two different densities, 1:8 and 1:12 for each line.

When cells reached >90% confluency, AggreWell800 plate (StemCell Technologies) was prepared by addition of 0.5 mL AggreWell rinsing solution (StemCell Technologies) and was centrifuged for 5 mins at 3,000 x g in order to remove air-bubbles from the microwells. Rinsing solution was carefully removed, washed with sterile DPBS and 1 mL of 2x Embryoid Body (EB) medium was added to each well. Cells were washed once with sterile DPBS and were incubated with 0.5 mL of pre-warmed TryplE for 5 mins at 37°C and 5% CO_2. Then cells were centrifuged in sterile DPBS for 5 mins at 400 x g and resuspended in 1x EB medium

supplemented with 10 µM of Y27632 (Table 2.2). Cells were counted and diluted using 1x EB medium to a final density of $4x10^6$ cells/mL. Subsequently, 1mL of the cell suspension containing $4x10^6$ cells was added to each AggreWell and the plate was centrifuged for 3 mins at 100 x g to ensure cells were distributed evenly across the microwells. The differentiating cells received a 75% medium change daily with 1x EB medium until day 4.

Component	Stock	Dilution	Final
mTeSR1			
VEGF	10 µg/mL	1:200	50 ng/mL
BMP4	10 µg/mL	1:200	50 ng/mL
SCF	10 µg/mL	1:500	20 ng/mL

Table 2.2 List of components for the Embryoid bodies (EB) medium (1X)

On day 4, T175 flasks containing of 15 mL factory medium (factory flasks) were prepared (Table 2.3). The EBs from each AggreWell were split across two T175 flasks. The EB medium was slowly aspirated and the EBs were carefully removed from the microwells with 2 mL of factory medium using a 5 mL serological stripette. This process was repeated twice until all EBs were removed from the microwells and the factory flasks were incubated 37°C and 5% CO_2. Factory medium was added weekly (10-15 mL) and macrophage/microglia precursors (pMacpre) started emerging in the supernatant approximately at day 14 -28. Cells were harvested and cultured for up to 2 weeks in microglia monocultures (pMGL) or in co-cultures with DNs (co-pMGL).

Component	Stock	Volume (mL)	Final
X-vivo 15		500	
Gluta-Max	100X	5	1X
IL-3	50 µg/mL	0.25	25 ng/mL
M-CSF	100 µg/mL	0.5	100 ng/mL
β-mercaptoethanol	1000X	0.5	1X

Table 2.3. List of components for the Factory Medium

2.1.4 Co-cultures of human iPSC-derived midbrain dopaminergic neurons and microglia (co-pMGL)

On day 45 of neuronal maturation, dopaminergic neurons were seeded with exogenous α-synuclein fibrils. On day 59 pMacpre were harvested from factories. Cell suspension was collected in 50ml Falcon tubes after having been filtered with 0.45 μm mesh filter system (Falcon). The cell suspension was centrifuged for 5 mins at 200 x g and re-suspended in Advanced DMEM/F12 microglia co-culture medium (Table 2.4). Cells were counted using Countess Automated Cell Counter (Invitrogen). In parallel, neuronal NBE+ medium was aspirated and the harvested pMacpre were added at a 1:1 ratio. Co-culture media was changed weekly until Day 73 when experiments were concluded.

Component	Stock	Volume (mL) per 100 mL	Final
Advanced DMEM/F12		96.4	1X
N2 Supplement	100X	1	1X
Gluta-Max	100X	1	1X
β-mercaptoethanol	1000X	0.5	1X
IL-34	100 μg/mL	0.1	100 ng/mL
Pen/Strep	100X	1	50U/mL

Table 2.4 List of components for microglia co-culture and monoculture medium

2.1.5 Microglia-like monocultures (pMGL)

pMacpre were harvested in factory medium as per the afore-mentioned method, centrifuged for 5 mins at 200 x g and re-suspended in Advanced DMEM/F12 microglia medium. Cells were counted using the Countess Automated Cell Counter and cultured in respective densities in cell culture plates pre-coated with 1 mL Geltrex. Medium was changed every 3-4 days for 2 weeks until cells obtained a pMGs like morphology.

2.1.6 Addition of *de novo* α-synuclein fibrils in iPSC-derived dopaminergic neurons and microglia

Generation of fibrils is described in section 2.3. Dopaminergic neurons were ''seeded'' with the exogenous α-synuclein fibrils on DIV45. The fibrils were sonicated for 1 min at 1s on/1s off and 30% amplitude and were added at a final 1μM concentration in NBE differentiation medium on the neurons following a full media change.

Similar methodology was followed for addition of the α-synuclein fibrils in microglia monocultures. On DIV7 of culture, medium was removed and replaced with medium supplemented with the fibrils.

2.1.7 Measurement of Cell Viability using lactate dehydrogenase (LDH) assay

Cell toxicity was measured with the Pierce LDH Cytotoxicity kit (ThermoFisher Scientific) according to the manufacturer's protocol. Briefly, conditioned media was collected from organotypic slices or from cell cultures and was centrifuged for 10 mins, at 4 °C and at 12,000 x g to discard cellular debris. Following, 50 µL of media was added in each well of a 96-well plate (Corning) and was incubated with 50 µL of reaction mix for 30 mins at RT. Incubation was terminated by addition of 50 µL of stop solution provided by the kit and the absorbance was read at two wavelengths, 490 and 680 nm using a CLARIOstar Plus (BMG Labtech, Ortenberg, Germany). A positive control was always included, and the background values were subtracted from the experimental values. The % cytotoxicity was calculated by the following formula:

$$\%Cytotoxicity = \frac{\text{Compound treated LDH activity} - \text{Spotaneous LDH activity}}{\text{Maximum LDH activity} - \text{Spotaneous LDH activity}}\ x100$$

2.2 Organotypic Slice Cultures

2.2.1 *Ex vivo* mice hippocampal slices

Organotypic brain hippocampal slices (OHS) were generated as previously described (Stoppini et al., 1991, McCarthy et al., 2021). Brains from transgenic A53T (TgA53T) mice pups (P5-P8) were dissected under sterile conditions and slices of 330 µm thickness were obtained using the Leica VT1200s Vibratome. Slices were dissected in ice cold dissection buffer consisted of Grey's Balanced Salt Solution (GBSS-Sigma), D-Glucose (Sigma), Kynurenic Acid (Sigma) and pH was adjusted to 7.1. Buffer was constantly perfused with 5% CO_2 and 95% O_2. Slices were cultured in organotypic slice culture media consisting of MEM (Gibco), horse serum heat inactivated (Gibco), HBSS (Gibco), Gluta-Max (Gibco), Pen/Strep, Fungizone, ddH_2O and-glucose with final pH=6.8-6.9 (Table 2.5) (McCarthy et al., 2021) via the interface method up in membranous 0.4 µm porous inserts (Millicell, Millipore) to 3 weeks. Culture media was fully replaced 3 times per week.

Addition of recombinant α-synuclein fibrils was carried out on DIV7 in a single treatment directly in the culture medium.

Component	Stock	Volume (mL) per 200 mL	Final
MEM	1X	100	1X
Horse serum (HI)	1X	50	1X
HBSS (-Ca, -Mg)	10X	2	1X
HEPES	1M	2	0.5M
Gluta-Max	100X	1	1X
L-Glutamine	100X	2	1X
Pen/Strep	100X	2	1X
Fungizone	250 µg/mL	2	12.5 µg/mL
ddH_2O		38	
D-glucose		1.3 g	

Table 2.5 List of components for mice organotypic hippocampal slices medium

2.2.2 *Ex vivo* live human cortical slices

Human neocortical brain slices were prepared from access tissue (cortical tissue outside the epileptic focus or glioma pathology, resected in order to gain access to the pathology) from patients undergoing surgery for epilepsy or brain tumour.

Approval from the ethics committee as well as written informed consent was obtained from all patients allowing the extra tissue from the surgery to be used in this study, as well as acute electrophysiological experiments from our collaborators' group in the Department of Pharmacology (Professor Somogyi). Tissue preparation was performed according to previously published protocols (Schwarz et al., 2019, Verhoog et al., 2013). Tissue integrity was carefully ensured, and it was transferred in ice-cold artificial cerebrospinal fluid (aCSF) (in mM: 110 choline chloride, 26 $NaHCO_3$, 10 D-glucose, 11.6 Na-ascorbate, 7 $MgCl_2$, 3.1 Na-pyruvate, 2.5 KCl, 1.25 NaH_2PO_4, and 0.5 $CaCl_2$) equilibrated with carbogen (95% O_2, 5% CO_2). The pia matter was carefully removed, the tissue chunk was trimmed perpendicular to the cortical surface and slices of 300 µm were obtained using Leica VT1200s Vibratome. Tissue and slices were constantly submerged in aCSF. Subsequently, slices were left to recover and were transferred on 0.4 µm porous membrane inserts (Millipore). Both human CSF and OHS slice medium were used for culture optimisation purposes. Slices were cultured in 5%CO_2, 37°C and 100% humidity for up to 3 weeks. Culture medium was fully replaced every two days.

2.3 Generation of α-synuclein fibrils

De novo generated α-synuclein was produced following the protocol developed at the Eli Lilly laboratories (UK) based on the protocols published by the Melki laboratory (Bousset et al., 2013a).

α-synuclein purification and assembly in fibrillar forms

Recombinant wild-type human α-synuclein was expressed in E. coli BL21 DE3 CodonPlus cells (Stratagene) and was purified by high performance liquid chromatography (HPLC) (Biorad) following published protocols (Tanudjojo et al., 2021, Ghee et al., 2005). The monomeric protein was firstly dialysed in exchange high-salt buffer (KCL) to remove any undesirable small contaminants, such as other proteins or salt molecules (Campos et al., 2019). Following, the monomeric protein was assembled into insoluble, higher molecular weight fibrillar polymorphs termed as ''fibrils'' (Bousset et al., 2013a) for 14 days in high-salt buffer (KCL). The structure of the fibrils was assessed with transmission electron microscopy (TEM) after adsorption of the fibrils onto carbon-coated 200 mesh grids and negative staining with 1% uranyl acetate, as previously described (Tanudjojo et al., 2021). The resulting α-synuclein fibrillar polymorphs were fragmented by sonication for 20 mins in 2 mL Eppendorf tubes in a Vial Tweeter powered by an ultrasonic processor UIS250v (250 W, 2.4 kHz; Hielscher Ultrasonic, Teltow, Germany) to generate fibrillar particles that are suitable for endocytosis, with an average size of 60-100 nm, as assessed by the TEM analysis. Their proteinase K proteolytic patterns were assessed by SDS-PAGE analysis after staining with Coomassie blue. To this end, *de novo* generated α-synuclein fibrillar polymorphs (1.4 mg/mL) in 150 mM KCl (Sigma), 50mM Tris-HCl (Sigma), pH 7.5 were treated at 37 °C by Proteinase K (3.8 µg/ml) (Roche). Aliquots

were removed at different time intervals following addition of the protease and transferred into Eppendorf tubes maintained at 90 °C containing sample buffer (50mM Tris-HCl, pH 6.8, 4% SDS (Sigma), 2% β-mercaptoethanol (Gibco), 12% glycerol (Sigma) and 0.01% bromophenol blue (Sigma) to immediately arrest cleavage. The tubes were incubated for 5 mins at 90 °C prior to SDS-PAGE (15%) analysis.

2.4 Molecular biology techniques

2.4.1 qRT-PCR

Total RNA was extracted from 12-well plate cell cultures using the RNeasy plus Mini Kit (Qiagen). Cultures were washed once with DPBS and lysed by addition of 350 µL RLT buffer (Qiagen) supplemented with 1% β-mercaptoethanol (Life Technologies). The RNA samples were purified for genomic DNA following the kit's instructions (Qiagen) and the quality of the samples was assessed by using a spectrophotometer (Nano-Drop 2000c). Sequentially, RNA was reversed transcribed into cDNA using the Omniscript RT kit (Qiagen) following the manufacturer's protocol. Quantitative real time PCR (qRT-PCR) was performed using the LightCycler 480 SYBR Green I Master Kit (Roche) in a 384-well PCR plate. In detail, 1 µL of cDNA was added in a final volume of 10 µl per reaction (5 ng of cDNA and 1 µM of both forward and reverse primers). The primers used in the present study are listed on Table 2.6 and they were designed using the Real-time PCR Primer and Probes Design Tool (GenScript). The GenBank accession number for the genes of interest were first acquired from Ensembl genome browser (species: human). The accession numbers were entered into the afore-mentioned Design Tool (GenScript) and only primers crossing exon junctions were selected with the following parameters: PCR amplicon size range, 50-200; primer melting point minimum, 52 °C, maximum, 56 °C, maximum, 60 °C. The samples were run in triplicate technical wells and the ΔΔCt values were calculated using the average Ct for each triplicate: ΔCt was generated by subtraction of the average Ct for reference housekeeping gene *GAPDH*, and then was normalised to the average ΔCt control samples.

Gene	Forward primer sequence (5' to 3')	Reverse primer sequence (3' to 5')
CSF1R	GGGAATCCCAGTGATAGAGCC	TTGGAAGGTAGCGTTGTTGGT
CX3CR1	AGTGTCACCGACATTTACCTCC	AAGGCGGTAGTGAATTTGCAC
TYROBP	ACTGAGACCGAGTCGCCTTAT	ATACGGCCTCTGTGTGTTGAG
APOE	GTTGCTGGTCACATTCCTGG	GCAGGTAATCCCAAAAGCGAC
LPL	AGGATGTGGCCCGGTTTATC	CCAAGGCTGTATCCCAAGAGAT
AXL	ATCAGCTTCGGCTAGGCAG	TCCGCGTAGCACTAATGTTCT
P2YR12	AAGAGCACTCAAGACTTTAC	GGGTTTGAATGTATCCAGTAAG
TMEM119	AGTCCTGTACGCCAAGGAAC	GCAGCAACAGAAGGATGAGG
TREM2	TCTGAGAGCTTCGAGGATGC	GGGGATTTCTCCTTCAAGA
MERTK	AGGACTTCCTCACTTTACTAAG	TGAACCCAGAAAATGTTGAC
GPR34	GAAGACAATGAGAAGTCATACC	TGTTGCTGAGAAGTTTTGTG
PROS1	AAAGATGTGGATGAATGCTC	TCACATTCAAAATCTCCTGG
C1QA	GTGACACATGCTCTAAGAAG	GACTCTTAAGCACTGGATTG
GAS6	CGAAGAAACTCAAGAAGCAG	AGACCTTGATCTCCATTAGG
GAPDH	TGGAAGGACTCATGACCACAG	CAGTGGGGACACGGAAGG

Table 2.6 List of primers used in the present study

2.4.2 Transcriptome analysis

The RNA sequencing was performed by the Wellcome Centre for Human Genetics (Oxford, UK) with Dr. Simon Engeldow. The transcriptomic analyses were performed by our collaborators, Dr. Devika Agarwal and Dr. David Sims.

2.4.2.1 Bulk RNA sequencing

Bulk RNA-Seq was performed to assess the neuronal and microglial responses to aggregation induced by 1 μM *de novo* α-synuclein fibrils in $SNCA^{TRIP}$ iPSC-derived neurons co-cultured with two different lines of HC iPSC-derived microglia (n=12). RNA samples were prepared using standard poly-A enrichment, 250-300 bp insert cDNA library which was prepared with the NEB Next® UltraTM RNA Library Prep Kit and sequenced on Illumina NovaSeq 6000 (S4) using 150 bp paired-end reads. Sequencing resulted in approximately 40 million reads per sample.

2.4.2.2 Human substantia nigra transcriptomic cell-type atlas

Filtered substantia nigra single nuclei count data with cell type annotations for 7 post-mortem individuals was downloaded from the Broad Institute Single Cell Portal [https://singlecell.broadinstitute.org/single_cell]. The count matrices for all individuals were merged to result in 40,453 SN single nuclei with 24 cell types encompassing all known resident cell classes as identified previously in the literature (Welch et al., 2019). For the purpose of cell type deconvolution analysis in this study, these cell types were merged into eight major subtypes: astrocytes, dopaminergic neurons, endothelial, excitatory and inhibitory neurons, microglia, oligodendrocytes and oligodendrocyte progenitor cells.

2.4.2.3 Cell-type deconvolution of bulk RNA sequencing samples

The cell-type composition of the bulk RNA-Seq samples was characterized using the MuSiC method (Wang et al., 2019), a cross-subject technique that utilises only the consistently expressed genes across multiple cells by up-weighting genes with low cross-subject variance (informative genes) and down-weighing genes with high cross- subject variance (non-informative genes). Furthermore, we accounted for a potential bias based on differing cell type numbers across the cell types in the reference single cell atlas by randomly down sampling the eight major resident cell types to the same number (n=50) 100 times and then estimating the cell type composition of the bulk samples and averaging the proportions across the bootstraps to obtain the final cell- type estimates.

2.4.2.4 Analysis of Bulk RNA sequencing data

Kallisto (v0.46.2) (Bray et al., 2016) was used to estimate abundance for Ensembl (release 102) protein-coding genes from RNA-Seq reads. Count data was imported into R (v4.1.0) using Tximport (v1.20.0) and genes with less than 10 reads across the 6 samples used in the comparison were filtered out. Differential gene expression was performed in DESeq2 (v1.32.0) (Love et al., 2014) using the Wald test with an FDR threshold of 0.05 and a log2 fold-change threshold of 0.25. Gene Set Enrichment Analysis (GSEA) was performed using the Fgsea package (v1.18.0) (Sergushichev, 2016) in R (v4.1.0) with KEGG pathways. Genes were ranked for GSEA using the Wald statistic and Fgsea (v.1.18.0) was run with 1000 permutations. Principal Component Analysis and all plotting was performed in R (v4.1.0).

2.4.2.5 Library preparation, sequencing and data processing of 10x Genomics Single cell data

mRNA barcoding was performed using the Chromium Single Cell 3′ Reagent Kit v3 (10x Genomics), following the manufacturer's instructions. For each sample, we targeted a 10,000-cell recovery. One library was prepared for each condition (non-seeding control: NSC, and α-synuclein fribril seeded: Fib). Libraries were sequenced with NovaSeq 6000 (Illumina) at Oxford's Wellcome Trust Centre for Human Genetics.

Alignment of Fastq files was done using CellRanger (v6.0.1) to map the two samples to the *Homo sapiens* GRCh38 2020, a reference provided by Cellranger (v6.0.1) software to create digital gene expression (DGE) matrices.

2.4.2.6 Analysis of 10x single cell data

The quality control, filtering, normalisation, integration, batch correction and finally differential expression for cell-type markers and between conditions (Fibrils vs NSC) of the resulting DGE matrices was carried out in Seurat (v4.0.6) in R (4.1.0).

Cell barcodes with <100 or >7,500 (NSC) or >6,000 (Fib) features >25% mitochondrial RNA, were discarded. The filtered DGE matrices were then normalised and scaled using SCTransform. The samples from the NSC and Fib conditions were then integrated, and batch corrected using the Canonical Correlation Analysis (CCA) anchor-based method using the common 3000 highly variable genes (HVGs) and 30 dimensions. The integrated cells were then clustered using the Louvain algorithm with multi-level refinement on the shared nearest neighbour graph with a resolution of 0.1, resulting in 6 clusters and an UMAP reduction performed for visualization, using the top 12 Principal Components (PCs).

2.4.2.7 Cell type annotation

For the clusters generated with unsupervised clustering, cell-type identity for each cell was predicted with Seurat's *TransferAnchor* and *TransferData* functions by projecting the PCA structure of a reference dataset onto the query. The reference dataset used for this purpose was the human substantia nigra single nuclei atlas mentioned previously (section 2.4.2.2). In order to use the dataset as a reference, the UMI count matrices for the 7 donors were normalised and scaled with SCTransform individually and then batch corrected and integrated using Seurats CCA based-anchor workflow, with 3000 HVGs and 50 CCA dimensions. Cell types were again broadly classified into 8 major cell types as done previously (section 2.4.2.2). The cell type identity for the iPSC 10x dataset was predicted by using the parameters: dims = 1:50, k.anchor=5 and k.weight=10 for the *TransferAnchors* and *TransferData* functions. This led to identifying a predicted identity for each cell in the iPSC dataset. The predicted cell types were further simplified as broad celltypes: neuronal (inhibitory neurons, excitatory neurons, dopaminergic neurons), microglia and other. In order to get a more cleaner cell type annotations for the 10x iPSC dataset, the top predicted broad cell type for each unsupervised Seurat cluster (based on frequency) was extrapolated to the whole Seurat cluster. This broad celltype extrapolated annotation was then utilised for all downstream analyses. Lastly, the broad predicted cell types were further checked by scoring each cluster for previously published gene signatures for microglia (Patir et al., 2019), adult neuronal & oligodendrocyte cell types and as well iPSC differentiation and maturation (Burke et al., 2020) by using the AddModuleScore function in Seurat.

2.4.2.8 Cluster specific markers

To further validate the predicted broad extrapolated cell type annotations, top cell-type specific markers (minimum log FC threshold =0.25, min.pct cell in either of the two populations = 0.15) were identified (one cell type vs all others) by using the Logistic Regression (LR) test while controlling for sequencing depth (nCount RNA) on the log normalised count data (RNA assay) data.

2.4.2.9 Differential expression: Treatment based markers

The logistic regression test was used to identify treatment related markers for each of the broad extrapolated cell-types. The Seurat object was sub-set to the relevant cell type and then renormalised and rescaled before differential expression with the LR test while accounting for sequencing depth as a latent variable to identify DEG (min.pct =0.10 & logFC threshold = 0.25) at 5% FDR between Fib vs NSC cells in the neuronal and microglial clusters separately.

2.4.2.10 Pathway analysis

Gene Ontology Biological process Gene Set Enrichment Analysis (GSEA) was performed for the differential expression results for treatment for the neuronal and microglial cell types by ranking the results based on the Log2FC and using the fgsea algorithm in the ClusterProfiler Biocondcutor package (v4.5.0.992) (Yu et al. 2012) with other parameters, such as min gene set size as 30 and maximum GeneSet size as 500 and eps set as 1E-50. Significantly up and down regulated GO terms based on Benjamini-Hochberg adjusted p-values were then visualized as a dotplot and Gene-Concept Network (CNET) plot.

2.4.2.11 Cell to cell communication analysis

A cell-cell interaction analysis was performed separately for cells from the NSC or the Fib treated sample by using the CellphoneDB database, a novel repository of ligands, receptors and their interactions (Efremova et al., 2020) and the CellphoneDB (v3.0.0) python package (https://github.com/ventolab/CellphoneDB). To identify biological relevant interactions, cell type enriched ligand-receptor interactions at a 10% threshold are identified between all the provided cell types by using the log-normalised count matrix and predicted and broad extrapolated cell-type annotations for NSC and Fib treated samples separately.

The *"statistical analysis"* method was used to identify significant cell-cell interactions at 5% FDR. Briefly, this method initially retrieves all the interactions that can potentially occur in the dataset and then randomly shuffles the cluster labels 10,000 times to estimate a null distribution of the mean of the average ligand-receptor expression for each ligand -receptor pair in each pairwise comparison between any two cell types. The P-value for the likelihood of a cell-type specificity of a given receptor -ligand complex is calculated based on the proportion of the means that are as high or higher than the actual mean (Efremova et al., 2020). Only the significant ligand-receptor interactions at 5% FDR in either conditions were then plotted as a dotplot showing the individual interactions or as a heatmap showing total number of significant interactions between the various annotated cell types with the ggplot2 (v3.3.6) and pheatmap (v1.0.12) libraries in R.

2.5 Biochemical Techniques

2.5.1 Estimation of protein concentration

The bicinchoninic acid (BCA) method was used to estimate protein concentration of samples. First, bovine serum albumin (BSA) (Sigma-Aldrich) standards were prepared to produce a standard curve of known concentrations (0-2 mg/mL) (Figure 2.1).

Standards and samples (diluted 1:10 if required) were added in triplicate (10 µL) to a clear non-sterile, flat-bottomed 96-well plate (Corning) before addition of the BCA reagents A and B (50:1 ratio) (ThermoFisher). Samples were incubated at 37°C for 30 minutes before absorbance was measure at 562 nm using a microplate reader (name of the plate reader we have in the lab). Protein concentration was determined by linear regression analysis and diluted to the required concentration before use.

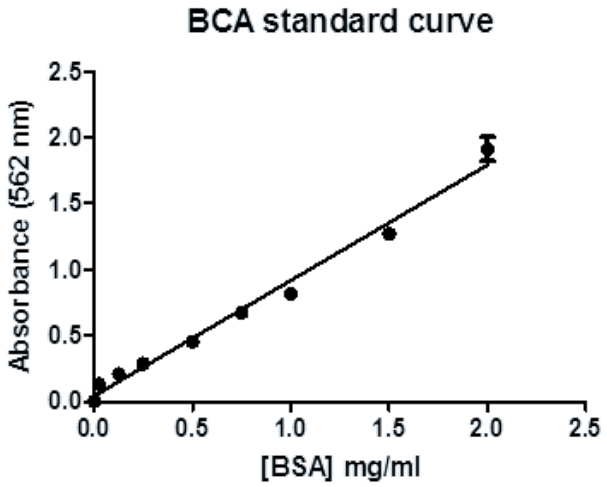

Figure 2.1 BCA Standard curve

2.5.2 Immunoblotting

Sample preparation

Cell cultures were lysed with ice-cold lysis buffer [0.1 M Tris-HCl, pH 7.4, 150 mM NaCl, 0.1% SDS, 1% Triton-X-100, N-Ethylmaleimide (NEM), 1 mM phenylmethylsulfonyl fluoride (PMSF) and 1X cOmplete™ Protease and 1X phosphatase inhibitor cocktails (Roche)]. Lysates were sonicated for 30 seconds at 30% amplitude power (Cycle ON 5 seconds, cycle OFF 5 seconds). Homogenized samples were clarified by centrifugation at 16,000×g at 4°C for 20 minutes. The supernatant was collected, and the protein concentration was determined using the BCA assay (Thermo Fisher Scientific) as per manufacturer's instructions. Equal amounts of protein across samples were added to NuPAGE LDS Sample Buffer 4X (Life Technologies), containing reducing agent 0.1 mM dithiothreitol (DTT).

SDS-PAGE electrophoresis and nitrocellulose membrane blotting

Protein samples were resolved using 4-12% SDS/PAGE (NuPAGE Novex Bis-Tris Gels; Life Technologies) and transferred onto a nitrocellulose membrane (Amersham Protran 0.45; GE Healthcare) using Invitrogen iBlot 2 transfer device. Once transfer was complete, protein loading was confirmed using Ponceau S, then nitrocellulose membranes were rinsed once in TBS-T and incubated with blocking solution for 1 hour (Table 2.7). Primary antibody (Table 2.8) was added, and blots were incubated for indicated times (table x) followed by 3 x 10 minutes' washes in TBS-T solution. Blots were then incubated with fresh blocking solution and appropriate secondary antibody conjugated to horseradish peroxidase for 1 hour. Then membranes were washed for 4 X 10 minutes in TBS-T solution and developed

with enhanced chemiluminescent (ECL) reagent (Amersham) using ChemiDoc MP Imaging System.

To re-probe membranes, blots were incubated in mild stripping buffer (Abcam) for 2 X 20 minutes, thoroughly rinsed in *dd*H_2O, incubated in blocking solution and were ready for another round of probing.

Relative quantification of the protein of interest to the loading control was measured using FIJI ImageJ.

Buffer	Recipe
Biochemical analysis	
1X Running Buffer	25 mM Tris-Base, 192 mM Glycine, 0.1% SDS, pH=8.6
SDS Sample Buffer	4x NuPage, 10X reducing agent, ddH_2O
Blocking Solution	25 mM Tris-Base, 135 mM NaCl, 2.5 mM kCl, 1mM $CaCl_2.2H_2O$, 0.1% Tween20, pH=7.4, 5% BSA
TBS-T	25 mM Tris-Base, 135 mM NaCl, 2.5 mM kCl, 1mM $CaCl_2.2H_2O$, 0.1% Tween20, pH=7.4
Immunofluorescence analysis (IF)	
Permeabilisation Buffer	PBS, 0.2% Triton-X100
Blocking Buffer	5% Normal goat serum (NGS), 0.2% Triton-X100

Table 2.7 Composition of buffers used for the present study

Measuring levels of insoluble and phosphorylated form of α-synuclein

For the detection of $pSyn^{S129}$ (phosphorylated α-synuclein on serine 129) in fibril-induced aggregates cells were lysed in ice-cold standard RIPA extraction buffer (Thermo Scientific) as described above. After homogenisation of samples, lysates were fractionated by ultracentrifugation for 2 h at 100,000 x g at 4°C. Intracellular aggregates are not soluble in 0.1% SDS, therefore, ultracentrifugation at the high speed (fractionation) allows to separate the soluble fraction (supernatant) from the insoluble fraction (pellet). The insoluble fraction was resolubilised in 2% SDS RIPA buffer (supplemented with NEM, PMSF and cOmplete™ protease and phosphatase inhibitors), then subjected to sonication (two cycles at 30% amplitude 1 second on, 1 second off for 30 secs) for 1 min on ice as described above.

Antibody	Supplier, cat no	Host species	Function, dilution
anti-phosphoS129 α-synuclein, clone EP1536Y	Abcam, ab51253	rabbit monoclonal	ICC (1:1000) WB (1:2000)
anti-tyrosine hydroxylase, clone LNC1	Millipore, MAB318	mouse monoclonal	ICC (1:1000)
anti-βIII tubulin/TUJ1	Biolegend, MMS-435P	mouse monoclonal	ICC (1:1500)
anti-MAP2	Abcam, ab5392	chicken polyclonal	ICC (1:2000)
anti-NeuN	Millipore, MAB377	mouse monoclonal	ICC (1:1000)
anti-Iba1	Fujifilm, Wako, 019-19741	rabbit monoclonal	ICC (1:500) WB (1:500)
anti-β-actin	Thermo Fisher, AM4302	mouse monoclonal	WB (1:10000)
Alexa Fluor 488-labelled anti-rabbit IgG H&L	Invitrogen, A11008	goat	ICC (1:1000)
Alexa Fluor 488-labelled anti-mouse IgG H&L	Invitrogen, A11001	goat	ICC (1:1000)
Alexa Fluor 568-labelled anti-rabbit	Invitrogen, A11011	goat	ICC (1:1000)
Alexa Fluor 647-labelled anti-chicken IgG H&L	Invitrogen, A21449	goat	ICC (1:1000)
Alexa Fluor 647-labelled anti-mouse IgG H&L	Invitrogen, A21235	goat	ICC (1:1000)
HRP-labelled anti-rabbit IgG H&L	Thermo Fisher, 31460	goat	WB (1:5000)
HRP-labelled anti-mouse IgG H&L	Thermo Fisher, 31402	goat	WB (1:5000)

Table 2.8 List of the primary and secondary antibodies used in the present study

2.5.3 Immunofluorescence

Confocal imaging of fixed specimen on coverslips

Coverslips with cells were washed twice with DPBS and fixed at RT with 4% paraformaldehyde (PFA) (VWR) in D-PBS for 10 mins. Following, coverslips were permeabilised and blocked with 5% normal goat serum (NGS) (Life Technologies) in DPBS with 0.2% Triton-X-100 (Sigma) at RT for 1 hr (Table 2.7). The coverslips were then incubated with primary antibodies overnight at 4°C on an orbital shaker at 5-10 revolutions per minute. The primary antibodies used in the present study are listed on table 2.8. Coverslips were washed three times with DPBS for 10 mins each wash and incubated with secondary antibodies for 1hr. Secondary antibodies used are listed on table 2.8. Following three washes with DPBS, coverslips were then mounted on microscope slides with Pro-Long Glass with Nuclei Blue (ThermoFisher). Images were acquired with Zeiss880 Confocal-Airyscan microscope equipped with a 40x or x63 oil objectives at 0.69-µm steps and Z-projected. Acquired images were processed with Image J software with FiJi image processing package. For measuring IBA1 microglia morphologies, 10 images were analysed per condition. For nuclei count, 15 images were acquired per condition, per differentiation and per line. The nuclei counts were blinded and quantified on FIJI ImageJ.

High-content imaging on Organotypic Slices

Before fixation, slices were transferred from the porous membrane culture insert to 24-well glass bottom imaging plates (Corning). Slices were fixed with 4% PFA for 45 mins at RT and washed three times with DPBS. Following, slices were incubated with ice cold 20% methanol (VWR) for 10 mins at RT. Sequentially, they

were washed once with DPBS and incubated with 1% Triton X-100 overnight at 4 °C on a shaker. Slices were then blocked with 20% BSA in 0.1% Triton X-100 in PBS for 4 hrs at RT. Primary antibodies were then added in 5% BSA in 0.1% Triton X-100 in PBS and the slices were incubated overnight at 4 °C on a shaker at 700 rpm. After two washes with PBS, the slices were incubated with secondary antibodies in 5% BSA in 0.1% Triton X-100 overnight at 4 °C on a shaker. After three washes with PBS and a 20-minute incubation with nuclei counterstain, Hoechst (Life Technologies), images were acquired using the Opera Phenix (Perkin Elmer). The method protocol that was used was PreciScan with 10x magnification for the pre-scan method and 20x magnification for the re-scan. The 40x water immersed lens was used to acquire example images and montage images were generated by stitching individual image fields together (Harmony software-Perkin Elmer).

2.5.4 Time-resolved FRET

The levels of pSYN were measured with the CisBio kit (Perkin Elmer, Waltham, MA USA) following the manufacturer's instructions. The CisBio assay measures the concentration of the analyte-pSYN in the case of this study by using similar chemical principles as the ELISA sandwich. The main component of the assay is the monoclonal antibody pair (Figure 2.2). Each antibody is covalently linked to an acceptor and donor fluorophore, which when are in close physical proximity fluoresce through Fluorescence Energy Transfer (FRET) principle. The high sensitivity of this assay originates from a time-resolved measurement of fluorescence (homology time resolved fluorescence, HTRF) that when combined with FRET allows a time delay (50-150 μseconds) immediately after the excitation and fluorescence reading. The time delay eliminates any non-specific and short-lived emissions that can act as background, such as compounds, proteins, medium).

Optimisation experiments were thoroughly carried out to determine the dynamic range of the assay specified for iPSC-derived co-cultures of human microglia and dopaminergic neurons. For the requirements of the assay, the dopaminergic neurons were 70,000 cells/well first in Geltrex-coated 96-well plates (Corning). Addition of the α-synuclein fibrils on neurons was performed on DIV45 and microglia were harvested and added at a 1:1 ratio on DIV59. CisBio was carried out following the two-week incubation period with microglia. On the day of the assay the co-cultures were lysed with CisBio lysis buffer (Perkin Elmer) and immediately homogenised at RT for 1 hr on a rocking platform. Following, lysates were snap frozen for 30 mins at -80°C to achieve complete content lysis.

Lysates were transferred onto specific HTRF 96-well plates (PerkinElmer). Each assay reaction consists of 20 µl: 16 µl of cell lysate is combined with 2 µl of acceptor-tagged antibody (d2) and 2 µl of cryptate donor tagged antibody (tb). Samples and fluorophores were mixed, covered, and incubated overnight at RT for maximum assay specificity. Samples were excited at 340 nm and emission values were measured at 620 nm and 665 nm using a CLARIOstar Plus (BMG Labtech, Ortenberg, Germany). FRET signal is proportional to the number of antigen-antibody complexes and therefore α-synuclein (oligomeric or S^{129}) intracellular concentrations. Data were normalised to total protein concentration as determined using a BCA assay (Thermo Scientific). FRET signal intensity was analysed by calculating fold change values based on the background-subtracted ratio of 665/620 nm.

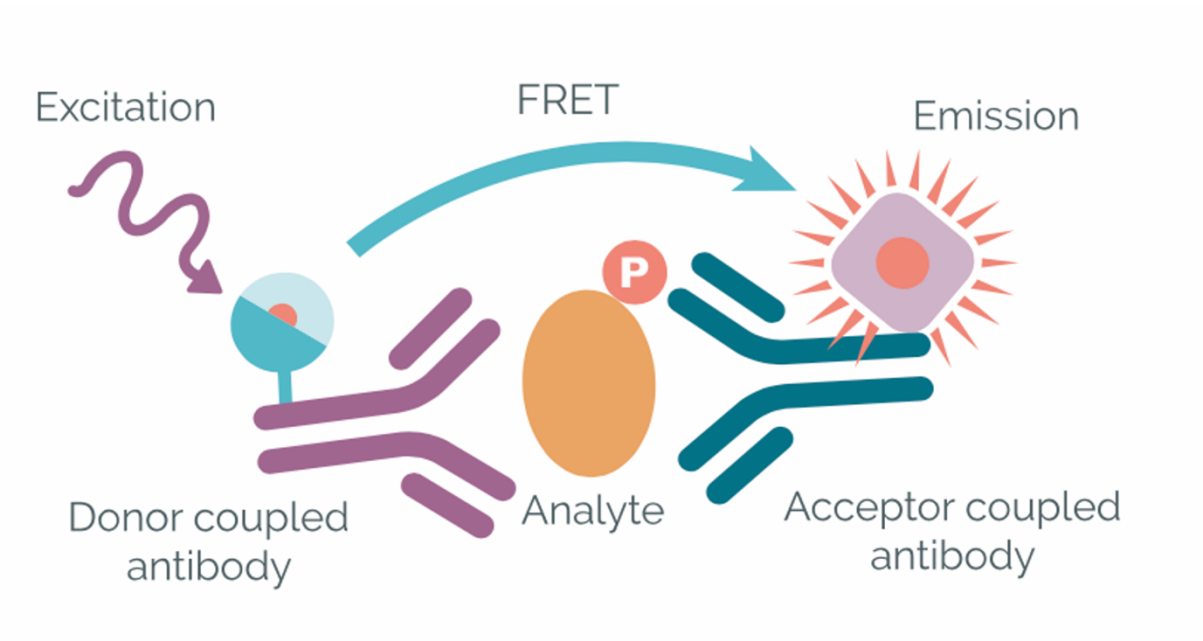

Figure 2.2 The homology time resolved fluorescence assay, Cisbio.

The acceptor and donor-tagged antibodies are mixed with the content of cell lysates and when the analyte of interest is present in the then the two antibodies come in proximity. The donor emits fluorescence upon excitation and the energy is transferred to the nearby acceptor, providing the acceptor with fluorescence. Donor fluorescence is also measured and the ratio with the acceptor fluorescence is calculated.

2.5.5 Proteome Profiler Array: Human XL cytokine array

Cytokines were detected in conditioned media of microglia and dopaminergic neurons co-cultured cells by using a human XL cytokine array kit (R&D systems). Dopaminergic neurons were plated at 800,000 cells/well in 12-well plate and microglia was added at a 1:1 ratio. Conditioned media was collected 2 weeks after microglia was added on the neurons. Large aggregates and cell debris was clarified by centrifugation at 1200 x g for 10 minutes at 4°C

Supernatants were processed according to the manufacturer's protocol. Each experimental condition requires one single membrane, therefore for biological significance media from three independent iPSC differentiations was pooled and assessed. Capture antibodies have been spotted in duplicates on nitrocellulose membranes and membranes were first blocked and following were incubated overnight with the pooled samples (Figure 2.3). The following day the membranes were incubated with the detection antibody cocktail mix. If a cytokine is present in the sample, then it binds with the detection antibody and is immobilised. Sequentially, streptavidin-HRP and chemiluminescent reagents are added on the membrane and light is produced at each spot in proportion to the cytokine bound. Intensity was measured using ChemiDoc MP imaging system (Biorad) and the intensity of each dot was measured by Studio Lite software.

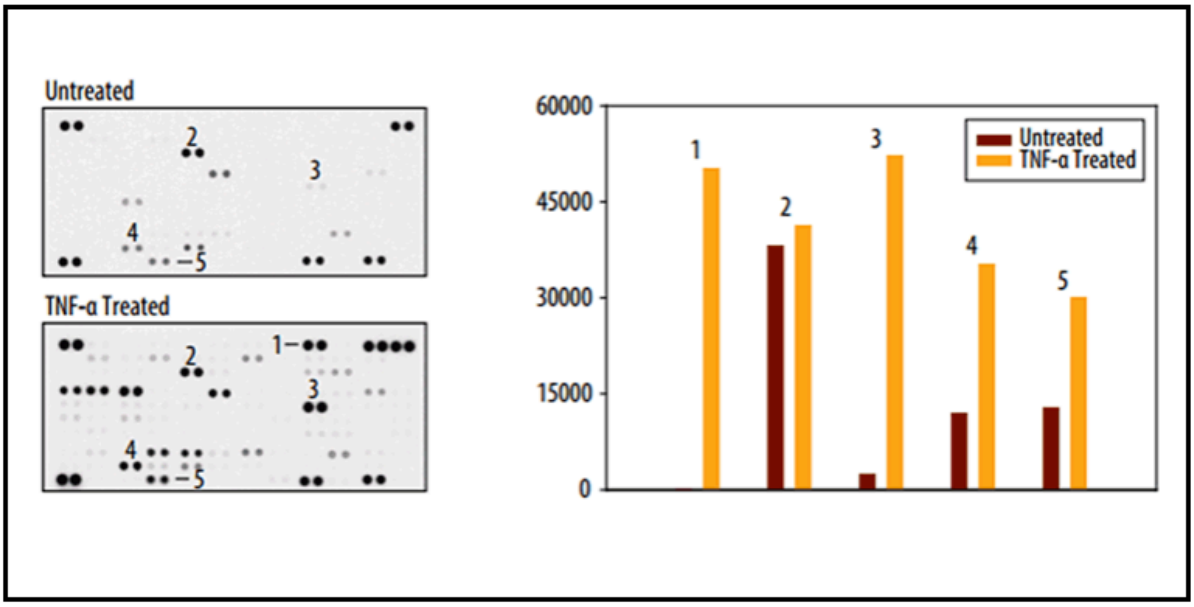

Figure 2.3 Principle of cytokine profiler array.

Example figure from the manufacturer's website demonstrates how the detection between an untreated and treated condition. Relative concentration of a cytokine is indicated by the dot's intensity and using an imaging software that can be plotted as relative intensity (arbitrary units, AU).

2.5.6 Immunoassay-Quanterix Simoa

Interleukin 6 (Il-6) was measured in conditioned medium of cultured OHS using an array digital technology (Quanterix, Lexington, MA), which uses a single-molecule enzyme-linked immune-array method, previously described (Rissin et al., 2010). SiMoA (Wilson et al., 2016) is a novel technology that employs highly sensitive immunoassays with lowest level of detection (LLOAD) ≤100 fg/mL. IL-6 was detected in the levels of pg/ml by interpolation to the calibration curves. The assay was carried out at the Eli Lilly laboratories.

2.6 Statistical Analysis

Statistical analysis was performed using GraphPad Prism (GraphPad, CA USA) v.9. For iPSC-derived experiments the *n* numbers represent one cell line differentiated once. The *n* biological replicates were defined as differentiations performed at least one cell-split apart and each clone was differentiated at least three times. The data were examined for normality and statistical tests were chosen accordingly. For normally distributed data, one-way ANOVA was performed followed by Tukey's multiple comparison test. For non-normally distributed data, the Kruskal-Wallis test was used followed by Dunn's multiple comparison test. A two-sided unpaired Student's *t*-test was used where indicated when two conditions were compared. The null hypothesis was rejected at a significance level of p=0.05.

2.7 Ethical approval

Ethical approval was obtained from the Oxford C REC Ethics Committee (No. 15/SC/0639) for the use of human tissue.

All animal procedures were performed in accordance with the Animals (Scientific Procedures) Act 1986 and were approved by the Eli Lilly Animal Welfare Board. It was in compliance with the ARRIVE guidelines.

Chapter 3: Set up of organotypic slices to study recombinant fibrils induced neuronal α-synuclein aggregation and microglia phenotypes

3.1 Introduction

3.1.1 Organotypic slices as *ex vivo* models of Parkinson's disease

Cellular *in vitro* models, either human or rodent have provided valuable insights regarding the molecular and biochemical pathways involved in neurodegeneration. However, the reductionist approach of using single cell types in culture does not model the interactions between different brain cell types that contribute to the pathogenesis of neurodegenerative diseases, such as Parkinson's and Alzheimer's disease (Croft et al., 2019b).

The limited efficacy of current therapeutic strategies against neurodegenerative disorders highlights their intrinsically complex aetiology and neuropathology and emphasises the need for research tools that more accurately recapitulate the disease's pathology, including cell non-autonomous effects (Slanzi et al., 2020). In this respect, organotypic slices offer several advantages. Tissue organotypic slices maintain the brain's architectural and structural hierarchy in a way that cellular models do not. By retaining the three-dimensional brain architecture, they also maintain some of the anatomical planes of connectivity in a way that the quite popular spherical organoids cannot (Arber et al., 2017). *Ex vivo* slices maintain the interactions and structural organisation between neuronal and non-neuronal cells, which is important since the involvement of the latter in neurodegeneration has become apparent. *In vitro* co-culture and tri-culture models have become

increasingly popular in the research field of neurodegeneration (Guttikonda et al., 2021). Nevertheless, they do not preserve the anatomical connections among the different brain cell types in the way that organotypic slices do. Another advantage that brain organotypic slices present, is that they maintain *ex vivo* the synaptic neuronal connections in a similar way to *in vivo*. Preserving this developmental phenotype intact is quite important in the study of neurodegenerative diseases (De Simoni et al., 2003). Microglia preserve their characteristic ramified homeostatic morphology *ex vivo* in a similar way they do *in vivo* in the rodent brain. Finally, organotypic brain slices preserve not only the synaptic connections, but also the neurovascular unit connections providing an experimental model that can overcome the *in vivo* impediments of the blood brain barrier.

The use of rodent brain organotypic slices mainly deriving from rat or mice brain was widely established in the early 1980s using the roller-tube method (Gahwiler, 1981). However, this method does not preserve the brain's structural and morphological architecture. This was enabled by the development of the interface method, which involves the long-term culture of brain slices on a porous membrane insert that allows the exchange of nutrients and oxygen between the sliced tissue and a culture media via capillary action (Stoppini et al., 1991).

As far as Parkinson's disease is concerned, the first organotypic slices to study the nigrostriatal system were developed in the mid-1990s as co-cultures between slices from the substantia nigra and the cortex and striatum (Ostergaard et al., 1996, Plenz and Kitai, 1998). Over the years, brain slices from other areas such as the subventricular zone and the hippocampus were also developed to study specifically the mechanistic effects of α-synuclein in Parkinson's disease neurodegeneration.

(Tonnesen et al., 2011, Elfarrash et al., 2019). The hippocampus, as a temporal lobe structure is involved in the regulation of learning and memory and is affected in Parkinson's disease with disease progression or from the early stages in certain patient subpopulations with associated cognitive decline (often referred to as dementia with Lewy bodies, DLB). Animal and human studies have revealed a direct link between dopamine transmission and hippocampal synaptic plasticity in memory and behaviour that could contribute to memory loss and the onset of neuropsychiatric symptoms in Parkinson's disease (Calabresi et al., 2013).

3.1.2 Organotypic slices as an *ex vivo* tool to model neuroinflammation in Parkinson's disease

Inflammation and activation of microglia and astrocytes in Parkinson's and Alzheimer's disease are undoubtedly important components in the cellular phase and progression of neurodegenerative diseases (De Strooper and Karran, 2016). Since organotypic brain slices maintain the three-dimensional connectivity planes between different regions and cellular types, they have been widely used to model and investigate interactions between the neuronal changes in Parkinson's and Alzheimer's disease and astroglia inflammatory mechanisms (Croft et al., 2019b).

It has been found using rodent hippocampal organotypic slices that microglia are activated around Aβ plaques and phagocytose insoluble aggregates (Fan and Tenner, 2004) (Croft et al., 2019b). Activated microglia have also been observed in *ex vivo* slices where neuronal α-synuclein aggregation was exogenously induced by the addition of synthetic fibrils (Roux et al., 2020, Elfarrash et al., 2019). Moreover, microglia inflammatory activation to these stimuli has been demonstrated by measuring mRNA levels of homeostatic, inflammatory, and chemotaxis-related markers (Delbridge et al., 2020). Transcriptomic studies have also revealed that the *ex vivo* inflammatory phenotype of rodent microglia is rather similar to the one observed *in vivo* and quite different to *in vitro* cultured microglia (Heng et al., 2008) (Delbridge et al., 2020). The highly dynamic microglia phenotype is preserved *ex vivo* even after the highly traumatic process of dissection and these early studies suggest that the use of brain organotypic slices is suitable for the study of microglial phenotypes in response to neuronal degeneration in Parkinson's and Alzheimer's disease.

3.1.3 α-synuclein *de novo* fibrils generation, seeded aggregation and phosphorylation on serine 129

Even though α-synuclein misfolding is a key event in the pathogenesis of Parkinson's disease, its physiological function remains poorly understood. It has been suggested that the loss of α-synuclein's normal function results in misfolding, or that loss of function may contribute to the disease, independent of the process of misfolding. In presynaptic terminals its function is not essential at least in animals when genetically knocked out, causing only subtle deficits such as an activity-dependent negative regulation of neurotransmission or impaired dilatation of the exocytic fusion pore (Sulzer and Edwards, 2019). Knockout of α-synuclein also leads to a reduction in the number of dopaminergic neurons during embryonic development, but not in any further damage later in life (Garcia-Reitboeck et al., 2013). Animal studies revealed that absence of all synucleins (α-, β-, γ-) caused axonal degeneration but not dopaminergic cell loss (Greten-Harrison et al., 2010).

Multiple lines of evidence indicate that neurodegeneration is caused by a toxic-gain of function as a result of α-synuclein assembly into fibrillar structures. These assemblies are generated in a self-templating manner that may also contribute to the propagation across interconnected neuronal networks as shown for other disease-associated proteins such as tau (Goedert, 2001). Based on this seeded aggregation model, monomeric α-synuclein misfolds and assembles into oligomeric species that form stable fibrils that are insoluble. High molecular weight, insoluble assemblies of α-synuclein are the main component of Lewy bodies and Lewy neurites in Parkinson's disease brains. Under physiological conditions *in vitro* α-synuclein monomers aggregate and form structurally similar aggregates to those found in the inclusions of parkinsonian brains (Spillantini et al., 1998). These pre-formed *de novo*

fibrils have been widely used in research as seeds that can be taken up by cells and imprint their conformation on the endogenous α-synuclein, recruit further endogenous monomeric protein, and propagate trans-neuronally (Bousset et al., 2013b, Karpowicz et al., 2019).

Bousset and colleagues, demonstrated that recombinant monomeric α-synuclein can assembly into two polymorphs in the presence of different salt concentrations (Bousset et al., 2013b). The authors observed by electron microscopy structures of "cylindrical" morphology termed fibrils and "ribbon-like" polymorphs under lower concentrations of salt (Bousset et al., 2013b). As far as their cytotoxicity is concerned, cell line seeding experiments suggested that α-synuclein fibrils were more efficient in triggering apoptotic events compared to the ribbons (Bousset et al., 2013b). These findings implied that different strains of α-synuclein may also be generated. In humans, the assembly of α-synuclein into different strains may explain the clinical heterogeneity that characterises synucleinopathies, such as Parkinson's disease, multiple systems atrophy (MSA) and dementia with Lewy bodies. Ultimately, the fact that *de novo* generated α-synuclein polymorphs can imprint their structural and morphological properties on the endogenous monomeric protein has enabled research to understand the molecular basis of α-synuclein seeded aggregation (Peng et al., 2018, Blumenstock et al., 2017).

The majority (>90%) of accumulated α-synuclein in the Lewy bodies is phosphorylated at serine 129 (pSyn129, pSYN), Whether phosphorylation of α-synuclein promotes or inhibits its aggregation remains elusive and under debate. Numerous *in vitro* and *in vivo* animal studies have shown that *de novo* fibrils can template the conversion of endogenous α-synuclein into aggregates that are

phosphorylated at serine129. The use of pSYN at serine129 has therefore been widely used as a marker for pathological forms of α-synuclein (Volpicelli-Daley et al., 2014). Phosphorylation at ser129 is detected in <5% of total α-synuclein in the healthy brain (Anderson et al., 2006, Fujiwara et al., 2002).

3.1.4 Human organotypic slices as a novel *ex vivo* tool to study neurodegeneration

One of the major drawbacks in using animals, especially rodents, to study human disease concerns the translational gap due to the species difference (Zeiss, 2017). Genome-wide association studies, as well as transcriptomic analyses have revealed major differences between humans and rodents (Breschi et al., 2017). This is especially important for the study of microglia in Parkinson's and Alzheimer's disease. There is overwhelming evidence that rodent microglia do not faithfully recapitulate the homeostatic or disease-associated transcriptomic signatures detected in humans (Smith and Dragunow, 2014, Gosselin et al., 2017a). One way to bypass this limitation is by using human brain organotypic slices. Over the years, human tissue obtained from neurosurgical procedures has proven extremely valuable as an acute electrophysiological research tool (Bernard et al., 2004, Kerkhofs et al., 2018). On the contrary to the preparation of rodent brain organotypic slices, human long-term slice culture was faced with the challenge of tissue preservation and viability. Nevertheless, advances in recent years provided encouraging data regarding neuronal connectivity and function by using electrophysiology readings (Eugène et al., 2014). Additionally, it has been shown that human brain slices can be cultured *in vitro* long-term up to three weeks and subjected to optogenetic modulation (Schwarz et al., 2019), therefore offering a means to study the living human brain.

3.1.5 Experimental workflow: α-synuclein seeded aggregation on mouse transgenic hippocampal organotypic slices

By obtaining mouse hippocampal organotypic slices and seeding them with *de novo* generated α-synuclein fibrils, I established a mouse *ex vivo* model to study the microglial and inflammatory response to neuronal seeded aggregation (Figure 3.1). I cultured the slices for 2 weeks. On day *in vitro* (DIV) 7, I added the fibrils in the culture media of hippocampal slices from transgenic A53T neonatal mouse pups (P5-P7). By using a high-content imaging platform, I designed an imaging pipeline that enabled me to measure microglia morphological activation by determining the total area they occupy on a single hippocampal slice.

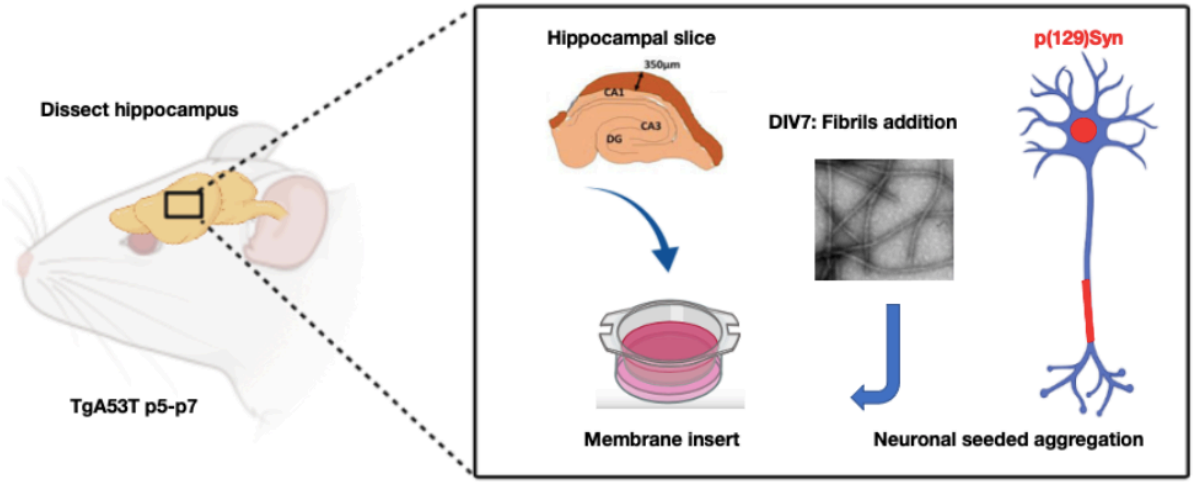

Figure 3.1 Assay workflow of modelling α-synuclein aggregation in organotypic hippocampal slices from A53T transgenic mice pups.

A53T pups (5-7 days old) were decapitated and from the whole cortex the hippocampus was isolated and obtained. Slices, with the structurally intact classical morphology (dentate gyrus-DG, hippocampal region CA1 and CA3) and thickness of 350 µm were acquired. Sequentially, slices were cultured on membrane porous inserts that allowed the exchange of oxygen and nutrients between the slice and the culture media. On day *in vitro* (DIV) 7, slices were inoculated with synthetic α-Synuclein fibrils. Slices were fixed and evaluated for the presence of endogenous α-synuclein neuronal aggregation as indicated by the pSYN [p(129) Ser] phosphorylation pathological marker.

3.1.6 Aims and objectives

The objectives of this chapter were to:

1. Generate *de novo* α-synuclein fibrils following previously published protocols and assess their cellular seeding efficacy
2. Establish long term cultures of hippocampal organotypic slices from transgenic mice expressing the A53T mutation (TgA53T)
3. Induce neuronal aggregation in the organotypic slices by addition of *de novo* fibrils
4. Culture human cortical slices from neurosurgical specimens as a first step towards the development of an *ex vivo* human model

3.2 Results

3.2.1 *De novo* generation of α-synuclein fibrils

3.2.1.1 Expression, purification, and assembly of α-synuclein into fibrils

In order to induce neuronal seeded aggregation in organotypic slices, my first aim was to generate *de novo* α-synuclein fibrils following previously published protocols (Bousset et al., 2013b), which were optimised and streamlined in the Eli Lilly laboratories (Indianapolis, USA and Windlesham, UK). Human monomeric α-synuclein was expressed in *E. coli* BL21 following transformation with a pRK5-αSyn^{WT} plasmid. Bacterial pellets were lysed, and lysates were subjected to multiple steps including size exclusion chromatography for monomeric α-synuclein purification (14 kDa) (Figure 3.2). For fibril generation, WT α-synuclein monomer was incubated in buffer containing 150 mM KCL at 37°C under continuous shaking for 14 days.

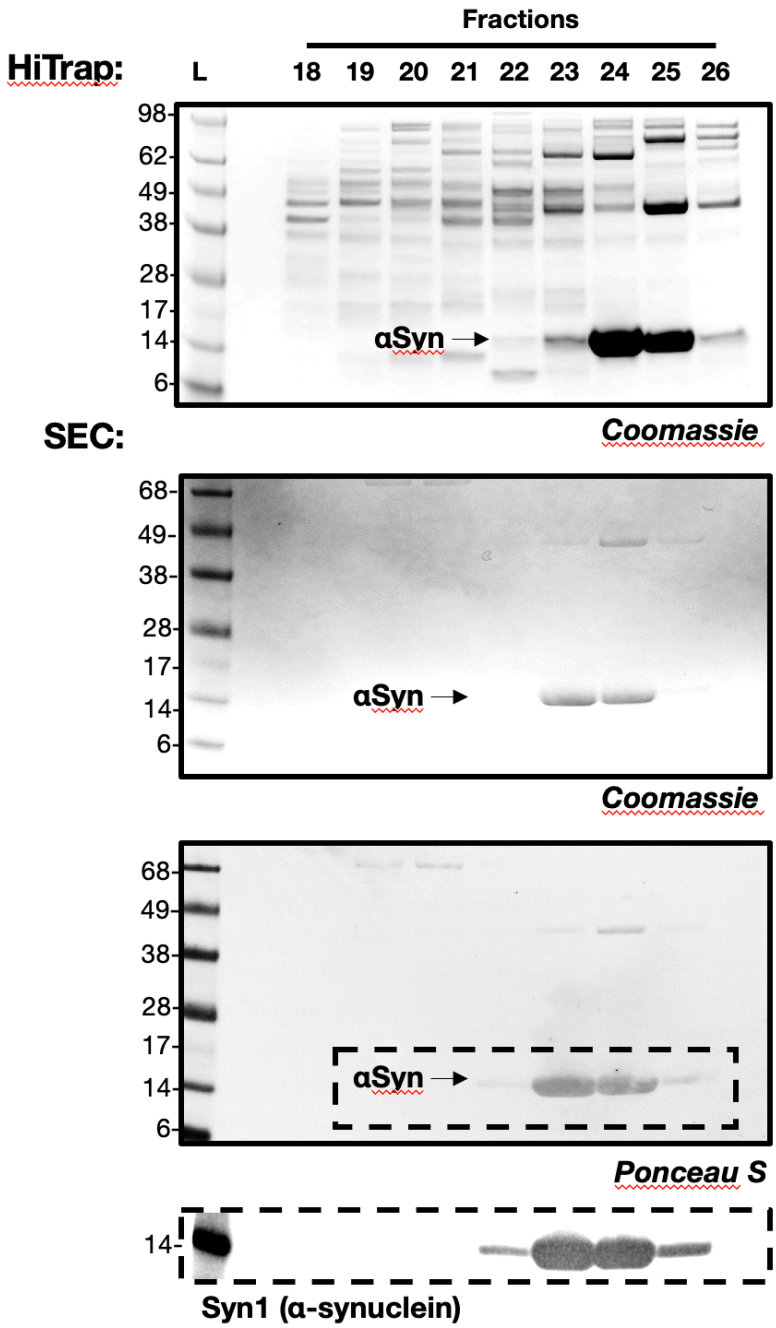

Figure 3.2 Expression and purification of recombinant α-synuclein monomer. Bacteria cultures (*E. coli* BL21) were transformed with pRK5-αSyn^{WT} plasmid. The cultures were incubated in big flasks and the final pellets were subjected to multiple steps of purification. The HiTrap chromatography yielded multiple fractions that were visualised on Coomassie gel (top gel). Fractions enriched with a 14 kDa protein were selected and further subjected to size exclusion chromatography (SEC). The resulting fractions were visualised on gels with Coomassie (middle gel) and PonceauS staining (bottom gel). The two fractions with the most visible bands at 14 kDa (dotted black box) were selected, pooled and further subjected to purification that resulted in generation of recombinant α-synuclein monomeric protein that was confirmed by immunoblotting. Purifications were carried out in collaboration with Dr. Jade Marsh and Dr. Dmitry Zenko.

3.2.1.2 Quality control and seeding efficiency of α-synuclein pre-formed fibrils

In vitro, the conversion of soluble α-synuclein into amyloid fibrils typically occurs after a lag phase that is followed by a rapid increase in fibril elongation and is concentration-dependent (Cremades et al., 2017). According to this model, soluble monomeric α-synuclein assembles into oligomers of different sizes and β-sheets content, which mature to protofibrils and via recruitment of monomers to stable fibrils (de Oliveira and Silva, 2019). This process was monitored with Thioflavin-T (ThT), a benzathiole dye that binds specifically to amyloid structures (Vassar and Culling, 1959). I used ThT to monitor the conversion of monomeric to fibrillar α-synuclein at different timepoints as shown in Figure 3.3. I observed an initial 10-fold increase in ThT fluorescence signal from DIV0 to DIV1, followed by a continuous increase in the signal intensity until approximately DIV7 when the signal reached a plateau and remained the same up to day DIV14 (Figure 3.3c).

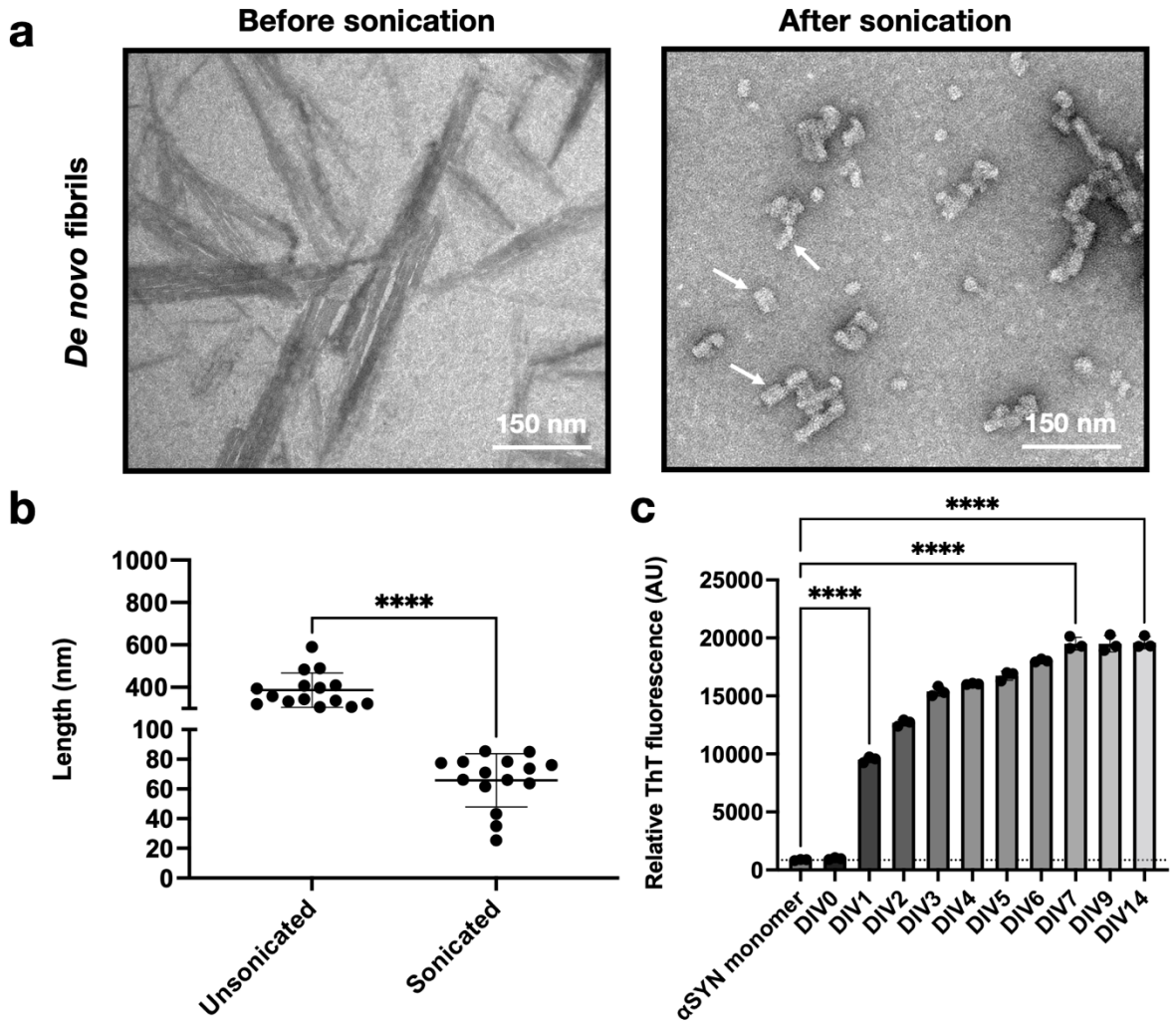

Figure 3.3 α-synuclein de novo fibrils and relative ThT fluorescence intensity signal signifying binding on amyloid β-sheet structures.

Monomeric recombinant α-synuclein was incubated at 37°C under continuous shaking conditions (500 rpm) for a period of 14 days *in vitro*. **a, b**. *De novo* fibrils were visualised with EM before and after being sonicated. White arrows point at individual fibrils following sonication and the length (nm) of individual fibrils was calculated. ****p<0.0001 by unpaired t-test. Scale bar at 150 nm. **c**. ThT was added daily until DIV7 and afterwards two additional readings were acquired on DIV9 and DIV14. Fluorescence was spectroscopically acquired at 450 nm. Each dot represents independent technical repeats and data are mean ± s.e.m. ****P<0.0001 by one-way ANOVA followed by Dunnett's multiple comparison test. EM images were acquired by our collaborator, Dr. Errin Johnson.

Following the detection of fibrils by ThT, I went on to confirm their presence by EM (Figure 3.3 a, b). I then assessed their seeding efficiency in a live cell-based aggregation assay that was established in our laboratory, using HEK295T cells stably expressing wild-type α-synuclein fused to its c-terminus to Venus fluorescent protein. I used two concentrations of fibrils (0.25 and 0.5 μM) for 48 h based on previous optimisation by other members of the laboratory. Formation of aggregates was observed in live cells within 12 h and confirmed by immunofluorescence microscopy, demonstrating that pSYN co-localised with Venus-positive inclusions as shown in Figure 3.4a.

I corroborated these immunostaining findings by immunoblotting, measuring pSYN levels in cells treated with fibrils relative to the non-seeded control (NSC) cells. I observed a 2-and 4-fold increase of the pSYN signal when the cells were seeded with 0.25 and 0.5 μM of fibrils, respectively as shown in Figure 3.4 b, c. As expected, no pSYN signal was detected in cell lysates after seeding with the α-synuclein monomer.

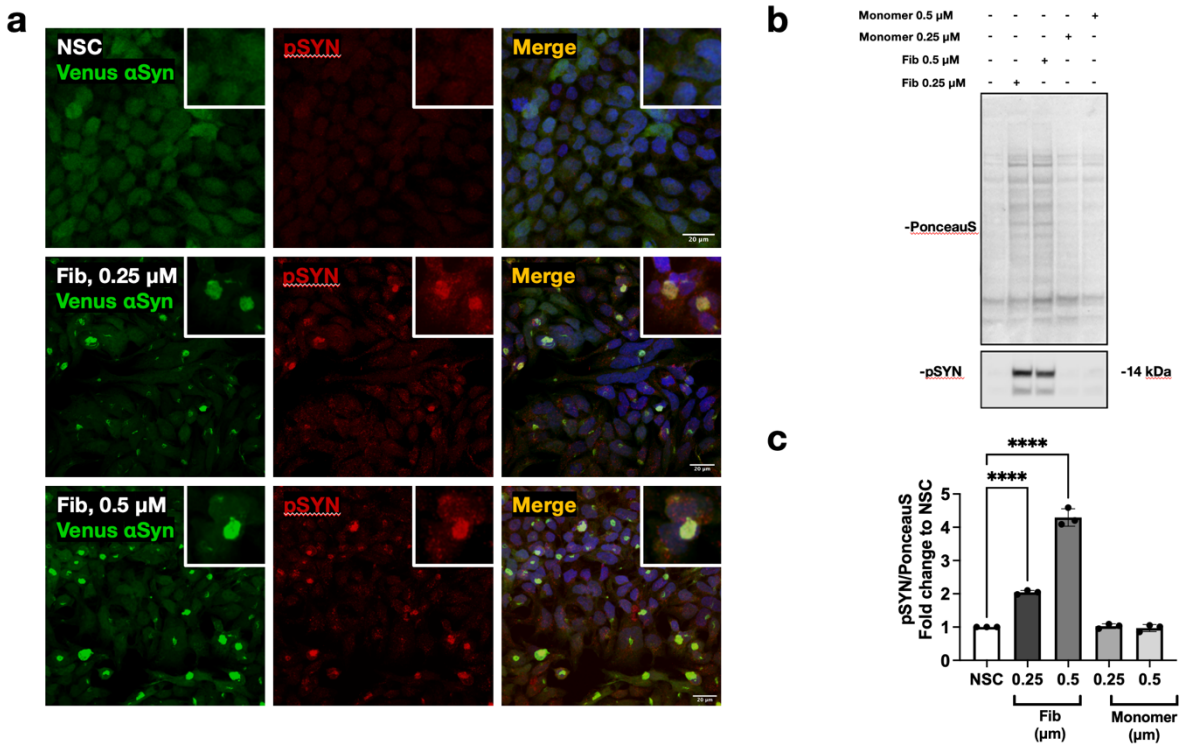

Figure 3.4 HEK295T α-synuclein-Venus cells were seeded with *de novo* generated fibrils.

a. At baseline no pSYN immunostaining was detected. After addition of fibrils endogenous α-synuclein-Venus was seeded to form inclusions which were stained with anti-pSYN antibodies. **b, c.** Immunoblotting showed increase pSYN levels when normalised to the total cell protein contents with 0.25 μM, which was almost doubled at the presence of 0.5 μM of fibrils. Cells treated with monomeric α-synuclein did not induce pSYN-positive inclusions. NSC, non-seeding control, Fib-fibrils. Scale bar at 20 μm. Each dot represents n=3 technical repeats and data are mean ± s.e.m. ****P<0.0001 by one-way ANOVA followed by Dunnett's multiple comparisons test.

3.2.2 *Ex vivo* TgA53T mouse hippocampal organotypic slices

3.2.2.1 Organotypic hippocampal slices preserve their structural architecture and cellular composition in *ex vivo* cultures

The first α-synuclein mutation associated with Parkinson's disease was the A53T substitution, that was found in a large Greek-Italian kindred with autosomal dominant early onset of Parkinson's disease (Polymeropoulos et al., 1997). Homozygous mice expressing the human A53T α-synuclein develop α-synuclein inclusions and an aggressive neurodegenerative phenotype associated with progressive motor dysfunction due to involvement of the spinal cord that leads to death (Lee et al., 2002). For my experiments, I used A53T heterozygotic mice because they develop α-synuclein pathology at a much slower rate and are therefore more suitable to assess whether α-synuclein *de novo* fibrils accelerate aggregation in the organotypic slice model as it was previously demonstrated *in vivo* (Prusiner et al., 2015).

Brain organotypic hippocampal slices (OHS) were cultured for 2 weeks on a porous membrane insert (Figure 3.5a, b). Macroscopically I observed that OHS maintained their anatomical organisation over the course of culture with macroscopically intact DG and CA1 region detected in each slice (Figure 3.5c).

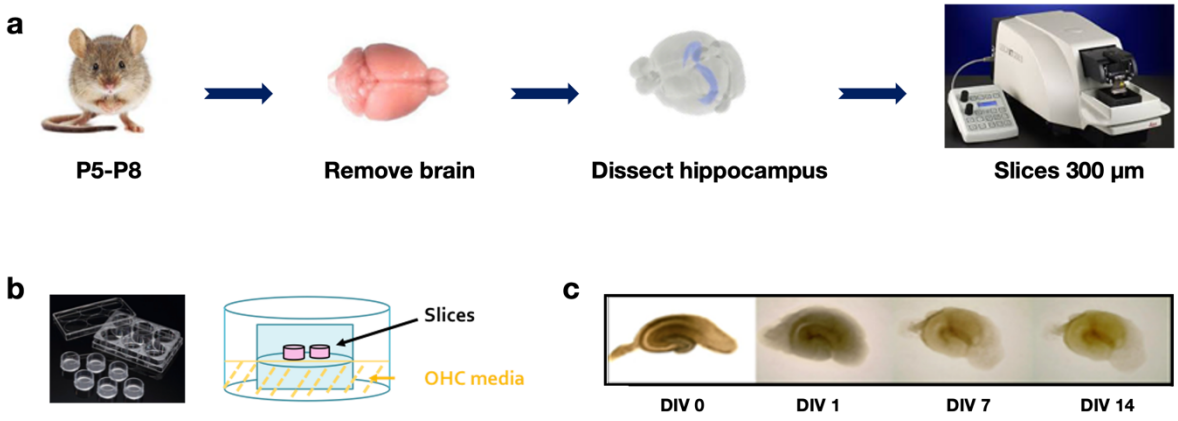

Figure 3.5 Workflow for acquiring organotypic hippocampal slices from transgenic A53T mice.

a. A53T mice pups (postnatal day 5-8) were obtained. The hippocampus was carefully dissected and perpendicular slices of 300 µm thickness were obtained. **b.** Organotypic hippocampal slices were cultured in 6-well plates on a membrane porous culture insert and culture media were changed every two days. **c.** Slices were cultured up to 14 days *in vitro* becoming transparent over time with preserved hippocampal structures such as the dentate gyrus (DG), the CA1 and CA3 region.

I examined the cellular complexity of the brain OHS by performing immunocytochemistry for neuronal, astrocytic and microglia specific markers. As expected, I observed preservation of the cellular heterogeneity: β3-tubullin (TUJ1) staining revealed a dense neuronal network with clearly identified hippocampal structures being preserved, DG, CA1 and CA3 (Figure 3.6). Staining was also detected with the astrocytic marker glial-fibrillary astrocytic protein (GFAP) and the microglia-specific marker, IBA1 as shown in Figure 3.6. Using the high content imaging software *Harmony* at Eli Lilly, I reconstructed the 3D morphology of the slices and I observed that astrocytes formed a glial scar on top of the slice, whereas microglia formed a dense network at the bottom of the slice and neurons were evenly distributed throughout the OHS (Figure 3.6 inner right panel). These data suggest that there is a degree of astrocytic scarring and microglial activation with time in culture.

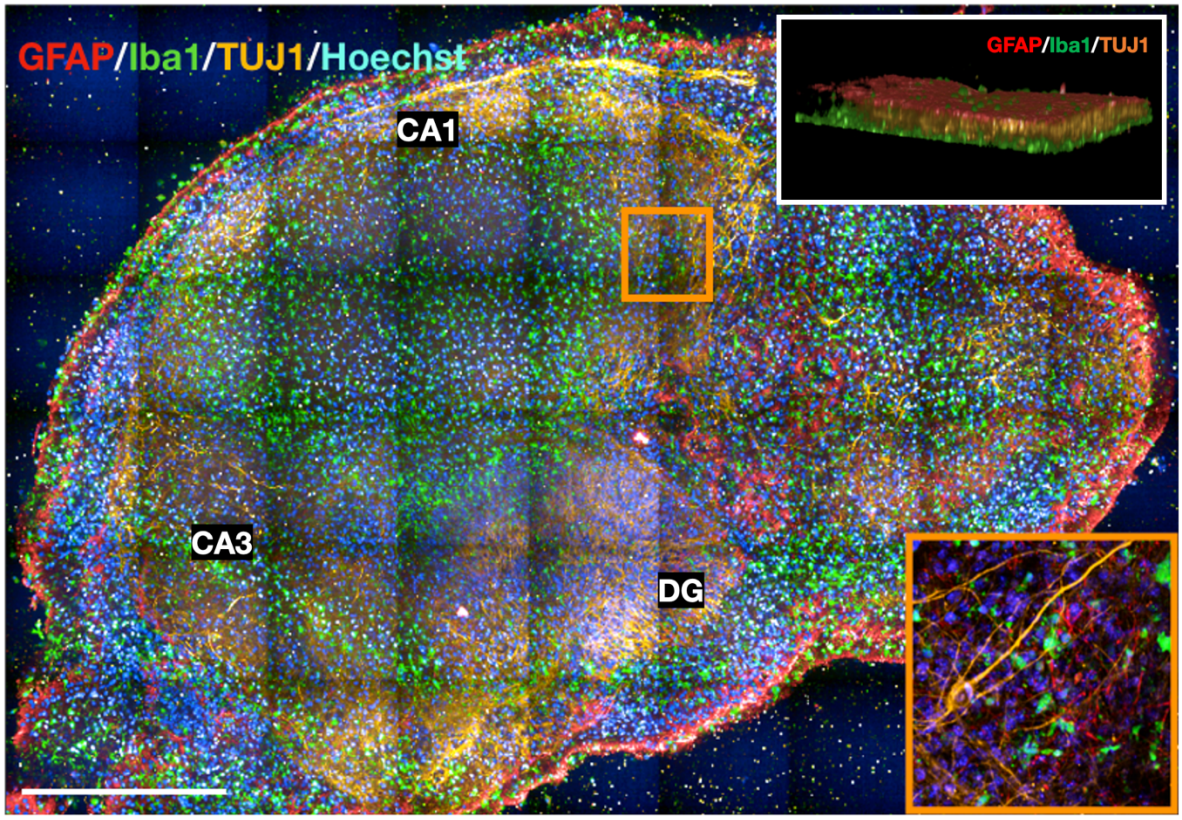

Figure 3.6 Long term organotypic hippocampal slices maintained their structural and cellular composition.

Organotypic hippocampal slices preserved their cellular heterogeneity as revealed by immunohistostaining for neuronal specific cytoskeleton marker βIII-tubullin (TUJ1), glial fibrillary astrocytic protein (GFAP) and homeostatic microglia marker, Iba1. The neuronal, microglia and astrocytic populations were evenly distributed across the slice. The classical hippocampal structures, DG, CA1 and CA3 were also visible as revealed by the neuronal staining. Images were acquired in Z-plane stacks confocal mode and merged to create a tiled image of a whole slice. 3D representation (white box) revealed that astrocytes (GFAP-red) were distributed on the top of the slice with the microglia (IBA1-green) being located at the bottom and the neurons (TUJ1-orange) evenly distributed throughout the slice. Images were acquired at the Eli Lilly laboratories (UK) using high throughput imaging system, Opera Phenix and the Harmony imaging software. Scale bar at 500 μm.

3.2.2.2 Addition of synthetic α-synuclein fibrils induced intraneuronal accumulation of pSYN and microglia activation

Our collaborators at Eli Lilly had previously optimised the culture conditions for the OHS and had additionally shown functional viability of OHS by performing calcium imaging electrophysiological studies (McCarthy et al., 2021). Therefore, once I had established that OHS maintained their structural architecture and cellular heterogeneity over a 2-week period, I then sought to induce neuronal aggregation by inoculating the slices with the aforementioned α-synuclein fibrils.

OHS from TgA53T mice pups were seeded with 1 μM of α-synuclein fibrils on DIV7. The fibrils were added as a single treatment directly in the culture media followed by media changes every two days thereafter until DIV14, when the slices were fixed and stained for pSYN and the microglia-specific marker, IBA1 (Figure 3.7a). As a positive control, OHS were treated with 1 μM of lipopolysaccharide (LPS). LPS is known to induce the activation of microglia (Boche et al., 2013, Wang et al., 2015a) into an M1-type phenotype that is typically associated with the secretion of cytokines and pro-inflammatory markers (Ye et al., 2020).

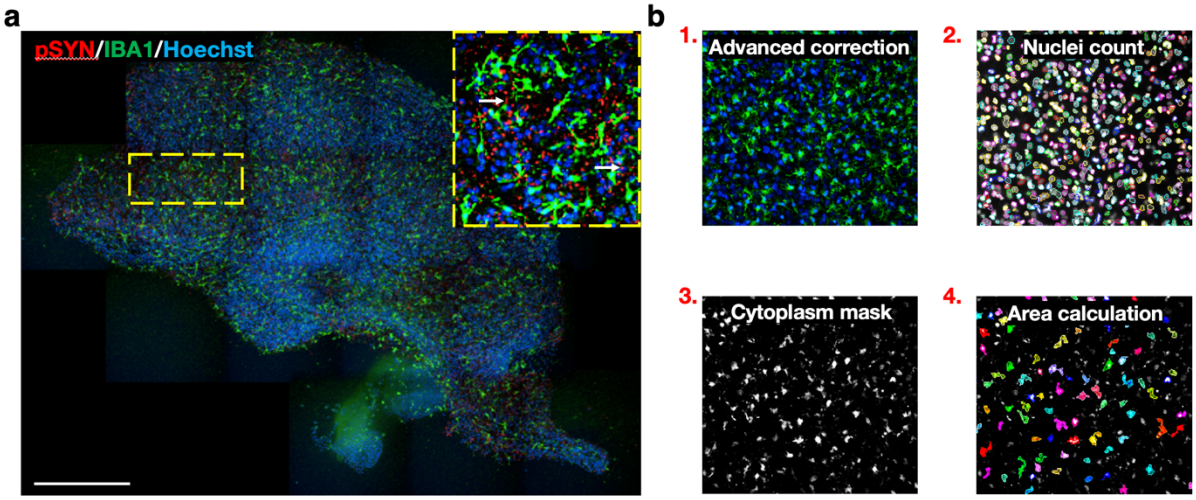

Figure 3.7 α-synuclein fibrils induced pSYN positive neuronal inclusions.

a. A53T organotypic hippocampal slices were seeded with α-synuclein fibrils on day DIV7 and were fixed after one week. Slices were stained for pSYN and microglial marker IBA1. Images were acquired in Z-stacks, maximum projected and merged to produce a whole tiled image. Yellow insert on top left corner depicts one single tile. White arrows show the pSYN positive inclusions **b.** Imaging pipeline designed to (1) correct the fluorescent background, (2) identify the total nuclei population, (3) identify nuclei positive objects with a cytoplasmic marker and (4) select and calculate the total surface (in μm^2) of the Iba1 cytoplasmic marker. Images acquired using Opera Phenix and 40x water immersed objective, Z-stacks max projected. Scale bar at 500 μM.

By using the *Harmony* software analysis, I designed an analysis pipeline that enabled me to measure the surface occupied by microglia on the slice surface in response to either fibril or LPS treatment (Figure 3.7b). The first step of the analysis included maximum projection of the acquired stack images and flatfield correction before being filtered to eliminate fluorescent background (Figure 3.7b1) (Katsikoudi et al., 2020). Then, the pipeline identified the nuclei (Figure 3.7b2) and from this population identified the microglia only cells by creating a mask, which then detected IBA1 positive cytoplasm (Figure 3.7b3). The surface of the selected IBA1-positive microglial cells was then calculated in μm^2 (Figure 3.7b4). I observed that microglia under basal conditions had the characteristic ramified homeostatic morphology

(Figure 3.8a). However, under LPS induced inflammatory activation microglia shortened their cellular bodies acquiring a distinguished amoeboid-like shape (Figure 3.8b). Similarly, after seeding with the α-synuclein fibrils, I observed that microglia lost their ramified homeostatic morphology (Figure 3.8c) and occupied significantly larger surface area on the OHS when compared to baseline conditions and the LPS treated slices (Figure 3.8d).

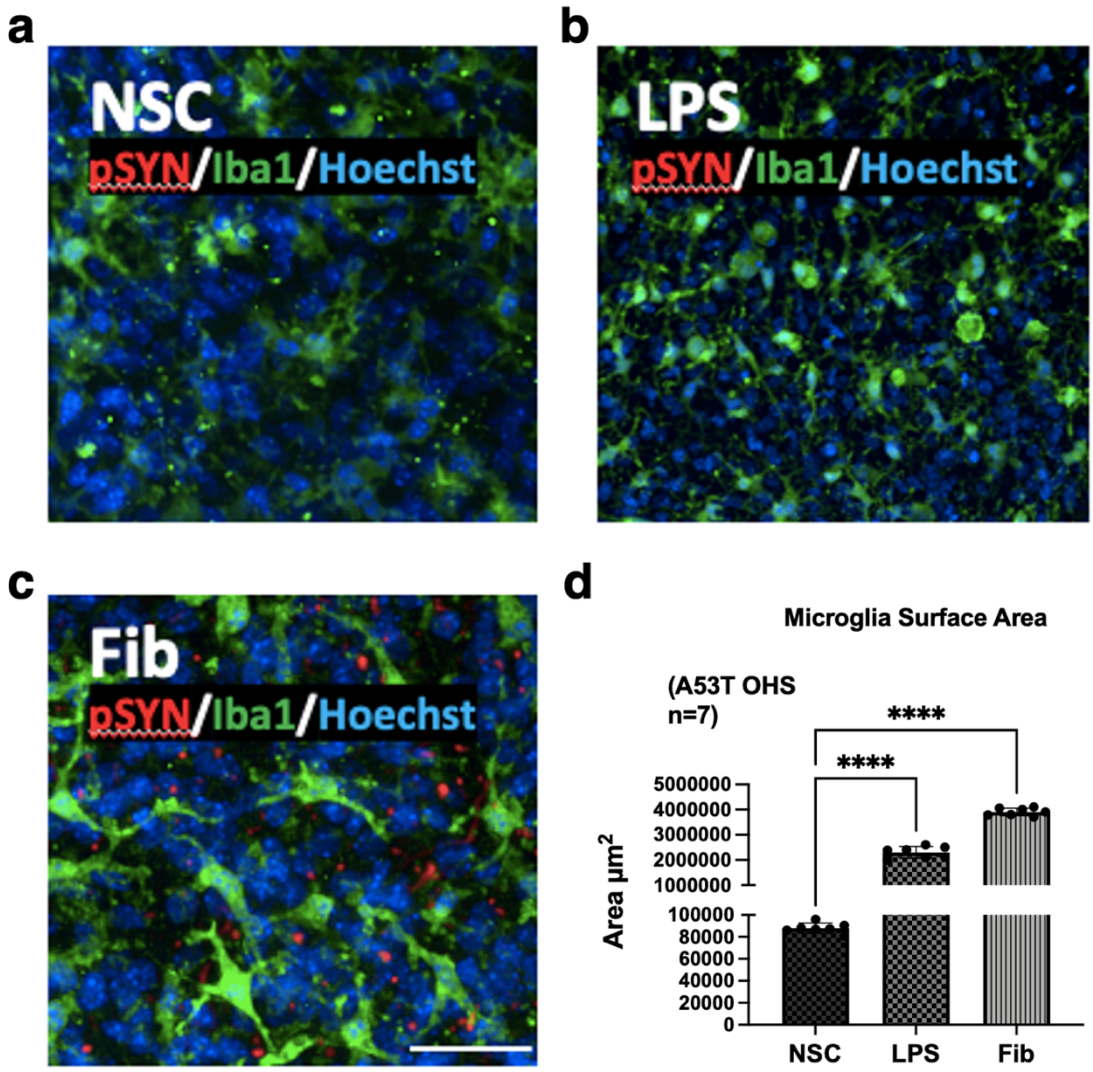

Figure 3.8 Microglia in organotypic hippocampal slices were activated in response to seeded intraneuronal α-synuclein aggregation.

a. IBA1 positive microglia exhibited a homeostatic ramified morphology under basal culture conditions. **b.** LPS at 10 ng/mL induced the microglia to acquire a predominantly amoeboid-like shape. **c.** Fibrils at 1 µM induced microglial activation similar to LPS as revealed by their primed activated morphology. **d.** Under baseline conditions microglia occupied an average of 87,931 μm^2 of the total surface area of the tissue slice. LPS induced a 26-fold increase of the surface area that microglia occupied, whereas the fibrils doubled that effect. Images are individual image fields from a single stitched organotypic slice image. Images were acquired using Opera Phenix and 40x water immersed objective, Z planes max projected. Scale bar at 20 µM. NSC-non seeding control, LPS-lipopolysaccharides, Fib-fibrils. Each dot represents n=7 biological repeats and data are mean ± s.e.m. ***P<0.001 by one-way ANOVA followed by Dunnett's multiple comparisons test.

“M1-type” activated microglia are primed to respond against pathogens or other antigenic stimuli by producing pro-inflammatory cytokines, such as IL-1β, IL-6 and TNFα. IL-6 has been described as a pleotropic cytokine that modulates microglial activation under various conditions, but it remains controversial whether it exerts beneficial or detrimental effects (Recasens et al., 2021). I assessed IL-6 secretion in my OHS model with an ultra-sensitive Simoa assay, following treatment with α-synuclein fibrils. For these experiments I collected conditioned media over the culture period of 2 weeks and compared the levels of IL-6 between seeded and control conditions. I observed that IL-6 secretion was significantly increased for all slices after dissection and reduced by approximately 50% after a week in culture and by 75% after two weeks (Figure 3.9). Levels of IL-6 were slightly higher in seeded OHS but this did not reach significance (Figure 3.9). These data suggest that IL-6 is not a specific response to aggregation.

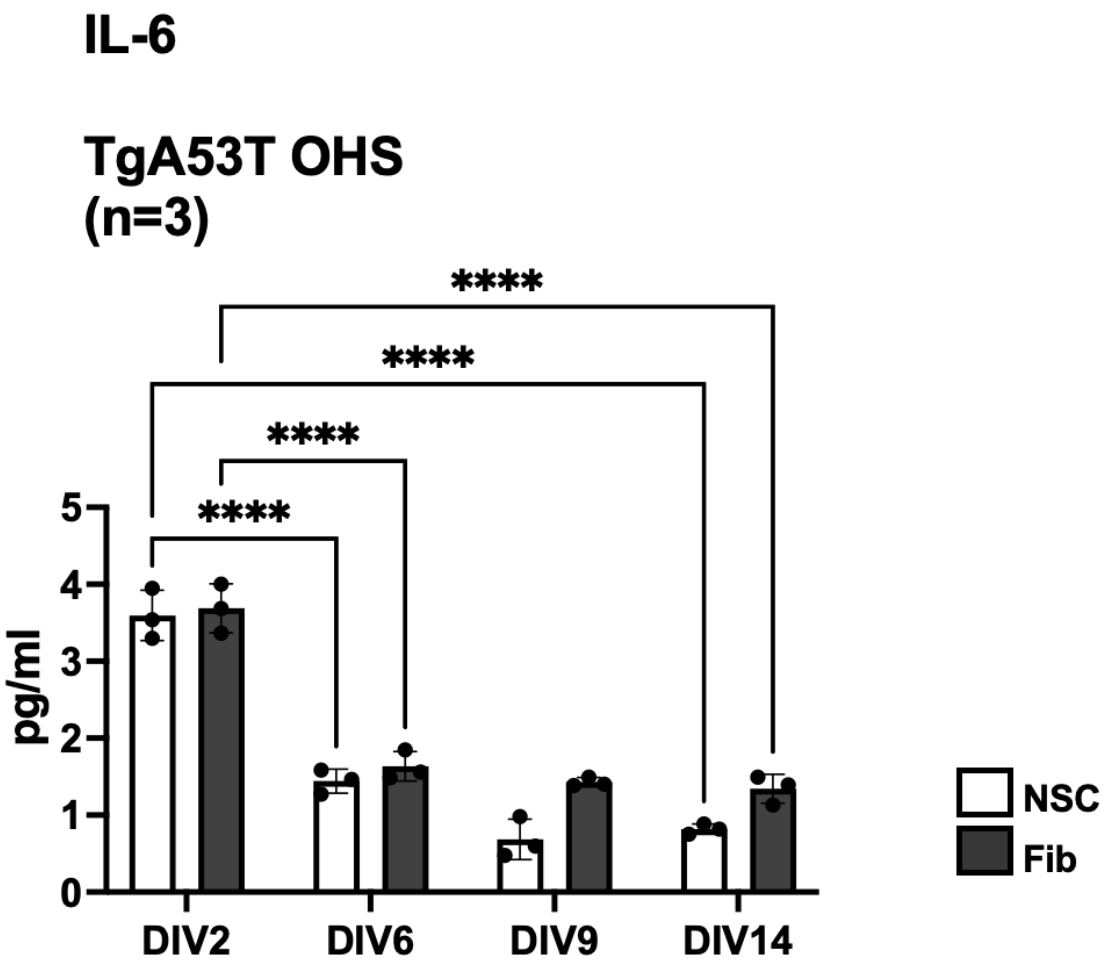

Figure 3.9 Secretion of pro-inflammatory cytokine IL-6 in the conditioned media of α-synuclein fibril treated A53T OHS.

Conditioned media was collected from OHS on DIV2, DIV6 and after the fibril treatment on DIV9 and DIV14 when the slices were fixed. IL-6 concentration (pg/mL) was measured. NSC-non seeding control, Fib-fibrils. Each dot represents n=3 technical repeats and conditioned media was pooled from n=7 slices. Data are mean ± s.e.m. ****p>0.05 by two-way ANOVA followed by Šídák's multiple comparisons test.

3.2.3 Pilot studies with human organotypic cultures

Having established the OHS model using mouse tissue, I attempted to adapt the protocol for the study of human long-term organotypic slice cultures with a view to develop a model of α-synuclein aggregation in the living human brain tissue and study neuron-microglial interactions. By working with my second academic supervisor, Associate Professor Olaf Ansorge and the team of Professor Peter Somogyi we obtained patient consent to use cortical tissue which was surgically removed from epilepsy or glioblastoma surgeries. The isolated tissue was constantly saturated with 5%CO_2 and 95%O_2. I obtained slices of two different thickness, 300 and 350 µm by cutting perpendicular to the pia matter (Figure 3.10a). The slices were cultured on the membrane porous inserts as used for mouse OHS. I first aimed to optimise the culture media. Previous studies had shown that human slices cultured with human cerebrospinal fluid preserved better their electrophysiological properties, including synaptic connectivity and action potential generation, when compared to an artificial culture media (Schwarz et al., 2017). However, I observed poor viability when I cultured the slices using human CSF as evidenced by the transition of the colour to yellow-ish and detachment of the slices from the membrane. I then used an artificial culture media similar to the one used for the mice OHS. Under these conditions I observed good viability as measured by lactate dehydrogenase (LDH) release in the culture media over a culture period of 18 days (Figure 3.10b). I also observed dense neuronal network using the neuronal dendritic marker, MAP2 (Figure 3.10c). In complementary experiments, Professor Somogyi's group labelled acute human slices with biocytin, and the team visualised GABAergic and pyramidal neurons (Figure 3.10d).

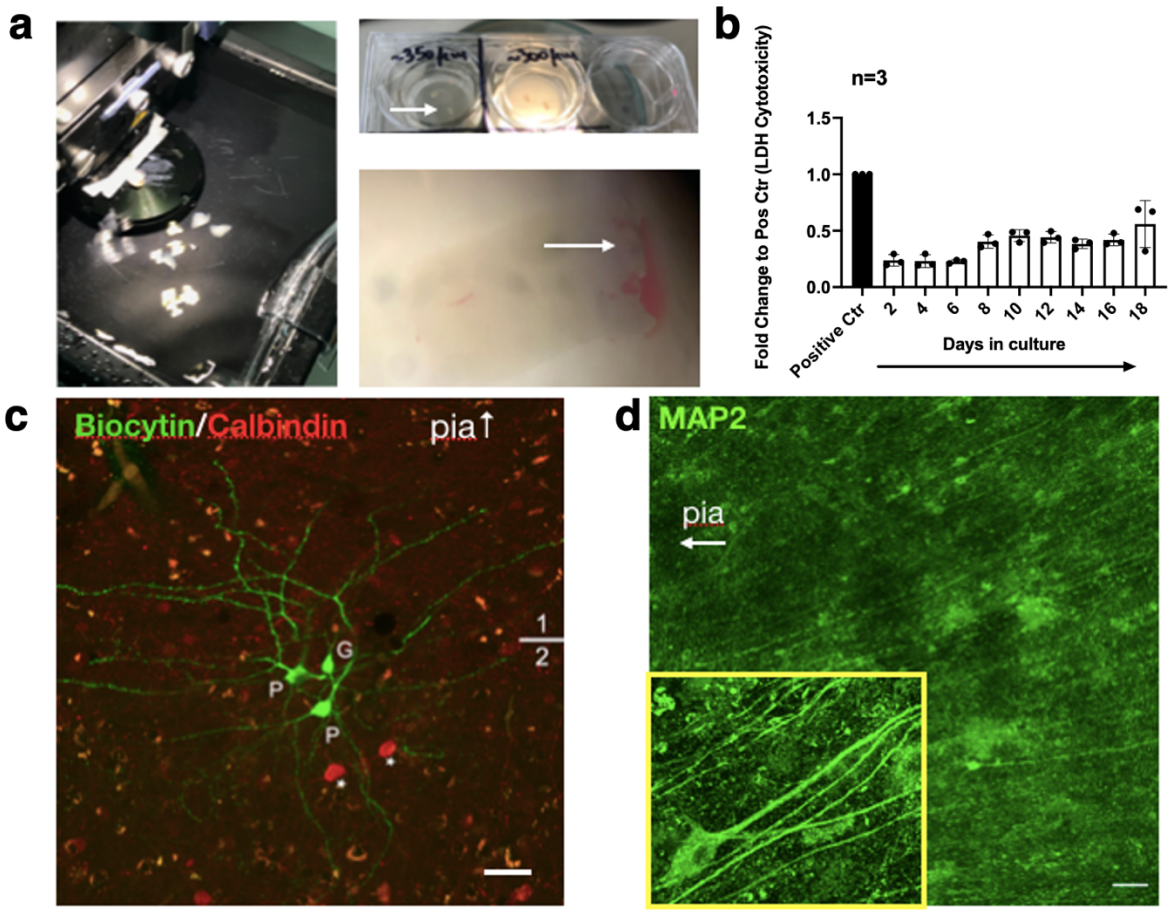

Figure 3.10 Workflow of human cortical slices as an organotypic culture model.

a. Small piece of surgically removed cortical tissue was cut perpendicular to the pia matter and the acquired slices had 300 and 350 µm thickness. Slices were cultured on membrane inserts (white arrow, top panel) and were stereoscopically evaluated daily (white arrow, bottom panel). **b.** Conditioned media was collected over a culture period of 18 days *in vitro* and LDH measurement revealed almost half-fold levels of cytotoxicity when compared to a positive control. **c.** MAP2-positive neurons on a fixed organotypic cortical slice. **d.** Pyramidal (P) and GABA-ergic (G) neurons as stained by biocytin. Neurons were in layer 2 of a human cortical slice taken from the right inferior temporal gyrus. Calbindin-D28k was detected in some GABAergic neurons (stars). Each dot represents n=3 biological repeats and data are mean ± s.e.m. followed by one-way ANOVA with Dunnett's multiple comparisons. Images acquired with Zeis Confocal Microscope, 20x objective, bar at 50 µm.

3.3 Discussion

Brain organotypic slices have emerged as an important research tool to study neurodegeneration in Parkinson's disease (Barth et al., 2021, Shrivastava et al., 2020). Their main advantage is that they maintain the three-dimensional organisation and cellular complexity of the brain. In this respect organotypic slices could bridge studies between the reductionist *in vitro* cultures and *in vivo* animal models (Ucar et al., 2021). Microglia, the brain's resident immune cells, may contribute to the progression of Parkinson's disease and other neurodegenerative diseases (Bachiller et al., 2018). In the OHS model, I have shown that mouse brain microglia preserve their characteristic ramified homeostatic morphology that has been documented *in vivo*, possibly because they maintain the connections with the other cell types thus representing a research system that is closer to the *in vivo* conditions compared to *in vitro* cultured microglia (Delbridge et al., 2020). Herein, I chose to use hippocampal slices rather than slices from SNc or the striatum (*in vivo* these regions are more affected by Lewy pathology) because they are more robust (Shrivastava et al., 2020), but also because of the involvement of the hippocampus in Parkinson's disease-related cognitive decline. I have shown that microglia become activated in the murine *ex vivo* slices following intra-neuronal pSYN aggregation induced by *de novo* α-synuclein fibrils.

Traditionally, the hippocampus, the temporal lobe structure responsible for the processes of memory and learning, has been implicated in Parkinson's disease dementia or dementia with Lewy bodies (DLB). Importantly, up to 25% of patients with Parkinson's have cognitive difficulties from the onset of their disease and dementia is detected in up to 80% of patients 20 years after their diagnosis (Gan et

al., 2021, Hely et al., 2008). The hippocampus is also closely connected with dopaminergic neurons. Excitatory glutamatergic projections from the hippocampus extend to the nucleus accumbens, which controls tonic inhibition of dopaminergic neurons (Lisman and Grace, 2005). Also, increased hippocampal activity promotes dopamine release within the nucleus accumbens (Goto and Grace, 2005). Studies performed using human post-mortem samples revealed that hippocampal atrophy and associated α-synuclein pathology in parkinsonian brains may underpin the onset of cognitive impairment, regardless the onset of dementia (Jokinen et al., 2009). For these reasons, the study of OHS is a relevant model in Parkinson's disease pathogenesis. My immunostaining showed that hippocampal neurons were successfully seeded with fibrils and developed α-synuclein aggregation.

Previous efforts to model tauopathies and synucleinopathies using *ex vivo* organotypic slices resided in viral overexpression of tau and α-synuclein (Croft et al., 2019a). However, in the present study I have demonstrated that a single treatment of TgA53T slices with *de novo* α-synuclein fibrils sufficed to result in pSYN positive inclusions. This has been recently reported during the course of my studies (Barth et al., 2021). In contrast to previous studies, I added the *de novo* fibrils in the culture media rather than using an injection form of treatment or a single drop on the slices (Elfarrash et al., 2019, Barth et al., 2021). I did so to avoid mechanical damage of the slices and reduce cellular stress. The pSYN burden induced in these slices was rather high and in accordance to previously described *in vivo* mouse models compared to wild-type mice (Luk et al., 2012b). The morphology of the pSYN inclusions in my model, was immunohistochemically similar to those observed in the brains of transgenic mice that were injected with *de novo* fibrils (Bétemps et al., 2014, Tarutani

et al., 2018). The inclusions appeared neuritic-like, as well as encircling the nucleus of the cell body. These observations support the concept of templated aggregation in neurodegeneration (Jucker and Walker, 2013, Goedert, 2001).

The diverse nature of α-synucleinopathies suggests that different pathological inclusions may be the result of distinct α-synuclein species (Peng et al., 2018). One limitation of my seeded organotypic model (Figure 3.1), was that the neuronal pSYN inclusions were the result of a single conformational α-synuclein strain. Evidence acquired with cryo-electron microscopy has showed for example, that the α-synuclein inclusions found in glia cytoplasm in multiple systems atrophy (MSA) are conformationally and biologically distinct from the inclusions of the Lewy bodies in Parkinson's disease (Peng et al., 2018, Li et al., 2018). Differential α-synuclein strain-related seeding properties have been also reported in mouse organotypic slices (Shrivastava et al., 2020). The seeding differences among fibrils polymorphs have been attributed to differential binding and uptake from the neurons and that results in impaired neuronal networks.

To overcome the argument of disease specificity and suitability of *de novo* seeds in neurodegeneration, α-synuclein and tau aggregates have been amplified *in vitro* from patients' brain extracts using protein misfolding cyclic amplification (PMCA). *De novo* α-synuclein fibrils have been shown to be structurally different from brain extracted and amplified fibrils (Strohäker et al., 2019). The reasons behind this remain elusive, however it is possible that post-translational modifications or different interacting partners may be responsible. Regardless the apparent differences between *de novo* and PMCA fibrils, access to human brain tissue remains limited. It is also unclear to what degree PMCA amplified fibrils recapitulate those found in the

brain. Taking these factors into consideration, I opted in using *de novo* α-synuclein fibrils for the majority of my studies.

Recent evidence from our own laboratory has demonstrated that human induced pluripotent derived dopaminergic neurons exhibit different phenotypes when seeded with various α-synuclein conformers, either *de novo* generated or templated from parkinsonian brain extracts (Tanudjojo et al., 2021). Strain-related microglia responses have also been reported *in vivo*. Injected PMCA α-synuclein fibrils from MSA brains induced higher IBA1 activation in wildtype mice compared to fibrils from Parkinson's disease and DLB brains (Strohäker et al., 2019). Another immunohistochemistry-based study in mice reported that differently prepared *de novo* α-synuclein fibrils induced varying degrees of IBA1-related activation (Liu et al., 2021). Specifically, strains prepared in mild acidic pH buffer without KCL resulted in enhanced IBA1 activation. It is possible that microglia exhibit different phenotypes when exposed to neurons seeded with different α-synuclein strains.

In my OHS I observed that microglia maintained their ramified homeostatic morphology in culture which suggests that the preparation of the slices does not cause persistent activation. This is supported by the transient elevation of IL-6 and the successful activation with LPS or fibrils subsequently. This is in contrast to cultures of purified microglia *in vitro* which reverse to macrophage-like cells and are not suitable for phenotypic studies (Timmerman et al., 2018).

Under homeostasis microglia monitor their microenvironment, provide support to neurons by secreting neurotrophic factors and maintain the neuronal synaptic plasticity by synaptic pruning. Microglia are activated in response to toxins, and this involves a morphological transformation, as well as secretion of pro-inflammatory

cytokines. I confirmed that in my model microglia acquired a rounded appearance after a single treatment with either LPS or endotoxin-free α-synuclein. Further activation mechanisms have been reported in literature that involve increased signalling of TLRs that result in microglia priming in organotypic slices (Coleman et al., 2020). It was previously observed that protective effects of microglia may occur without their activation: In a similar OHS set up, treated with oligomer enriched Aβ peptide, the microglia did not transition to a morphological activation state yet exhibited neuronal protection (Richter et al., 2020). Inherently, ramified microglia are not “resting’’ but actively maintaining homeostatic functions.

Interestingly, I found subtle differences in the morphology of microglia under the two conditions: LPS induced a classical amoeboid shape, whereas the microglia located around neuronal pSYN-positive inclusions were primed, with shorter dendritic branches compared to the homeostatic ramified microglia and at places were bipolar (Figure 3.8). This compilation of various shapes has been characterised as an ‘’intermediate’’ state of activation and demonstrates the versatile morphological phenotypes of microglia (Davis et al., 2017). However, due to their dynamic nature, correlating microglia morphology with their function remains challenging. pSYN microglia inclusions in OHS from TgA53T mice have been reported before (Barth et al., 2021). Nevertheless, this is not something I observed in my set up. That can be explained by the cell-to cell propagation model. Microglia inclusions appeared in literature with a 2–3-week delay following neuronal inclusions suggesting that longer-term in culture may have been required to observe this phenotype.

I further sought to correlate microglia morphological activation under conditions of seeding with secretion of the pro-inflammatory cytokine IL-6, by

examining its concentrations (pg/mL) in the cultured media of organotypic slices over time (Figure 3.9). I observed increased levels of IL-6 within the first two days of the culture, which is a consequence of acute injury from the slicing procedure. The levels of IL-6 decreased on DIV6 and under baseline conditions were further reduced on DIV9 and remained stable until the end of the culture period on DIV14. In fibril treated slices, IL-6 levels were also reduced by DIV6 as expected but the levels from DIV9 onwards were slightly higher compared to non-seeded slices. Although not significant nevertheless, this finding is consistent with the activated morphology in response to neuronal α-synuclein aggregation and suggested an early activation stage, possibly similar to the now obsolete "M1-subtype". This phenotype was characterised by secretion of pro-inflammatory cytokines, such as IL-6, IL-1β and TNFα that promote apoptotic and cytotoxic events, whereas "M2-subtype" has not been correlated with protective effects. It should be noted that transcriptomic studies have now shown that activated microglia in neurodegeneration fall into many various sub-groups and this will be discussed I more detail in subsequent chapters (Ransohoff, 2016).

Two unforeseen circumstances necessitated the early termination of these studies: Firstly, the Eli Lilly UK facilities closed in October 2019, and I did not have access to necessary equipment and mice to perform further experiments. Secondly, the coronavirus epidemic and recurrent lockdowns severely disrupted the access to human neurosurgical specimens for further development of the human model. Outstanding questions that I would have liked to pursue include the following: (1) assess additional markers of microglial phagocytosis, such as complement components C3α and C3β using a combination of ELISA in media and qPCR

following RNA extraction. (2) Deplete microglia from the culture slices using pharmacological agents and assess whether this has beneficial or detrimental effects to neurons following seeded aggregation. (3) Attempt to seed aggregates in human slices and measure neuronal viability based on neurofilament release (Ishii et al., 1979, Goldman et al., 1983) and histology as well as microglial changes.

Overall, this data gave initial promising evidence that microglia are activated in response to intraneuronal aggregation. To bypass the limitations imposed by external factors, and study in more detail this neuron-microglial interaction, I sought to set up a human iPSC-based co-culture model under conditions of intraneuronal α-synuclein aggregation. These findings are described in Chapters 4 and 5.

Chapter 4: A microglia-neuronal co-culture system to decipher the microglial response to intraneuronal α-synuclein aggregation

4.1 Introduction

4.1.1 Modelling the cellular pathology of Parkinson's disease using human stem cells

The introduction of iPSCs by Yamanaka in 2006 (Takahashi and Yamanaka, 2006), transformed cell-based research because they offer an enduring source, which can provide different cell types that retain genomic information from patients (Figure 4.1) (Santostefano et al., 2015). It is well documented that there are variations of protein peptides and isoforms, as well as post-translational modifications between human and mouse cells. Therefore, the study of human iPSC-based models circumvents the species differences when studying disease-causing proteins (de Rus Jacquet et al., 2021).

iPSC-derived midbrain dopaminergic neurons (DN) have been extensively used to investigate pathogenic mechanisms in Parkinson's disease. Even though reprogramming removes epigenetic modifications, disease-related phenotypes arise from the patient's genetic composition that could represent the earliest stages of the disease (Studer et al., 2015). So far, most iPSC-based models investigate the effects of monogenic mutations, such as the triplication of the α-synuclein gene (*SNCA*) (Tanudjojo et al., 2021, Sánchez-Danés et al., 2012a, Devine et al., 2011). Although *SNCA* mutations or multiplications are very rare, these iPSC lines exhibit α-synuclein accumulation or susceptibility to aggregation and associated phenotypic

abnormalities that may be relevant to sporadic Parkinson's disease. However, when compared to healthy controls, iPSC lines deriving from patients with sporadic Parkinson's disease do not manifest obvious α-synuclein accumulation (Soldner et al., 2009, Sánchez-Danés et al., 2012b).

Neuroinflammation in Parkinson's disease has been shown in post-mortem brains where there is microglial activation and in patients who exhibit elevated inflammatory markers in the cerebrospinal fluid (McGeer and McGeer, 2008). Nevertheless, the exact role of microglia using iPSC-based models remains unexplored. An iPSC-derived co-culture system of microglia and dopaminergic neurons could determine microglial phenotypes in Parkinson's disease and whether their activation results in protective effects or instead, acceleration of the pathology (Simmnacher et al., 2020). Recent meta-analysis data has revealed that so far 385 human neuronal iPSC-derived lines have been generated in a total of 67 original research studies demonstrating the wide range of available data from iPSC derived research in Parkinson's disease (Tran et al., 2020). However, iPSC-based research for Parkinson's is still lacking models that incorporate the non-neuronal phase of the disease, such as microglia and astrocytes.

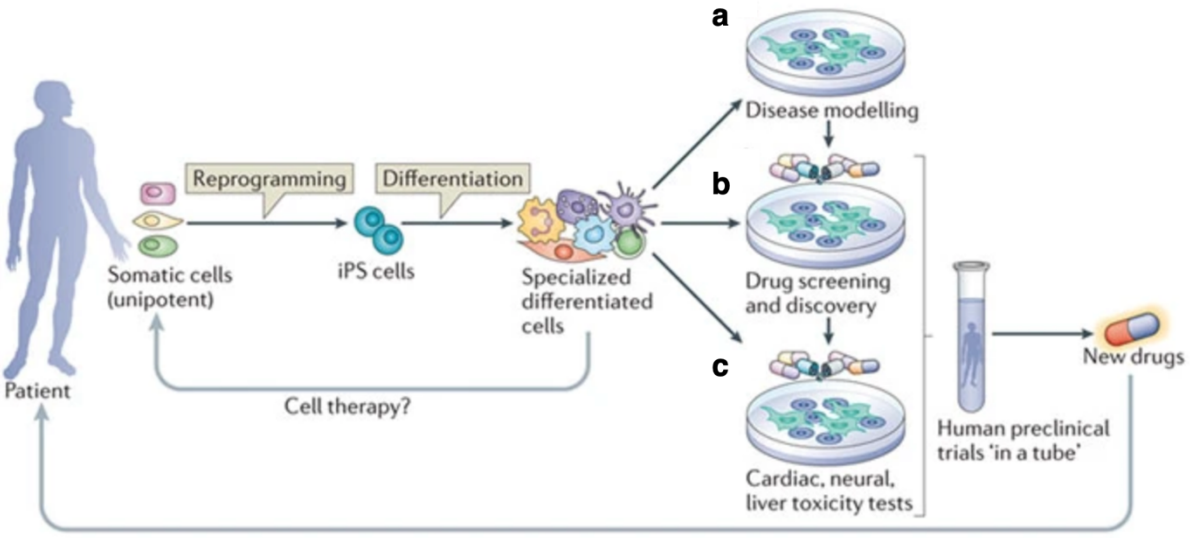

Figure 4.1 Generation, differentiation and applications of human iPSC-derived cells.

Adult somatic cells (unipotent) from any patient can be obtained and reprogrammed into induced pluripotent stem cells (iPSCs). iPSCs can be differentiated into various cell types that can be used for an array of applications. **a**. Human iPSCs are a popular *in vitro* tool to model disease phenotypes to achieve greater understanding of the molecular mechanisms, for example in the case of Parkinson's disease. **b**. Further, iPSCs are widely used in drug screening and discovery to determine the effects of candidate drugs and compounds, as well as characterise target pathways. **c**. Additionally, iPSCs are a useful tool to establish the cardiac, neural and liver toxicity of the drug compounds. That concept in combination with the screening studies represent what is termed as human preclinical (*in vitro*) trials ''in a tube'', one of the earliest stages in the drug discovery process. Image adapted from (Bellin et al., 2012).

4.1.2 Differentiation of dopaminergic neurons

Anatomically, midbrain dopaminergic neurons are derived from the substantia nigra pars compacta (SNc) (A9 group) and the mesolimbic ventral tegmental area (VTA) (A10 group). They are large, unmyelinated cells and a single neuron can generate thousands of synapses. Additionally, they are anatomically and functionally a heterogenous neuronal group with projections and connections across various brain nuclei systems. Their heterogeneity is striking at the molecular level, but dopaminergic neurons share commonalities regarding the core molecules involved in the synthesis of dopamine e.g., tyrosine hydroxylase (TH) and dopa decarboxylase (DDC)(Poulin et al., 2018). Because of their extensive arborisations and spontaneous pacing, dopaminergic neurons are under heavy metabolic stress and have a high bioenergetic demand. Nevertheless, it remains unclear whether these properties contribute to the selective vulnerability of dopaminergic neurons from SNc in Parkinson's disease (Hartfield et al., 2014). Due to their extreme diversity, it is important that stem cells differentiate into dopaminergic neuronal subtypes, which are relevant to areas that are vulnerable to Parkinson's disease, such as the SNc.

To date, several protocols have described the generation of midbrain dopaminergic neurons from iPSCs (Gonzalez et al., 2013, Gantner et al., 2020, Arenas et al., 2015). One of the best protocols is the floor-plate by using small molecules (Kriks et al., 2011). The superiority of the aforementioned protocol lies on the high yield of dopaminergic neurons (>50-70%), as well as the fact that it follows *in vitro* the *in vivo* developmental pathways by applying an array of small molecules. The Studer group developed a novel floor-plate protocol to differentiate midbrain dopaminergic neurons that were successfully engrafted *in vivo* demonstrating complete specification of the generated cells (Kriks et al., 2011). This group induced

iPSCs into a primitive neuroectoderm by inhibiting the TGFβ/activin/nodal/bone morphogenetic protein (BMP) pathways, which signal via SMAD 2/3 and SMAD 1/5 (Bond et al., 2012). The dual SMAD inhibition was further refined by addition of sonic hedgehog (SHH) and fibroblast growth factor 8 α (FGF8α) that directed neural induction towards an anterior floor plate identity (Simmnacher et al., 2020). Moreover, activating the canonical WNT/β-catenin signalling pathway by addition of a GSK3β inhibitor, CHIR99021 resulted in formation of midbrain dopaminergic neurons from stem cells after 11 days (Kriks et al., 2011). The work by the Studer group was ground-breaking and the use of CHIR99021 was critical in generating high-specificity midbrain dopaminergic neurons from patient stem cells. Those are characterised by a high percentage of TH-positive cells, as well as co-expression of transcription factors FOXA2 and LMX1A, which drive neurogenesis of dopaminergic neurons (Arenas et al., 2015). By day 25 the floor-plate protocol resulted in the generation of midbrain dopaminergic neurons as shown by immunocytochemistry where cells co-expressed neuronal specific marker, TUJ1 (β3-tubullin) and dopaminergic specific marker, TH (Kriks et al., 2011). The neurons generated from this protocol were also characterised by expression of TFF3, EBF1/3 and TTR which are specific to human brain SNc neurons. Furthermore, the iPSC-derived neurons were cultured for several weeks *in vitro* and were shown to acquire electrophysiological properties that are characteristic of mature dopaminergic neurons.

4.1.3 Microglia differentiation

Although the generation of human iPSC-derived neuronal subtypes was achieved early, protocols for the successful differentiating human microglia-like cells were not available until 2016 (Speicher et al., 2019). A key limitation was the fact that CNS microglia follow a different embryonic ontogenesis compared to peripheral tissue resident macrophages. More specifically, microglia progenitors have been described *in vitro* to originate from the yolk sac and they are *PU.1* and *Irf8* dependent (Kierdorf et al., 2013b), but independent from Myb, which is a transcription factor necessary for the generation of haematopoietic macrophages (Figure 4.2) (Gomez Perdiguero et al., 2015a). The definitive proof that microglia are derived from mesoderm came from genetic studies in mice that lack the myeloid cell transcription factor PU.1 and resulted in complete absence of microglia in the brain (McKercher et al., 1996). Based on this observation several protocols have been developed to generate microglia-like cells form iPSCs that are independent of the primitive haematopoietic fate (Abud et al., 2017, Haenseler et al., 2017a, Muffat et al., 2016, Douvaras et al., 2017).

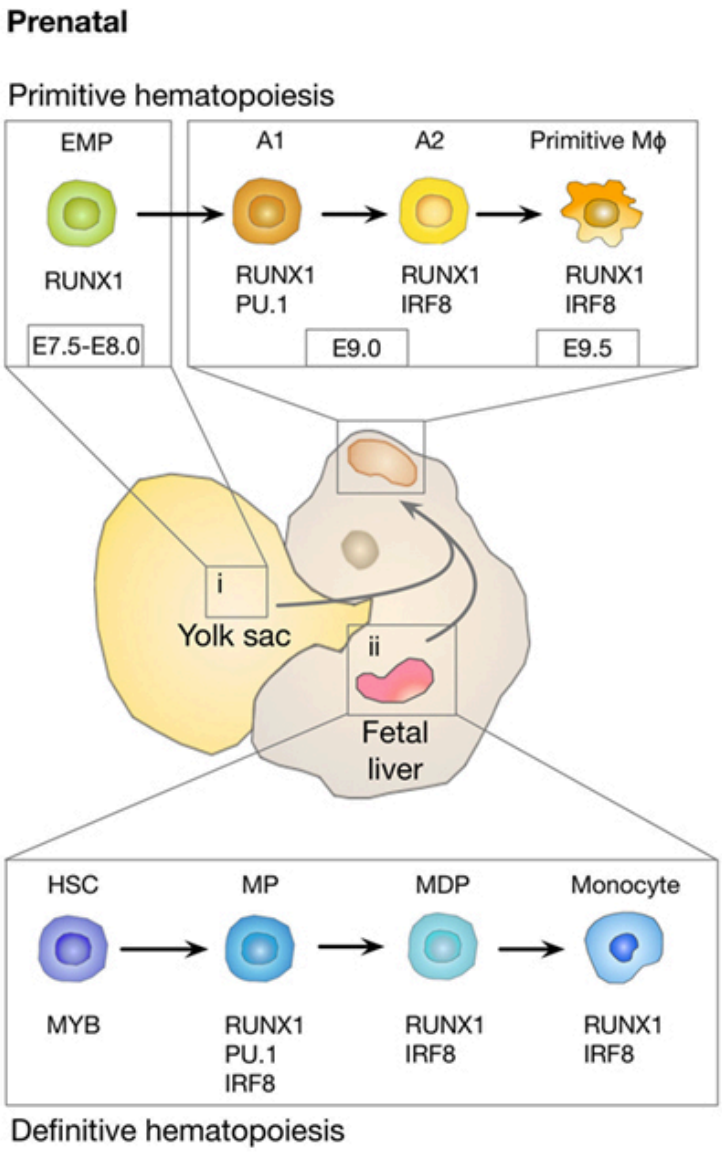

Figure 4.2 Ontological origin of macrophage subpopulations in the central nervous system (CNS).

The first wave of myeloid cell development occurs in the yolk sac (i) between E7.0 and E8.0 with a process that is termed primitive haematopoiesis and results in generation of erythromyeloid progenitors (EMP). EMP cells further become A1 (cKit^{+}, CX3CR1^{-}) and A2 (CX3CR1^{+}) that ultimately give rise to microglia, perivascular macrophages (pvMϕ), choroid plexus macrophages (cpMϕ) and meningeal macrophages (mMϕ). Microglia originate from yolk sac cell progenitors, whereas non-parenchymal CNS macrophages are derived from foetal liver (ii) progenitor cells as part of the definitive haematopoiesis. Image adapted from (Sevenich, 2018).

Study of microglia ontogeny in humans is not as simple as in mice yet it is assumed that the developmental processes are similar (Haenseler et al., 2017a). As soon as microglia enter the brain they mature alongside the neurons. Cortical neurons exhibit spontaneous electrical activity after microglia migration during the 20th week of gestation and onwards (Moore et al., 2011). Haenseler and colleagues further optimised a previously published protocol (Buchrieser et al., 2017) and generated macrophage precursors, Myb independent and *PU.1* and *RUNX.1* dependent that when co-cultured with iPSC-derived cortical neurons fully matured into microglia (Haenseler et al., 2017a).

According to this protocol, which recapitulated the conditions of microglial development in the embryo, the first critical step was the formation of embryoid bodies (EB) from cultured stem cells (Haenseler et al., 2017a). The EBs were cultured with bone morphogenetic protein 4 (BMP4) to induce mesoderm formation, vascular endothelial growth factor (VEGF) for the endothelial precursors fate and stem cell factor (SCF) for haematopoietic precursors. According to the authors, the EBs were further transferred and cultured in big flasks, termed as ''factories'' and were cultured with interleukin 3 (IL-3) and macrophage colony-stimulating factor (M-CSF) to induce myeloid differentiation (Haenseler et al., 2017a). Most of the EBs extended adherent stromal cells developing cystic yolk sac-like structures. Following 3-4 weeks of culture the authors observed production of embryonic-like precursors in the supernatant, which were described as a uniform population of large, round cells with obvious filopodia and ruffles. The macrophage precursors were simply harvested from the supernatant. Macrophage precursors fully matured into microglia when co-cultured with cortical neurons recapitulating *in vivo* conditions. Isolated microglia

from the co-cultures expressed key microglia genes (Butovsky et al., 2014b), such as *MERTK*, *GPR34*, *PROS1*, *C1QA*, *GAS6* and *P2RY12* compared to foetal microglia and also expressed *TREM2*, *APOE* and *APP* among other genes (Haenseler et al., 2017a).

Overall, understanding of microglial ontogeny led to the development of protocols that reproduce *in vivo* events of development in the human brain. What is also important is that the iPSC-derived microglia can be co-cultured with neurons maintaining their signature and retaining the neuronal maturity and functionality *in vitro* for several weeks.

4.1.4 Microglia and neurodegeneration

Microglia are the main tissue resident macrophages of the CNS. Microglia are long-living cells that regenerate through self-renewal. Tissue resident macrophages are a heterogeneous population of immune cells performing functions ranging from regulation of local homeostasis to inflammation response and resolution. Microglia account for 10-15% of all glial cells in the brain and similar to peripheral macrophages outside the brain they serve homeostatic functions and are the first line of defence against infections or toxins (von Bartheld et al., 2016). During embryogenesis and development, microglia contribute to neurogenesis, oligodendrogenesis and myelinogenesis (Ueno et al., 2013). Additionally, they modulate synaptogenesis, neuronal circuit formation by synaptic pruning and preservation of neurons by secreting neurotrophic factors (Streit, 2006). In the adult brain microglia continue their homeostatic functions that include synaptic pruning and neuronal support, surveillance of the microenvironment and activation under conditions of injury, presence of pathogens and neurological disease.

Different microglia subtypes have been described across brain regions but the precise regional differences are not fully resolved (de Haas et al., 2008). Homeostatic microglia are extremely motile as their processes continuously explore and survey the local environment (Nimmerjahn et al., 2005). It has been suggested that the term ‘’activated’’ microglia may be misleading as it does not cover the full functional phenotypic spectrum they adopt when activated in response to specific perturbations (Perry et al., 2010). Earlier studies had proposed a dichotomy of microglia activation phenotypes by introducing the M1 (classically activated via toll-like receptors or interferon γ-IFNγ) and M2 phenotypes (alternatively activated by interleukins IL-4 or IL-13) (Martinez et al., 2008), which essentially translates as progression from

homeostasis to a partial and full activation. However, M1 and M2 activation does not reflect the vast microglia activation phenotypes, particularly under conditions of neurodegeneration (Perry et al., 2010).

Alzheimer's disease heritability enrichment studies have unequivocally revealed microglial involvement in the disease by identifying microglia-specific genes, such as *TREM2* where mutations have been linked to increased risk of disease onset. It has long been proposed that in Alzheimer's disease activated microglia are a cause rather than a consequence of the disease's pathology (Griffin et al., 1989). In Parkinson's disease similar heritability studies have yielded mixed results. Yet, a recent meta-analysis study highlighted *P2RY12* as an example of a microglia causal gene underlying a Parkinson's disease association signal (Andersen et al., 2021). In Alzheimer's disease, activated microglia localise around the extracellular Aβ plaque deposits and the presence of insoluble amyloid deposits activates the resident tissue microglia. The role of microglia in tau pathology, whether it is a consequence, or a contributor remains under investigation. Studies have shown that microglial secreted factors, such as nitric oxide (NO) may lead to initiation of tau aggregation in neurites (Gorlovoy et al., 2009). Other studies have also reported involvement of microglia in synaptic loss and spreading of tau (Asai et al., 2015, Hopp et al., 2018). In Parkinson's disease, the α-synuclein inclusions in neurons activates microglia in the striatum and SNc, as observed in Parkinsonian post-mortem brain tissue and animal models (Duffy et al., 2018, McGeer et al., 2003, McGeer and McGeer, 1998). Microglial contribution to neurodegeneration has been hypothesised as a positive feedback loop where the degenerative neurons secrete molecules that activate microglia, which in turn secrete

additional neurotoxic molecules that further promote degeneration by sustaining a self-perpetuating neurotoxic cycle (Song and Colonna, 2018) (Figure 4.3).

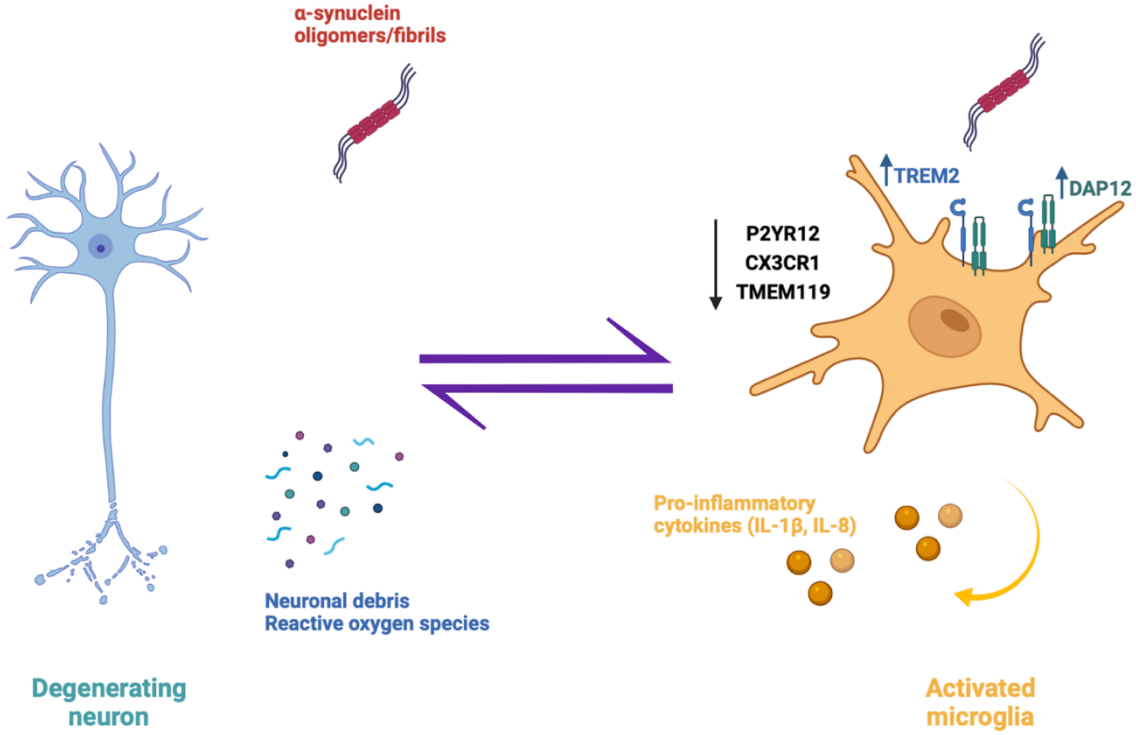

Figure 4.3 Suggested positive feedback loop for microglia's involvement in neurodegeneration of Parkinson's disease.

Degenerating neurons release debris and reactive oxygen species due to accumulation of insoluble proteins, such as α-synuclein. Aggregated α-synuclein or phosphorylated tau are secreted in the extracellular space (either free or engulfed in vesicles) and are taken up by microglia. These neuronal changes activate microglia which secrete pro-inflammatory cytokines (IL-1β, IL-8) and undergo phenotypic transition. Genes encoding receptors that participate in the homeostatic neuron-microglia communication (such as *P2YR12*, *CX3CR1*, *TMEM119*) are down-regulated and expression of phagocytosis-mediating receptors such as TREM2 and its adaptive receptor DAP12 (TYROBP) is increased. A key question in the field of neuroinflammation and neurodegeneration is at which point and how microglia cease to be protective and switch to a detrimental state.

4.1.5 Parkinson's disease related mutations, LRRK2 and GBA: is there a link to microglial responses?

The most common genetic cause of Parkinson's disease is mutations in the gene encoding leucine rich repeat kinase 2 (*LRRK2*). LRRK2 is an unusually large protein of 2527 amino acids with several functional domains, including a kinase domain (Li et al., 2014b). Although several mutations have been reported so far of varying pathogenicity, the *G2019S* point mutation is the most common (Zimprich et al., 2004, Monfrini and Di Fonzo, 2017). *G2019S* and other *LRRK2* mutations increase the protein's kinase activity and have been described as gain-of-function mutations (West et al., 2005, Greggio et al., 2006). The LRRK2 kinase activity has been implicated in endo-lysosomal trafficking, synaptic function, cell proliferation, cytoskeleton dynamics and possibly inflammation (Nguyen and Krainc, 2018, Manzoni, 2017, Russo et al., 2014). Increased LRRK2 activity has been observed in idiopathic Parkinson's disease cases and neurons that had been previously exposed to mitochondrial toxins demonstrating a wider possible role in the pathology of the sporadic form of the disease (Di Maio et al., 2018).

Heterozygous mutations in *GBA1* gene constitute the most common genetic risk factor for Parkinson's disease with 7-10% of the patients harbouring *GBA1*-associated mutations (O'Regan et al., 2017). Patients with concurrent mutations on *LRRK2* (G2019S) and *GBA1* (L444P or E326K) manifest disease symptoms earlier than patients with mutations in either of the two genes (Spitz et al., 2015). The product of *GBA1* is a protein called glucocerebrosidase 1 (GCase), which is a lysosomal hydroxylase that catalyses hydrolysis of glucosylceramide to glucose and ceramide and only becomes active when transferred to the acidic lumen of the lysosome. Mutations may cause disruption in the folding or lysosomal targeting of GBA, thus

impairing the function of this enzyme in the lysosome (Do et al., 2019). Impaired glucocerebrosidase may lead to Parkinson's pathogenesis by disrupting lysosomal homeostasis, enhancing stress in the endoplasmic reticulum, or by contributing to mitochondrial impairment.

Post-mortem brains from individuals with *LRRK2* mutations have demonstrated variability in terms of α-synuclein pathology (Zimprich et al., 2004). It has been reported that half of the patients with *LRRK2* mutations and two thirds of those with the *G2019S* mutation develop Lewy-like pathologies (Kalia et al., 2015, Henderson et al., 2019). *GBA1* mutation carriers with Parkinson's disease develop extensive Lewy-like pathology with distribution that resembles the one observed in dementia with Lewy bodies (Neumann et al., 2009b). However, not all *GBA1* mutation carriers develop α-synuclein pathology.

LRRK2 is highly expressed in peripheral blood monocytes and its expression is reportedly higher than in neurons (Thévenet et al., 2011). Expression of *LRRK2* has also been reported in macrophages and microglia but the exact role of the kinase in microglia function remains poorly understood (Moehle et al., 2012). Given the expression of *LRRK2* by immune cells and its association in Parkinson's and Crohn's disease (Barrett et al., 2008), it is possible that there is a link between α-synuclein pathology and LRRK2 function in microglia. A recent study using iPSC-derived neurons and microglia reported that LRRK2 regulates microglia response to inflammatory IFNγ signalling by modulating immune metabolic re-programming (Panagiotakopoulou et al., 2020). Additionally, studies in *LRRK2* (G2019S) mutant mice showed a tendency of recruitment of pro-inflammatory monocyte-derived macrophages in the brain suggesting role of LRRK2 kinase in chemotaxis (Xu et al.,

2022). Nevertheless, it remains elusive how *LRRK2* mutations affect the response of microglia to Lewy-like neuronal pathology.

Microglia express the highest levels of *GBA1* mRNA and mutations in *GBA1* may affect their homeostatic signature in similar ways to macrophages in Gaucher's disease (Zhang et al., 2013, Brunialti et al., 2021). PET scans have revealed microglia activation in Lewy-susceptible brain regions of patients with the *GBA1* mutations (Mullin et al., 2021). Experiments using isolated *in vitro* primary microglia have revealed a possible role of microglial glucocerebrosidase in detoxifying neuronal signals (Brunialti et al., 2021). Similar to the *LRRK2* mutations, it remains unexplored how *GBA1* mutations affect microglial phenotypic responses to dopaminergic neuronal pathology.

4.1.6 Co-culture assay workflow: α-synuclein seeded aggregation of patient derived dopaminergic neurons followed by addition of microglia precursors

In this chapter, I established a novel iPSC-based co-culture model to investigate chronic microglial responses to intraneuronal α-synuclein pathology (Figure 4.4). To do so, I matured dopaminergic neurons until day *in vitro* 45 (DIV45) and then seeded them with a single treatment of *de novo* generated α-synuclein fibrils (described in Chapter 3). To maximise the intraneuronal pathology I used neurons derived from familial Parkinson's disease patients with a triplication in the *SNCA* gene ($SNCA^{TRIP}$). Two weeks after seeding (i.e., DIV59), which the lab had previously demonstrated is the period needed for sufficient intraneuronal aggregation to occur (Tanudjojo et al., 2021), I harvested and added iPSC-derived microglial precursors to the neuronal cultures at 1:1 ratio. The microglia derived from healthy controls and co-cultured with neurons for further two weeks to achieve mature microglial phenotypes as previously shown (Haenseler et al., 2017a). The experiments were terminated at DIV73 for phenotypic analysis.

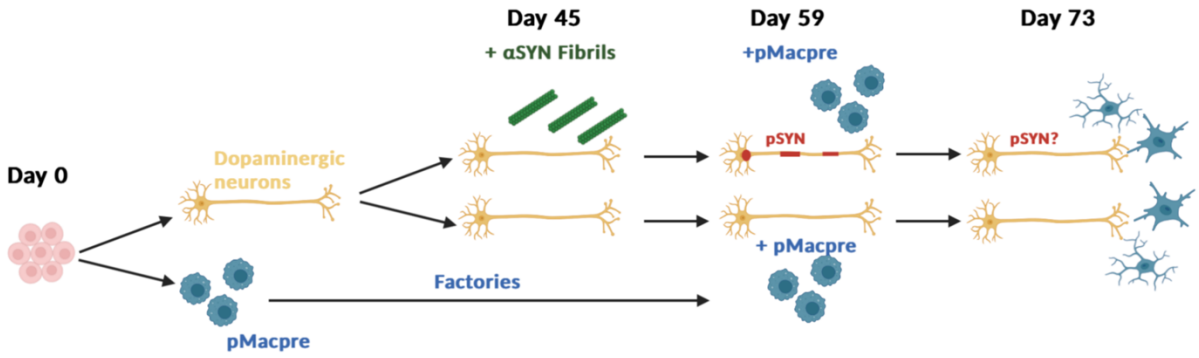

Figure 4.4 Chronic iPSC-derived co-culture system to study microglia effects on neurons containing α-synuclein aggregates.

Stem cells from SNCA^{TRIP} patients and healthy control (HC) individuals were differentiated independently into dopaminergic neurons and microglia, respectively. Dopaminergic neurons were re-plated in various plate formats on DIV21 and were seeded on DIV45 at a single treatment (1 µM) with the *de novo* generated α-synuclein fibrils. Two weeks later, on DIV59, HC factories were harvested, and macrophage/microglial precursors (pMacpre) were added on seeded and non-seeded control dopaminergic neurons following a 1:1 plating ratio. The pMacpre matured in the presence of neurons and the main components of the co-culture media (IL-34) into microglia (co-pMGL). On DIV73 the co-cultures were assayed for various readouts.

4.1.7 Aims and Objectives

The objectives of this chapter were to:

1. Generate human iPSC-derived dopaminergic neurons
2. Generate iPSC-derived microglia and assess their maturation after co-culturing them with human dopaminergic neurons
3. Asses the effect of microglia in response to seeded neuronal aggregation by measuring levels of pSYN.
4. Determine the effects of *LRRK2* and *GBA1* mutations on microglial clearance of neuronal pSYN
5. Investigate the role of phagocytosis in the clearance of α-synuclein fibrils

4.2 Results

4.2.1 Dopaminergic neurons express neuronal and dopaminergic specific markers

To set up a neuronal-microglia co-culture system of α-synuclein seeded aggregation, my first aim was to generate iPSC-derived dopaminergic neurons, which expressed neuronal and dopaminergic specific markers. The floor plate differentiation protocol from the Studer group has been modified and is described below. Among the modifications included were the replacement of one of the original dual SMAD inhibitors (SB431542 10 μM to A83-01 2 μM, which is a more potent TGFβ inhibitor), the increase of SHH levels (from 100 ng/mL to 300 ng/mL) and FGF8α (100 ng/mL to 200 ng/mL). This modification yielded a higher percentage of TH-positive neurons which maintained their electrophysiological properties from 60% in the published studies (Arenas et al., 2015) to 76% (Tanudjojo et al., 2021). The differentiating stem cells were subjected to daily media changes followed by exposure to an array of small molecules with the aim to generate neural progenitors by DIV10 with the floor plate induction and to a series of neuronal growth factors that aimed to generate dopaminergic neurons by DIV21, as per the Studer floor-plate protocol (Figure 4.5).

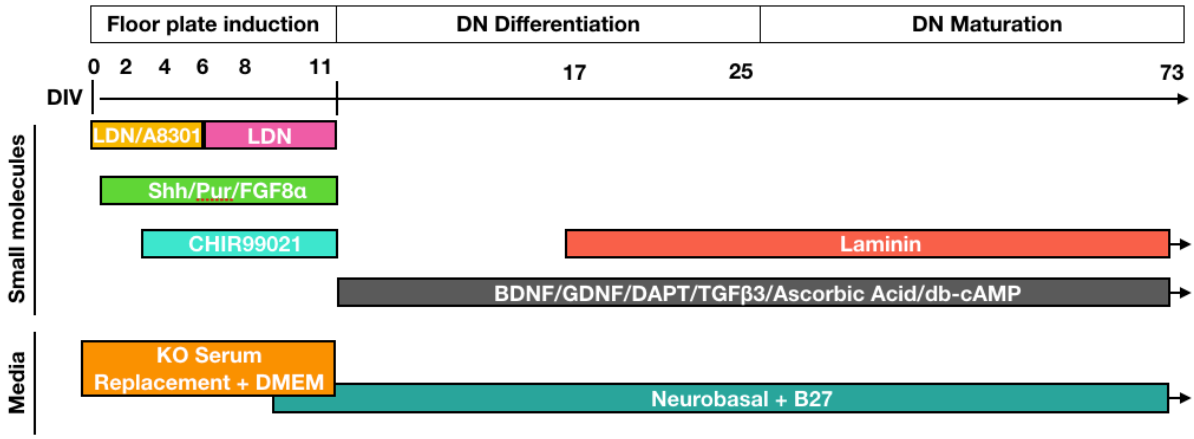

Figure 4.5 Floor plate differentiation protocol for generation of dopaminergic neurons from human iPSCs.

Dopaminergic neurons were generated using the protocol modified from Kriks et al. (2011). The protocol involves two important steps with the first one being the floor plate induction by a series of small molecules and sequentially the acquisition of a neuronal dopaminergic fate. Stem cells (SNCA triplications) were differentiated in a monolayer and subjected to daily media changes with corresponding small molecules and factors up to day 21. Cells were then re-plated in various plate formats and treated with mitomycin-C (MMC) on day 23 to inhibit proliferation of non-neuronal mitotic cells. Dopaminergic neurons were matured until day 45 before use in assays.

Differentiation of stem cells was initiated once stem cells reached confluency. The cells were maintained in monolayer from DIV0 until DIV21 (Figure 4.6a). Approximately by DIV20-DIV21 neuronal projections emerged in gaps which is an indicator that neurons formed and were ready to be dissociated. Three days post re-plating the cells were treated with mitomycin C (MMC) to inhibit proliferation of non-neuronal cells and neurons appeared with shorter projections (Figure 4.6b top). By DIV35 neurons had formed a more complex network (Figure 4.6b middle), which maturated further by DIV45, when the neurons were ready to be seeded with the α-synuclein fibrils (Figure 4.6b bottom).

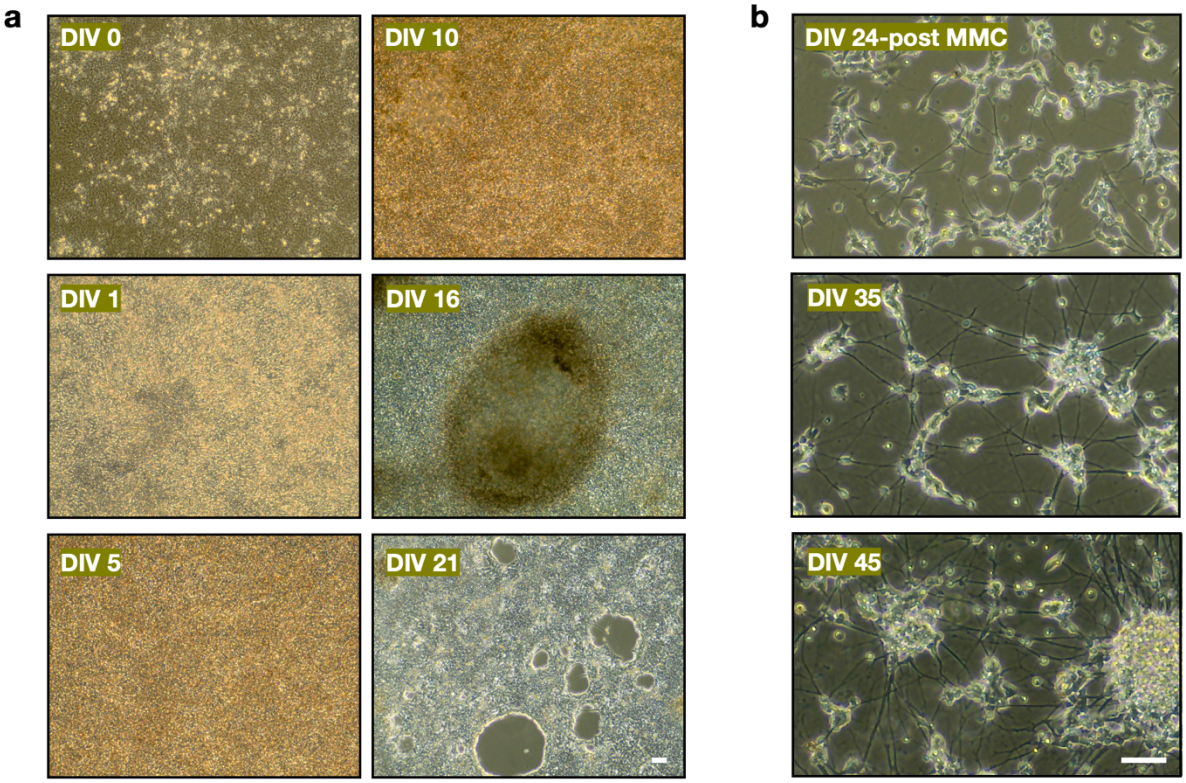

Figure 4.6 Time-course photo journal of differentiating cells to dopaminergic neurons from DIV0 to DIV45.

a. Differentiation of iPSCs in a monolayer was initiated when stem cells reached an approximate confluency of 90%. Typical morphology of iPSC at DIV0 with large nuclear to cytoplasmic ration. As observed under brightfield microscopy, the morphology was similar until DIV10. Ridges started appearing on DIV11 and were maintained until DIV14-16. By DIV21 large gaps formed within the monolayer in which neuronal projections were obvious and indicated that the cells were ready to be dissociated and re-plated in various cell culture plate formats. **b.** Three days later following MMC treatment neurons had shorter projections which grew in a dense network by DIV45. Scale bar at 10 µm.

Once the cells were differentiated and maintained until DIV73, I assessed their composition by immunocytochemistry for neuronal specific markers, including cytoskeletal βIII tubulin (TUJ1), nucleic NeuN and dopaminergic specific marker, TH (Figure 4.7a). Additionally, I confirmed that the neurons also expressed dendritic specific marker, microtubule associated protein 2, MAP2 (Figure 4.7a). I also confirmed that 83 % percentage expressed TUJ1 and MAP2, signifying neuronal phenotype and 79 % TH, a widely used marker of dopaminergic phenotype (Figure 4.7b). The Studer group that developed the floor-plate based protocol confirmed thoroughly dopaminergic neuronal identity by also staining for LIM homeobox transcription factor 1 alpha, LMX1A and by measuring gene expression of dopamine transporter (*DAT*) and G-protein-coupled, inwardly rectifying potassium channel (*KCNJ6*), which are markers expressed *in vivo* by dopaminergic neurons of the SNc (Kriks et al., 2011).

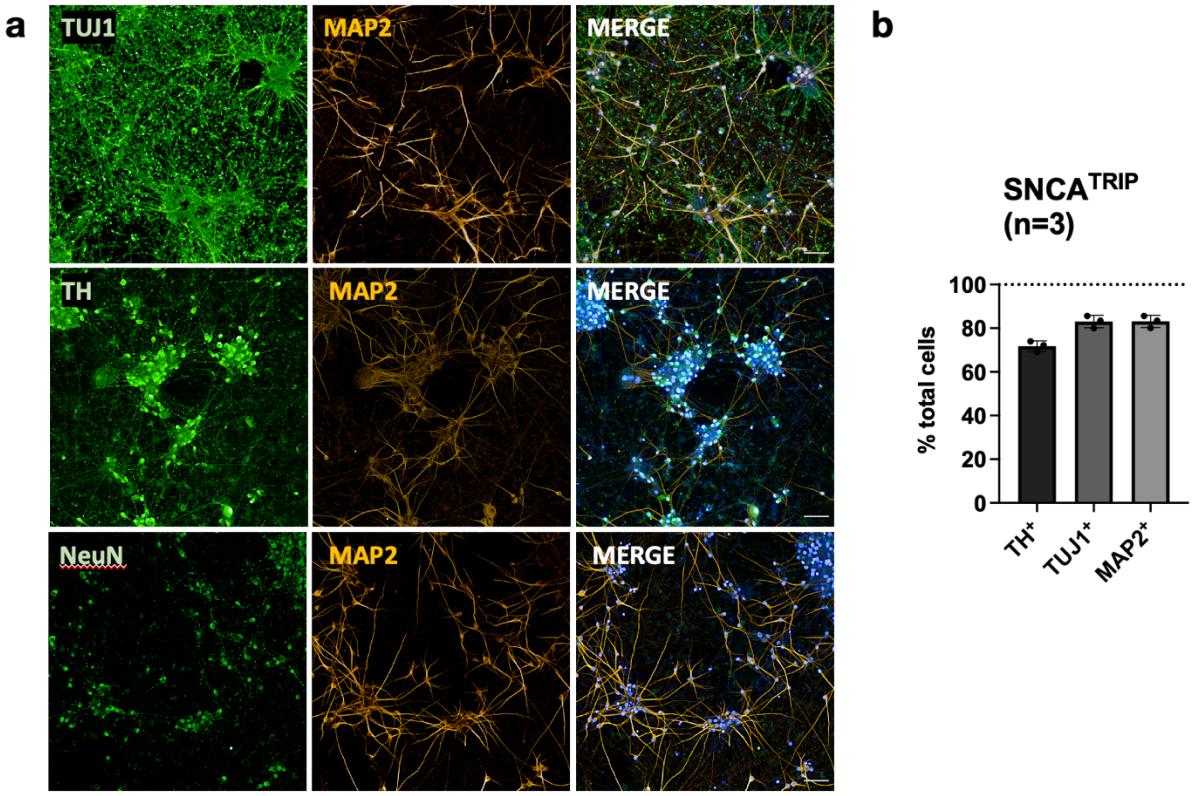

Figure 4.7 Characterisation of human iPSC-derived dopaminergic neurons by immunocytochemistry (ICC).

a. Representative images of dopaminergic neurons fixed on DIV73 and stained for pan-neuronal markers, such as cytoskeletal βIII tubulin (TUJ1) and nuclei specific, NeuN. Additionally, neurons expressed dopaminergic specific marker, tyrosine hydroxylase (TH) and all above markers co-localised with dendritic specific marker, MAP2. Imaging was performed using high-throughput imaging system, Opera Phenix. Scale bar at 20 μm**. b.** Quantification of TUJ1 and MAP2 and revealed 83% positive neurons and quantification of TH showed 79% positive dopaminergic neurons. Each dot corresponds to one neuronal line differentiated once and data are mean ± s.e.m. from n=3 independent differentiations.

4.2.2 Generation of human iPSC derived microglia

Human stem cells were differentiated in microglia cells following the protocol first described in our collaborator's laboratory, Dr Sally Cowley (Dunn School of Pathology, University of Oxford) (Haenseler et al., 2017a). Once stem cells reached confluency (DIV0) they were transferred to Aggrewells (STEMCELL Technologies) where they formed EBs of defined size (Figure 4.8). EBs were cultured for four days with daily media feeds supplemented with BMP4, VEGF and SCF. On DIV4, EBs were re-suspended and transferred in big flasks where they were cultured with X-Vivo media supplemented with IL-3 and macrophage colony-stimulating factor (M-CSF) aiming to induce and promote myeloid differentiation. It was very important that during the first couple of weeks, the so-called factories remained un-disturbed. That enabled attachment of the EBs which formed cystic, yolk-sac-like structures by putting out surrounding adherent stromal cells. After 4 weeks in culture and weekly addition of fresh factory media, embryonic-like macrophage precursors emerged into the supernatant as a uniform population of round cells, termed macrophage/microglia precursors (pMacpre). These were harvested by collecting supernatant followed by media replenishment and the factories were maintained in culture for up to 6 months undergoing several weekly harvests. According to the authors of the originally published protocol, the factories yielded a total of 10 to 43-fold higher number of cells when compared to the number of input iPSCs, as well as other published protocols (Haenseler et al., 2017a).

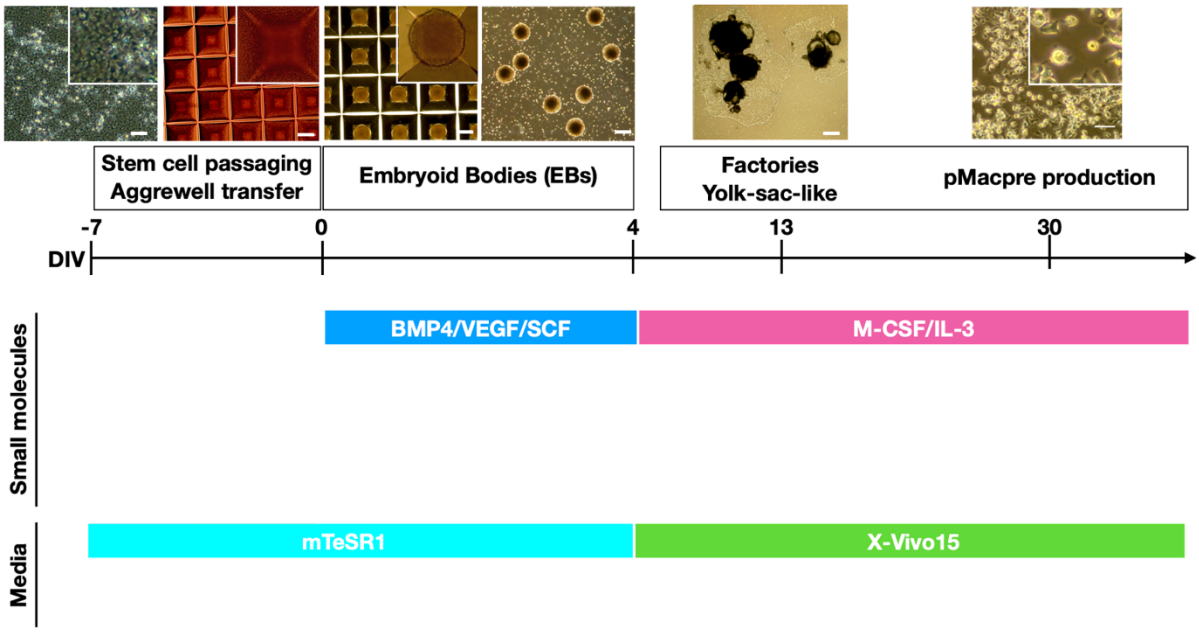

Figure 4.8 Timeline of microglia differentiation via Embryonic Bodies formation that recapitulated *in vivo* embryonic development.

When stem cells reached confluency >90%, they were re-plated and transferred to plates containing aggrewells on DIV0. Each well of a 24-wp contained 300 small aggrewells and the cells congregated towards the bottom of each aggrewell by soft centrifugation. After one day in culture, cells formed EBs which were subjected to daily media changes. The media base was mTeSR1 supplemented with BMP4, VEGF and SCF. On DIV4, the EBs were carefully transferred to big culture flasks and were cultured with X-vivo media supplemented with M-CSF and IL-3. After one week in culture, most of the EBs attached on the flask surfaces forming a yolk sac-like structure. After approximately 4 weeks, a uniform cell population of round shape emerged within the supernatant. These cells were macrophage/microglia precursors (pMacpre) and were harvested by supernatant collection. Harvests occurred frequently followed by addition of fresh factory media and the factories were maintained in culture for up to 6 months. Scale bar at 20 μm.

Having successfully replicated the protocol for microglia differentiation, I further sought to confirm microglia identity of the harvested pMacpre cells when cultured alone or with dopaminergic neurons. The culture media for mono and co-cultures was carefully designed and optimised to support microglia survival and development while cultured alone or in the presence of neurons. In detail, microglia survival is dependent on the tyrosine kinase receptor CSF1 therefore, the media was supplemented with IL-34, which is an alternative CSF1R ligand produced in the brain. Neuronal compatibility was achieved with addition of the N2 supplement instead of B27. The latter compromised microglia activity as it contained corticosterone, catalase and superoxide dismutase (SOD). Therefore, the media used for all subsequent mono and co-cultures was advanced DMEM/F12 supplemented with N2 and 100 ng/mL of IL-34 to achieve neuronal compatibility and microglia survival. Additionally, the presence of IL-34 supported formation of ramified morphology (Haenseler et al., 2017a). The harvested pMacpre that were cultured in monocultures are termed from here after as microglia-like cells, pMGL, whereas co-cultured pMacpre are termed as co-pMGL.

Firstly, I wanted to confirm the presence of microglia in mono and co-cultures by assessing their morphology under brightfield microscope and by immunofluorescent staining for microglia specific marker ionised calcium-binding adapter molecule 1, IBA1 encoded by *AIF1*. IBA1 is a pan-microglia cytosolic marker that is always expressed by these cells regardless of their phenotype (Jurga et al., 2020). pMGL and co-pMGL under baseline conditions manifested the characteristic homeostatic ramified morphology (Figure 4.9 upper panels) and were positive for IBA1 marker (Figure 4.9 bottom panels).

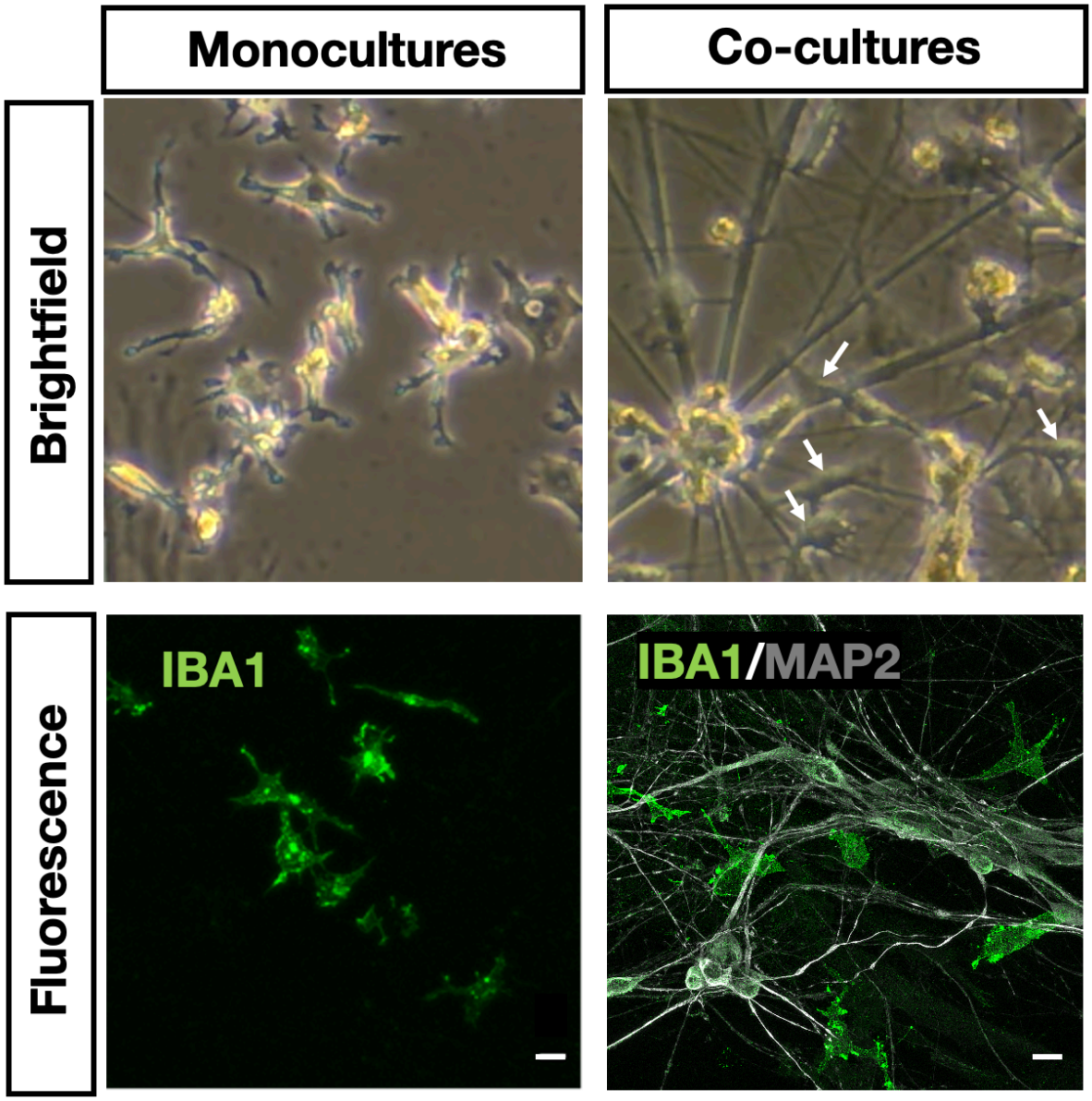

Figure 4.9 pMGL (monocultures) and co-pMGL (co-cultures) acquired ramified morphology and expressed the microglial specific marker, IBA1.

When pMacpre were harvested they were cultured alone or with dopaminergic neurons. They matured in culture and acquired the characteristic ramified morphology under baseline conditions. Under brightfield microscopy co-pMGL were also observed in close proximity to dopaminergic neurons (indicated by the white arrows). Immunofluorescence confirmed microglia identity in mono and co-cultures by positive staining of pan-microglial marker, IBA1. Scale bar at 20 μm.

To assess the extent to which pMacpre mono- and co-cultured resemble microglia on a gene expression level, I performed RT-qPCR and compared the gene expression profile of 9 consensus microglia genes in pMGL and co-pMGL to dopaminergic neuronal monocultures (Figure 4.10). I used a previously published set of primers for the following key microglia genes: *MERTK*, *GPR34*, *PROS1*, *C1QA*, *GAS6*, *TMEM119*, *P2YR12* and *TREM2* as identified in the literature (Haenseler et al., 2017a, Butovsky et al., 2014a). All these genes were strongly expressed in both pMGL and co-pMGL microglia when compared to neuronal monocultures (DN) where there was no expression. *MERTK*, *GPR34*, *PROS1*, *C1QA*, *TMEM119* and *P2RY12* had significantly higher expression in co-pMGL compared to pMGL. Interestingly, *GAS6* and *TREM2* expression was significantly higher in pMGL microglia compared to co-pMGL.

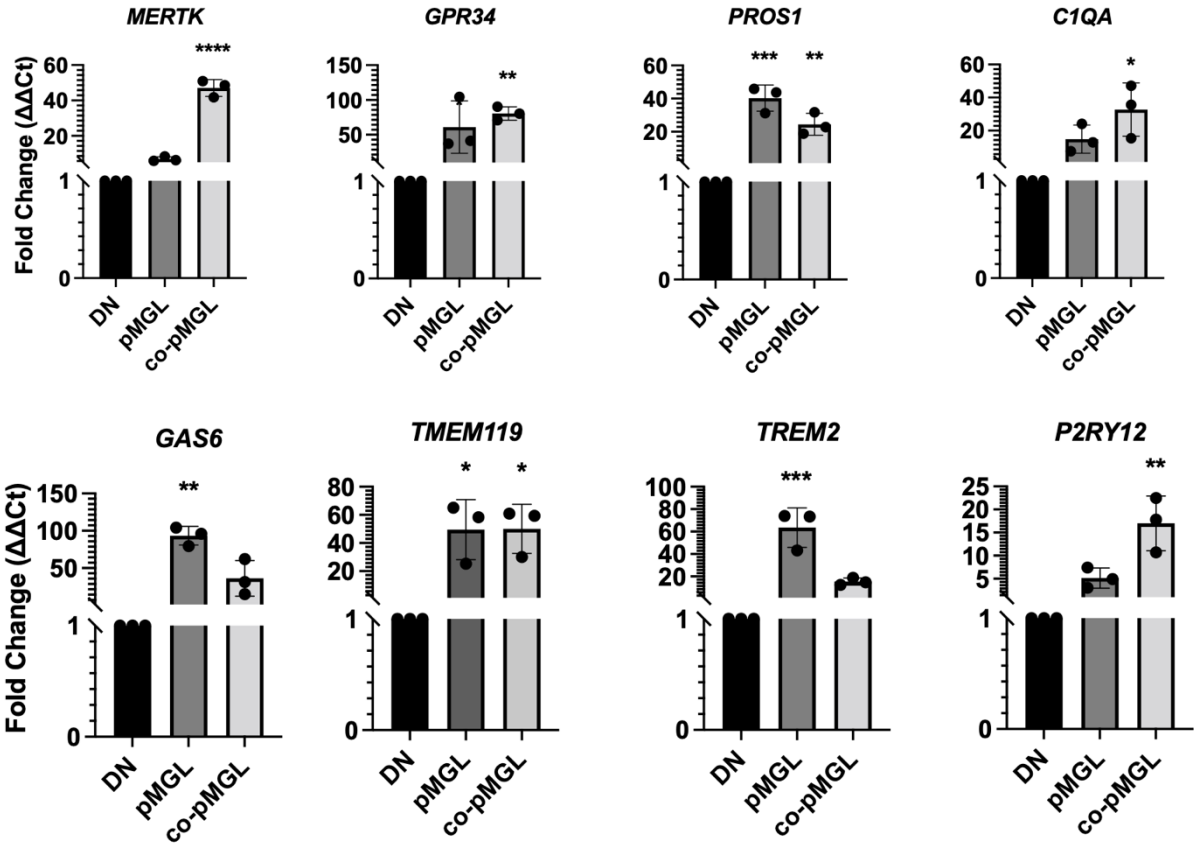

Figure 4.10 iPSC-derived mono and co-cultured microglia express consensus microglia markers.

Monocultured (pMGL) and co-cultured microglia (co-pMGL) expressed key microglia markers as revealed by RT-qPCR. Fold change was calculated using the ΔΔCT method with normalisation to dopaminergic neuronal monocultures (DN). Literature search identified 9 consensus microglia expressed genes: *MERTK*, *GPR34*, *PROS1*, *C1QA*, *GAS6*, *TMEM119, TREM2* and *P2RY12*. Each dot represents one independent differentiation for one microglia and one neuronal clone (n=3 differentiations per clone with technical repeats for RT-qPCR). *p<0.0177, ** p<0.0082, ***p<0.0002, **** p<0.0001 by one-way ANOVA followed by Dunnet's multiple comparison test.

The identity of the cells in the co-cultures was further determined on a transcriptomic level by performing bulk RNA-sequencing. Cell type deconvolution was performed by our collaborator, Dr. Devika Aggarwall in Dr. David Sims's laboratory, who compared the dopaminergic neurons and microglia (co-pMGL) that I generated and cultured together to a multi-subject human single-cell atlas of SNpc using the MuSiC method. The cell-type composition of the bulk RNA-sequencing samples from two independent experiments using one neuronal iPSC line and two iPSC lines of healthy control microglia confirmed the dopaminergic fate of the generated neurons, as well as the presence of microglia (Figure 4.11). More specifically, there were about 80-85% dopaminergic neurons in my samples and about 15% of microglia. The absence of astrocytes was also confirmed.

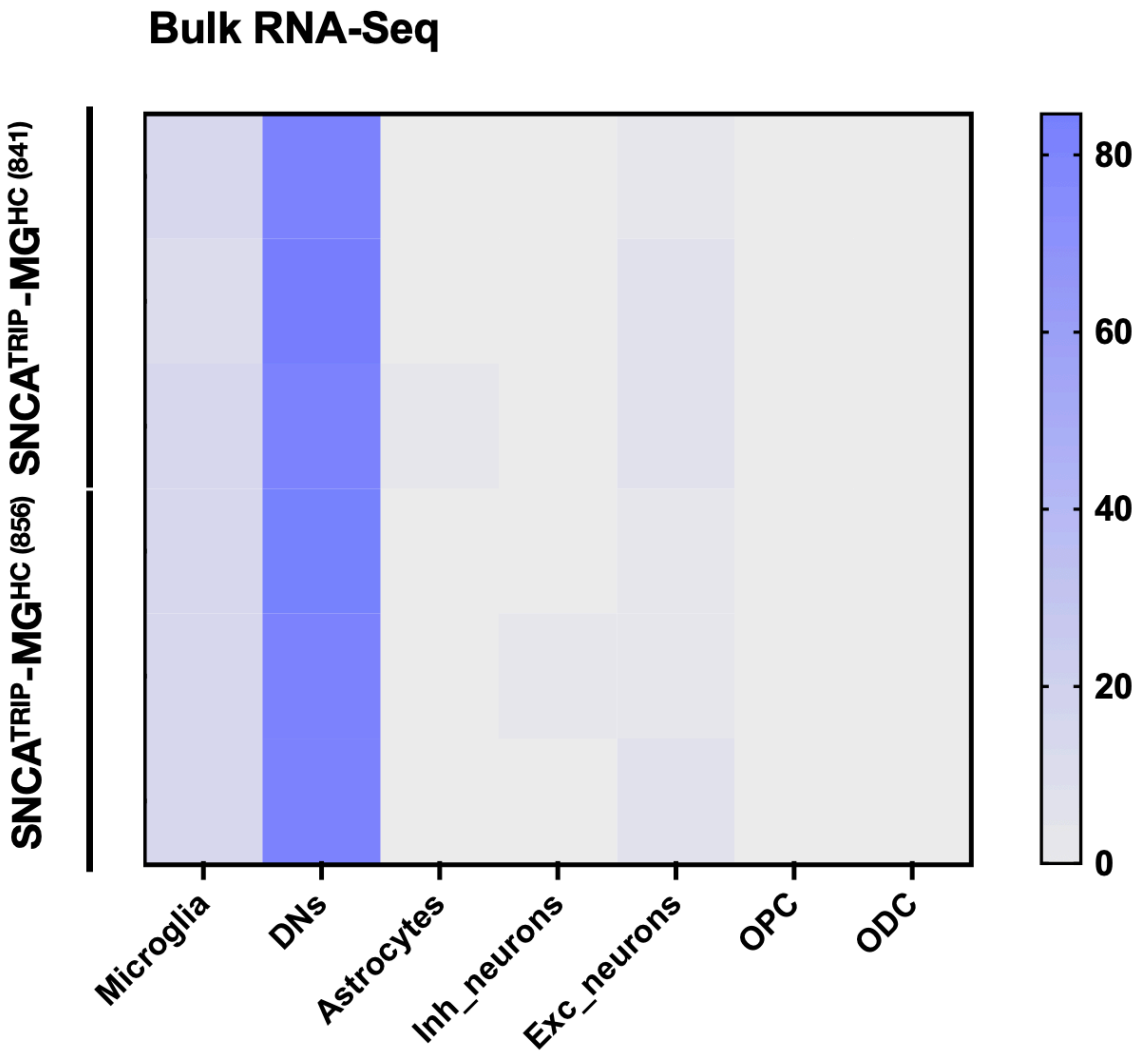

Figure 4.11 Dopaminergic neuron identity and microglia identified by bulk RNA-Sequencing.

Transcriptomic analysis from iPSC-derived co-cultures demonstrated that 80-85% of the identified neurons were dopaminergic and there were approximately 15% microglia cells identified when compared to a multi-subject human single cell atlas of the substantia nigra. Transcriptomic analysis was performed on two healthy control lines differentiated into microglia (SFC841 and SFC856) and one $SNCA^{TRIP}$ line. Each line was differentiated once (n=6 independent differentiations). The data in this figure was analysed by Dr Devika Agarwall and Dr David Sims.

4.2.3 *De novo* generated α-synuclein fibrils induce neurotoxic, pSYN positive inclusions in SNCA^{TRIP} dopaminergic neurons

To determine whether addition of the *de novo* generated α-synuclein fibrils that I generated, template aggregation of endogenously expressed neuronal α-synuclein as the lab had previously shown (Tanudjojo et al., 2021), I measured α-synuclein phosphorylation at Ser129 (pSYN), which is an abundant pathological modification found in Lewy bodies (Fujiwara et al., 2002). α-Synuclein fibrils (1 μM) were added once to SNCA^{TRIP} dopaminergic neurons on DIV45 and half-media changes were performed every three days thereafter and assayed 4 weeks after seeding. I found that α-synuclein fibrils induced aggregation and localisation of pSYN positive inclusions in the neurites and cell bodies of dopaminergic neurons (Figure 4.12a, b). Additionally, using a homology time resolved FRET assay, I observed increased pSYN levels in seeded neurons when compared to their non-seeding control (Figure 4.12c). Using imaging software ImageJ (Fiji), I then counted the number of nuclei between the non-seeding and fibril seeding groups; I found approximately 25% reduction in neurons under seeding conditions (Figure 4.12d).

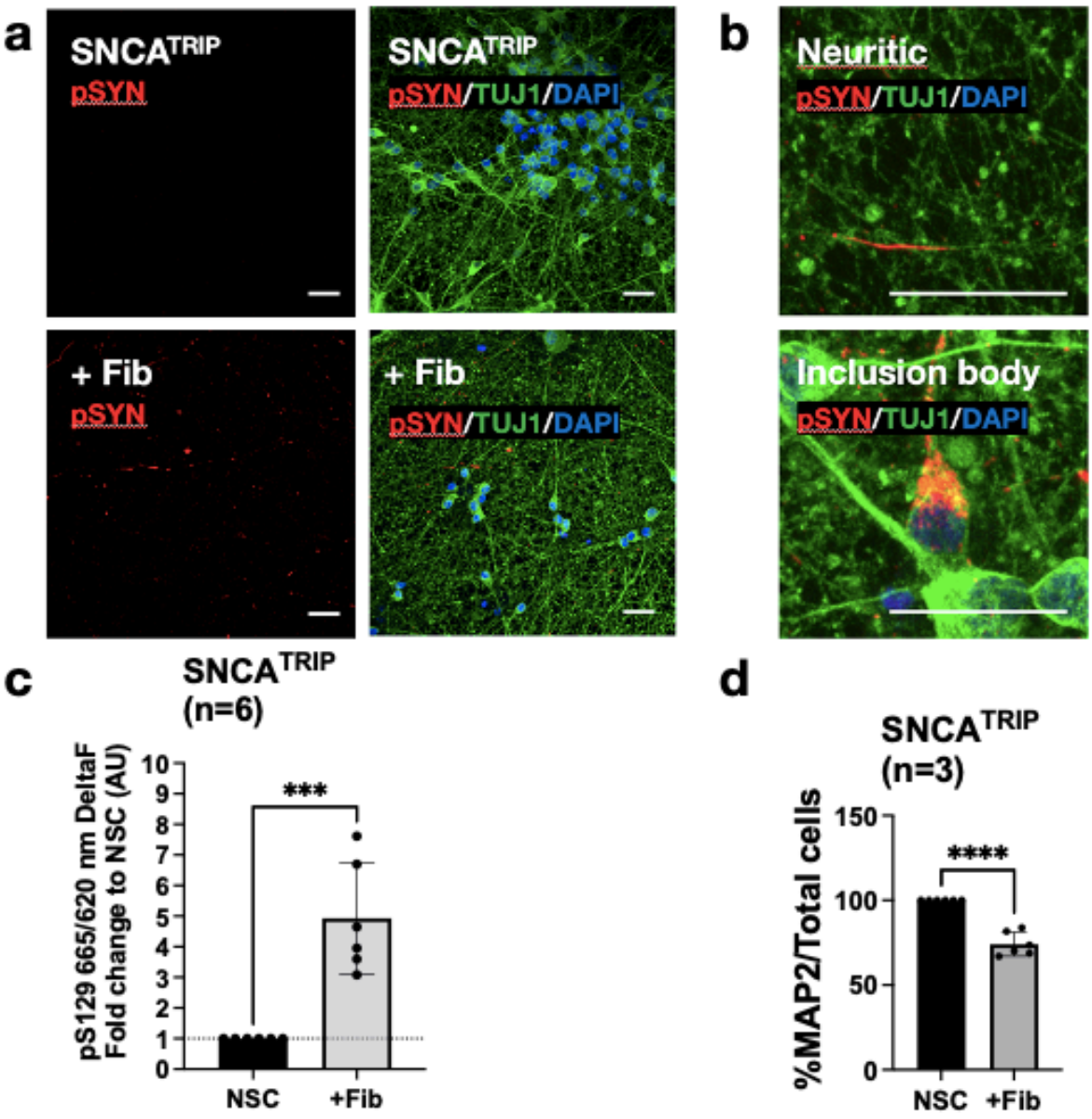

Figure 4.12 α-Synuclein seeded aggregation in SNCA^{TRIP} iPSC-derived dopaminergic neurons resulted in increased pSYN levels and reduced number of surviving MAP2-positive nuclei.

a. α-Synuclein fibrils (+Fib) seeded aggregation of endogenous α-synuclein in SNCA^{TRIP} dopaminergic neurons as detected by the presence of pathological pSYN positive inclusions, scale bar at 20 µm. **b.** The pSYN positive inclusions were localised in axons (neuritic) or soma (inclusion body), scale bar at 40 µm. **c.** Time resolved FRET assay revealed an approximate 4-fold increase of the pSYN levels when compared to NSC. Each dot represents one independent differentiation of the same clone (n=6), ***p<0.0004 by unpaired t-test. **d.** 25% reduction in the number of MAP2 positive nuclei 4 weeks after seeding. Each dot represents one independent differentiation of the same clone (n=6 differentiations with technical repeats), ****p<0.0001 by t-test.

Data is shown as mean ± s.e.m. NSC: non-seeded control, +Fib: α-synuclein fibrils. Images are representative of three independent differentiations.

4.2.4 Microglia reduced pSYN levels when co-cultured with dopaminergic neurons containing α-synuclein aggregates

As sentinels, microglia are the first CNS cell type to sense stress and homeostatic disturbances in the brain microenvironment. Therefore, I sought to investigate their effects on stressed, fibril-seeded dopaminergic neurons. To do so I set up a novel chronic model of iPSC-derived co-culture as explained in section 4.1.5 and shown schematically in Figure 4.4. In summary, dopaminergic neurons from patients with $SNCA^{TRIP}$ were seeded with fibrils and two weeks later were co-cultured with microglia from healthy control subjects for further two weeks.

pMacpre differentiated into microglia (co-pMGL) in the presence of neurons within the course of two weeks and brightfield microscopy observations captured their morphological transition towards their characteristic ramified morphology (Figure 4.13).

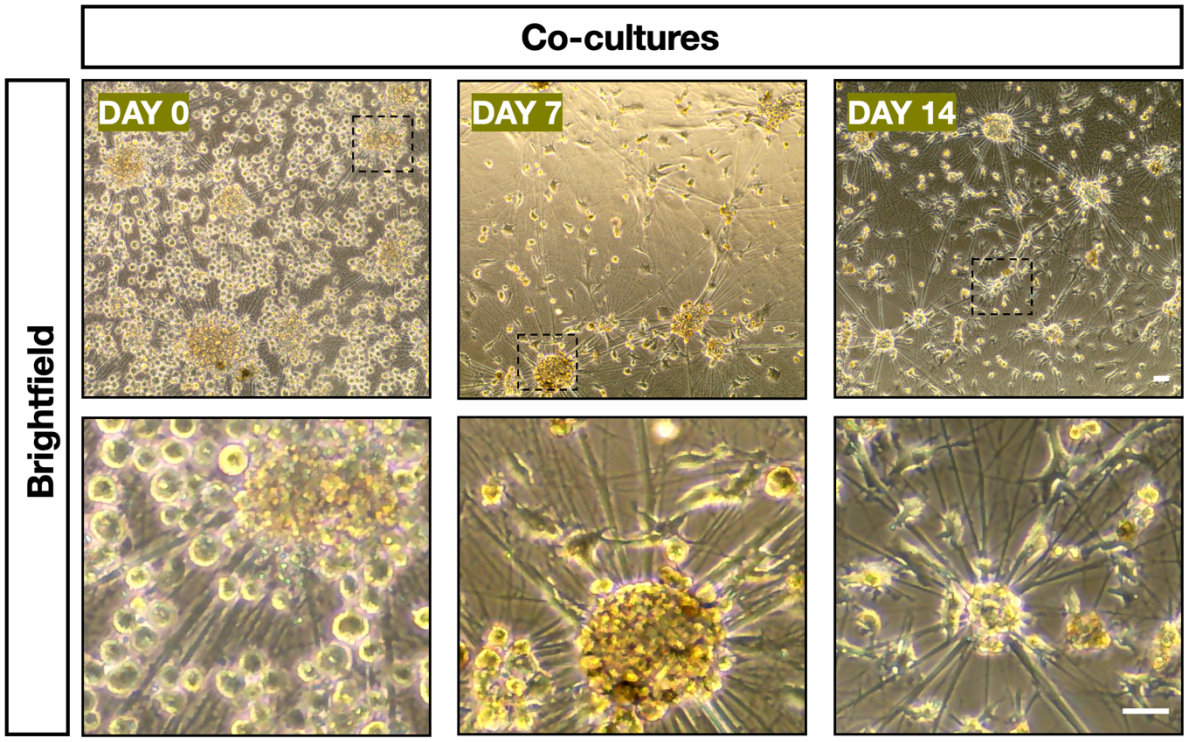

Figure 4.13 Progressive morphological maturation of pMacpre into co-cultured microglia (co-pMGL).

Harvested pMacpre maintained their uniform round shape when added to dopaminergic neurons (top left panel). After 7 days of co-culturing the majority of co-pMGL had settled down among the dopaminergic neurons and two weeks later under baseline conditions microglia had acquired their characteristic ramified morphology among the neurons. Images are representative of six independent differentiations (3 differentiations of two different iPSC healthy control lines) and acquired with brightfield microscope. Scale bar at 20 µm.

Microglia were further assessed in the co-cultures under baseline and seeded aggregation conditions by staining for the pan-microglia marker, IBA1 (Figure 4.14). Under basal conditions, microglia appeared ramified, with branches and processes that resemble homeostatic, surveillant phenotypes (Leyh et al., 2021). In contrast, in seeded co-cultures, microglia localised around neuronal clusters and appeared rounder with shorter cellular processes (Figure 4.14a). I quantified their morphology

by counting three distinct morphological states, ramified, bipolar and round cells using imaging processing software, whilst being blinded for the conditions (Figure 4.14b). I found that there was approximately a 20% reduction in ramified cells and 18% increase in round/activated cells in co-cultures with aggregates when compared to controls.

I then went on to measure the levels of pSYN in the seeded co-cultures compared to neuronal monocultures using homology time resolved FRET assay. Interestingly, I found that the pSYN levels were significantly reduced in seeded co-cultures when compared to neurons alone (Figure 4.14c). I then sought to determine whether the reduction in pSYN levels was due to loss of neurons. For this reason, I counted the number of MAP2 and IBA1 positive cells in non-seeded and seeded co-cultures using the cell counting plugin of ImageJ (Fiji) and expressed their numbers as a percentage of all the detected cells. The number of MAP2 positive cells remained approximately the same in unseeded and seeded co-cultures, as did the number of IBA1 positive microglia (Figure 4.14d and e, respectively).

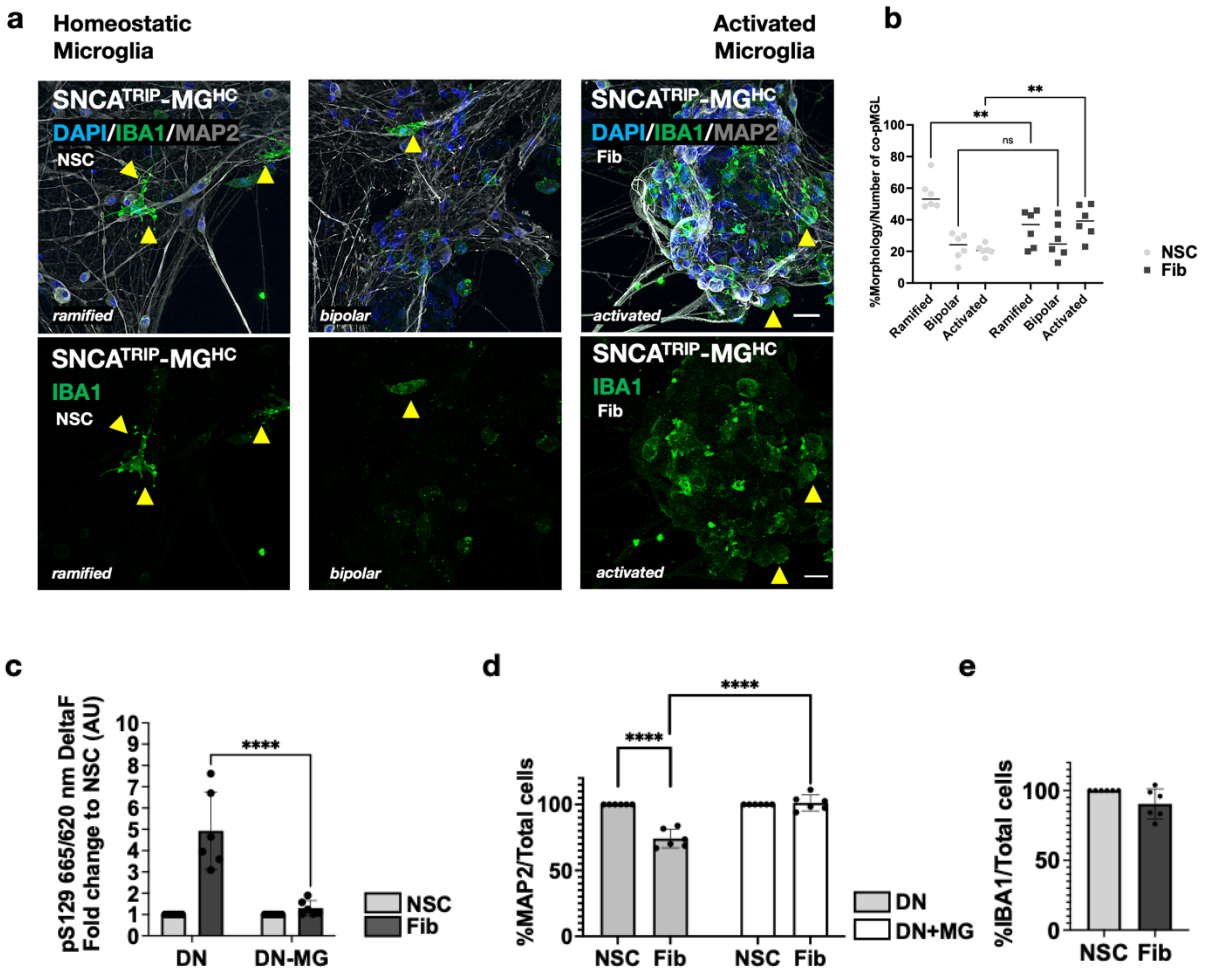

Figure 4.14 Microglial transition to morphologically activated phenotypes, reduces levels of pSYN and rescue neuronal loss when co-cultured with α-synuclein seeded dopaminergic neurons.

a. Representative images of SNCA^{TRIP}-MG^{HC} co-cultures on DIV73, 4 weeks following neuronal seeding with α-synuclein fibrils. Three broad morphological phenotypes of microglia were observed under NSC and Fib conditions: ramified, bipolar and activated. Ramified microglia displayed dendritic like branches extending from the cell body. Bipolar cells presented a rod-like morphology, whereas activated cells had a round, amoeboid-like shaped cell body (yellow arrows). Scale bar at 20 μm. **b.** Morphological quantification revealed 56% ramified and 20% activated microglia in NSC. However, 34% of microglia were ramified and 38% were activated in fibril-seeded co-cultures. **c.** Time resolved FRET assay, revealed that in the presence of microglia pSYN levels were significantly reduced compared to neuronal monocultures. Each dot represents an independent differentiation with one SNCA^{TRIP} clone and two different HC lines each differentiated three times. ****p<0.0001 by two-way ANOVA followed by Sidak's multiple comparisons test. **d.** ImageJ (Fiji) was used to count MAP2 co-stained neuronal nuclei in monocultures (DN) and co-cultures (DN-MG) ****p<0.0001 by two-way ANOVA followed by Sidak's multiple comparisons test

e. IBA1 co-stained nuclei quantification in co-cultures. Data is shown as mean ± s.e.m. NSC: non-seeded control, Fib: α-synuclein fibrils

4.2.5 Physical contact between microglia and dopaminergic neurons was required for reduction of pSYN levels.

In the brain the microglia-neuron crosstalk is largely mediated by a direct physical contact between the two cell types, but secreted signals or extracellular vesicles have also been implicated (Yang et al., 2018, Butovsky et al., 2014a). I therefore sought to examine whether the phenotype observed required microglia to be in direct contact with the dopaminergic neurons. To this end I used 24 well plate trans-well inserts where microglia were cultured on the porous membrane of the insert, and the neurons were cultured directly below on glass coverslips (Figure 4.15). The timelines of the experiment were as previously described (Figure 4.4). Aggregation was measured by immunofluorescence staining and quantification of the area of pSYN inclusions using ImageJ (Fiji). This analysis showed a significantly higher pSYN signal when microglia were not in contact with neurons (Figure 4.13b).

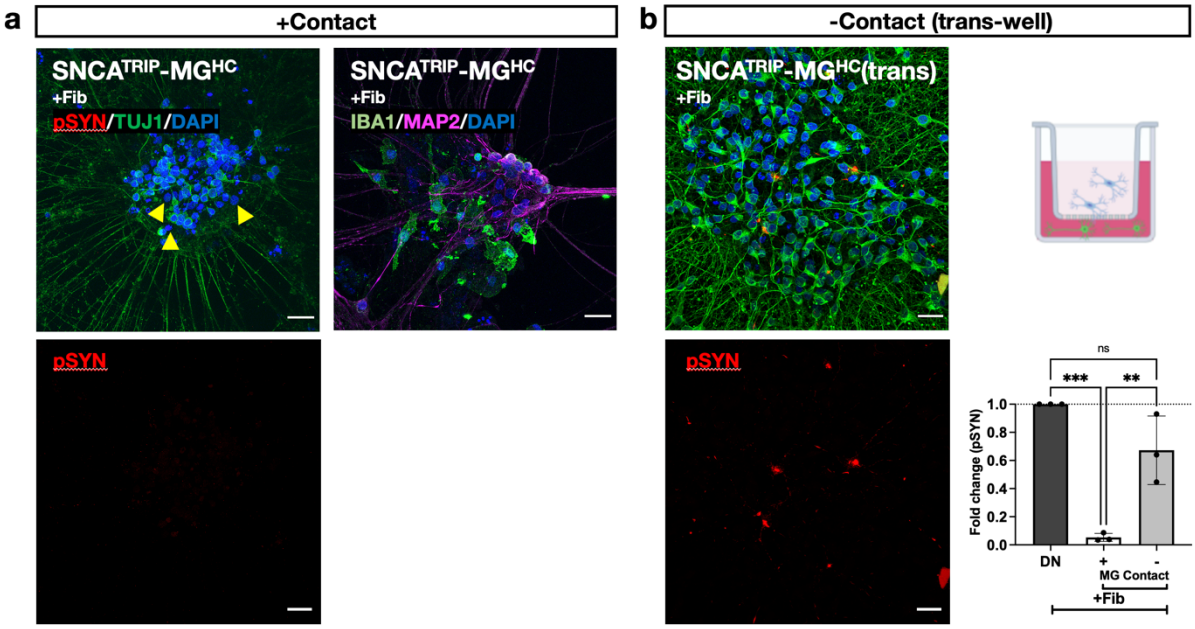

Figure 4.15 pSYN inclusions decreased when microglia were cultured in direct contact with dopaminergic neurons.

a. Representative confocal images of co-cultures where microglia were in direct contact with the dopaminergic neurons. Due to immunocytochemistry antibody incompatibility microglia could not be visualised in conjunction to the pSYN marker. Therefore, seeded co-cultures are visualised in two different combinations. Yellow arrows indicate representative microglia positive nuclei. Images are representative of three independent differentiations. Scale bar at 20 µm. **b.** Representative confocal images of seeded dopaminergic neurons whilst microglia were cultured in a trans-well insert. Schematic illustration of a 24 well plate trans-well insert. The seeded dopaminergic neurons were cultured on glass coverslips and harvested microglia were added on the porous membrane insert. The exchange of nutrients from the co-culture media was facilitated by the 0.2 µm diameter of the membrane's pores. The pixel area of pSYN positive inclusions was reduced significantly when microglia was in physical contact with the dopaminergic neurons (+contact) compared to the trans-well seeded co-cultures (-contact). Data is expressed as fold change to seeded neuronal monocultures (DN) (1.0). Each dot corresponds to one independent differentiation with one SNCA^{TRIP} clone and microglia clone differentiated three times. **p< 0.0001 by one-way ANOVA followed by Tukey's multiple comparisons test. Data is shown as mean ± s.e.m.

4.2.6 Effect of microglial LRRK2 and GBA mutations on neuronal α-synuclein aggregation.

I used iPSC lines derived from patients with *LRRK2* (*G2019S*) and *GBA* (*N370S*) mutations to assess the effects of these PD-associated mutations on microglial function in my model. I differentiated and co-cultured microglia from LRRK2 and GBA patients with SNCA^{TRIP} dopaminergic neurons following the same timelines and procedures as previously described. I observed that the levels of pSYN were reduced in co-cultures with LRRK2 and GBA iPSC-derived microglia when compared to their non-seeded co-culture controls following a similar phenotypic response to HC microglia (Figure 4.16).

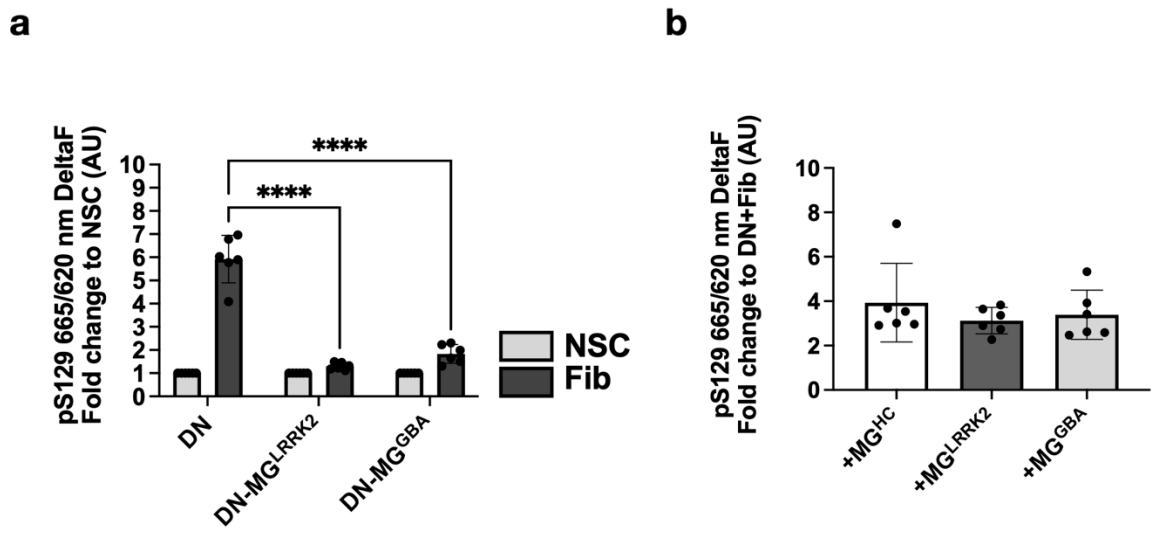

Figure 4.16 pSYN levels are not affected by microglial LRRK2 or GBA mutations.

a. Time resolved FRET assay specific for human pSYN, revealed that in the presence of LRRK2 or GBA mutant microglia, pSYN levels were also reduced as observed with HC microglia. ****p<0.0001 by two-way ANOVA followed by Sidak's multiple comparisons test **b.** Fold change of pSYN signal of co-cultures with HC, LRRK2 and GBA-derived microglia to their corresponding seeded neuronal monocultures. Each dot represents one independent differentiation with one neuronal clone and two microglial clones each differentiated three times. Data is shown as mean ± s.e.m.- Fib: non-seeding control, Fib: α-synuclein fibrils.

4.2.7 Phagocytosis may be relevant to the clearance of aggregates

To assess the potential mechanisms by which fibrillar α-synuclein is degraded by microglia, I assessed the effect of phagocytosis in monocultures. For these experiments, I used 10 μM of cytochalasin D which is an inhibitor of actin polymerisation and was previously used to inhibit phagocytosis in iPSC-derived microglia (Haenseler et al., 2017b). I initially performed a time-course experiment to determine the optimal duration of treatment with cytochalasin D without toxicity using the LDH assay (Figure 4.17a). Based on these results I treated microglia with 1 μM of fibrils with or without pre-treatment for 1 hr with cytochalasin D, followed by lysis at 24h and immunoblotting. I observed that α-synuclein levels were almost undetectable when cells were pre-treated with cytochalasin D (Figure 4.17 b,c), suggesting a role of the cytoskeleton and potentially phagocytosis in the uptake of aggregates as previously observed (Haenseler et al., 2017b).

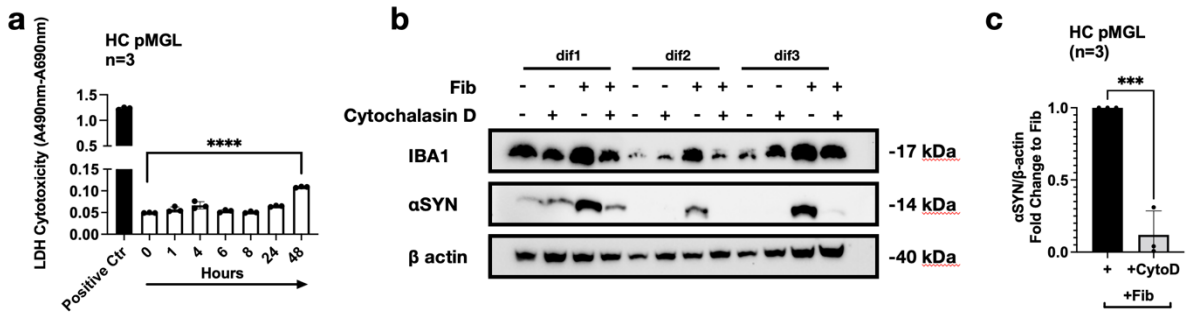

Figure 4.17 HC iPSC-derived microglia uptake exogenous α-synuclein fibrils via phagocytosis.

a. Time-course examination of 10 μM cytochalasin D revealed toxicity at 48 h but not at earlier time-points ****$p<0.05$ by one-way ANOVA followed by Dunnett's multiple comparisons test. **b.** HC microglia uptake exogenously added α-synuclein fibrils which is blocked by cytochalasin D. **c**. Quantification of fibrillar α-synuclein uptake following inhibition of phagocytosis. Each dot represents one independent differentiation. *$p<0.05$ by unpaired t-test (left graph) and **$p<0.05$ by one-way ANOVA followed by Tukey's multiple comparisons test and data is shown as mean ± s.e.m. Fib: α-synuclein fibrils, +CytoD: pre-treatment with cytochalasin D plus α-synuclein fibrils

4.3 Discussion

Human iPSC-derived models are well established and widely used in translational research and drug discovery. Efforts to model neuroinflammation in neurodegenerative diseases, such as Parkinson's and Alzheimer's using iPSC-derived neurons and microglia has only recently been investigated. The exact role of microglia in the onset and progression of Parkinson's disease remains elusive. Herein, I have developed a novel *in vitro* model using an iPSC-derived co-culture system to study microglia responses following seeded intraneuronal α-synuclein aggregation (Figure 4.4). $SNCA^{TRIP}$ iPSC-derived dopaminergic neurons were successfully differentiated and used to maximise the burden of aggregated α-synuclein. Stem cells from healthy individuals were successfully differentiated into human microglia to assess their response to pathology. The successful generation of this model was confirmed with immunostaining, morphological analysis and transcriptomics. Importantly, pSYN burden was significantly reduced when the $SNCA^{TRIP}$ dopaminergic neurons were co-cultured with healthy control microglia. The removal of aggregates was associated with improved neuronal survival based on neuronal counts (Figure 4.14d) and required direct physical contact between the two cell types (Figure 4.15). Taken together, this data demonstrates that iPSC-derived microglia-neuronal co-cultures can be used to study phenotypic microglial phenotypes and identify potential beneficial effects.

Since the floor plate model was firstly published (Kriks et al., 2011), several groups have introduced small modifications that have resulted in high-specificity yields of dopaminergic neurons (Jonikas et al., 2018, Fedele et al., 2017, Luo et al., 2020). The modified floor plate protocol developed in our lab yields dopaminergic

neurons with an approximate 60-70% brain region homology when compared to a human multi-subject single-cell atlas of the substantia nigra (Tanudjojo et al., 2021). I have confirmed the reproducibility of our modified floor-plate differentiation protocol using immunocytochemistry specific markers for dopaminergic neurons, and by bulk-RNA sequencing. The RNA sequencing also revealed small numbers of excitatory and inhibitory neurons, as well as astrocytes. Another challenge in the *in vitro* iPSC-modelling of neurodegeneration is the possibility of an altered age disease phenotype. Re-programming cells to a pluripotent state has been shown to delete the epigenome and modify age-related phenotypes, which potentially might be relevant to disease progression (Huh et al., 2016). To overcome this, the field has used fibroblasts which have been directly differentiated into induced neurons that have been used to model late-onset neurodegenerative diseases (Vierbuchen et al., 2010). However, protocols for induced neuron differentiation lack core neuronal subtype markers and have reduced viability (Abernathy et al., 2017, Carter et al., 2020). An alternative solution for the age-related disease phenotypes *in vitro* has been the telomerase manipulation of neurons (Vera et al., 2016).

Increased copy (either duplication or triplication) of the *SNCA* gene, which encodes the α-synuclein protein results in early onset autosomal forms of Parkinson's disease and contributes to accelerated progression and aggressiveness of the clinical symptoms (Oliveira et al., 2015). Our research group has established the differentiation of dopaminergic neurons from both healthy individuals, but also $SNCA^{TRIP}$ patients and demonstrated the higher seeding capacity of $SNCA^{TRIP}$ neurons using multiple clones (Haenseler et al., 2017c, Heman-Ackah et al., 2017, Tanudjojo et al., 2021). Since my research focused on assessing microglia phenotypes under

conditions of advanced neuronal pathology, for consistency I used a single $SNCA^{TRIP}$ clone and two different healthy control iPSC lines for microglial generation each differentiated three times for the majority of the experiments.

The protocols that mimic the developmental pathway of microglia differ substantially regarding their starting points and their length. For example, Muffat and colleagues generated EBs by treating iPSC colonies with collagenase IV in low-adherence tissue culture plates (Muffat et al., 2016). Following the generation of EBs, the authors reported that they used the same medium throughout the duration of the protocol, which contained colony stimulate factor 1 (csf1) and IL-34. The adhered EBs reportedly formed cystic structures, termed as ‘’yolk-sac EBs” that produced microglia precursors expressing the *PU.1* transcription factor, as well as pan-microglia markers, such as IBA1 and TMEM119. Other published protocols started by passaging stem cells as single cells (Abud et al., 2017). However, some protocols resulted in the generation of monocytes, which under further exposure to chemical cues and factors within the culture media acquired microglia-like properties. Generation of human microglia-like cells through monocytes is controversial given the distinct lineage of brain microglia compared to peripheral tissue resident macrophages. As an example, Pandya and colleagues (Pandya et al., 2017) initially reported treatment of iPSC colonies with BMP4, VEGF and SCF, but these cells expressed haematopoietic surface markers CD34 and CD43 and though positive for microglia signature markers their purity was as low as 9%. Given the current evidence, the most critical element for iPSC-derived microglia that resembles the human microglia and follow the *in vivo* developmental path, is the formation of yolk-sac like structures via formation of EBs. In my experiments, I followed step by step

the protocol published from our collaborators at the Dunn School of Pathology (Haenseler et al., 2017a) (Cowley Lab) and my qPCR results demonstrated that my pMGL and co-pMGL expressed an array of key microglia genes.

Additionally, a notable observation is that some microglia genes, such as *GPR34*, *C1QA, P2YR12* were expressed significantly higher in co-pMGL rather than pMGL. That can be explained by the fact that co-pMGL were co-cultured with neurons and therefore, achieving higher degrees of maturation through their interactions with neurons. Significant expression of *GPR34, MERTK* and *CI1QA* has been confirmed by comparative transcriptomic analysis in iPSC-derived microglia of various protocols, which follows closely the *in vivo* foetal and adult microglia signature (Aubert et al., 2021).Metabotropic receptor P2Y12 is a key component in the bi-directional communication with neurons and it signals and promotes microglia branching, as well as participating in chemotactic mechanisms (Eyo and Wu, 2013). GPR34, a G-protein coupled receptor belonging to the same superfamily as P2YR12, is implicated in pathways regulating axonal growth, as well as microglial morphology and phagocytosis (Preissler et al., 2015). *GPR34* is also a homeostatic microglial gene and part of the neurodegenerative disease phenotype as its expression is reduced over time in disease (Krasemann et al., 2017a).

Based on previous studies from our research group on neuronal monocultures, I used the same concentration (1μM) of the *de novo* α-synuclein fibrils to induce pSYN pathology on $SNCA^{TRIP}$ dopaminergic neurons. I observed accumulation of pSYN positive inclusions in neurites and cell bodies of neurons. Our laboratory has previously shown that these inclusions co-localised with p62, a marker of inclusion pathology (Tanudjojo et al., 2021). Time resolved FRET assay revealed a significant

increase in pSYN levels in dopaminergic neurons, when assayed 4 weeks after fibrils addition, which resulted in approximately 25% of neuronal death. It is highly likely that the process of inclusion formation caused neuronal death, and this was mitigated by the addition of microglia (Figure 4.14d). The factors that mediate this protective response are not clear.

Neuroinflammation and 'reactive' microglia have been long associated with Parkinson's disease, yet the nature of any causal relationship remains elusive. The human iPSC-derived co-culture system to study the microglia phenotypes in response to intraneuronal α-synuclein aggregation is to my knowledge the first to be reported (Figure 4.4). Microglia secrete trophic factors that support the surrounding tissues and by selective synapse elimination and axonal pruning they contribute to the formation of functional neuronal circuits (Neumann et al., 2009a). It has also been reported that *in vitro*, human iPSC-derived microglia are mostly ramified around neuronal clusters (Haenseler et al., 2017a). Indeed, I observed that soon after addition of harvested pMacpre, ramified microglia mostly localised around neuronal clusters. Furthermore, the neuronal axonal morphology changed over the co-cultured time. It is therefore possible that selective phagocytosis of axonal terminals with aggregates is a likely mechanism by which aggregates are removed in this system. In addition, microglia secrete brain derived neurotrophic factor (BDNF) and other trophic signals which may enhanced neuronal health (Huang and Reichardt, 2001).

According to the prion-like paradigm, misfolded proteins such as α-synuclein and tau are released in the extracellular space and propagate to neighbouring cells (Goedert, 2001). Effective clearance of such proteotoxic species by microglia may be a key response to limit neurodegeneration. In this respect, the reduction in neuronal

pSYN levels was associated with improved dopaminergic neuronal survival in the seeded co-cultures when compared to seeded neuronal monocultures (Figure 4.12d). It is highly likely that microglia uptake released aggregated α-synuclein assemblies and facilitate their degradation as previously reported (Scheiblich et al., 2021). Reduction of the pathological burden leads to improved neuronal health (Stefanis, 2012). Neuroprotective microglial effects were also observed in other neurodegenerative diseases. For example, in the early stages of Alzheimer's disease microglia were reported to reduce Aβ plaques (Frenkel et al., 2008, Simard et al., 2006). However, chronic neurodegeneration and persistent stress have been correlated with loss of microglial phagocytic activity, increased accumulation of Aβ and microglia-related neurotoxic effects (Onuska, 2020). A neuroprotective microglial effect has also been reported in the zebra fish of ALS expressing human TDP43 (Svahn et al., 2018).

Interestingly, in fixed seeded HC microglia-SNCA^{TRIP} dopaminergic neuron co-cultures I found that microglia shortened their ramifications and enlarged their cell body. As discussed in Chapter 3, primed and activated microglia shorten their processes and enlarge their cell bodies, acquiring an amoeboid-like shape. Morphological activation of iPSC-derived microglia in *in vitro* models of Parkinson's disease neuroinflammation has also been reported recently in the literature (Badanjak et al., 2021). Several studies have reported morphological activation of microglia under conditions of protein misfolding and aggregation in other neurodegenerative disorders (Plescher et al., 2018, Franco-Bocanegra et al., 2021, Sanchez-Guajardo et al., 2010). In my model, I observed a highly dynamic transition from ''resting'', ramified microglia to round, amoeboid-like shaped, activated microglia through an

intermediate activation stage of bipolar-like shape (Figure 4.14) (Okajima and Tsuruta, 2018). I visualised and evaluated microglial morphology using the IBA1 marker, as its expression has been correlated with microglia motility (Franco-Bocanegra et al., 2019). Clustering of activated microglia is more pronounced around Aβ plaques in Alzheimer's disease (Franco-Bocanegra et al., 2019). Similarly, I observe a significant transition to round, activated microglia under seeding conditions and clustering around dopaminergic neurons. Although I have not generated immunocytochemical evidence of clustering around pathological pSYN positive inclusions due to antibody limitations, imaging data suggests that microglia migrated towards the site of the pathology.

It is noteworthy that activated microglia were also present under baseline conditions. Under physiological conditions round microglia exhibit chemotactic motility with the aim to restore homeostasis (Franco-Bocanegra et al., 2019). Therefore, the detection of activated microglia does not always imply the presence of pathological microglia. Transcription factor PU.1 encoded by *SPI1* among other functions may be involved in the morphological transition of microglia (Okajima and Tsuruta, 2018). Interestingly, *SPI1* was expressed in microglia under non-seeded and seeded conditions with an upregulation trend in the later as revealed, by the whole transcriptome RNA-Seq analysis (Chapter 5). PU.1 is involved in the downstream pathways of CSF1R signalling, which is essential for microglia survival and proliferation (Elmore et al., 2014). This could explain the observed morphological motility and plasticity.

Human iPSC-derived LRRK2 (G2019S) and GBA microglia co-cultured with seeded $SNCA^{TRIP}$ dopaminergic neurons resulted in decreased pSYN levels similar to

healthy controls (Figure 4.16). Small interfering RNA (siRNA) knockdown of *LRRK2* in mouse microglia-like cells, BV2 resulted in reduced phagocytotic activity (Marker et al., 2012). Human iPSC-derived LRRK2 macrophages produced with the same protocol as described in my study displayed co-localisation of endogenous LRRK2 with late phagocytic markers RAB9 and LAMP1 rather than early endosomal marker RAB5 and it was suggested that LRRK2 may function in alternative phagosome components other than the direct route to proteolysis (Lee et al., 2020). These observations could possibly point towards increased phagocytotic activity of microglia and therefore, reduced pSYN signal in my model. iPSC-derived dopaminergic neurons from GBA patients reportedly displayed disease-relevant phenotypes and increased levels of α-synuclein (Schöndorf et al., 2014). To my knowledge, studies on GBA-derived human microglia have not been reported yet. My results suggest that GBA is not critical for the observed phenotype. Consistent with what has been previously shown in the literature (Scheiblich et al., 2021, Haenseler et al., 2017c), iPSC-derived microglia displayed increased α-synuclein uptake after treatment with *de novo* α-synuclein fibrils, which was significantly reduced when phagocytosis was blocked with cytochalasin D (Figure 4.17).

Microglia participate in a dynamic bi-directional communication with neurons, and this is facilitated via secretion of chemokines and neurotransmitters, as well as purinergic signalling (Szepesi et al., 2018). The data presented here showed that microglia require direct contact with the neurons to promote the clearance of pSYN inclusions. Recently, it was reported that monocultured microglia can degrade fibrillar α-synuclein via tunnelling nanotubes (Scheiblich et al., 2021). Therefore, beyond axonal phagocytosis, F-actin intercellular connections could be formed between

microglia and neurons to facilitate degradation of pathological forms of α-synuclein. To further investigate this interaction future work could utilise microfluidic devices (Katsikoudi et al., 2020).

Overall, work in this chapter led to the development of a new iPSC-based model of neuron-microglial interaction in the context of Parkinson's pathology and identified a protective microglial phenotype.

Chapter 5: Microglial phenotypes in response to neuronal α-synuclein aggregation

5.1 Introduction

5.1.1 Homeostatic microglia

The unique transcriptional homeostatic signature of microglia was firstly identified in mice (Butovsky et al., 2014b, Hickman et al., 2013). Despite the differences in the gene expression pattern between mouse and human microglia, a number of these homeostatic genes are expressed across species, including the purinergic receptor P2Y12 (*P2RY12*), transmembrane protein 119 (*TMEM119*), G-protein coupled receptor 34 (*GPR34*), β-hexosaminidase subunit β (*Hexb*), colony stimulating factor receptor 1 (*CSF1R*), fractalkine receptor CX3C-chemokine receptor 1 (*CX3CR1*) and the calcium-binding protein allograft inflammatory factor 1 (*AIF1*, also known as *IBA1*) (Galatro et al., 2017b).

To study the versatility of the microglia phenotypes, it is imperative to firstly understand the mechanisms behind the homeostatic phenotypes. For example, persistent activation of the CSF1R by its ligand CSF1 promotes microglia development and further activation by the additional ligand IL-34, drives tissue-specific signalling pathways (Butovsky and Weiner, 2018). Further studies have also revealed several transcription factors that regulate microglial phenotypes such as PU.1 (encoded by *SPI1*), which is a master regulator of myeloid cells (Friedman, 2007) and serves an essential role in lineage determination (Heinz et al., 2010). Additionally, secondary transcription factors are involved in microglia homeostatic regulation, such

as IRF8, which is essential for generation of mature microglia precursors (Kierdorf et al., 2013a). TGFβ1 is a factor involved in the homeostatic microglial transition *in vivo*.

Microglial function is also regulated by inhibitory signals that supress unwanted inflammatory over-activity that may arise with tissue destruction (Hanisch and Kettenmann, 2007). These checkpoint mechanisms include microglia-neuronal communication through receptor-ligand interactions, such as CX3CR1-CX3CL1, soluble molecules in the brain's milieu, such as TGFβ1 and intracellular regulators, such as transcription factors like MafB (Butovsky et al., 2015, Matcovitch-Natan et al., 2016). These mechanisms can be detrimental when persistent microglia activity is required.

5.1.2 Disease-associated microglia

Studies in Alzheimer's disease have reported conflicting results on the contribution of microglia to the onset and progression of the disease (Deardorff and Grossberg, 2017, Wang et al., 2016, Guillot-Sestier et al., 2015). Some studies have reported that microglia acquire pro-inflammatory phenotypes, which have been correlated to disease acceleration (Tejera and Heneka, 2016, Yamasaki et al., 2014). It is likely that microglia exert protective effects at the early stages of neurodegeneration but switch phenotypes towards more advanced stages.

The Amit group uncovered a unique disease-associated microglia (DAM) subtype by using a mouse model of Alzheimer's disease and by performing parallel single-cell analysis with chromatin profiling, single-molecule FISH, immunohistochemistry, genetic perturbation and computational modelling (Keren-Shaul et al., 2017). This DAM subtype of microglia express typical pan-microglia markers, such as *IBA1* whilst simultaneously have downregulated homeostatic genes, such as *P2RY12*, *CX3CR1* and *TMEM119* (Deczkowska et al., 2018). Furthermore, DAM express an array of genes related to phagocytosis, lysosomal and lipid metabolism pathways, such as *APOE*, *Lpl*, *Axl*, *TYROBP* and *TREM2*. A few of these aforementioned genes especially TREM2, have also been identified as major Alzheimer's disease-related risk factors (Lambert et al., 2013).

Although DAM genes were initially reported in a transgenic mouse model associated with 5 familial Alzheimer's disease mutations, in areas associated with Aβ pathology, these findings were further confirmed in models of tauopathies (Ajami et al., 2018, Friedman et al., 2018a), ALS (Friedman et al., 2018a, Keren-Shaul et al., 2017) and MS (Krasemann et al., 2017b). DAM microglial signatures were also confirmed in post mortem brains from patients with Alzheimer's disease (Friedman et

al., 2018a), further supporting the notion that they constitute a neurological disease related microglial subtype independent of a specific aetiology (Deczkowska et al., 2018).

5.1.3 Disease-associated microglia: universal sensors of neurodegeneration and their molecular patterns

Various stress signals known as DAMPs and PAMPs are recognised via patterns recognition receptors (PRRs) and initiate immune responses (Janeway, 1989, Matzinger, 1994). The shared patterns among various pathogens resulted in a small group of sensors that respond to a wide variety of pathogens. It has been proposed that initiation of the DAM phenotype is manifestation of this fundamental principle (Deczkowska et al., 2018). Neurodegeneration associated molecular patterns (NAMPs) across various neurological disorders are recognised by an array of receptors expressed on microglia and trigger their transition to DAM (Figure 5.1). NAMPs include molecules on apoptotic neuronal cells, lipid degradation products and extracellular aggregated proteins, such as α-synuclein.

The presence of DAM has been detected under conditions of apoptotic neuronal death (Wang et al., 2015b, Keren-Shaul et al., 2017, Krasemann et al., 2017a). Additionally, injection of labelled apoptotic neuronal bodies in wild type mice resulted in emergence of phagocytotic microglia displaying engulfing morphologies and transcriptomic profiles similar to DAM ($Apoe^{hi}$, $Clec7a^{hi}$, $TMEM119^{low}$, $P2RY12^{low}$) (Deczkowska et al., 2018). These data suggested that apoptosis precedes the emergence of DAM and that TREM2 is a key component in the DAM induction, since it is a direct receptor to an array of NAMPs (Keren-Shaul et al., 2017, Deczkowska et al., 2018).

The Tyro3/Axl/Mer receptor tyrosine kinase complex also recognises molecules on apoptotic cells (Lemke, 2017). Particularly, it has been reported that *Axl* expression in Alzheimer's disease and ALS mouse models was increased compared to homeostatic microglia phenotypes (Fourgeaud et al., 2016, Keren-Shaul et al.,

2017). However, it remains unclear whether the receptor tyrosine kinases are a universal sensor for NAMPs across neurodegeneration. Induction of the DAMP phenotype also includes down-regulation of *P2RY12*, whose product also recognises apoptotic molecules across neurological disorders (Rodrigues et al., 2015).

Induction of DAM is only one aspect of a complex signalling mechanisms that may be linked to neurodegeneration, as dysregulation of other brain cells may also contribute (Mosher and Wyss-Coray, 2014). Microglia as sentinels can detect any changes in their microenvironment but whether neuronal or glial signals lead to DAM phenotypes in Parkinson's disease remains unknown.

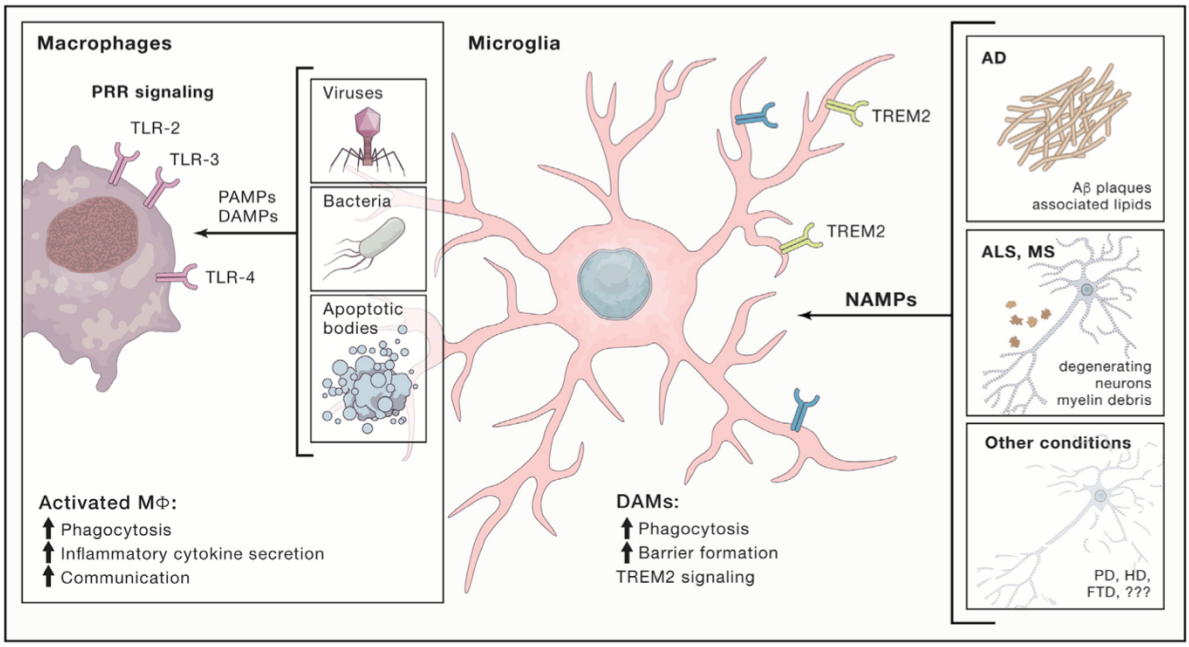

Figure 5.1 Disease Associated Microglia phenotype: a universal phenotype across neurodegeneration.

In analogy to the peripheral immune system, where pathogens and damage associated signals (DAMPs and PAMPs) are recognised via PRRs, it has been suggested that microglia are equipped to respond to neuronal damage (NAMPs) via activation of specific array of receptors, such as TREM2 and P2YR12. Image adapted from (Deczkowska et al., 2018).

5.1.4 TREM2 function and role in Parkinson's disease

TREM2 is a transmembrane receptor and part of the immunoglobulin superfamily that was first identified in monocyte-derived cells and mouse macrophages (Bouchon et al., 2000). *TREM2* is expressed in cells of the myeloid lineage but regulation of its expression remains elusive. Among the promoters of the *TREM2* gene is PU.1, a master regulator of myeloid cell fate (Satoh et al., 2014). TREM2 recognises a variety of ligands, such as phospholipids, sulfatides, bacterial lipopolysaccharides and DNA (Wang et al., 2015b, Cannon et al., 2012). The receptor's extracellular region includes a single immunoglobulin domain and a stalk region and it is followed by a transmembrane domain and a short intracellular domain with no motifs (Ulland and Colonna, 2018).

The transmembrane domain of TREM2 associates with the adaptor proteins DNA-X activation protein 12 (DAP12, also known as TYRO protein tyrosine kinase-binding protein TYROBP) and DAP10. DAP12 is required for the expression of TREM2 on the cell surface and transmission of intracellular signals via recruitment of the tyrosine-protein kinase SYK (Konishi and Kiyama, 2018). DAP10 initiates intracellular signal cascades via recruitment of phosphatidylinositol 3-kinase (PI3K) (Peng et al., 2010). Activation of TREM2-DAP12-DAP10 triggers protein and lipid phosphorylation cascades that results in mobilisation of Ca^{2+}, activation of integrin, re-arrangement of the cytoskeleton, mechanistic target of rapamycin (mTOR), signalling of mitogen-activated protein kinase (MAPK) and metabolic signals (Figure 5.2) (Ulland et al., 2017, Peng et al., 2010).

TREM2-deficient microglia have reduced capacity to maintain their cellular homeostasis, resulting in reduced activation and clustering around misfolded proteins, such as Aβ (Ulland et al., 2017). In Alzheimer's disease animal models,

absence of TREM2 results in decreased microglial cellular fitness by increased activation of AMP-activated protein kinase (AMPK), of Unc-51-like autophagy activating kinase 1 (ULK1) and ultimately, autophagy (Ulland et al., 2017).

Since the discovery that *TREM2* mutations are risk factors for Alzheimer's disease (Colonna and Wang, 2016, Guerreiro et al., 2013, Song et al., 2017), several studies have investigated the involvement of TREM2 in other neurodegenerative diseases, such as Parkinson's disease. An *in vivo* study reported that *TREM2* overexpression in the MPTP mouse model attenuated neurodegeneration and neuroinflammation (Ren et al., 2018). *In vitro*, knockdown of *TREM2* in BV2 microglial cells enhanced α-synuclein induced inflammatory responses (Guo et al., 2019). These results indicate that the role of TREM2 in Parkinson's disease pathology remains elusive.

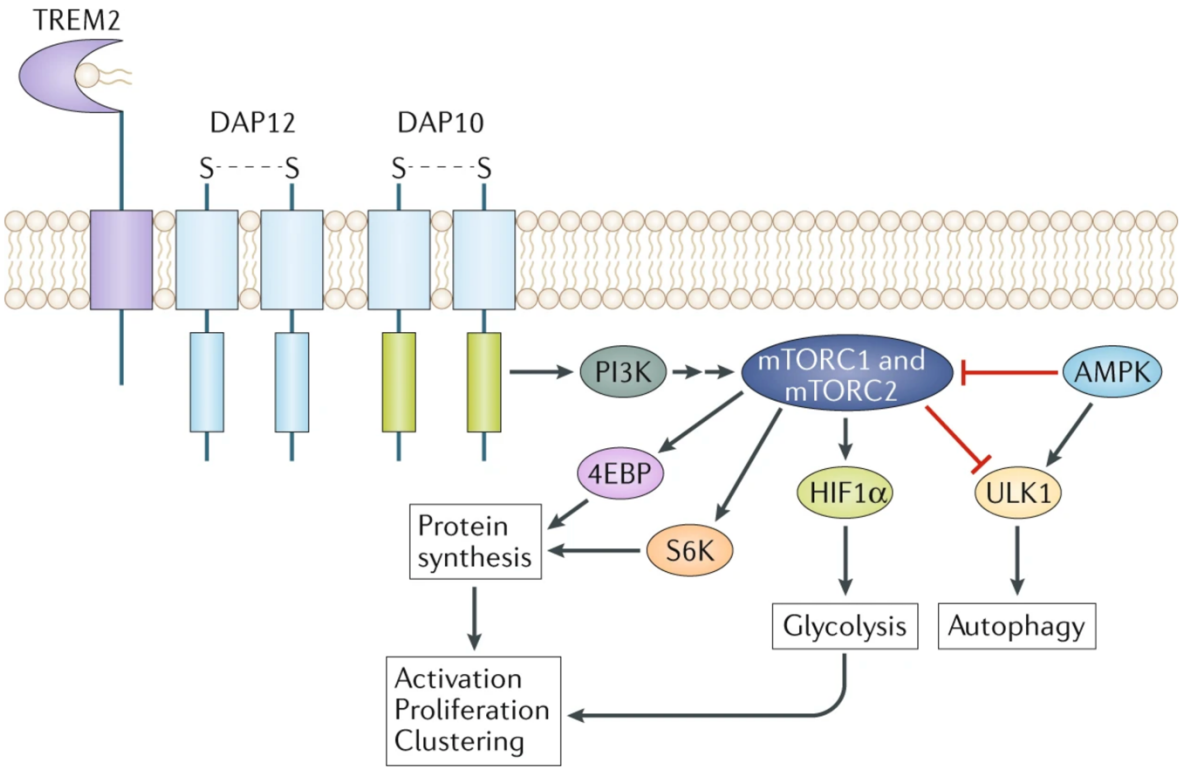

Figure 5.2 TREM2 and downstream pathways upon receptor activation.

Ligand binding on microglial TREM2 results in activation of its adaptive receptors, DAP12 and DAP10 which sequentially activate PI3K. Activation of PI3K results in activation of the mechanistic target of rapamycin complexes 1 and 2 (mTORC1 and mTORC2), which are responsible for metabolic regulation and inhibition of autophagy. S-----S indicates a disulphide bridge. 4EBP, eukaryotic translation initiation factor 4E-binding protein; DAP, DNAX-activation protein; HIF1α, hypoxia-inducible factor 1α; S6K, ribosomal protein S6 kinase. Image adapted from (Ulland and Colonna, 2018).

5.1.5 Disease associated microglia phenotype is initiated by a TREM2 independent mechanism

After identifying the unique microglial subtype, the Amit group sought to investigate whether there were any potential regulators that may trigger initiation of the DAM phenotype (Keren-Shaul et al., 2017). To do so, they performed single-cell RNA sequencing on whole brains from wild type and the Alzheimer's disease mouse model that expresses five familial gene mutations (5XFAD) with or without *TREM2* expression. Their analysis suggested that DAM are generated through a two-step process following activation of homeostatic microglia. The first intermediate stage, which is independent of TREM2 signalling involves reduction of critical homeostatic checkpoints, such as *CX3CR1* and *P2RY12* and simultaneous upregulation of genes, such as *APOE* and TREM2 adaptor, *TYROBP*. The intermediate DAM programme is followed by a TREM2-dependent activation, which involves increased expression of genes implicated in phagocytosis and lipid metabolism, such as *Lpl*. Interestingly, the authors reported that no stage 2 DAM cells were observed without having been firstly initiated through the intermediate stage, suggesting that the DAM activation is a mechanistically coupled temporal event that requires transition through both stages (Keren-Shaul et al., 2017).

5.1.6 Cytokine levels in Parkinson's disease

The discovery of DAM in Alzheimer's disease transformed our understanding of microglia heterogeneity in the brain. Based on the NAMPs principle it is expected that DAM subtypes exist in Parkinson's disease as well. Induction of the DAM phenotype aims initially towards protection of the microenvironment. An important research topic in Parkinson's disease associated inflammation is whether microglia secret pro-inflammatory cytokines and neurotrophic factors or aggravate the pathology via secretion of anti-inflammatory factors that are detrimental to dopaminergic neurons (Joers et al., 2017).

Evaluation of secreted cytokines can provide helpful insights regarding the possible pathogenic impact of microglia, which has been briefly discussed in Chapter 3. Elevated levels of pro-inflammatory cytokines TNFα, IL-1β and IL-6 have been reported in the CSF of Parkinson's disease patients (Mogi et al., 2007, Müller et al., 1998). However, levels of other inflammatory markers, such as fractalkine (CX3CL1), Flt3 ligand, C-reactive protein, interferon gamma-induced protein 10 (IP-10), monocyte chemotactic protein 1 (MCP-1) and macrophage inflammatory protein 1β (MIP-1β) are not significantly elevated in patients when compared to healthy control individuals (Shi et al., 2011, Lindqvist et al., 2013). TGF-β levels, a factor involved in microglia activation is elevated in the patient CSF (Vawter et al., 1996). Elevated cytokine levels have also been observed in the plasma of Parkinson's disease patients, such CCL3 (also known as MIP-α) (Lindqvist et al., 2013).

5.1.7 Uptake and clearance of α-synuclein by microglia

Part of the homeostatic functions of microglia *in vivo* is clearance of cellular debris, dying cells and aggregation-prone proteins when they sense changes in their microenvironment. It has been suggested that chronic inflammation may contribute to aggravated α-synuclein pathology (Brundin et al., 2008) that may be explained by defected mechanisms regarding the uptake and clearance of α-synuclein.

It has also been suggested that spread of α-synuclein pathology may be facilitated by cell-to-cell transmission involving either neuronal or glial cells (Desplats et al., 2009, Rostami et al., 2017). To this end, mechanisms such as exocytosis and endocytosis, exosome uptake or direct transmission through the cellular milieu have been proposed (Emmanouilidou et al., 2010, Flavin et al., 2017, Freundt et al., 2012) and may limit efficient microglia clearance (Choi et al., 2020). Uptake of α-synuclein *de novo* fibrils has been studied and reported in human iPSC-derived microglia through phagocytosis (Haenseler et al., 2017c). Additionally, it has been recently demonstrated that *in vitro* human microglia can degrade fibrillar α-synuclein through F-actin nanotube structures (Scheiblich et al., 2021). Understanding the mechanisms behind α-synuclein clearance is imperative. Enhancing the microglial clearance of the protein may prove a valuable therapeutic strategy for the treatment of synucleinopathies.

5.1.8 Aims and Objectives

In the previous chapter I described a new microglial-dopaminergic neuronal co-culture model that I established to study the microglial response following seeded aggregation of iPSC-derived $SNCA^{TRIP}$ dopaminergic neurons.

The objectives of this chapter were to:

1. Perform targeted and genome-wide transcriptomic studies in wild type microglia when co-cultured with α-synuclein seeded dopaminergic neurons
2. Study the role of DAM-related *TREM2* in mono and co-cultured iPSC-derived microglia
3. Measure microglial cytokines that are secreted in response to neuronal seeded aggregation

5.2 Results

5.2.1 Whole transcriptome analysis of iPSC-derived microglial-dopaminergic neuronal co-cultures following neuronal α-synuclein seeded aggregation

To obtain an initial overview of the microglial and corresponding neuronal molecular changes in the model, we performed bulk RNA-sequencing in iPSC-derived co-cultures under baseline conditions vs seeded aggregation. $SNCA^{TRIP}$ neurons and HC microglia were analysed at DIV73. To ensure reproducibility, two different iPSC lines were used for microglia differentiations, as well as independent differentiation replicates (Rs). The bioinformatic analysis was performed by our collaborators, Dr. Devika Agarwal and Dr. David Sims. Principal component analysis (PCA) illustrated that samples were clustered based on the microglia cell line (SFC856 and SFC841) used for the co-cultures (Figure 5.3).

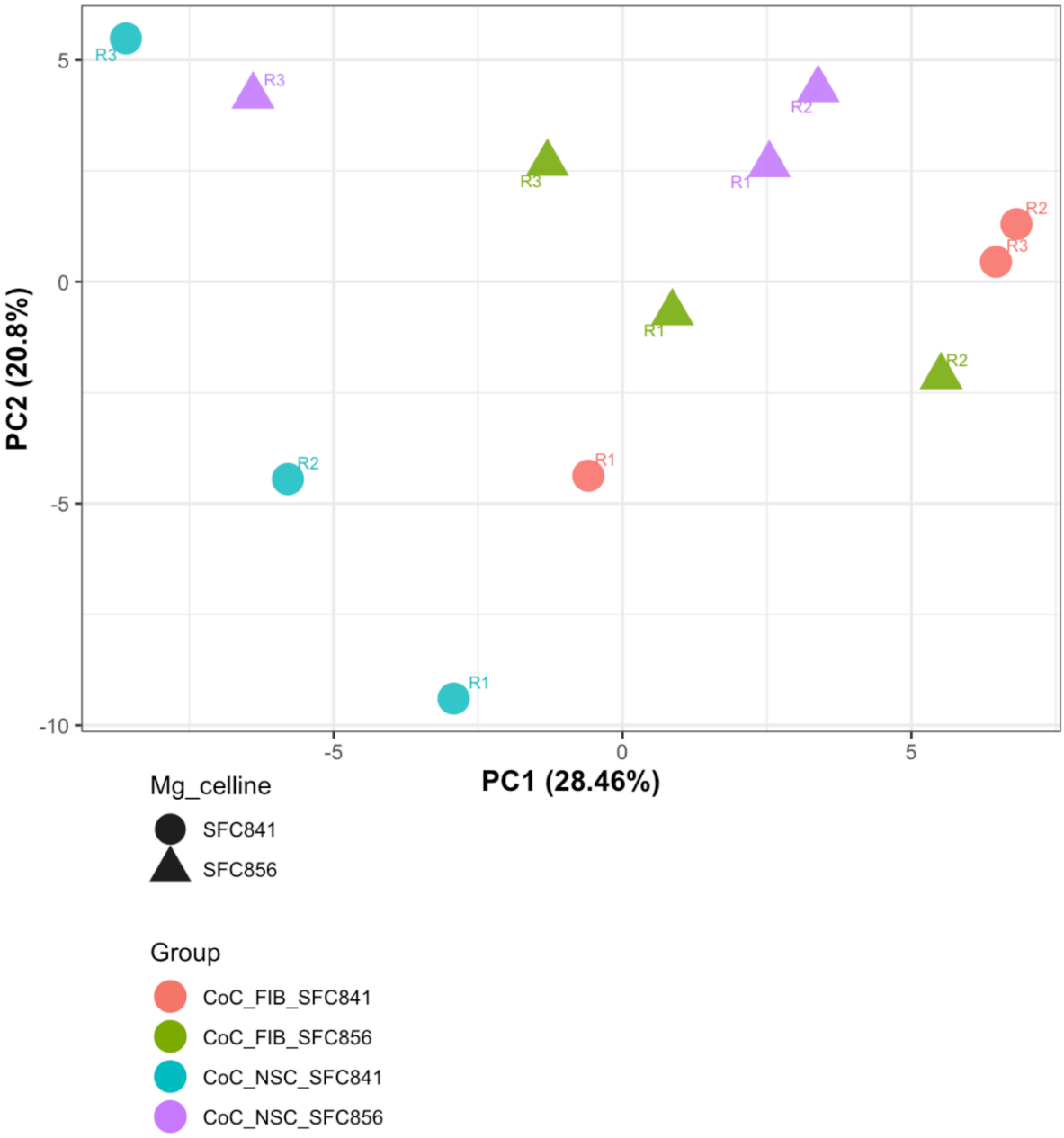

Figure 5.3 Principal component analysis by bulk RNA-Seq in seeded co-cultures versus non-seeded co-cultures revealed better clustering for one of the two stem cell lines used for the microglia differentiations.

Principal component analysis showed that samples clustered by the cell line used for microglia differentiation in the co-cultures (SFC856 vs. SFC841). n=3 differentiations (R1, R2, R3) per condition and per microglia iPSC line. Data analysis for this figure was performed by Dr. Devika Agarwal and Dr. David Sims.

Based on the separation patterns described in the PCA plots, co-culture replicates with the SFC856 microglia cell line that yielded closer clustering on PC1-PC2 were analysed further for differential gene expression using DESeq2, to identify significant differences in genes between baseline and aggregation across the three replicates. A total of 20 genes were significantly upregulated under conditions of seeded aggregation, whilst 9 were downregulated (Figure 5.4a). Using the human protein atlas online database, only 3 genes (*BTBD7*, *FKBP9* and *SSH2*) had a microglia cell type specificity whilst 3 genes (*SMURF1*, *PI4KB* and *SYNPO2*) had a shared specificity between neurons and microglia. Even though this analysis did not yield significant differences at genome-wide comparison, most likely due to low number of replicates to account for the variability between differentiations, we observed a trend for down-regulation of homeostatic genes such as *TMEM119* and up-regulation of DAM genes such as *SPI1*, *Axl*, *CLEC7A*, *SYK*, *CTSD*, *APOE*, *B2M* (Figure 5.4b)

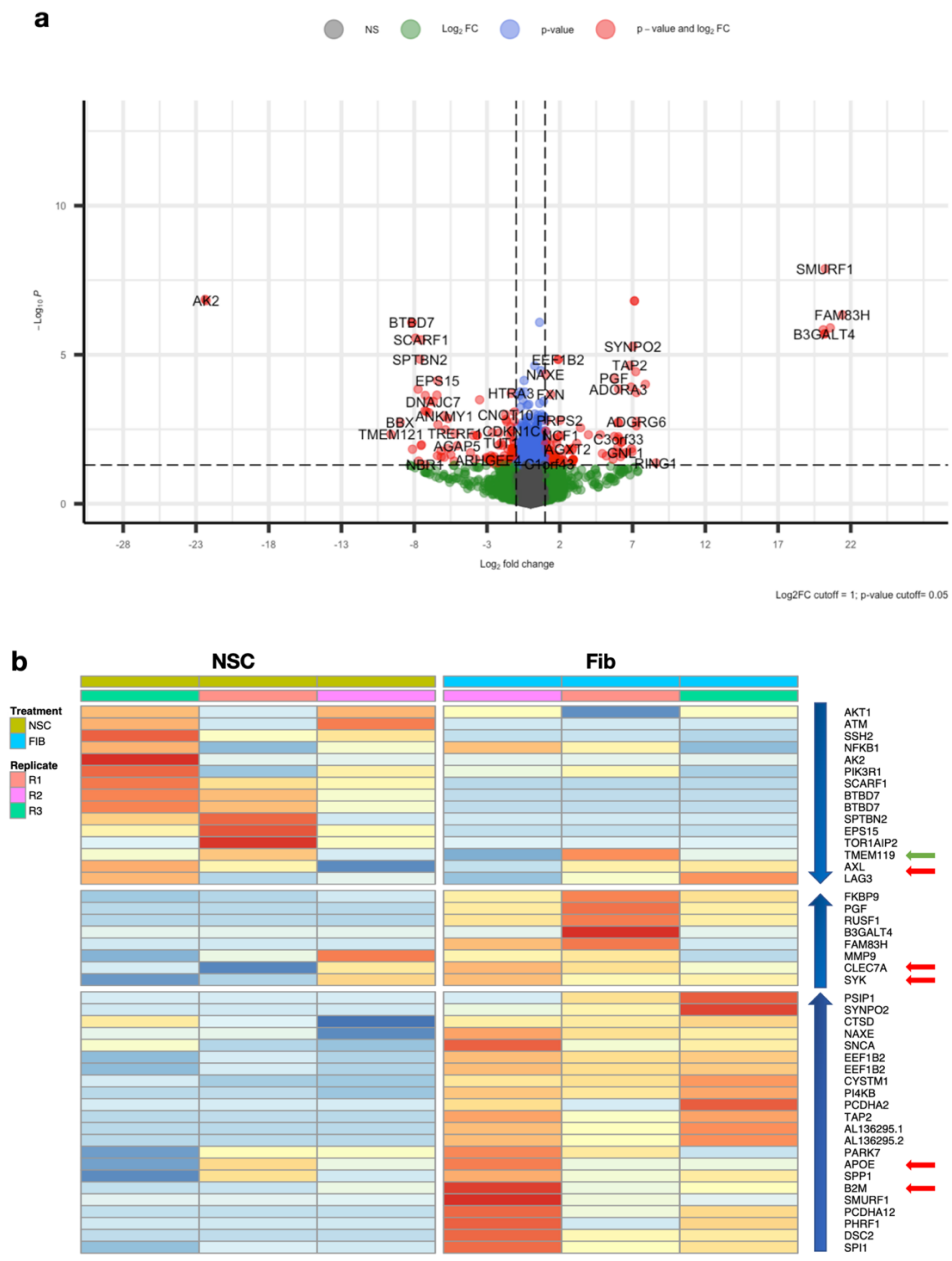

Figure 5.4 Differential gene expression by bulk RNA-Seq in co-cultures of microglia with either fibril seeded (Fib) or non-seeded control (NSC) neurons.

a. Volcano plot of all the differentially expressed genes between Fib vs NSC co-cultures at DIV73. Genes with | $\log_2$ fold-change | > 1 and adjusted p-value < 0.05 were defined as differentially expressed and are depicted in red (n=3 differentiations using the SFC856 HC line for microglia). **b.** Heatmap of Rlog transformed z-score values across samples with ward clustering of genes for differentially expressed and key microglial genes with up-and down regulation trends in seeded vs. non-seeded co-cultures across three independent differentiations (R1, R2, R3). Arrows indicate

homeostatic (green) and DAM (red) genes. The data in this figure was analysed by Dr. Devika Agarwal and Dr. David Sims.

5.2.2 Microglia express homeostatic and disease-associated genetic markers

To further assess whether co-pMGL in my co-culture model expressed key homeostatic, and disease associated genetic markers as identified in the literature (Figure 5.5a), I performed targeted gene expression analysis using qPCR at DIV73, i.e., 2-weeks after the microglia were added to seeded neurons and 4-weeks after seeded aggregation of neurons. I observed a significant down-regulation of three homeostatic genes: *P2RY12*, *CX3CR1* and *TMEM119* (Figure 5.5b). The DAM genes, *TYROBP*, *TREM2*, *APOE*, *LPL*, *AXL* were significantly upregulated when compared to the corresponding unseeded control co-cultures (Figure 5.5c).

Given the importance of TREM2 in the transition to a DAM phenotype and the fact that both *TREM2* and *TYROBP* were upregulated in my co-culture model under aggregation conditions, I further investigated the primary downstream components of the TREM2/DAP12 (TYROBP) complex by qPCR. *CSF1R*, *PLC* γ, *PI3K* and *AkT* expression was significantly upregulated when compared to their corresponding baseline control and there was a trend for increased Src kinase expression (Figure 5.5d, e).

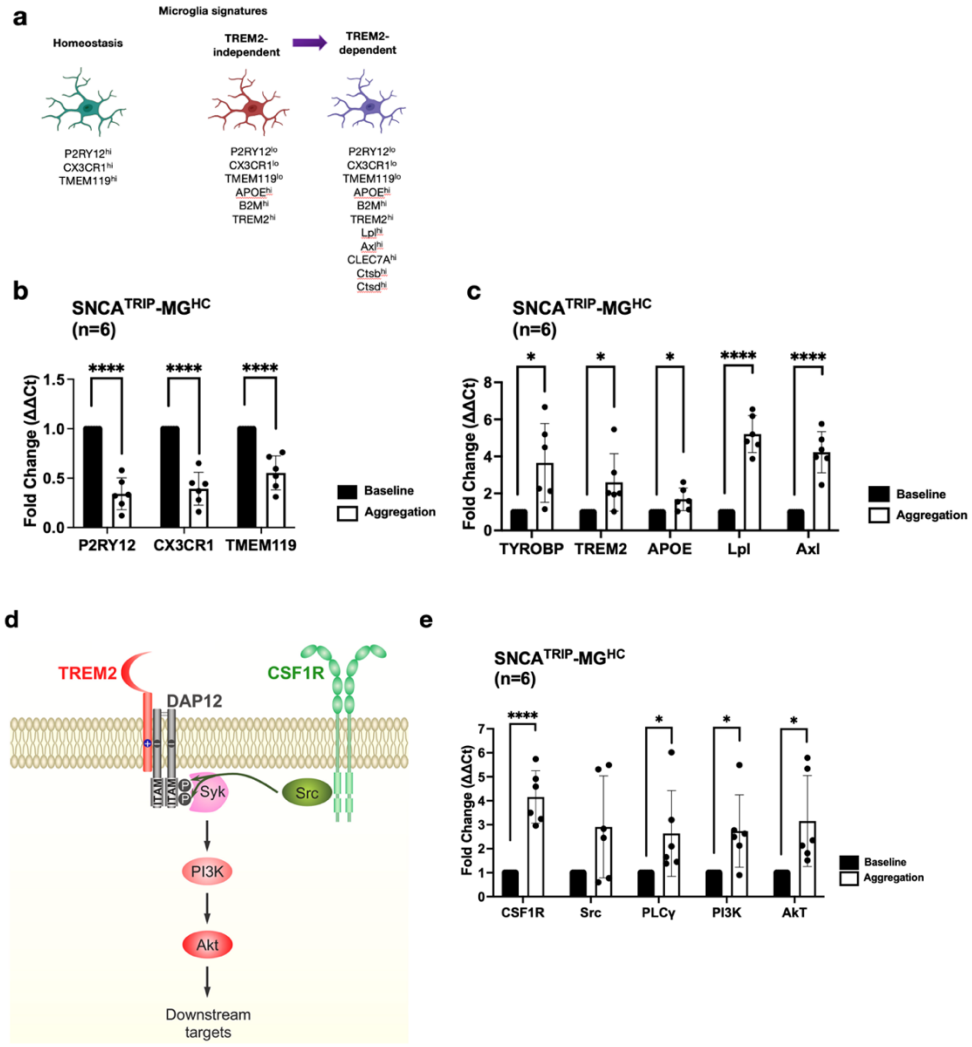

Figure 5.5 Co-cultured microglia express key homeostatic and DAM genes.

a. Examples of homeostatic and DAM-related genes microglial genes whose expression changes in neurodegeneration. **b.** Quantification of the relative expression of three key homeostatic markers (*P2RY12*, *CX3CR1*, *TMEM119*) and **c.** five DAM markers (*TYROBP*, *TREM2*, *APOE*, *Lpl*, *Axl*). Relative expression was calculated using the $2^{-\Delta\Delta Ct}$ method, with *GAPDH* as an endogenous control and normalization to non-seeding control (NSC: Baseline). Each dot represents one independent differentiation for two microglia clones (each differentiated 3 times) and one neuronal $SNCA^{TRIP}$ clone (with technical repeats for RT-qPCR). *, **** $p<0.0001$ by individual unpaired t-tests. **d.** Schematic representation of the primary downstream components of the TREM2/DAP12 receptor complex in microglia. Image adapted from (Konishi and Kiyama, 2020). **e.** Quantification of the relative expression of the TREM2 primary downstream components. Relative expression was calculated using the $2^{-\Delta\Delta Ct}$ method, with *GAPDH* as an endogenous control and normalization to non-seeding control (NSC: Baseline). Each dot represents one independent differentiation for two microglia clones (each differentiated 3 times) and one neuronal $SNCA^{TRIP}$ clone (with technical repeats for RT-qPCR). *, **** $p<0.0001$ by individual unpaired t-tests

5.2.3 Assessment of TREM2 function on the uptake or degradation of α-synuclein fibrils

Based on my qPCR data and the expression trends from the whole transcriptome analysis, I went on to assess TREM2 function using pharmacological and genetic approaches. In initial experiments I examined the effect of anti-TREM2 antibodies (Wang et al., 2020) provided by Eli Lilly (antibody antagonists A and B) on the uptake of fibrillar α-synuclein. For these studies, I harvested microglia precursors and cultured them as monocultures (pMGL) for 7 days. On DIV7, I pre-treated cells with antibodies for 1 h followed by the addition of fibrils and then microglial cell lysis 24 h later. I monitored α-synuclein levels by immunoblotting (Figure 5.6a). My data showed a trend for increased α-synuclein levels following TREM2 inhibition but with significant variability between replicates, which requires further experiments to conclude (Figure 5.6b, c)

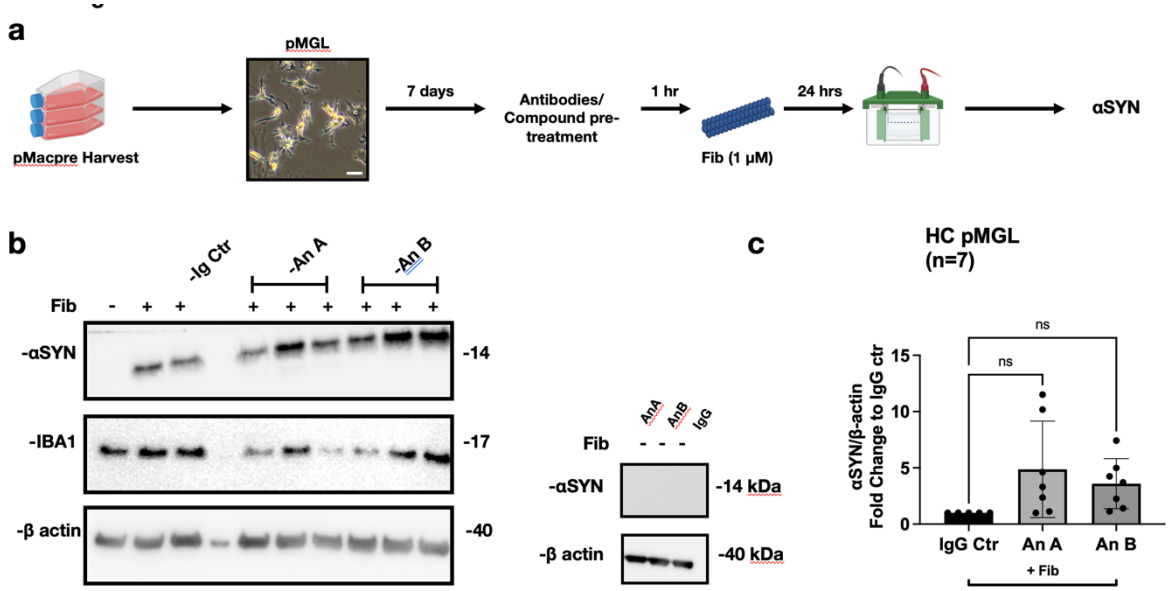

Figure 5.6 Uptake of fibrillar α-synuclein in HC iPSC-derived microglia was not modified by addition of TREM2-specific antibodies.

a. Schematic illustration of the monoculture model to study pharmacological manipulation of the phenotype. Scale bar at 20 µm. **b.** HC monocultured iPSC-derived microglia were pre-treated with two TREM2 specific antagonistic antibodies and one IgG control provided by the Eli Lilly laboratories (USA) followed by 24 h incubation with α-synuclein fibrils (top blots). Cells were also pre-treated with the antibodies in the absence of fibrils as a control (right smaller blot) **c.** Quantification of the immunoblotting. All immunoblotting data is first exported as ratio of α-synuclein levels to housekeeping β-actin. Each dot represents one independent differentiation. ns by one-way ANOVA followed by Tukey's multiple comparisons test and data is shown as mean ± s.e.m. An A and B: Antagonists A and B, Fib: α-synuclein fibrils, IgG Ctr: antibody IgG control

To more definitively investigate the role of TREM2, I used a previously published TREM2 knockout (KO) IPSC line and its isogenic control that was generated using CRISPR/Cas9 (Figure 5.7).

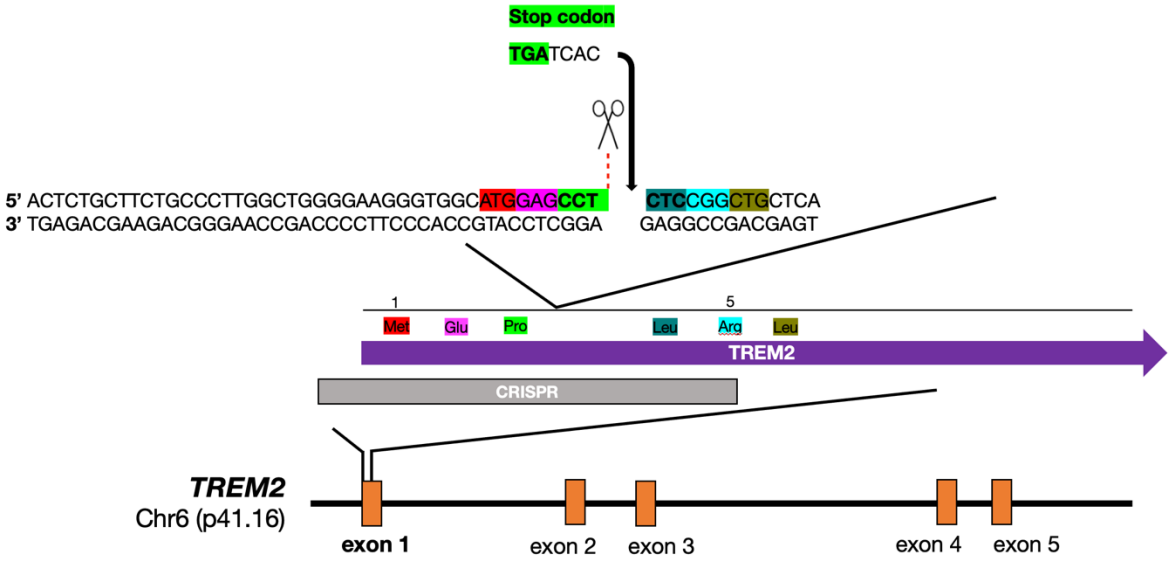

Figure 5.7 Generation of the TREM2 KO iPSC line.

The CRISPR/Cas9 was used to knockout the TREM2 gene of a parental line by targeting the 5' end of exon 1. Following, a homologous template encoding a TGA stop codon (green highlighted sequence) accompanied by four extra bases (TCAC) was inserted and homology arms were used for homology directed repair (HDR). The edited line (BIONi010-C) is considered homozygous knock-out of the human *TREM2* gene (Hall-Roberts et al., 2020, Rasmussen et al., 2014).

Firstly, I confirmed TREM2 KO in iPSC-derived microglia by immunoblotting (Figure 5.8a). It is noteworthy that the isogenic line had less TREM2 as seen by the immunoblotting. Re-programming a somatic cell into a pluripotent epigenetic state using the virus mediated transduction (Table 2.1) delivers the reprogramming factors into random places on the somatic chromatin. This integration could lead to inactivation of various genes with negative downstream effects (Byrne, 2008), which could explain reduced expression of the target protein on the isogenic line, due to a faulty generation method. Following, I used my previously described α-synuclein up-take assay (Fig 5.6a) to compare the response in the TREM2 KO line vs its isogenic (ISO) control. I found that TREM2-KO does not have an effect on the uptake of α-

synuclein when compared to isogenic HC microglia at baseline (Figure 5.8b, c). However, in the presence of cytochalasin D (previously described in Chapter 4), I observed a significant increase in the residual levels of α-synuclein in the TREM2-KO microglia compared to controls (Figure 5.8d, e).

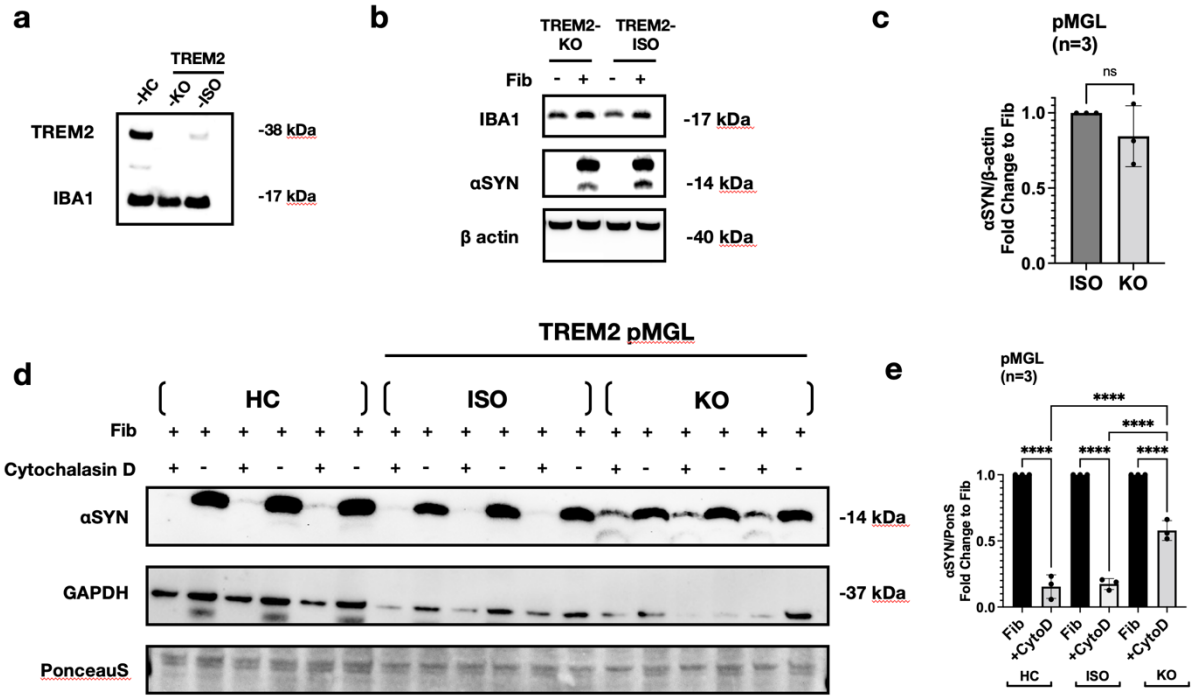

Figure 5.8 TREM2 does not influence the uptake of α-synuclein fibrils in iPSC-derived microglia cells.

a. Immunoblotting of iPSC-derived microglia lysates confirmed the knockout of TREM2 by CRISPR/Cas9. **b, c.** TREM2 KO does not influence the uptake of exogenous α-synuclein fibrils. **d.** Representative immunoblot for α-synuclein in microglia treated with cytochalasin D (+) or baseline (-) across three independent differentiations of HC, TREM2 KO and ISO microglia. Cytochalasin D pre-treatment increased the residual levels of exogenous α-synuclein in TREM2 KO microglia. **e.** Quantification of cytochalasin D uptake inhibition expressed as fold-change to the fibril treated cells. All immunoblotting data were calculated as the ratio α-synuclein levels to PonceauS and shown as fold change to the fibril only treated controls, which were the set baseline. Each dot represents one independent differentiation. **p<0.01, ****p<0.001 by one-way ANOVA followed by Tukey's multiple comparisons test and

data is shown as mean ± s.e.m. Fib: α-synuclein fibrils, +CytoD: pre-treatment with cytochalasin D followed by α-synuclein fibrils.

Finally, I investigated whether the TREM2 KO modifies the observed phenotype in my co-culture model, i.e., reduction of the levels of neuronal pSYN by HC microglia (Chapter 4). My pilot data (n=2) suggest that TREM2 is dispensable for this phenotype (Figure 5.9).

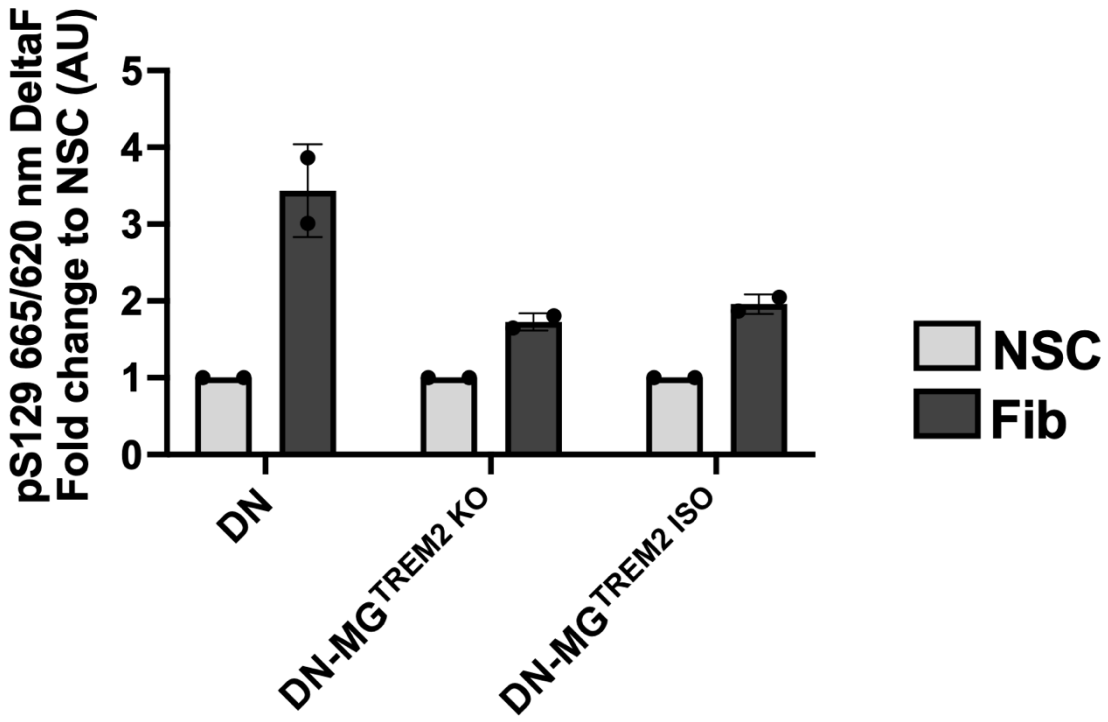

Figure 5.9 TREM2 KO does not modify the microglial effect on neuronal pSYN levels.

pSYN levels measured by HTRF were equally reduced in neurons co-cultured with TREM2 KO microglia or isogenic control microglia (n=2). For these two differentiations, Dr. Benedict Tanudjojo generated the iPSC-derived dopaminergic neurons.

5.2.4 Pilot single-cell RNA sequencing analysis identifies distinct microglia and neuronal clusters in iPSC-derived co-cultures with neuronal α-synuclein aggregation

Unique populations of microglia with disease-specific signatures have been identified through transcriptome analyses on the single cell level (Keren-Shaul et al., 2017, Grubman et al., 2021, Patir et al., 2019). Therefore, I performed pilot experiments to determine whether I can identify specific microglial signatures and/or subpopulations in response to neuronal α-synuclein aggregation. Quality control-based filtering in both baseline and seeded conditions excluded cells with mitochondria percentage above 25% and cells with less than 100 genes, yielded a total of 6,571 cells and 20,264 genes in the non-seeded control and 4,713 cells and 19,324 genes in seeded co-cultures. Using previously published datasets for microglia specific genes (Patir et al., 2019), as well as markers for iPSC-derived neuronal differentiation and maturation (Burke et al., 2020) and a reference mapping with a substantia nigra single nuclei atlas (Welch et al., 2019), the analysis identified specific microglial and neuronal clusters (Figure 5.10a). Heatmap of broad cell-type extrapolated markers revealed specific expression of microglial and neuronal markers in the corresponding clusters (Figure 5.10b). Additionally, UCell, an R package for scoring gene signatures in single-cell datasets identified previously reported clusters (Popova et al., 2021). The authors constructed a ‘’report card’’ where they identified conserved microglial clusters across human and murine experimental models. Hereby, the analysis demonstrated the presence of a) the universal homeostatic signature, b) the axonal tract microglia (ATM), suggestively maintained under universal culture conditions and c) the *ex vivo* signature (Popova et al., 2021), which is similar to the recently identified *ex vivo* ‘’activated microglia’’, exAM signature

which is composed by a cluster of cells enzymatically digested without any inhibitors expressing prominent stress related gene signatures, such as *Fos*, *Dusp1*, *Hspa1* and *Jun* (Marsh et al., 2020) (Figure 5.10c). Specifically, under seeded conditions in the co-cultures the exAM and homeostatic signatures were reduced (Figure 5.10d).

To further investigate the context-dependent crosstalk of the different identified cell types that enable physiological processes to proceed, specifically between microglia and neurons, we performed pilot analysis using the interactive CellPhoneDB database, a novel repository of ligands, receptors and their interactions (Efremova et al., 2020). Interestingly this analysis revealed increased interactions between neurons and microglia under fibril-treated conditions (Figure 5.11a) with the CD74/MIF being the most prominent signalling interaction between microglia and neurons (Figure 5.11b). Comparison of DGE trends between the non-seeded and seeded treatments in the neuronal and microglia cell type clusters identified a total of 186 differentially expressed genes (56 up and 67 down at logfc > 0.25 and adjusted < 0.05) in the microglial cluster following neuronal aggregation (Figure 5.12a) and gene set enrichment analysis (GSEA) identified the top 20 upregulated (p. adjusted < 0.05) and downregulated pathways for both neuronal and microglial clusters (Figure 5.12b). The identified pathways in the microglial cluster are also represented in the form of node diagrams showing the leading genes involved in the pathways (Figure 5.13). This analysis revealed a down regulation in antigen presentation and upregulation in oxidative phosphorylation and mitochondria translation, which are pathways related to the metabolic maintenance of microglia and IL10 signalling that may have anti-inflammatory effects.

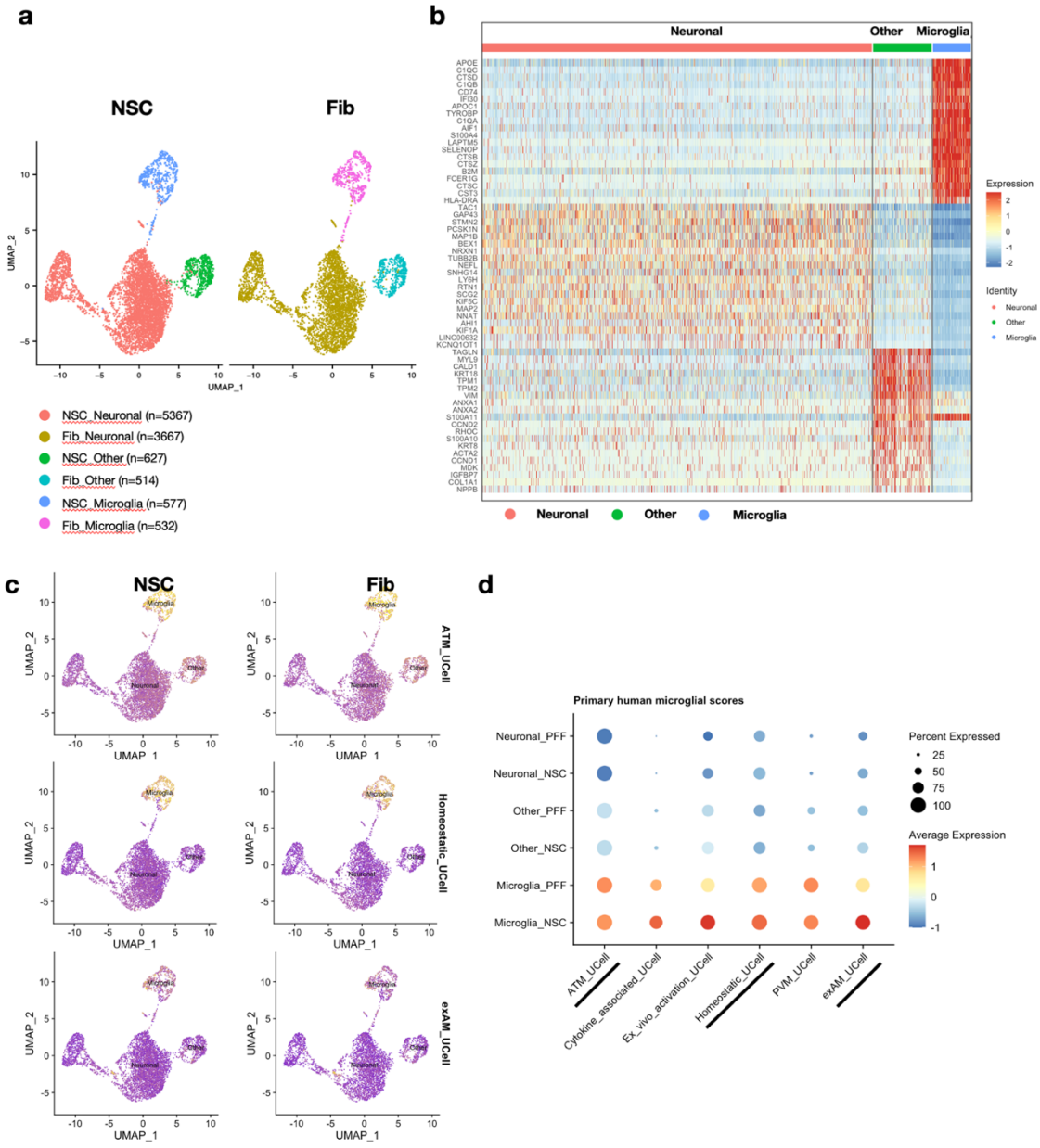

Figure 5.10 Single cell RNA-Seq analysis revealed microglial and neuronal specific clusters.

a. Uniform manifold approximation and projection (UMAP) showed identified broad clusters (neuronal, microglial and other) and cell numbers in the conditions of baseline (NSC) and seeded aggregation (Fib). **b.** Heatmap represents the top 20 differential markers among a broader classification of the clusters in neuronal, microglial and other cell types. Microglial cells highly expressed specific markers, such as *AIF1*, *C1QA*, *C1QB*, *C1QC* and *CTSD* while neuronal cells highly expressed specific markers such as *MAPT*, *STMN2* and *TUBB2B*. **c, d.** UCell calculation of previously published signatures in the iPSC single cell data. The data in this figure was analysed by Dr. Devika Agarwall and Dr. David Sims and iPSC-derived neurons were generated by Dr. Benedict Tanudjojo for all the co-cultures analysed in these pilot experiments

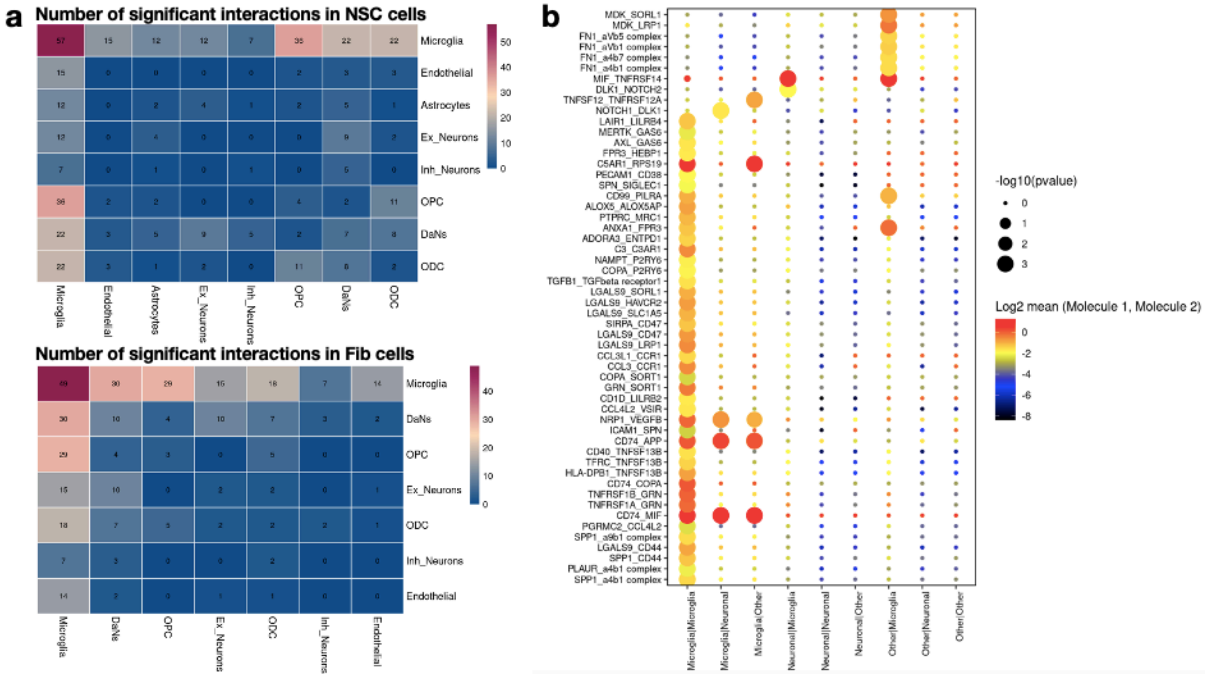

Figure 5.11 Single cell RNA-Seq analysis identified treatment specific cell-to cell communication microglial-neuronal pairs.

a. Heatmaps showing the total number of significant interactions between cell types at P ≤0.05 in the NSC (top) and aggregated (bottom) cell types. Note the enhanced interactions between DaNs and microglia under aggregation conditions. **b.** The CellPhoneDB analysis identified significant interactions between cell-specific pairs, including microglia and neurons in the seeded aggregation (Fib). Between microglia-microglia and microglia-neurons the CD74/MIF pair was significantly upregulated under conditions of seeded aggregation. The same was observed for the CD74-APP interaction. The p value for significant interactions was <0.05 and p values are indicated by dot size. The means of the average expression level of interacting molecule 1 in cluster 1 and interacting molecule 2 in cluster 2 are indicated by colour. The analysis was performed by Dr. Devika Agarwal and Dr. David Sims.

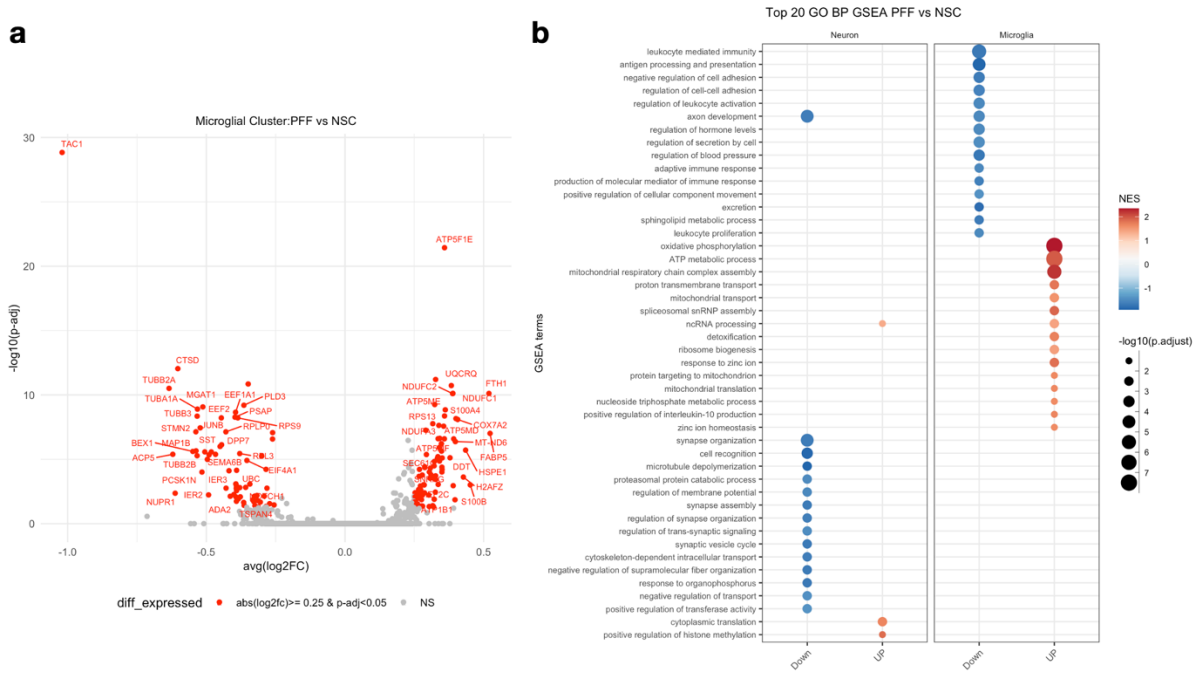

Figure 5.12 Single cell RNA-Seq analysis identified differentially expressed genes and their pathways within microglial and neuronal subpopulations under fibril-treated conditions.

a. Volcano plot represents significant differential expressed genes in the microglia cluster under seeded aggregation conditions. Among the downregulated genes are CTSD and STMN2. **b.** GSEA analysis was carried out to categorise the expressed genes in corresponding biological pathways for both neuronal and microglial clusters between the two conditions. The top 20 significant (p.adjusted < 0.05), up (NES > 0) and down regulated (NES < 0) pathways for each are plotted. The data in this pilot experiment were analysed by Dr. Devika Agarwal and Dr. David Sims and further replicates were planned to validate the results.

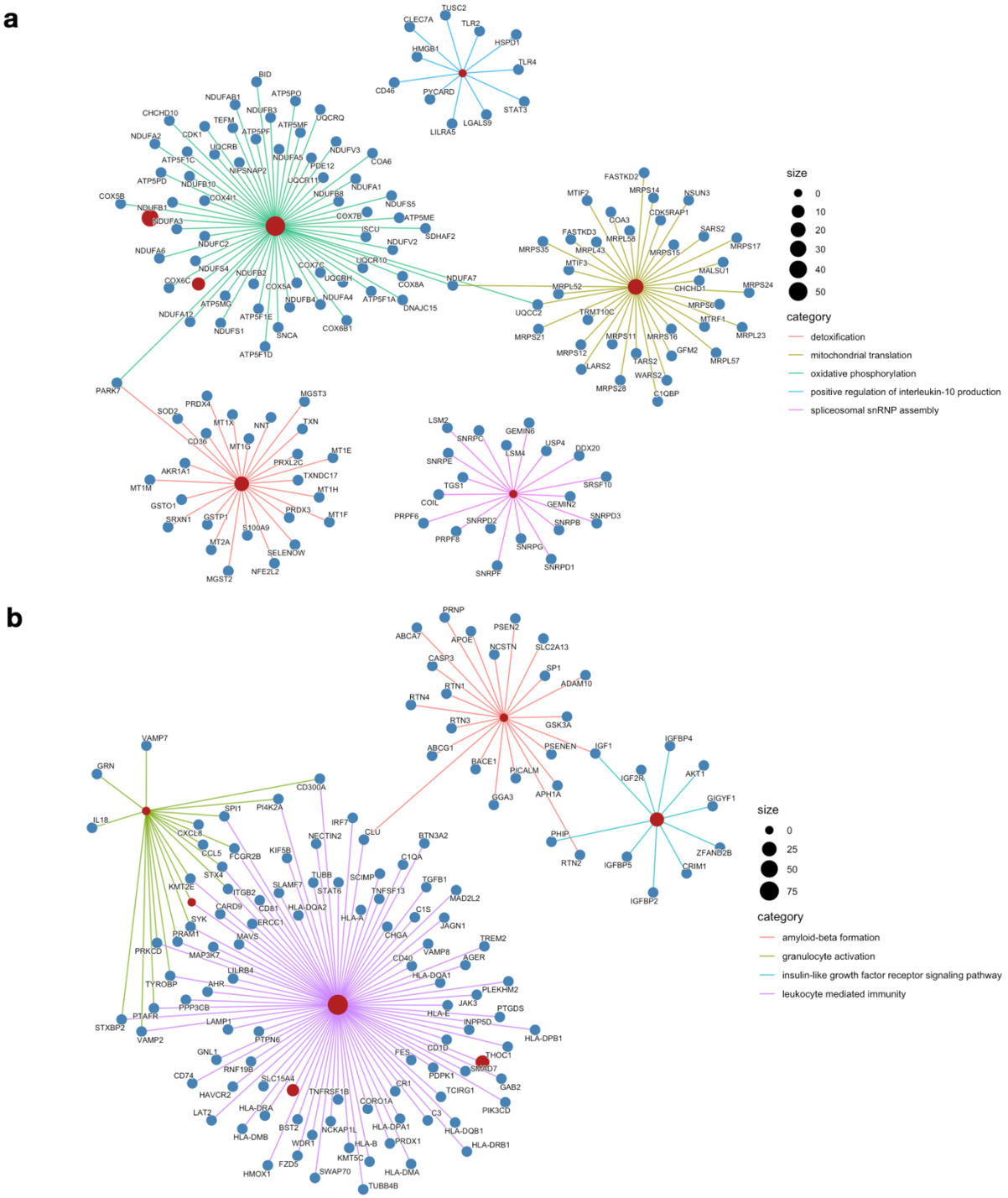

Figure 5.13 Gene Set Enrichment Analysis identified the microglial pathways that were differentially regulated under seeding conditions.

Gene-Concept Network (CNET) plots showing the **(a)** upregulated and **(b)** downregulated pathways for the microglial cluster. The data in this pilot experiment were analysed by Dr. Devika Agarwal and Dr. David Sims and further replicates were planned to validate the results.

5.2.5 Secreted cytokine profile in seeded iPSC-derived co-cultures

The single cell transcriptomic analysis suggests that the beneficial effects of microglia in my model were associated with activation of anti-inflammatory signals. I sought to corroborate this finding by assessing the profile of secreted cytokines in conditioned media collected from baseline and seeded co-cultures. To this end, media were pooled from three independent differentiations on DIV73 (at the time of cell lysis) and assayed using a membrane-based proteome array of 105 cytokines and chemokines and their qualitative analysis via changes in detected intensity (AU). Since this secretome analysis was a qualitative measurement, I chose to plot as differentially expressed cytokines those with > 1-fold increase and < 1-fold decrease compared to the baseline condition. As such, there were in total 30 differentially secreted cytokines in the conditioned media of co-cultures with aggregates compared to the non-seeded control (Figure 5.14a). Further, I plotted some noteworthy cytokines with relevance to Parkinson's disease and other neurodegenerative diseases according to existing literature (Hall et al., 2016, Jeong et al., 2021, Tansey et al., 2022) (Figure 5.14b). Strikingly, the secretion of IL-10 and the related cytokine IL-22 were increased under conditions of aggregation vs baseline, in agreement with the transcriptomic data that implicate IL-10 signalling pathways. It is noteworthy that TNF-alpha (TNFα), a key cytokine in microglial-mediated cytotoxicity, that is down-regulated by IL-10 signalling (Shin et al., 1999) was not detected under these conditions.

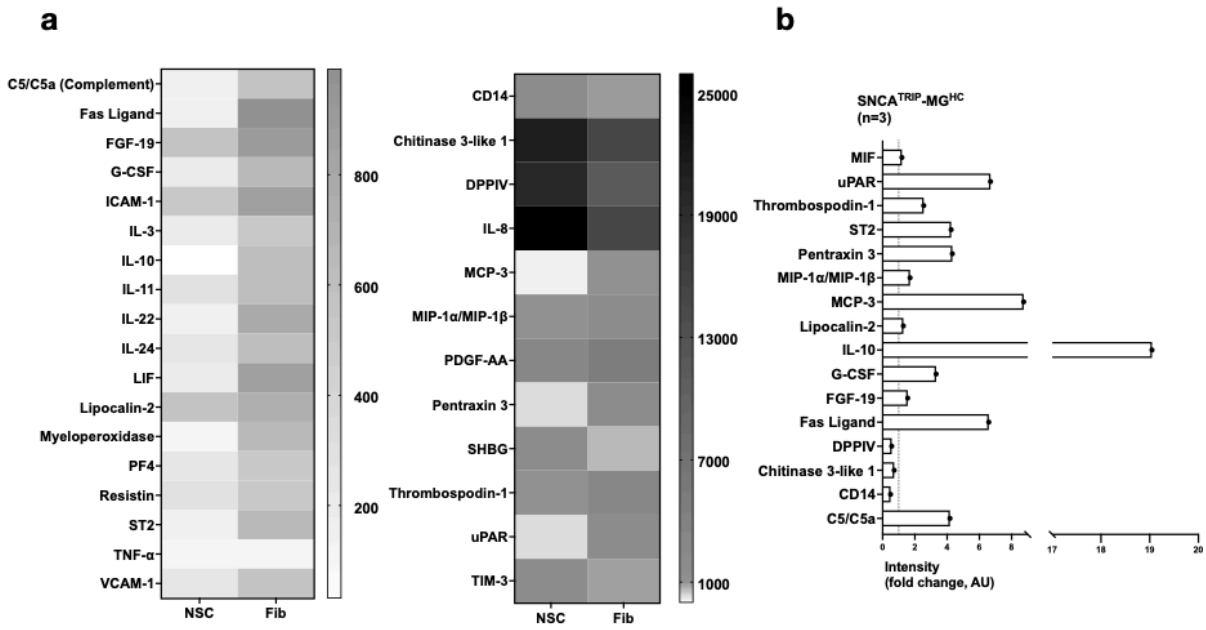

Figure 5.14 Secretome analysis of microglia co-cultured with α-synuclein seeded dopaminergic neurons.

a. Heatmaps display the profile of the released cytokines in conditioned media in non-seeded (NSC) and seeded (Fib) co-cultures. The right heatmap focuses on the cytokines with intensity values up to 1000 AU. Conditioned media were pooled from three independent differentiations (n=3) and data were expressed as intensity AU. **b**. Note-worthy up-and down regulated cytokines. Data are shown as fold-change of intensity (AU) of seeded co-cultures (Fib) to non-seeded co-cultures (NSC) (Baseline=1).

5.3 Discussion

In the everchanging microenvironment of the brain, microglia display a remarkable phenotypic spectrum of plasticity that ranges from morphological changes, secreted cytokines and surface markers to diverse transcriptomic signatures. Based on these changes microglia can be defined as neurotoxic or neuroprotective. However, much ought to be investigated to correlate microglia phenotypes with function.

The unique DAM subtype identified by the Amit group animal models of Alzheimer's disease changed the field's perception regarding microglia. Ever since, approaches using the new advances in RNA-sequencing techniques aimed to identify unique sub-populations of microglia that correlate with different stages of neurodegenerative diseases. Herein, I hypothesised that microglia in my model would express DAM-related markers, that follow the expression trends reported in literature (Keren-Shaul et al., 2017, Deczkowska et al., 2018).

Whole transcriptome analysis revealed upregulation trends in genes such as, *SYK*, *CLEC7A*, *APOE* and *B2M,* which have been associated with DAM (Figure 5.4b) (Keren-Shaul et al., 2017). Additionally, other homeostatic genes as reported in literature (Butovsky et al., 2014b), such as *Olfml3* and *Sall* displayed a trend towards downregulation (data not shown). *SMURF1* was a hit significantly upregulated in my co-culture model (Figure 5.4a). Smad ubiquitin regulator factor 1 (SMURF1) and SMURF2 were originally identified as antagonists of the TGFβ/BMP pathway (Kavsak et al., 2000, Ebisawa et al., 2001, Murakami et al., 2003) and accumulating evidence has also suggested a crosstalk of the SMADs proteins between the aforementioned pathway and other signalling cascades (Ulloa et al., 1999, Park, 2005). In addition to

these roles, SMURF1 has reportedly exhibited anti-inflammatory function by supressing pro-inflammatory signals via K48-linked polyubiquitination of the adaptor MYD88 (Lee et al., 2011b). Also, an anti-inflammatory role is supported by evidence of SMURF1-mediated ubiquitination and degradation of TRAF proteins (Li et al., 2010). SMURF1 has also been suggested to promote degradation of p53 (Nie et al., 2010), which promotes apoptosis. Another study suggested that upregulation of *SMURF1*, which further degrades p53 could inhibit apoptosis of dopaminergic neurons (Gao et al., 2016). SMURF1 does not ubiquitinate α-synuclein and therefore, a direct effect on its degradation is unlikely (Tofaris et al., 2011). Given the suggested protective function of microglia in my model, it is possible that SMURF1 promotes an anti-inflammatory response and protects the dopaminergic neurons from apoptosis. Future work could involve knockdown of *SMURF1* in microglia and dopaminergic neuronal monocultures treated with α-synuclein fibrils to study the exact role of this gene in each cell type in response to α-synuclein fibrils.

By RT-qPCR I observed clear down-regulation in homeostatic genes, such as *P2RY12*, *CX3CR1*, *TMEM119* and significant up-regulation of DAM-related genes, such as *TYROBP*, *APOE*, *Lpl*, *Axl* and *TREM2* (Figure 5.5b, c). However, bulk RNA-Seq analysis did not reveal significant differences on the aforementioned genes. This discrepancy may be explained as follows: Firstly, for accurate RT-qPCR results the selection of a reference gene is important. Several studies have reported that levels of conventional reference genes, such as *GAPDH* and *β-actin* may be altered under the studied experimental conditions (Derveaux et al., 2010, Guénin et al., 2009). A study compared the stability of expression levels of GAPDH and *β-actin* to the levels of *Stx5α* and *Hnrnpab* using periphery macrophages under LPS stimulation and

suggested that the later had more stable expression levels (Tanaka et al., 2017). Another study using periphery macrophages reported altered levels of *GAPDH* following LPS treatment due malonylation, a post-translational modification (Galván-Peña et al., 2019). However, there is no report of altered levels of *GAPDH* in human iPSC-derived microglia so far. Secondly, a comparison at genome-wide level may require more replicates to account for the inherent variability between differentiations.

A consistent result from the qPCR analysis was the up-regulation of TREM2 and associated signalling factors. Upon its activation, TREM2 and its adaptive receptor DAP12 (TYROBP) initiate intracellular downstream cascades that utilise the PI3K-AkT network. Once AkT is activated it phosphorylates a plethora of substrates within the cytoplasm and the nucleus, which in turn activate a range of pathways related to cell survival, proliferation, differentiation, migration and glucose metabolism (Xiao et al., 2010, Zhou et al., 2000). Activation of the PI3K-AkT pathway in microglia has been shown to be neuroprotective (Bhat et al., 2021) and qPCR revealed upregulation of these downstream components (Figure 5.5 d, e). The role of TREM2, before or during the early phase of Alzheimer's disease is to phagocytose amyloid peptides without triggering inflammatory responses and thus, increased levels of TREM2 in early stages of DAM may be neuroprotective (Gratuze et al., 2018, Keren-Shaul et al., 2017, Parhizkar et al., 2019). However, the lack of TREM2 effect in my co-culture model, using either a KO iPSC line or TREM2-targeting suggests that alternative phagocytosis receptors such as TLR4 may be more relevant. It was previously shown that the TLR family, such as TLR2 and TLR4 are critical for α-synuclein phagocytosis (Fellner et al., 2013). Recent studies in primary murine macrophages showed a negative feedback loop between TLR4 activation and IL-10

secretion (Alexander et al., 2021). That could explain the secreted levels of IL-10 in my co-cultures and the absence of TLR4 as a hit in the pilot single cell RNA-Seq analysis.

Uptake of *de novo* fibrils has been reported as a relative quick process occurring within 15 mins of treatment; yet degradation is a much slower process resulting in increased accumulation of the protein after 24 hr (Scheiblich et al., 2021). siRNA knockdown of TREM2 in BV2 cells has been linked with increased inflammatory responses and neuronal apoptosis (Guo et al., 2019). However, it remains elusive whether TREM2 is involved in α-synuclein processing. The results from my monoculture experiments with TREM2-specific blocking antibodies (Eli-Lilly) did not consistently increase the levels of fibrillar α-synuclein following uptake, as well as the lack of a significant effect on pSYN levels in TREM2-KO co-cultures suggest that under these experimental conditions TREM2 may not be essential for clearance of α-synuclein (Figure 5.6, 5.9). However, further investigations are required to fully conclude whether TREM2 is involved in the clearance of the fibrils given the variability observed in my monoculture experiments. One explanation may be that the concentration of the TREM2 antibodies was saturated in the cultures and therefore, the epitope specificities between the two antagonists were obscured. Further work will involve concentration titration experiments to identify the optimal concentration window for this assay. It will also be important to perform antibody-target engagement studies. Techniques, such as fluorescence correlation spectroscopy have been used to explore antibody diffusion and protein-protein interactions in biological matrices (Lagerkvist et al., 2001, Hung et al., 2019). Another possibility would also be the use of mass-spectroscopy to screen the proteome for evidence of

ligand-target binding (Cousins et al., 2018). Further, in the case of a transmembrane target, such as TREM2, engagement of the antibody with the target leads to subsequent interaction with additional cell surface and downstream targets (Sengers et al., 2016). Engagement of the Lilly antibodies on TREM2 could be studied by measuring the expression of the downstream molecules, such as Syk and adaptive receptor DAP12 (Figure 5.5d). Additionally, the concentration of soluble TREM2 generated by shedding from receptor shedding (Filipello et al., 2022) within the conditioned media could be also measured with ELISA. *TREM2* expression was upregulated in my co-culture model by RT-qPCR and therefore, future work would involve time-course studies to investigate the exact temporal stage when and if DAM TREM2 contributes to α-synuclein pathology.

Pilot studies using single cell RNA-Seq analysis of co-cultured cells revealed distinct clusters of neurons and microglia in non-seeded and seeded co-cultures with cluster-specific expressed genes, such as *TYROBP*, *TREM2*, *B2M*, *AIF1* for microglia and *STMN2* and *TUBB2B* for neurons (Figure 5.10). Analysis on the significant interactions between cell types revealed a shift from baseline to the seeded conditions that involved downscaling of microglia-microglia interactions and upscaling of microglia-dopaminergic neuronal interactions (Figure 5.11a). This observation combined with the finding of complement secretion, as well as microglia clustering around aggregated neurons based on morphology (Chapter 4), all suggest early signs of synaptic pruning. Microglia phagocytose apoptotic bodies through a variety of receptors, including Axl (Fourgeaud et al., 2016) and are mobilised in an orchestrated fashion towards the vicinity of damaged and apoptotic neurons (Damisah et al., 2020). However, no overt neuronal death was observed (Chapter 4).

Transcription factor PU.1, encoded by *SPI1* is involved in microglial polarisation, both under homeostatic and activation conditions (Okajima and Tsuruta, 2018). *Axl* and *SPI1* were upregulated in my model (RT-qPCR and whole transcriptome analysis). This finding in combination with the detected increased neuro-microglial interaction resulting in reduced pSYN levels and morphological transitions (Chapter 4) all suggest that microglia mobilise around neurons with aggregates possibly to "trim" damaged neuronal sub-compartments containing aggregated α-synuclein. Advanced imaging techniques could be used in future work to visualise and further delineate these processes.

Further analysis on cellular interactions revealed prominent treatment specific interaction in the CD74-MIF signalling axis (Figure 5.11b). CD74, an integral membrane protein has been previously reported upregulated in microglia around Aβ plaques and neurofibrillary tangles (Bryan et al., 2008) and macrophage migration inhibitory factor (MIF) is released as an inflammatory response/activation. Various cell types, including neurons and microglia release MIF as a pro-inflammatory signal. In Alzheimer's disease MIF is released following activation of the PI3K-AkT signalling cascade (Su et al., 2017). Additionally, it has been reported that MIF-related inflammation is associated with amyloid pathology and tau hyperphosphorylation during the early stages of Alzheimer's (Oikonomidi et al., 2017). Interestingly, secretion of MIF was also detected in conditioned media of co-cultures under both baseline and seeded aggregation conditions, with 1.2-fold increase in the later (Figure 5.14). Further work is needed to confirm MIF levels with sensitive assays, such as ELISA or MSD in biological replicates.

To further elaborate biological functions that are engaged by microglia in the presence of aggregated dopaminergic neurons, pathway and gene ontology (GO) analysis was performed (Figures 5.12-5.13). Oxidative stress emanating from cellular responses to misfolded proteins is prominent feature in neurodegeneration. Glial-induced oxidative stress responses further damage the neurons and α-synuclein induced microglial activation leads to increased production of nitric oxide (NO) (Béraud et al., 2011). However, a balance in the oxidative phosphorylation of many immune cells is important for the transition between damaging inflammatory and restorative responses (Pålsson-McDermott and O'Neill, 2020). Microglial phagocytosis is a highly demanding metabolic process and highly dependent on oxidative phosphorylation for production of ATP (Aldana, 2019). In my model preliminary data points toward enhanced oxidative phosphorylation and mitochondria translation pathways. This may reflect increased oxidative burst as microglia are phagocytosing neuronal aggregates. Mitochondria deficiency and mass loss has been linked to neurodegeneration in the *in vivo* 5XFAD mouse model of Alzheimer's disease (Ulland et al., 2017). Moreover, changes in the expression of cytoskeleton related genes are consistent to what has been observed before, where iPSC-derived monocultured microglia cleared α-synuclein fibrils via polymerisation of globular actin into filaments and microtubules (Scheiblich et al., 2021). The same study reported amplified mitochondria alteration and enhanced production of ROS in the presence of α-synuclein fibrils. Our analysis demonstrated similar findings suggesting possible early stages of mitochondria mobilisation with enhanced levels of ROS in the attempt to clear the neuronal misfolded proteins. Mitochondria transfer might be a part of a rescue strategy (Davis et al., 2014). Nevertheless, this need to be

further elucidated. Further work is currently under way with more technical and temporal replicates to analyse at higher sequencing depth co-cultured cells. Even though the co-culture model is more disease-relevant, the reductionist monoculture models can provide valuable information in cell type specific mechanisms. It is important to include further time points and different concentrations of fibrils to decipher whether my observed phenotype, which points towards rescue and metabolically active microglia would shift to damaging, persistent inflammatory events.

Assessment of cytokine secretion in the co-culture model revealed a number of interesting changes: Chitinase 3-like (CHI3L1) (also known as YKL-40) has been reported as a biomarker for Alzheimer's disease and other neurodegenerative diseases particularly for disease progression with increased levels in the CSF of patients (Comabella et al., 2010, Craig-Schapiro et al., 2010). In Parkinson's disease, increased CSF CHI3L1 levels have been correlated with accelerated cognitive decline (Hall et al., 2016). Some studies have reported expression of CHI3L1 by microglia (Hellwig et al., 2015) and other by astrocytes (Craig-Schapiro et al., 2010). In the seeded co-cultures, I observed a downregulation trend in the levels of CHI3L1, which would possibly suggest a reduced inflammatory response by microglia. Dipeptidyl peptidase IV (DPPIV) is a serine protease best known for inactivating glucagon-like peptide (GLP-1). GLP-1 has been positively associated with Parkinson's disease-like symptoms in animal models (Athauda and Foltynie, 2016) and DPPIV inhibitors in a case study were described to increase GLP-1 levels with overall beneficial effects (Jeong et al., 2021). Similarly, in my seeded co-cultures I observed a qualitative downregulation trend in DPPIV levels.

TNFα levels are elevated in the MPTP animal model of PD, and in clinical samples (De Lella Ezcurra et al., 2010, Sriram et al., 2002). Additionally, TNFα is a potent stimulator of γ-secretase, which leads to increased levels of Aβ peptide in Alzheimer's disease (Liao et al., 2004). It is noteworthy that TNFα secretion was not detected in my model. Matrix metalloproteinases are proteases that remodel the extracellular matrix and MMP9 has been suggested that to contribute to neuronal degeneration in Parkinson's and Alzheimer's disease by inducing neuronal death (Lorenzl et al., 2004). Nevertheless, the levels of MMP9 in the conditioned media between seeded and unseeded conditions in the co-cultures remained unchanged. Glial-secreted lipocalin-2, which regulates cell differentiation, apoptotic death and cellular uptake of iron, has been associated with neurotoxic effects *in vitro* (Lee et al., 2012, Bi et al., 2013) and *in vivo* in the MPTP and 6-hydroxydopamine (6-OHDA) animal models of Parkinson's disease (Kim et al., 2016). Yet, a recent study conducted in Parkinson's disease patients, yielded negative results regarding levels of lipocalin-2 in the serum of patients (Xiong et al., 2022). Lipocalin-2 was slightly upregulated in my seeded co-cultures and whether this is relevant to Parkinson's pathogenesis remains to be seen.

Microglial complement activation results in generation of soluble fragments, such as C3a and C5a that further interact with receptors to activate phagocytosis (Monk et al., 2007) and the later also possesses chemotactic properties (Yao et al., 1990). Fibrillar Aβ can activate the complement system *in vitro* and *in vivo* (Bradt et al., 1998, Matsuoka et al., 2001). Additionally, oligomeric α-synuclein has been shown to bind on C5 and promote microglial activation, which ultimately leads to cell toxicity in animals overexpressing human A53T α-synuclein that were injected with

exogenous α-synuclein fibrils (Ma et al., 2021). Secreted levels of C5a were significantly higher in seeded co-cultures and based on published observations this suggests phagocytosis activation and possible interaction with fibrillar forms of α-synuclein. Additionally, complement components C1q and C3 have shown to mediate early synaptic loss in the J20 transgenic animal model of Alzheimer's disease (Hong et al., 2016). It could be that microglia in my co-cultures are in the early stages of that activation. Chemokine MCP-3, alternatively known as CLL7 is one of the many ligands for chemokine receptor 2, CCR2 and is required for infiltration of macrophages into inflamed tissues. Of note, deletion of CCR2 and another binding chemokine, CCL2 in the MPTP Parkinson's mouse model did not protect against dopaminergic neurodegeneration possibly due to overcompensation via CCL7 signalling (Pattarini et al., 2007). CCL7 is highly secreted in my seeded co-cultures and given its chemotactic role that could be another explanation behind microglia mobilisation towards aggregated dopaminergic neurons (findings in Chapter 4). Interestingly, levels of Fas ligand (Fasl) were high in the seeded co-cultures and their origin can be either microglial or neuronal. Absence of Fas expression in the MPTP mouse model appeared to protect the loss of dopaminergic neurons within the SNpc (Hayley et al., 2004).

The most exciting finding from the secretome analysis was the discovery of increased levels of IL-10 and IL-22, which belongs to the IL-10 family, in the conditioned media of seeded co-cultures. This was consistent with the GO analysis on the single cell level which identified up-regulation of the pathways related to IL-10 production (Figure 5.13a). It has been shown that *in vitro* IL-10 inhibits the secretion of pro-inflammatory cytokines preventing microglial hyperactivation (Lobo-Silva et al.,

2017). IL-10 acts by supressing pro-inflammatory cytokines, such as TNFα (van der Poll et al., 1994), IL-6 (Wang et al., 1994) and IL-8 . Additionally, genetic deletion of IL10 in mice resulted in enhanced inflammation-induced tau pathology (Weston et al., 2021) and animal studies have reported that IL-10 based therapeutic approaches. Specifically, in Alzheimer's disease crossed APP/PS1 mouse model IL-10 suppressed neuroinflammation, enhanced neurogenesis and improvement of spatial cognitive dysfunction (Guillot-Sestier et al., 2015). On the other hand, no protection was observed when IL-10 was overexpressed with AAV in the spine of transgenic mice expressing A53T mutant α-synuclein (Cockey et al., 2021) a model with extensive pathology. Nevertheless, the lack of response may be related to the limitation of the model or differences between human and mouse systems which are well established as previously discussed. The role of IL-10 and potential down-stream pathways in the human co-culture model warrants further validation and characterisation. Interestingly IL-8, which is a pro-inflammatory cytokine and negatively regulated by IL-10 (Moore et al., 2001), was reduced in this model. IL-8 levels are lower in CSF from Parkinson's disease patients compared to Parkinson's dementia (Janelidze et al., 2015) and have been correlated with cognitive impairment and more advanced disease (Hall et al., 2018). It should be noted that the secretome membrane profiler used in this study is a qualitative measurement. Therefore, future work would involve a more specific and sensitive quantification of IL-10 through ELISA or MSD.

A recent study compared murine and human iPSC-derived microglia on the single-cell level across experimental models that included *in vitro* cultures and *ex vivo* organoids (Popova et al., 2021). Based on this, the iPSC-derived microglial signatures

in my co-cultures were compared to the aforementioned ‘’report card’’. According to the authors cytokine and chemokine gene expression is better preserved in a human-related environment, which was confirmed in my samples (Figure 5.10d). An additional microglial cluster, the axonal tract microglia (ATM) was also confirmed in my co-cultures, which is maintained across culturing conditions. UCell analysis revealed a condition-specific *ex vivo* signature in my co-cultures, which was reduced under conditions of seeded aggregation. Recently, it was demonstrated that enzymatic dissociation of human tissue results in enhanced artificial transcriptome signatures within microglial clusters, termed as exAM (Marsh et al., 2020). The exAM and *ex vivo* signatures of the ‘’report card’’ are very similar except for a few genes. Marsh and colleagues (2020) overcame this fact by introducing transcriptional and translational enzymatic inhibitors at multiple steps of the RNA extraction protocol and eliminated the *ex vivo* signature (Marsh et al., 2020). The authors concluded that a proper baseline, which is not confounded by the *ex vivo* signature is critical to delineate subtle transcriptomic differences between a control and a treatment group. It is highly likely that some signatures in my microglial cluster, such as DAM related genes are obscured by the enhanced *ex vivo* signature in my samples under the baseline conditions. Therefore, future work involving enzymatic dissociation of my iPSC-derived co-cultures ought to involve enzymatic inhibitors.

The “two-faces’’ of DAM have long been appreciated in the field of neurodegeneration (Hickman et al., 2008, Keren-Shaul et al., 2017). Microglia adopt a disease-associated phenotype with the aim to clear amyloid or α-synuclein accumulation and protect their microenvironment. It has been suggested that the early-phase neuroprotective DAM become overwhelmed and detrimental as the

disease evolves (Onuska, 2020). In the iPSC-derived co-culture system, HC microglia displayed enhanced morphological plasticity, activation and clustering around $SNCA^{TRIP}$ dopaminergic neurons, where the pSYN inclusions were more pronounced. Further, transcriptomic studies revealed distinct microglia population under conditions of α-synuclein seeding aggregation, which acquired some of the DAM signatures. Single-cell studies can provide valuable information to the field particularly when they deconvolute disease-specific genetic risks to biological pathways, cellular and regional specific expressions. Recently, a human single-nuclei transcriptomics atlas for the SNc was reported where Parkinson's disease genetic risk was reportedly associated with dopaminergic neurons of the SNc, as well as with oligodendrocytes (Agarwal et al., 2020). It is noteworthy that the study did not find any genetic Parkinson's disease risk implications associated to microglia or astrocytes, possibly suggesting a negative causal relationship between neuroinflammation and onset of Lewy neuropathology. Nevertheless, more similar studies that will include a variety of samples to reflect amongst others the different Braak stages, are necessary to delineate the exact relationship of neuroinflammation and disease progression.

Overall, the transcriptomic and secretome analysis in my model suggest that microglia are in a neuroprotective state where prominent inflammatory activation remained in check. It should be noted that microglia were cultured for 2 weeks with the dopaminergic neurons, and it is possible that a full transition to DAM with pro-inflammatory phenotype has not yet occurred. Future studies would benefit from assessment of phenotypes at 4 week or longer, as this may show whether the microglia shift towards a possible detrimental state. Importantly, stabilisation of the

identified microglial state, for example by IL-10 or related signalling factors, could offer a potential therapeutic strategy.

Chapter 6: General Discussion

Aggregation of α-synuclein into filamentous inclusions is critical in the pathogenesis of Parkinson's disease and related disorders (Spillantini and Goedert, 2018). In this process, physiological monomeric α-synuclein misfolds and assembles to form oligomeric species and higher molecular weight assemblies that are causatively linked to the death of dopaminergic neurons. However, the precise mechanisms underpinning the aggregation process and aggregate-induced toxicity remain unclear. Microglia internalise and degrade α-synuclein in order to restore the disturbed homeostasis in the brain's microenvironment. A defect in this process, possibly due to their persistent activation causes the transition of microglia from beneficial to cytotoxic (Halliday and Stevens, 2011, Onuska, 2020). However, we still do not know whether microglial activation is linked to or it is independent of α-synuclein aggregation.

The phenotypic heterogeneity of microglia transitioning from homeostasis to disease states was first thoroughly described using an Alzheimer's disease mouse model harnessing advancements in single cell RNA-sequencing technologies that have enabled the systematic untangling of microglia heterogeneity (Krasemann et al., 2017a, Keren-Shaul et al., 2017, Mrdjen et al., 2018) . Although the DAM phenotype is now considered a general response to neurodegeneration, little is known about microglial phenotypes in Parkinson's disease. DAM phenotypes have been shown to differ between mouse models and human brain tissue (Mathys et al., 2017, Alsema et al., 2020, Zhou et al., 2020). One explanation may be the fact that isolated human

tissues taken from terminal stages of either Alzheimer's or Parkinson's disease differ from the dynamic models and phenotypes that develop over shorter time-points.

In this thesis I used human models to investigate microglial phenotypes in response to α-synuclein aggregation. Specifically, by setting up a novel human iPSC-derived co-culture model between dopaminergic neurons and microglia I endeavoured to explore the microglial phenotypes following α-synuclein aggregation within dopaminergic neurons. Additionally, mechanistic studies in microglial monocultures aimed to explore the relevance of TREM2 in α-synuclein uptake and processing given the importance of this receptor in the DAM transitioning phenotype (Krasemann et al., 2017b, Keren-Shaul et al., 2017).

Relevant experimental models of Parkinson's disease ought to recapitulate not only the main neuropathological hallmarks that include neuronal degeneration and fibrillar α-synuclein aggregation, but also the inflammatory component that occurs simultaneously. My work using *ex vivo* brain organotypic slices re-enforces this notion. Modelling proteopathic lesions in a brain-like environment allows the investigation of cell-type specific phenotypes in response to the pathogenic protein inclusions (Barth et al., 2021, Croft et al., 2019b). Further, in the case of aggregated α-synuclein it permits the investigation of cell-to-cell release and uptake that mimics those *in vivo* events between interconnected regions (Jucker and Walker, 2018, Peng et al., 2020a). Murine brain organotypic slices offer an experimental environment for mechanistic studies of protein transmission, microglial activation and mobilisation towards the sites of pathology. However, it is imperative that the translational gap between the human brain environment and the mouse is acknowledged. A significant limitation also includes the fact that those slices originated from a postnatal brain and

thereby, not recapitulating the ageing aspect of neurodegeneration in the human brain. Additionally, transcriptomic studies have now demonstrated significant differences in disease related genes between the two species (Zhou et al., 2020, Lin et al., 2014, Hodge et al., 2019, Friedman et al., 2018a, Miller et al., 2010). Long-term human organotypic slices were established in the past few years (Schwarz et al., 2019, Schwarz et al., 2017) and recently it was shown that α-synuclein inclusions can be induced in human cultured slices (Barth et al., 2021). The transition from murine to human slices is an exciting step forward towards a true human brain experimental set up that offers a promising platform for therapeutic explorations.

Microglia identity is driven by their ontogeny and embryonic lineage, as well as their environment (Bennett and Bennett, 2020). Most of the latest protocols for the generation of human iPSC-derived microglia (Haenseler et al., 2017a, Muffat et al., 2016, Abud et al., 2017) mirror their primitive haematopoietic lineage by utilisation of factors that drive PU.1 and IRF8 dependence and simultaneous MYB independence (Buchrieser et al., 2017, Bian et al., 2020). Mesoderm/haemogenic endothelium/myeloid differentiation can be achieved by a combination of recombinant factors, such as BMP4, SCF, VEGF, IL-3, M-CSF within the differentiation culture media. However, further maturation of microglia requires signals from their microenvironment and *in vitro* this can be achieved via co-culturing with other CNS cell types, mainly being neurons and astrocytes (Haenseler et al., 2017a, Abud et al., 2017, Park et al., 2018, Guttikonda et al., 2021, Takata et al., 2017). Modelling the complexity of neurodegeneration in faithful *in vitro* models is key in the development of future therapeutics. In this study, I generated an iPSC-derived co-culture model of dopaminergic neurons and microglia following adjusted

protocols that have been previously reported to mirror the differentiation lineages of both cell types (Kriks et al., 2011, Haenseler et al., 2017a).

Persistent microglia activation exacerbates neuronal damage; however, the early stage neuroprotective role of microglia in neurodegeneration is not fully understood (Hickman et al., 2018). Throughout my iPSC-derived co-cultures, I observed a reduction in the pathological levels of pSYN, which appeared to be dependent on direct contact between neurons and microglia and complemented by rescuing of neuronal death. The importance of communication between the two cell types was re-enforced by the initial observations of the single cell RNA-seq CellPhoneDB analysis which revealed an increase in the number of microglial and dopaminergic neuronal interactions. Neuroprotection has been observed *in vivo* and *in vitro* in models of Aβ accumulation and α-synuclein and TDP43 aggregation in ALS (Choi et al., 2020, Xie et al., 2022, Frenkel et al., 2008). Further work in our laboratory includes monitoring of this phenotype over longer periods of time to determine a potential transition of microglia from beneficial to detrimental stages. In my opinion, this co-culture model may be further used to examine potential biomarkers at early disease stages that can be monitored and explored for therapeutical interventions.

To delineate and further interpretate the observed phenotype we performed transcriptomic studies using initially bulk and more recently single-cell RNA sequencing. With deconvolution analyses the former revealed defined clusters of cell-specific populations in my iPSC-derived co-cultures accompanied with a couple of significant hits that provided us with directions for our future research. On the single-cell level disease-specific microglia populations and pathways were identified that will require further validation. In this regard further sequencing experiments have

already been performed and the results will be available in the near future. This withstanding, an anti-inflammatory phenotype has emerged from the data so far, in particular increased secretion of IL-10 and parallel decreased secretion of IL-8 combined with upregulation of IL-10 GO pathway from the initial single-cell RNA sequencing analysis.

TREM2 has emerged as an important mediator of microglial physiology and genetic variants have been implicated primarily in Alzheimer's disease and other neurodegenerative diseases (Filipello et al., 2022). TREM2 and related signalling factors were up-regulated in my model. However, my initial functional studies using antibodies and a TREM2 KO iPSC line do not support an essential role for TREM2 in the documented phenotype. Acute TREM2 pharmacological inhibition with blocking antibodies revealed a trend towards increased uptake or impaired degradation of α-synuclein fibrils in genetically edited *TREM2* microglia monocultures. These TREM2-KO microglial monocultures treated with the phagocytosis inhibitor cytochalasin D also had increased residual levels of α-synuclein. This combination suggests that TREM2 most likely participates for functions regarding phagocytosis of α-synuclein fibrils. Levels of sTREM2 are reportedly increased in the CSF of Parkinson's disease patients and positively correlate with the CSF α-synuclein levels (Peng et al., 2020b). Inhibition of TREM2 signalling may have also led to activation of compensatory mechanisms, such as increased TLR4 activation, which is a receptor for α-synuclein.

An important limitation of my model that could also potentially impact on my observations regarding TREM2 function is the conformation of α-synuclein assemblies that I used. TREM2 has an array of binding ligands, and different conformers of fibrillar α-synuclein may bind with different affinity. In this respect it

would be interesting to test the effect of brain amplified conformers generated through PMCA as the lab has recently studied in neurons (Tanudjojo et al., 2021) or oligomers which are thought to cause microglia activation and microgliosis (Garcia et al., 2022).

Despite the numerous failures in clinical trials in Parkinson's and Alzheimer's disease, advances in the field of ''omics'' and biomarkers have reshaped our approach to therapeutic strategies for neurodegeneration and eventually a precision medicine approach (Di Meco and Vassar, 2021). My hope is that my doctorate research has contributed towards our understanding of the multifaceted neurobiology of Parkinson's disease and has generated relevant research tools that can be explored further for the development of disease-modifying therapies for the patients.

REFERENCES

ABERG, M. A., ABERG, N. D., PALMER, T. D., ALBORN, A. M., CARLSSON-SKWIRUT, C., BANG, P., ROSENGREN, L. E., OLSSON, T., GAGE, F. H. & ERIKSSON, P. S. 2003. IGF-I has a direct proliferative effect in adult hippocampal progenitor cells. *Mol Cell Neurosci,* 24**,** 23-40.

ABERNATHY, D. G., KIM, W. K., MCCOY, M. J., LAKE, A. M., OUWENGA, R., LEE, S. W., XING, X., LI, D., LEE, H. J., HEUCKEROTH, R. O., DOUGHERTY, J. D., WANG, T. & YOO, A. S. 2017. MicroRNAs Induce a Permissive Chromatin Environment that Enables Neuronal Subtype-Specific Reprogramming of Adult Human Fibroblasts. *Cell Stem Cell,* 21**,** 332-348.e9.

ABUD, E. M., RAMIREZ, R. N., MARTINEZ, E. S., HEALY, L. M., NGUYEN, C. H. H., NEWMAN, S. A., YEROMIN, A. V., SCARFONE, V. M., MARSH, S. E., FIMBRES, C., CARAWAY, C. A., FOTE, G. M., MADANY, A. M., AGRAWAL, A., KAYED, R., GYLYS, K. H., CAHALAN, M. D., CUMMINGS, B. J., ANTEL, J. P., MORTAZAVI, A., CARSON, M. J., POON, W. W. & BLURTON-JONES, M. 2017. iPSC-Derived Human Microglia-like Cells to Study Neurological Diseases. *Neuron,* 94**,** 278-293 e9.

AFLAKI, E., BORGER, D. K., MOAVEN, N., STUBBLEFIELD, B. K., ROGERS, S. A., PATNAIK, S., SCHOENEN, F. J., WESTBROEK, W., ZHENG, W., SULLIVAN, P., FUJIWARA, H., SIDHU, R., KHALIQ, Z. M., LOPEZ, G. J., GOLDSTEIN, D. S., ORY, D. S., MARUGAN, J. & SIDRANSKY, E. 2016. A New Glucocerebrosidase Chaperone Reduces α -Synuclein and Glycolipid Levels in iPSC-Derived Dopaminergic Neurons from Patients with Gaucher Disease and Parkinsonism. *J Neurosci,* 36**,** 7441-52.

AGARWAL, D., SANDOR, C., VOLPATO, V., CAFFREY, T. M., MONZÓN-SANDOVAL, J., BOWDEN, R., ALEGRE-ABARRATEGUI, J., WADE-MARTINS, R. & WEBBER, C. 2020. A single-cell atlas of the human substantia nigra reveals cell-specific pathways associated with neurological disorders. *Nature Communications,* 11**,** 4183.

AGOSTINHO, P., MADEIRA, D., DIAS, L., SIMÕES, A. P., CUNHA, R. A. & CANAS, P. M. 2020. Purinergic signaling orchestrating neuron-glia communication. *Pharmacol Res,* 162**,** 105253.

AGUZZI, A. & LAKKARAJU, A. K. K. 2016. Cell Biology of Prions and Prionoids: A Status Report. *Trends Cell Biol,* 26**,** 40-51.

AJAMI, B., BENNETT, J. L., KRIEGER, C., TETZLAFF, W. & ROSSI, F. M. V. 2007. Local self-renewal can sustain CNS microglia maintenance and function throughout adult life. *Nature Neuroscience,* 10**,** 1538-1543.

AJAMI, B., SAMUSIK, N., WIEGHOFER, P., HO, P. P., CROTTI, A., BJORNSON, Z., PRINZ, M., FANTL, W. J., NOLAN, G. P. & STEINMAN, L. 2018. Single-cell mass cytometry reveals distinct populations of brain myeloid cells in mouse neuroinflammation and neurodegeneration models. *Nat Neurosci,* 21**,** 541-551.

ALDANA, B. I. 2019. Microglia-Specific Metabolic Changes in Neurodegeneration. *Journal of Molecular Biology,* 431**,** 1830-1842.

ALEXANDER, A. F., KELSEY, I., FORBES, H. & MILLER-JENSEN, K. 2021. Single-cell secretion analysis reveals a dual role for IL-10 in restraining and resolving the TLR4-induced inflammatory response. *Cell Reports,* 36**,** 109728.

ALLIOT, F., LECAIN, E., GRIMA, B. & PESSAC, B. 1991. Microglial progenitors with a high proliferative potential in the embryonic and adult mouse brain. *Proceedings of the National Academy of Sciences of the United States of America,* 88**,** 1541-1545.

ALSEMA, A. M., JIANG, Q., KRACHT, L., GERRITS, E., DUBBELAAR, M. L., MIEDEMA, A., BROUWER, N., HOL, E. M., MIDDELDORP, J., VAN DIJK, R., WOODBURY, M., WACHTER, A., XI, S., MÖLLER, T., BIBER, K. P., KOOISTRA, S. M., BODDEKE, E. & EGGEN, B. J. L. 2020. Profiling Microglia From Alzheimer's Disease Donors and Non-demented Elderly in Acute Human Postmortem Cortical Tissue. *Front Mol Neurosci,* 13**,** 134.

ANDERSEN, M. S., BANDRES-CIGA, S., REYNOLDS, R. H., HARDY, J., RYTEN, M., KROHN, L., GAN-OR, Z., HOLTMAN, I. R. & PIHLSTRØM, L. 2021. Heritability Enrichment Implicates Microglia in Parkinson's Disease Pathogenesis. *Ann Neurol,* 89**,** 942-951.

ANDERSON, J. P., WALKER, D. E., GOLDSTEIN, J. M., DE LAAT, R., BANDUCCI, K., CACCAVELLO, R. J., BARBOUR, R., HUANG, J., KLING, K., LEE, M., DIEP, L., KEIM, P. S., SHEN, X., CHATAWAY, T., SCHLOSSMACHER, M. G., SEUBERT, P., SCHENK, D., SINHA, S., GAI, W. P. & CHILCOTE, T. J. 2006. Phosphorylation of Ser-129 is the dominant pathological modification of alpha-synuclein in familial and sporadic Lewy body disease. *J Biol Chem,* 281**,** 29739-52.

ANSARI, K. A. & JOHNSON, A. 1975. Olfactory function in patients with Parkinson's disease. *J Chronic Dis,* 28**,** 493-7.

APPEL-CRESSWELL, S., VILARINO-GUELL, C., ENCARNACION, M., SHERMAN, H., YU, I., SHAH, B., WEIR, D., THOMPSON, C., SZU-TU, C., TRINH, J., AASLY, J. O., RAJPUT, A., RAJPUT, A. H., JON STOESSL, A. & FARRER, M. J. 2013. Alpha-synuclein p.H50Q, a novel pathogenic mutation for Parkinson's disease. *Mov Disord,* 28**,** 811-3.

ARBER, C., LOVEJOY, C. & WRAY, S. 2017. Stem cell models of Alzheimer's disease: progress and challenges. *Alzheimers Res Ther,* 9**,** 42.

ARCURI, C., MECCA, C., BIANCHI, R., GIAMBANCO, I. & DONATO, R. 2017. The Pathophysiological Role of Microglia in Dynamic Surveillance, Phagocytosis and Structural Remodeling of the Developing CNS. *Frontiers in molecular neuroscience,* 10**,** 191-191.

ARENAS, E., DENHAM, M. & VILLAESCUSA, J. C. 2015. How to make a midbrain dopaminergic neuron. *Development,* 142**,** 1918-36.

ASAI, H., IKEZU, S., TSUNODA, S., MEDALLA, M., LUEBKE, J., HAYDAR, T., WOLOZIN, B., BUTOVSKY, O., KÜGLER, S. & IKEZU, T. 2015. Depletion of microglia and inhibition of exosome synthesis halt tau propagation. *Nat Neurosci,* 18**,** 1584-93.

ATHAUDA, D. & FOLTYNIE, T. 2016. The glucagon-like peptide 1 (GLP) receptor as a therapeutic target in Parkinson's disease: mechanisms of action. *Drug Discov Today,* 21**,** 802-18.

AUBERT, A., STUDER, F., COLOMBO, B. M. & MENDOZA-PARRA, M. A. 2021. A Core Transcription Regulatory Circuitry Defining Microglia Cell Identity Inferred from the Reanalysis of Multiple Human Microglia Differentiation Protocols. *Brain Sci,* 11.

BABA, M., NAKAJO, S., TU, P. H., TOMITA, T., NAKAYA, K., LEE, V. M., TROJANOWSKI, J. Q. & IWATSUBO, T. 1998. Aggregation of alpha-synuclein in Lewy bodies of sporadic Parkinson's disease and dementia with Lewy bodies. *Am J Pathol,* 152**,** 879-84.

BACHILLER, S., JIMÉNEZ-FERRER, I., PAULUS, A., YANG, Y., SWANBERG, M., DEIERBORG, T. & BOZA-SERRANO, A. 2018. Microglia in Neurological Diseases: A Road Map to Brain-Disease Dependent-Inflammatory Response. *Frontiers in Cellular Neuroscience,* 12.

BADANJAK, K., MULICA, P., SMAJIC, S., DELCAMBRE, S., TRANCHEVENT, L.-C., DIEDERICH, N., RAUEN, T., SCHWAMBORN, J. C., GLAAB, E., COWLEY, S. A., ANTONY, P. M. A., PEREIRA, S. L., VENEGAS, C. & GRÜNEWALD, A. 2021. iPSC-Derived Microglia as a Model to Study Inflammation in Idiopathic Parkinson's Disease. *Frontiers in Cell and Developmental Biology,* 9.

BADIMON, A., STRASBURGER, H. J., AYATA, P., CHEN, X., NAIR, A., IKEGAMI, A., HWANG, P., CHAN, A. T., GRAVES, S. M., UWERU, J. O., LEDDEROSE, C., KUTLU, M. G., WHEELER, M. A., KAHAN, A., ISHIKAWA, M., WANG, Y. C., LOH, Y. E., JIANG, J. X., SURMEIER, D. J., ROBSON, S. C., JUNGER, W. G., SEBRA, R., CALIPARI, E. S., KENNY, P. J., EYO, U. B., COLONNA, M., QUINTANA, F. J., WAKE, H., GRADINARU, V. & SCHAEFER, A. 2020. Negative feedback control of neuronal activity by microglia. *Nature,* 586**,** 417-423.

BANDRES-CIGA, S., DIEZ-FAIREN, M., KIM, J. J. & SINGLETON, A. B. 2020. Genetics of Parkinson's disease: An introspection of its journey towards precision medicine. *Neurobiol Dis,* 137**,** 104782.

BARAK, V., ACKER, M., NISMAN, B., KALICKMAN, I., ABRAHAMOV, A., ZIMRAN, A. & YATZIV, S. 1999. Cytokines in Gaucher's disease. *Eur Cytokine Netw,* 10**,** 205-10.

BARRETT, J. C., HANSOUL, S., NICOLAE, D. L., CHO, J. H., DUERR, R. H., RIOUX, J. D., BRANT, S. R., SILVERBERG, M. S., TAYLOR, K. D., BARMADA, M. M., BITTON, A., DASSOPOULOS, T., DATTA, L. W., GREEN, T., GRIFFITHS, A. M., KISTNER, E. O., MURTHA, M. T., REGUEIRO, M. D., ROTTER, J. I., SCHUMM, L. P., STEINHART, A. H., TARGAN, S. R., XAVIER, R. J., LIBIOULLE, C., SANDOR, C., LATHROP, M., BELAICHE, J., DEWIT, O., GUT, I., HEATH, S., LAUKENS, D., MNI, M., RUTGEERTS, P., VAN GOSSUM, A., ZELENIKA, D., FRANCHIMONT, D., HUGOT, J. P., DE VOS, M., VERMEIRE, S., LOUIS, E., CARDON, L. R., ANDERSON, C. A., DRUMMOND, H., NIMMO, E., AHMAD, T., PRESCOTT, N. J., ONNIE, C. M., FISHER, S. A., MARCHINI, J., GHORI, J., BUMPSTEAD, S., GWILLIAM, R., TREMELLING, M., DELOUKAS, P., MANSFIELD, J., JEWELL, D., SATSANGI, J., MATHEW, C. G., PARKES, M., GEORGES, M. & DALY, M. J. 2008. Genome-wide association defines more than 30 distinct susceptibility loci for Crohn's disease. *Nat Genet,* 40**,** 955-62.

BARTH, M., BACIOGLU, M., SCHWARZ, N., NOVOTNY, R., BRANDES, J., WELZER, M., MAZZITELLI, S., HÄSLER, L. M., SCHWEIGHAUSER, M., WUTTKE, T. V., KRONENBERG-VERSTEEG, D., FOG, K., AMBJØRN, M., ALIK, A., MELKI, R., KAHLE, P. J., SHIMSHEK, D. R., KOCH, H., JUCKER, M. & TANRIÖVER, G. 2021. Microglial inclusions and neurofilament light chain release follow neuronal α-synuclein lesions in long-term brain slice cultures. *Molecular Neurodegeneration,* 16**,** 54.

BELLIN, M., MARCHETTO, M. C., GAGE, F. H. & MUMMERY, C. L. 2012. Induced pluripotent stem cells: the new patient? *Nature Reviews Molecular Cell Biology,* 13**,** 713-726.

BENDOR, J. T., LOGAN, T. P. & EDWARDS, R. H. 2013. The function of α-synuclein. *Neuron,* 79**,** 1044-66.

BENNETT, M. L. & BENNETT, F. C. 2020. The influence of environment and origin on brain resident macrophages and implications for therapy. *Nature Neuroscience,* 23**,** 157-166.

BÉRAUD, D., TWOMEY, M., BLOOM, B., MITTEREDER, A., TON, V., NEITZKE, K., CHASOVSKIKH, S., MHYRE, T. R. & MAGUIRE-ZEISS, K. A. 2011. α-Synuclein Alters Toll-Like Receptor Expression. *Front Neurosci,* 5**,** 80.

BERNARD, C., ANDERSON, A., BECKER, A., POOLOS, N. P., BECK, H. & JOHNSTON, D. 2004. Acquired dendritic channelopathy in temporal lobe epilepsy. *Science,* 305**,** 532-5.

BÉTEMPS, D., VERCHÈRE, J., BROT, S., MORIGNAT, E., BOUSSET, L., GAILLARD, D., LAKHDAR, L., MELKI, R. & BARON, T. 2014. Alpha-synuclein spreading in M83 mice brain revealed by detection of pathological α-synuclein by enhanced ELISA. *Acta Neuropathologica Communications,* 2**,** 29.

BHAT, S. A., HENRY, R. J., BLANCHARD, A. C., STOICA, B. A., LOANE, D. J. & FADEN, A. I. 2021. Enhanced Akt/GSK-3 β /CREB signaling mediates the anti-inflammatory actions of mGluR5 positive allosteric modulators in microglia and following traumatic brain injury in male mice. *J Neurochem,* 156**,** 225-248.

BI, F., HUANG, C., TONG, J., QIU, G., HUANG, B., WU, Q., LI, F., XU, Z., BOWSER, R., XIA, X. G. & ZHOU, H. 2013. Reactive astrocytes secrete lcn2 to promote neuron death. *Proc Natl Acad Sci U S A,* 110**,** 4069-74.

BIAN, Z., GONG, Y., HUANG, T., LEE, C. Z. W., BIAN, L., BAI, Z., SHI, H., ZENG, Y., LIU, C., HE, J., ZHOU, J., LI, X., LI, Z., NI, Y., MA, C., CUI, L., ZHANG, R., CHAN, J. K. Y., NG, L. G., LAN, Y., GINHOUX, F. & LIU, B. 2020. Deciphering human macrophage development at single-cell resolution. *Nature,* 582**,** 571-576.

BIBER, K., NEUMANN, H., INOUE, K. & BODDEKE, H. W. 2007. Neuronal 'On' and 'Off' signals control microglia. *Trends Neurosci,* 30**,** 596-602.

BIJU, K. C., SANTACRUZ, R. A., CHEN, C., ZHOU, Q., YAO, J., ROHRABAUGH, S. L., CLARK, R. A., ROBERTS, J. L., PHILLIPS, K. A., IMAM, S. Z. & LI, S. 2013. Bone marrow-derived microglia-based neurturin delivery protects against dopaminergic neurodegeneration in a mouse model of Parkinson's disease. *Neurosci Lett,* 535**,** 24-9.

BIOSA, A., SANDRELLI, F., BELTRAMINI, M., GREGGIO, E., BUBACCO, L. & BISAGLIA, M. 2017. Recent findings on the physiological function of DJ-1: Beyond Parkinson's disease. *Neurobiol Dis,* 108**,** 65-72.

BLUMENSTOCK, S., RODRIGUES, E. F., PETERS, F., BLAZQUEZ-LLORCA, L., SCHMIDT, F., GIESE, A. & HERMS, J. 2017. Seeding and transgenic overexpression of alpha-synuclein triggers dendritic spine pathology in the neocortex. *EMBO Molecular Medicine,* 9**,** 716-731.

BOCHE, D., PERRY, V. H. & NICOLL, J. A. 2013. Review: activation patterns of microglia and their identification in the human brain. *Neuropathol Appl Neurobiol,* 39**,** 3-18.

BOND, A. M., BHALALA, O. G. & KESSLER, J. A. 2012. The dynamic role of bone morphogenetic proteins in neural stem cell fate and maturation. *Dev Neurobiol,* 72**,** 1068-84.

BONIFATI, V., RIZZU, P., VAN BAREN, M. J., SCHAAP, O., BREEDVELD, G. J., KRIEGER, E., DEKKER, M. C., SQUITIERI, F., IBANEZ, P., JOOSSE, M., VAN DONGEN, J. W., VANACORE, N., VAN SWIETEN, J. C., BRICE, A., MECO, G., VAN DUIJN, C. M., OOSTRA, B. A. & HEUTINK, P. 2003. Mutations in the DJ-1 gene associated with autosomal recessive early-onset parkinsonism. *Science,* 299**,** 256-9.

BOUCHON, A., DIETRICH, J. & COLONNA, M. 2000. Cutting edge: inflammatory responses can be triggered by TREM-1, a novel receptor expressed on neutrophils and monocytes. *J Immunol,* 164**,** 4991-5.

BOUSSET, L., PIERI, L., RUIZ-ARLANDIS, G., GATH, J., JENSEN, P. H., HABENSTEIN, B., MADIONA, K., OLIERIC, V., BOCKMANN, A., MEIER, B. H. & MELKI, R. 2013a. Structural and functional characterization of two alpha-synuclein strains. *Nat Commun,* 4**,** 2575.

BOUSSET, L., PIERI, L., RUIZ-ARLANDIS, G., GATH, J., JENSEN, P. H., HABENSTEIN, B., MADIONA, K., OLIERIC, V., BÖCKMANN, A., MEIER, B. H. & MELKI, R. 2013b. Structural and functional characterization of two alpha-synuclein strains. *Nature Communications,* 4**,** 2575.

BRAAK, H., DE VOS, R. A., BOHL, J. & DEL TREDICI, K. 2006. Gastric alpha-synuclein immunoreactive inclusions in Meissner's and Auerbach's plexuses in cases staged for Parkinson's disease-related brain pathology. *Neurosci Lett,* 396**,** 67-72.

BRAAK, H. & DEL TREDICI, K. 2008. Invited Article: Nervous system pathology in sporadic Parkinson disease. *Neurology,* 70**,** 1916-1925.

BRAAK, H., DEL TREDICI, K., RÜB, U., DE VOS, R. A., JANSEN STEUR, E. N. & BRAAK, E. 2003a. Staging of brain pathology related to sporadic Parkinson's disease. *Neurobiol Aging,* 24**,** 197-211.

BRAAK, H., GHEBREMEDHIN, E., RÜB, U., BRATZKE, H. & DEL TREDICI, K. 2004. Stages in the development of Parkinson's disease-related pathology. *Cell Tissue Res,* 318**,** 121-34.

BRAAK, H., RÜB, U., GAI, W. P. & DEL TREDICI, K. 2003b. Idiopathic Parkinson's disease: possible routes by which vulnerable neuronal types may be subject to neuroinvasion by an unknown pathogen. *J Neural Transm (Vienna),* 110**,** 517-36.

BRADT, B. M., KOLB, W. P. & COOPER, N. R. 1998. Complement-dependent proinflammatory properties of the Alzheimer's disease beta-peptide. *J Exp Med,* 188**,** 431-8.

BRAY, N. L., PIMENTEL, H., MELSTED, P. & PACHTER, L. 2016. Near-optimal probabilistic RNA-seq quantification. *Nat Biotechnol,* 34**,** 525-7.

BRESCHI, A., GINGERAS, T. R. & GUIGÓ, R. 2017. Comparative transcriptomics in human and mouse. *Nature Reviews Genetics,* 18**,** 425-440.

BREYDO, L., WU, J. W. & UVERSKY, V. N. 2012. A-synuclein misfolding and Parkinson's disease. *Biochim Biophys Acta,* 1822**,** 261-85.

BRUNDIN, P., LI, J. Y., HOLTON, J. L., LINDVALL, O. & REVESZ, T. 2008. Research in motion: the enigma of Parkinson's disease pathology spread. *Nat Rev Neurosci,* 9**,** 741-5.

BRUNDIN, P. & MELKI, R. 2017. Prying into the Prion Hypothesis for Parkinson's Disease. *J Neurosci,* 37**,** 9808-9818.

BRUNIALTI, E., VILLA, A., MEKHAEIL, M., MORNATA, F., VEGETO, E., MAGGI, A., DI MONTE, D. A. & CIANA, P. 2021. Inhibition of microglial β-glucocerebrosidase hampers the microglia-mediated antioxidant and protective response in neurons. *Journal of neuroinflammation,* 18**,** 220-220.

BRYAN, K. J., ZHU, X., HARRIS, P. L., PERRY, G., CASTELLANI, R. J., SMITH, M. A. & CASADESUS, G. 2008. Expression of CD74 is increased in neurofibrillary tangles in Alzheimer's disease. *Molecular Neurodegeneration,* 3**,** 13.

BUCHRIESER, J., JAMES, W. & MOORE, M. D. 2017. Human Induced Pluripotent Stem Cell-Derived Macrophages Share Ontogeny with MYB-Independent Tissue-Resident Macrophages. *Stem Cell Reports,* 8**,** 334-345.

BUELL, A. K., GALVAGNION, C., GASPAR, R., SPARR, E., VENDRUSCOLO, M., KNOWLES, T. P. J., LINSE, S. & DOBSON, C. M. 2014. Solution conditions determine the relative importance of nucleation and growth processes in α-synuclein aggregation. *Proceedings of the National Academy of Sciences,* 111**,** 7671-7676.

BURKE, E. E., CHENOWETH, J. G., SHIN, J. H., COLLADO-TORRES, L., KIM, S.-K., MICALI, N., WANG, Y., COLANTUONI, C., STRAUB, R. E., HOEPPNER, D. J., CHEN, H.-Y., SELLERS, A., SHIBBANI, K., HAMERSKY, G. R., DIAZ BUSTAMANTE, M., PHAN, B. N., ULRICH, W. S., VALENCIA, C., JAISHANKAR, A., PRICE, A. J., RAJPUROHIT, A., SEMICK, S. A., BÜRLI, R. W., BARROW, J. C., HILER, D. J., PAGE, S. C., MARTINOWICH, K., HYDE, T. M., KLEINMAN, J. E., BERMAN, K. F., APUD, J. A., CROSS, A. J., BRANDON, N. J., WEINBERGER, D. R., MAHER, B. J., MCKAY, R. D. G. & JAFFE, A. E. 2020. Dissecting

transcriptomic signatures of neuronal differentiation and maturation using iPSCs. *Nature Communications,* 11**,** 462.

BURMANN, B. M., GEREZ, J. A., MATEČKO-BURMANN, I., CAMPIONI, S., KUMARI, P., GHOSH, D., MAZUR, A., ASPHOLM, E. E., ŠULSKIS, D., WAWRZYNIUK, M., BOCK, T., SCHMIDT, A., RÜDIGER, S. G. D., RIEK, R. & HILLER, S. 2020. Regulation of α-synuclein by chaperones in mammalian cells. *Nature,* 577**,** 127-132.

BURRÉ, J., SHARMA, M., TSETSENIS, T., BUCHMAN, V., ETHERTON, M. R. & SÜDHOF, T. C. 2010. Alpha-synuclein promotes SNARE-complex assembly in vivo and in vitro. *Science,* 329**,** 1663-7.

BUTOVSKY, O., JEDRYCHOWSKI, M. P., CIALIC, R., KRASEMANN, S., MURUGAIYAN, G., FANEK, Z., GRECO, D. J., WU, P. M., DOYKAN, C. E., KINER, O., LAWSON, R. J., FROSCH, M. P., POCHET, N., FATIMY, R. E., KRICHEVSKY, A. M., GYGI, S. P., LASSMANN, H., BERRY, J., CUDKOWICZ, M. E. & WEINER, H. L. 2015. Targeting miR-155 restores abnormal microglia and attenuates disease in SOD1 mice. *Ann Neurol,* 77**,** 75-99.

BUTOVSKY, O., JEDRYCHOWSKI, M. P., MOORE, C. S., CIALIC, R., LANSER, A. J., GABRIELY, G., KOEGLSPERGER, T., DAKE, B., WU, P. M., DOYKAN, C. E., FANEK, Z., LIU, L., CHEN, Z., ROTHSTEIN, J. D., RANSOHOFF, R. M., GYGI, S. P., ANTEL, J. P. & WEINER, H. L. 2014a. Identification of a unique TGF-beta-dependent molecular and functional signature in microglia. *Nat Neurosci,* 17**,** 131-43.

BUTOVSKY, O., JEDRYCHOWSKI, M. P., MOORE, C. S., CIALIC, R., LANSER, A. J., GABRIELY, G., KOEGLSPERGER, T., DAKE, B., WU, P. M., DOYKAN, C. E., FANEK, Z., LIU, L., CHEN, Z., ROTHSTEIN, J. D., RANSOHOFF, R. M., GYGI, S. P., ANTEL, J. P. & WEINER, H. L. 2014b. Identification of a unique TGF-β-dependent molecular and functional signature in microglia. *Nat Neurosci,* 17**,** 131-43.

BUTOVSKY, O. & WEINER, H. L. 2018. Microglial signatures and their role in health and disease. *Nature reviews. Neuroscience,* 19**,** 622-635.

BUTOVSKY, O., ZIV, Y., SCHWARTZ, A., LANDA, G., TALPALAR, A. E., PLUCHINO, S., MARTINO, G. & SCHWARTZ, M. 2006. Microglia activated by IL-4 or IFN-gamma differentially induce neurogenesis and oligodendrogenesis from adult stem/progenitor cells. *Mol Cell Neurosci,* 31**,** 149-60.

BYRNE, J. A. 2008. Generation of isogenic pluripotent stem cells. *Human Molecular Genetics,* 17**,** R37-R41.

CALABRESI, P., CASTRIOTO, A., DI FILIPPO, M. & PICCONI, B. 2013. New experimental and clinical links between the hippocampus and the dopaminergic system in Parkinson's disease. *The Lancet Neurology,* 12**,** 811-821.

CAMPOS, L. A., SHARMA, R., ALVIRA, S., RUIZ, F. M., IBARRA-MOLERO, B., SADQI, M., ALFONSO, C., RIVAS, G., SANCHEZ-RUIZ, J. M., ROMERO GARRIDO, A., VALPUESTA, J. M. & MUÑOZ, V. 2019. Engineering protein assemblies with allosteric control via monomer fold-switching. *Nature Communications,* 10**,** 5703.

CANNON, J. P., O'DRISCOLL, M. & LITMAN, G. W. 2012. Specific lipid recognition is a general feature of CD300 and TREM molecules. *Immunogenetics,* 64**,** 39-47.

CARDONA, A. E., PIORO, E. P., SASSE, M. E., KOSTENKO, V., CARDONA, S. M., DIJKSTRA, I. M., HUANG, D., KIDD, G., DOMBROWSKI, S., DUTTA, R., LEE, J. C., COOK, D. N., JUNG, S., LIRA, S. A., LITTMAN, D. R. & RANSOHOFF, R. M. 2006. Control of microglial neurotoxicity by the fractalkine receptor. *Nat Neurosci,* 9**,** 917-24.

CARLSON, J. D., NEUMILLER, J. J., SWAIN, L. D., MARK, J., MCLEOD, P. & HIRSCHAUER, J. 2014. Postoperative delirium in Parkinson's disease patients following deep brain stimulation surgery. *J Clin Neurosci,* 21**,** 1192-5.

CARTER, J. L., HALMAI, J. & FINK, K. D. 2020. The iNs and Outs of Direct Reprogramming to Induced Neurons. *Front Genome Ed,* 2**,** 7.

CASTRIOTO, A., KISTNER, A., KLINGER, H., LHOMMÉE, E., SCHMITT, E., FRAIX, V., CHABARDÈS, S., MERTENS, P., QUESADA, J. L., BROUSSOLLE, E., POLLAK, P., THOBOIS, S. C. & KRACK, P. 2013. Psychostimulant effect of levodopa: reversing sensitisation is possible. *J Neurol Neurosurg Psychiatry,* 84**,** 18-22.

CERRI, S., MUS, L. & BLANDINI, F. 2019. Parkinson's Disease in Women and Men: What's the Difference? *J Parkinsons Dis,* 9**,** 501-515.

CHANG, D., NALLS, M. A., HALLGRÍMSDÓTTIR, I. B., HUNKAPILLER, J., VAN DER BRUG, M., CAI, F., KERCHNER, G. A., AYALON, G., BINGOL, B., SHENG, M., HINDS, D., BEHRENS, T. W., SINGLETON, A. B., BHANGALE, T. R. & GRAHAM, R. R. 2017. A meta-analysis of genome-wide association studies identifies 17 new Parkinson's disease risk loci. *Nat Genet,* 49**,** 1511-1516.

CHARTIER-HARLIN, M. C., KACHERGUS, J., ROUMIER, C., MOUROUX, V., DOUAY, X., LINCOLN, S., LEVECQUE, C., LARVOR, L., ANDRIEUX, J., HULIHAN, M., WAUCQUIER, N., DEFEBVRE, L., AMOUYEL, P., FARRER, M. & DESTÉE, A. 2004. Alpha-synuclein locus duplication as a cause of familial Parkinson's disease. *Lancet,* 364**,** 1167-9.

CHEN, S. K., TVRDIK, P., PEDEN, E., CHO, S., WU, S., SPANGRUDE, G. & CAPECCHI, M. R. 2010. Hematopoietic origin of pathological grooming in Hoxb8 mutant mice. *Cell,* 141**,** 775-85.

CHOI, I., ZHANG, Y., SEEGOBIN, S. P., PRUVOST, M., WANG, Q., PURTELL, K., ZHANG, B. & YUE, Z. 2020. Microglia clear neuron-released α-synuclein via selective autophagy and prevent neurodegeneration. *Nature communications,* 11**,** 1386-1386.

COCKEY, S. G., MCFARLAND, K. N., KOLLER, E. J., BROOKS, M. M. T., GONZALEZ DE LA CRUZ, E., CRUZ, P. E., CEBALLOS-DIAZ, C., ROSARIO, A. M., LEVITES, Y. R., BORCHELT, D. R., GOLDE, T. E., GIASSON, B. I. & CHAKRABARTY, P. 2021. Il-10 signaling reduces survival in mouse models of synucleinopathy. *npj Parkinson's Disease,* 7**,** 30.

COLEMAN, L. G., ZOU, J. & CREWS, F. T. 2020. Microglial depletion and repopulation in brain slice culture normalizes sensitized proinflammatory signaling. *Journal of Neuroinflammation,* 17**,** 27.

COLLABORATORS, G. B. D. N. 2019. Global, regional, and national burden of neurological disorders, 1990-2016: a systematic analysis for the Global Burden of Disease Study 2016. *Lancet Neurol,* 18**,** 459-480.

COLONNA, M. & BUTOVSKY, O. 2017. Microglia Function in the Central Nervous System During Health and Neurodegeneration. *Annu Rev Immunol,* 35**,** 441-468.

COLONNA, M. & WANG, Y. 2016. TREM2 variants: new keys to decipher Alzheimer disease pathogenesis. *Nat Rev Neurosci,* 17**,** 201-7.

COMABELLA, M., FERNÁNDEZ, M., MARTIN, R., RIVERA-VALLVÉ, S., BORRÁS, E., CHIVA, C., JULIÀ, E., ROVIRA, A., CANTÓ, E., ALVAREZ-CERMEÑO, J. C., VILLAR, L. M., TINTORÉ, M. & MONTALBAN, X. 2010. Cerebrospinal fluid chitinase 3-like 1 levels are associated with conversion to multiple sclerosis. *Brain,* 133**,** 1082-93.

COUSINS, E. M., GOLDFARB, D., YAN, F., ROQUES, J., DARR, D., JOHNSON, G. L. & MAJOR, M. B. 2018. Competitive Kinase Enrichment Proteomics Reveals that Abemaciclib Inhibits GSK3 β and Activates WNT Signaling. *Mol Cancer Res,* 16**,** 333-344.

CRAIG-SCHAPIRO, R., PERRIN, R. J., ROE, C. M., XIONG, C., CARTER, D., CAIRNS, N. J., MINTUN, M. A., PESKIND, E. R., LI, G., GALASKO, D. R., CLARK, C. M., QUINN, J. F., D'ANGELO, G., MALONE, J. P., TOWNSEND, R. R., MORRIS, J. C., FAGAN, A. M. & HOLTZMAN, D. M. 2010. YKL-40: a novel prognostic fluid biomarker for preclinical Alzheimer's disease. *Biol Psychiatry,* 68**,** 903-12.

CREMADES, N., CHEN, S. W. & DOBSON, C. M. 2017. Structural Characteristics of alpha-Synuclein Oligomers. *Int Rev Cell Mol Biol,* 329**,** 79-143.

CROFT, C. L., CRUZ, P. E., RYU, D. H., CEBALLOS-DIAZ, C., STRANG, K. H., WOODY, B. M., LIN, W. L., DETURE, M., RODRIGUEZ-LEBRON, E., DICKSON, D. W., CHAKRABARTY, P., LEVITES, Y., GIASSON, B. I. & GOLDE, T. E. 2019a. rAAV-based brain slice culture models of Alzheimer's and Parkinson's disease inclusion pathologies. *J Exp Med,* 216**,** 539-555.

CROFT, C. L., FUTCH, H. S., MOORE, B. D. & GOLDE, T. E. 2019b. Organotypic brain slice cultures to model neurodegenerative proteinopathies. *Molecular Neurodegeneration,* 14**,** 45.

CUMMINGS, J. L. 1992. Depression and Parkinson's disease: a review. *Am J Psychiatry,* 149**,** 443-54.

DAFINCA, R., SCABER, J., ABABNEH, N., LALIC, T., WEIR, G., CHRISTIAN, H., VOWLES, J., DOUGLAS, A. G., FLETCHER-JONES, A., BROWNE, C., NAKANISHI, M., TURNER, M. R., WADE-MARTINS, R., COWLEY, S. A. & TALBOT, K. 2016. C9orf72 Hexanucleotide Expansions Are Associated with Altered Endoplasmic Reticulum Calcium Homeostasis and Stress Granule Formation in Induced Pluripotent Stem Cell-Derived Neurons from Patients with Amyotrophic Lateral Sclerosis and Frontotemporal Dementia. *Stem Cells,* 34**,** 2063-78.

DAMISAH, E. C., HILL, R. A., RAI, A., CHEN, F., ROTHLIN, C. V., GHOSH, S. & GRUTZENDLER, J. 2020. Astrocytes and microglia play orchestrated roles and respect phagocytic territories during neuronal corpse removal in vivo. *Science Advances,* 6**,** eaba3239.

DAVID, S. & KRONER, A. 2011. Repertoire of microglial and macrophage responses after spinal cord injury. *Nat Rev Neurosci,* 12**,** 388-99.

DAVIS, B. M., SALINAS-NAVARRO, M., CORDEIRO, M. F., MOONS, L. & DE GROEF, L. 2017. Characterizing microglia activation: a spatial statistics approach to maximize information extraction. *Scientific Reports,* 7**,** 1576.

DAVIS, C. H., KIM, K. Y., BUSHONG, E. A., MILLS, E. A., BOASSA, D., SHIH, T., KINEBUCHI, M., PHAN, S., ZHOU, Y., BIHLMEYER, N. A., NGUYEN, J. V., JIN, Y., ELLISMAN, M. H. & MARSH-ARMSTRONG, N. 2014. Transcellular degradation of axonal mitochondria. *Proc Natl Acad Sci U S A,* 111**,** 9633-8.

DAWSON, T. M., GOLDE, T. E. & LAGIER-TOURENNE, C. 2018. Animal models of neurodegenerative diseases. *Nature Neuroscience,* 21**,** 1370-1379.

DAY, J. O. & MULLIN, S. 2021. The Genetics of Parkinson's Disease and Implications for Clinical Practice. *Genes (Basel),* 12.

DE BIASE, L. M., SCHUEBEL, K. E., FUSFELD, Z. H., JAIR, K., HAWES, I. A., CIMBRO, R., ZHANG, H. Y., LIU, Q. R., SHEN, H., XI, Z. X., GOLDMAN, D. & BONCI, A. 2017. Local Cues Establish and Maintain Region-Specific Phenotypes of Basal Ganglia Microglia. *Neuron,* 95**,** 341-356.e6.

DE HAAS, A. H., BODDEKE, H. W. & BIBER, K. 2008. Region-specific expression of immunoregulatory proteins on microglia in the healthy CNS. *Glia,* 56**,** 888-94.

DE LELLA EZCURRA, A. L., CHERTOFF, M., FERRARI, C., GRACIARENA, M. & PITOSSI, F. 2010. Chronic expression of low levels of tumor necrosis factor-alpha in the substantia nigra

elicits progressive neurodegeneration, delayed motor symptoms and microglia/macrophage activation. *Neurobiol Dis,* 37**,** 630-40.

DE OLIVEIRA, G. A. P. & SILVA, J. L. 2019. Alpha-synuclein stepwise aggregation reveals features of an early onset mutation in Parkinson's disease. *Communications Biology,* 2**,** 374.

DE RUS JACQUET, A., DENIS, H. L., CICCHETTI, F. & ALPAUGH, M. 2021. Current and future applications of induced pluripotent stem cell-based models to study pathological proteins in neurodegenerative disorders. *Molecular Psychiatry,* 26**,** 2685-2706.

DE SIMONI, A., GRIESINGER, C. B. & EDWARDS, F. A. 2003. Development of rat CA1 neurones in acute versus organotypic slices: role of experience in synaptic morphology and activity. *J Physiol,* 550**,** 135-47.

DE STROOPER, B. & KARRAN, E. 2016. The Cellular Phase of Alzheimer's Disease. *Cell,* 164**,** 603-15.

DEARDORFF, W. J. & GROSSBERG, G. T. 2017. Targeting neuroinflammation in Alzheimer's disease: evidence for NSAIDs and novel therapeutics. *Expert Rev Neurother,* 17**,** 17-32.

DECZKOWSKA, A., KEREN-SHAUL, H., WEINER, A., COLONNA, M., SCHWARTZ, M. & AMIT, I. 2018. Disease-Associated Microglia: A Universal Immune Sensor of Neurodegeneration. *Cell,* 173**,** 1073-1081.

DEL TREDICI, K., RÜB, U., DE VOS, R. A., BOHL, J. R. & BRAAK, H. 2002. Where does parkinson disease pathology begin in the brain? *J Neuropathol Exp Neurol,* 61**,** 413-26.

DELBRIDGE, A. R. D., HUH, D., BRICKELMAIER, M., BURNS, J. C., ROBERTS, C., CHALLA, R., RAYMOND, N., CULLEN, P., CARLILE, T. M., ENNIS, K. A., LIU, M., SUN, C., ALLAIRE, N. E., FOOS, M., TSAI, H.-H., FRANCHIMONT, N., RANSOHOFF, R. M., BUTTS, C. & MINGUENEAU, M. 2020. Organotypic Brain Slice Culture Microglia Exhibit Molecular Similarity to Acutely-Isolated Adult Microglia and Provide a Platform to Study Neuroinflammation. *Frontiers in Cellular Neuroscience,* 14.

DELEERSNIJDER, A., GERARD, M., DEBYSER, Z. & BAEKELANDT, V. 2013. The remarkable conformational plasticity of alpha-synuclein: blessing or curse? *Trends Mol Med,* 19**,** 368-77.

DERVEAUX, S., VANDESOMPELE, J. & HELLEMANS, J. 2010. How to do successful gene expression analysis using real-time PCR. *Methods,* 50**,** 227-30.

DESPLATS, P., LEE, H. J., BAE, E. J., PATRICK, C., ROCKENSTEIN, E., CREWS, L., SPENCER, B., MASLIAH, E. & LEE, S. J. 2009. Inclusion formation and neuronal cell death through neuron-to-neuron transmission of alpha-synuclein. *Proc Natl Acad Sci U S A,* 106**,** 13010-5.

DEVINE, M. J., RYTEN, M., VODICKA, P., THOMSON, A. J., BURDON, T., HOULDEN, H., CAVALERI, F., NAGANO, M., DRUMMOND, N. J., TAANMAN, J. W., SCHAPIRA, A. H., GWINN, K., HARDY, J., LEWIS, P. A. & KUNATH, T. 2011. Parkinson's disease induced pluripotent stem cells with triplication of the α-synuclein locus. *Nat Commun,* 2**,** 440.

DI MAIO, R., HOFFMAN, E. K., ROCHA, E. M., KEENEY, M. T., SANDERS, L. H., DE MIRANDA, B. R., ZHARIKOV, A., VAN LAAR, A., STEPAN, A. F., LANZ, T. A., KOFLER, J. K., BURTON, E. A., ALESSI, D. R., HASTINGS, T. G. & GREENAMYRE, J. T. 2018. LRRK2 activation in idiopathic Parkinson's disease. *Sci Transl Med,* 10.

DI MECO, A. & VASSAR, R. 2021. Chapter Eight - Early detection and personalized medicine: Future strategies against Alzheimer's disease. *In:* TEPLOW, D. B. (ed.) *Progress in Molecular Biology and Translational Science.* Academic Press.

DIAO, J., BURRÉ, J., VIVONA, S., CIPRIANO, D. J., SHARMA, M., KYOUNG, M., SÜDHOF, T. C. & BRUNGER, A. T. 2013. Native α-synuclein induces clustering of synaptic-vesicle mimics via binding to phospholipids and synaptobrevin-2/VAMP2. *eLife,* 2**,** e00592-e00592.

DICKSON, D. W. 2012. Parkinson's disease and parkinsonism: neuropathology. *Cold Spring Harb Perspect Med,* 2.

DICKSON, D. W., BRAAK, H., DUDA, J. E., DUYCKAERTS, C., GASSER, T., HALLIDAY, G. M., HARDY, J., LEVERENZ, J. B., DEL TREDICI, K., WSZOLEK, Z. K. & LITVAN, I. 2009. Neuropathological assessment of Parkinson's disease: refining the diagnostic criteria. *Lancet Neurol,* 8**,** 1150-7.

DO, J., MCKINNEY, C., SHARMA, P. & SIDRANSKY, E. 2019. Glucocerebrosidase and its relevance to Parkinson disease. *Molecular Neurodegeneration,* 14**,** 36.

DOORN, K. J., BREVÉ, J. J., DRUKARCH, B., BODDEKE, H. W., HUITINGA, I., LUCASSEN, P. J. & VAN DAM, A. M. 2015. Brain region-specific gene expression profiles in freshly isolated rat microglia. *Front Cell Neurosci,* 9**,** 84.

DORSEY, E. R., SHERER, T., OKUN, M. S. & BLOEM, B. R. 2018. The Emerging Evidence of the Parkinson Pandemic. *Journal of Parkinson's Disease,* 8**,** S3-S8.

DOUVARAS, P., SUN, B., WANG, M., KRUGLIKOV, I., LALLOS, G., ZIMMER, M., TERRENOIRE, C., ZHANG, B., GANDY, S., SCHADT, E., FREYTES, D. O., NOGGLE, S. & FOSSATI, V. 2017. Directed Differentiation of Human Pluripotent Stem Cells to Microglia. *Stem Cell Reports,* 8**,** 1516-1524.

DUBOIS, B. & PILLON, B. 1997. Cognitive deficits in Parkinson's disease. *J Neurol,* 244**,** 2-8.

DUFFY, M. F., COLLIER, T. J., PATTERSON, J. R., KEMP, C. J., LUK, K. C., TANSEY, M. G., PAUMIER, K. L., KANAAN, N. M., FISCHER, D. L., POLINSKI, N. K., BARTH, O. L., HOWE, J. W., VAIKATH, N. N., MAJBOUR, N. K., EL-AGNAF, O. M. A. & SORTWELL, C. E. 2018. Lewy body-like alpha-synuclein inclusions trigger reactive microgliosis prior to nigral degeneration. *Journal of neuroinflammation,* 15**,** 129-129.

DUFFY, P. E. & TENNYSON, V. M. 1965. Phase and Electron Microscopic Observations of Lewy Bodies and Melanin Granules in the Substantia Nigra and Locus Caeruleus in Parkinson's Disease*†. *Journal of Neuropathology & Experimental Neurology,* 24**,** 398-414.

EBISAWA, T., FUKUCHI, M., MURAKAMI, G., CHIBA, T., TANAKA, K., IMAMURA, T. & MIYAZONO, K. 2001. Smurf1 interacts with transforming growth factor-beta type I receptor through Smad7 and induces receptor degradation. *J Biol Chem,* 276**,** 12477-80.

EDWARDS, L., QUIGLEY, E. M., HOFMAN, R. & PFEIFFER, R. F. 1993. Gastrointestinal symptoms in Parkinson disease: 18-month follow-up study. *Mov Disord,* 8**,** 83-6.

EFREMOVA, M., VENTO-TORMO, M., TEICHMANN, S. A. & VENTO-TORMO, R. 2020. CellPhoneDB: inferring cell–cell communication from combined expression of multi-subunit ligand–receptor complexes. *Nature Protocols,* 15**,** 1484-1506.

ELFARRASH, S., JENSEN, N. M., FERREIRA, N., BETZER, C., THEVATHASAN, J. V., DIEKMANN, R., ADEL, M., OMAR, N. M., BORAIE, M. Z., GAD, S., RIES, J., KIRIK, D., NABAVI, S. & JENSEN, P. H. 2019. Organotypic slice culture model demonstrates inter-neuronal spreading of alpha-synuclein aggregates. *Acta Neuropathologica Communications,* 7**,** 213.

ELMORE, M. R. P., NAJAFI, A. R., KOIKE, M. A., DAGHER, N. N., SPANGENBERG, E. E., RICE, R. A., KITAZAWA, M., MATUSOW, B., NGUYEN, H., WEST, B. L. & GREEN, K. N. 2014.

Colony-stimulating factor 1 receptor signaling is necessary for microglia viability, unmasking a microglia progenitor cell in the adult brain. *Neuron,* 82**,** 380-397.

EMMANOUILIDOU, E., MELACHROINOU, K., ROUMELIOTIS, T., GARBIS, S. D., NTZOUNI, M., MARGARITIS, L. H., STEFANIS, L. & VEKRELLIS, K. 2010. Cell-produced alpha-synuclein is secreted in a calcium-dependent manner by exosomes and impacts neuronal survival. *The Journal of neuroscience : the official journal of the Society for Neuroscience,* 30**,** 6838-6851.

EUGÈNE, E., CLUZEAUD, F., CIFUENTES-DIAZ, C., FRICKER, D., LE DUIGOU, C., CLEMENCEAU, S., BAULAC, M., PONCER, J. C. & MILES, R. 2014. An organotypic brain slice preparation from adult patients with temporal lobe epilepsy. *J Neurosci Methods,* 235**,** 234-44.

EYO, U. B. & WU, L.-J. 2013. Bidirectional Microglia-Neuron Communication in the Healthy Brain. *Neural Plasticity,* 2013**,** 456857.

FAN, R. & TENNER, A. J. 2004. Complement C1q expression induced by Abeta in rat hippocampal organotypic slice cultures. *Exp Neurol,* 185**,** 241-53.

FANNING, S., SELKOE, D. & DETTMER, U. 2021. Vesicle trafficking and lipid metabolism in synucleinopathy. *Acta Neuropathol,* 141**,** 491-510.

FARFEL-BECKER, T., VITNER, E. B., PRESSEY, S. N., EILAM, R., COOPER, J. D. & FUTERMAN, A. H. 2011. Spatial and temporal correlation between neuron loss and neuroinflammation in a mouse model of neuronopathic Gaucher disease. *Hum Mol Genet,* 20**,** 1375-86.

FATTORELLI, N., MARTINEZ-MURIANA, A., WOLFS, L., GERIC, I., DE STROOPER, B. & MANCUSO, R. 2021. Stem-cell-derived human microglia transplanted into mouse brain to study human disease. *Nature Protocols,* 16**,** 1013-1033.

FEDELE, S., COLLO, G., BEHR, K., BISCHOFBERGER, J., MÜLLER, S., KUNATH, T., CHRISTENSEN, K., GÜNDNER, A. L., GRAF, M., JAGASIA, R. & TAYLOR, V. 2017. Expansion of human midbrain floor plate progenitors from induced pluripotent stem cells increases dopaminergic neuron differentiation potential. *Scientific Reports,* 7**,** 6036.

FELLNER, L., IRSCHICK, R., SCHANDA, K., REINDL, M., KLIMASCHEWSKI, L., POEWE, W., WENNING, G. K. & STEFANOVA, N. 2013. Toll-like receptor 4 is required for α-synuclein dependent activation of microglia and astroglia. *Glia,* 61**,** 349-60.

FERNANDES, H. J., HARTFIELD, E. M., CHRISTIAN, H. C., EMMANOULIDOU, E., ZHENG, Y., BOOTH, H., BOGETOFTE, H., LANG, C., RYAN, B. J., SARDI, S. P., BADGER, J., VOWLES, J., EVETTS, S., TOFARIS, G. K., VEKRELLIS, K., TALBOT, K., HU, M. T., JAMES, W., COWLEY, S. A. & WADE-MARTINS, R. 2016. ER Stress and Autophagic Perturbations Lead to Elevated Extracellular alpha-Synuclein in GBA-N370S Parkinson's iPSC-Derived Dopamine Neurons. *Stem Cell Reports,* 6**,** 342-56.

FILIPELLO, F., GOLDSBURY, C., YOU, S. F., LOCCA, A., KARCH, C. M. & PICCIO, L. 2022. Soluble TREM2: Innocent bystander or active player in neurological diseases? *Neurobiology of Disease,* 165**,** 105630.

FLAVIN, W. P., BOUSSET, L., GREEN, Z. C., CHU, Y., SKARPATHIOTIS, S., CHANEY, M. J., KORDOWER, J. H., MELKI, R. & CAMPBELL, E. M. 2017. Endocytic vesicle rupture is a conserved mechanism of cellular invasion by amyloid proteins. *Acta Neuropathol,* 134**,** 629-653.

FLÜGEL, A., BRADL, M., KREUTZBERG, G. W. & GRAEBER, M. B. 2001. Transformation of donor-derived bone marrow precursors into host microglia during autoimmune CNS inflammation and during the retrograde response to axotomy. *J Neurosci Res,* 66**,** 74-82.

FOLEY, J. A., FOLTYNIE, T., ZRINZO, L., HYAM, J. A., LIMOUSIN, P. & CIPOLOTTI, L. 2017. Apathy and Reduced Speed of Processing Underlie Decline in Verbal Fluency following DBS. *Behav Neurol,* 2017**,** 7348101.

FORNO, L. S. 1969. Concentric hyalin intraneuronal inclusions of Lewy type in the brains of elderly persons (50 incidental cases): relationship to parkinsonism. *J Am Geriatr Soc,* 17**,** 557-75.

FORNO, L. S. & NORVILLE, R. L. 1976. Ultrastructure of Lewy bodies in the stellate ganglion. *Acta Neuropathol,* 34**,** 183-97.

FOURGEAUD, L., TRAVÉS, P. G., TUFAIL, Y., LEAL-BAILEY, H., LEW, E. D., BURROLA, P. G., CALLAWAY, P., ZAGÓRSKA, A., ROTHLIN, C. V., NIMMERJAHN, A. & LEMKE, G. 2016. TAM receptors regulate multiple features of microglial physiology. *Nature,* 532**,** 240-244.

FRANCO-BOCANEGRA, D. K., GOURARI, Y., MCAULEY, C., CHATELET, D. S., JOHNSTON, D. A., NICOLL, J. A. R. & BOCHE, D. 2021. Microglial morphology in Alzheimer's disease and after A β immunotherapy. *Scientific Reports,* 11**,** 15955.

FRANCO-BOCANEGRA, D. K., MCAULEY, C., NICOLL, J. A. R. & BOCHE, D. 2019. Molecular Mechanisms of Microglial Motility: Changes in Ageing and Alzheimer's Disease. *Cells,* 8.

FRENKEL, D., PUCKETT, L., PETROVIC, S., XIA, W., CHEN, G., VEGA, J., DEMBINSKY-VAKNIN, A., SHEN, J., PLANTE, M., BURT, D. S. & WEINER, H. L. 2008. A nasal proteosome adjuvant activates microglia and prevents amyloid deposition. *Ann Neurol,* 63**,** 591-601.

FREUNDT, E. C., MAYNARD, N., CLANCY, E. K., ROY, S., BOUSSET, L., SOURIGUES, Y., COVERT, M., MELKI, R., KIRKEGAARD, K. & BRAHIC, M. 2012. Neuron-to-neuron transmission of alpha-synuclein fibrils through axonal transport. *Ann Neurol,* 72**,** 517-24.

FRIEDMAN, A. D. 2007. Transcriptional control of granulocyte and monocyte development. *Oncogene,* 26**,** 6816-28.

FRIEDMAN, B. A., SRINIVASAN, K., AYALON, G., MEILANDT, W. J., LIN, H., HUNTLEY, M. A., CAO, Y., LEE, S.-H., HADDICK, P. C. & NGU, H. 2018a. Diverse brain myeloid expression profiles reveal distinct microglial activation states and aspects of Alzheimer's disease not evident in mouse models. *Cell reports,* 22**,** 832-847.

FRIEDMAN, B. A., SRINIVASAN, K., AYALON, G., MEILANDT, W. J., LIN, H., HUNTLEY, M. A., CAO, Y., LEE, S. H., HADDICK, P. C. G., NGU, H., MODRUSAN, Z., LARSON, J. L., KAMINKER, J. S., VAN DER BRUG, M. P. & HANSEN, D. V. 2018b. Diverse Brain Myeloid Expression Profiles Reveal Distinct Microglial Activation States and Aspects of Alzheimer's Disease Not Evident in Mouse Models. *Cell Rep,* 22**,** 832-847.

FUJIWARA, H., HASEGAWA, M., DOHMAE, N., KAWASHIMA, A., MASLIAH, E., GOLDBERG, M. S., SHEN, J., TAKIO, K. & IWATSUBO, T. 2002. alpha-Synuclein is phosphorylated in synucleinopathy lesions. *Nat Cell Biol,* 4**,** 160-4.

GAHWILER, B. H. 1981. Organotypic monolayer cultures of nervous tissue. *J Neurosci Methods,* 4**,** 329-42.

GALATRO, T. F., HOLTMAN, I. R., LERARIO, A. M., VAINCHTEIN, I. D., BROUWER, N., SOLA, P. R., VERAS, M. M., PEREIRA, T. F., LEITE, R. E. P., MÖLLER, T., WES, P. D., SOGAYAR, M. C., LAMAN, J. D., DEN DUNNEN, W., PASQUALUCCI, C. A., OBA-SHINJO, S. M., BODDEKE, E., MARIE, S. K. N. & EGGEN, B. J. L. 2017a. Transcriptomic analysis of purified human cortical microglia reveals age-associated changes. *Nat Neurosci,* 20**,** 1162-1171.

GALATRO, T. F., HOLTMAN, I. R., LERARIO, A. M., VAINCHTEIN, I. D., BROUWER, N., SOLA, P. R., VERAS, M. M., PEREIRA, T. F., LEITE, R. E. P., MÖLLER, T., WES, P. D., SOGAYAR, M. C., LAMAN, J. D., DEN DUNNEN, W., PASQUALUCCI, C. A., OBA-SHINJO, S. M., BODDEKE, E. W. G. M., MARIE, S. K. N. & EGGEN, B. J. L. 2017b. Transcriptomic analysis of purified human cortical microglia reveals age-associated changes. *Nature Neuroscience,* 20**,** 1162-1171.

GALLARDO, G. 2019. Microglia seeding the brain for α-synuclein pathology. *Science Translational Medicine,* 11**,** eaax9563.

GALVAGNION, C., BUELL, A. K., MEISL, G., MICHAELS, T. C., VENDRUSCOLO, M., KNOWLES, T. P. & DOBSON, C. M. 2015. Lipid vesicles trigger α-synuclein aggregation by stimulating primary nucleation. *Nat Chem Biol,* 11**,** 229-34.

GALVÁN-PEÑA, S., CARROLL, R. G., NEWMAN, C., HINCHY, E. C., PALSSON-MCDERMOTT, E., ROBINSON, E. K., COVARRUBIAS, S., NADIN, A., JAMES, A. M., HANEKLAUS, M., CARPENTER, S., KELLY, V. P., MURPHY, M. P., MODIS, L. K. & O'NEILL, L. A. 2019. Malonylation of GAPDH is an inflammatory signal in macrophages. *Nature communications,* 10**,** 338-338.

GAN, J., LIU, S., WANG, X., SHI, Z., SHEN, L., LI, X., GUO, Q., YUAN, J., ZHANG, N., YOU, Y., LV, Y., ZHENG, D. & JI, Y. 2021. Clinical characteristics of Lewy body dementia in Chinese memory clinics. *BMC Neurol,* 21**,** 144.

GANTNER, C. W., COTA-CORONADO, A., THOMPSON, L. H. & PARISH, C. L. 2020. An Optimized Protocol for the Generation of Midbrain Dopamine Neurons under Defined Conditions. *STAR Protocols,* 1**,** 100065.

GAO, J., KANG, X. Y., SUN, S., LI, L., ZHANG, B. L., LI, Y. Q. & GAO, D. S. 2016. Transcription factor Six2 mediates the protection of GDNF on 6-OHDA lesioned dopaminergic neurons by regulating Smurf1 expression. *Cell Death & Disease,* 7**,** e2217-e2217.

GARCIA, P., JÜRGENS-WEMHEUER, W., URIARTE HUARTE, O., MICHELUCCI, A., MASUCH, A., BRIOSCHI, S., WEIHOFEN, A., KONCINA, E., COOWAR, D., HEURTAUX, T., GLAAB, E., BALLING, R., SOUSA, C., KAOMA, T., NICOT, N., PFANDER, T., SCHULZ-SCHAEFFER, W., ALLOUCHE, A., FISCHER, N., BIBER, K., KLEINE-BORGMANN, F., MITTELBRONN, M., OSTASZEWSKI, M., SCHMIT, K. J. & BUTTINI, M. 2022. Neurodegeneration and neuroinflammation are linked, but independent of alpha-synuclein inclusions, in a seeding/spreading mouse model of Parkinson's disease. *Glia,* 70**,** 935-960.

GARCIA-REITBOECK, P., ANICHTCHIK, O., DALLEY, J. W., NINKINA, N., TOFARIS, G. K., BUCHMAN, V. L. & SPILLANTINI, M. G. 2013. Endogenous alpha-synuclein influences the number of dopaminergic neurons in mouse substantia nigra. *Exp Neurol,* 248**,** 541-5.

GEIRSDOTTIR, L., DAVID, E., KEREN-SHAUL, H., WEINER, A., BOHLEN, S. C., NEUBER, J., BALIC, A., GILADI, A., SHEBAN, F., DUTERTRE, C. A., PFEIFLE, C., PERI, F., RAFFO-ROMERO, A., VIZIOLI, J., MATIASEK, K., SCHEIWE, C., MECKEL, S., MÄTZ-RENSING, K., VAN DER MEER, F., THORMODSSON, F. R., STADELMANN, C., ZILKHA, N., KIMCHI, T., GINHOUX, F., ULITSKY, I., ERNY, D., AMIT, I. & PRINZ, M. 2019. Cross-Species Single-Cell Analysis Reveals Divergence of the Primate Microglia Program. *Cell,* 179**,** 1609-1622.e16.

GHEE, M., MELKI, R., MICHOT, N. & MALLET, J. 2005. PA700, the regulatory complex of the 26S proteasome, interferes with alpha-synuclein assembly. *FEBS J,* 272**,** 4023-33.

GIASSON, B. I., DUDA, J. E., MURRAY, I. V., CHEN, Q., SOUZA, J. M., HURTIG, H. I., ISCHIROPOULOS, H., TROJANOWSKI, J. Q. & LEE, V. M. 2000. Oxidative damage linked

to neurodegeneration by selective alpha-synuclein nitration in synucleinopathy lesions. *Science,* 290**,** 985-9.

GIASSON, B. I., MURRAY, I. V., TROJANOWSKI, J. Q. & LEE, V. M. 2001. A hydrophobic stretch of 12 amino acid residues in the middle of alpha-synuclein is essential for filament assembly. *J Biol Chem,* 276**,** 2380-6.

GIBB, W. R., SCOTT, T. & LEES, A. J. 1991. Neuronal inclusions of Parkinson's disease. *Mov Disord,* 6**,** 2-11.

GINHOUX, F., GRETER, M., LEBOEUF, M., NANDI, S., SEE, P., GOKHAN, S., MEHLER, M. F., CONWAY, S. J., NG, L. G., STANLEY, E. R., SAMOKHVALOV, I. M. & MERAD, M. 2010. Fate mapping analysis reveals that adult microglia derive from primitive macrophages. *Science,* 330**,** 841-5.

GINHOUX, F., LIM, S., HOEFFEL, G., LOW, D. & HUBER, T. 2013. Origin and differentiation of microglia. *Frontiers in Cellular Neuroscience,* 7.

GOEDERT, M. 2001. Alpha-synuclein and neurodegenerative diseases. *Nat Rev Neurosci,* 2**,** 492-501.

GOLDMAN, J. E., YEN, S. H., CHIU, F. C. & PERESS, N. S. 1983. Lewy bodies of Parkinson's disease contain neurofilament antigens. *Science,* 221**,** 1082-4.

GOMEZ PERDIGUERO, E., KLAPPROTH, K., SCHULZ, C., BUSCH, K., AZZONI, E., CROZET, L., GARNER, H., TROUILLET, C., DE BRUIJN, M. F., GEISSMANN, F. & RODEWALD, H.-R. 2015a. Tissue-resident macrophages originate from yolk-sac-derived erythro-myeloid progenitors. *Nature,* 518**,** 547-551.

GOMEZ PERDIGUERO, E., KLAPPROTH, K., SCHULZ, C., BUSCH, K., AZZONI, E., CROZET, L., GARNER, H., TROUILLET, C., DE BRUIJN, M. F., GEISSMANN, F. & RODEWALD, H. R. 2015b. Tissue-resident macrophages originate from yolk-sac-derived erythro-myeloid progenitors. *Nature,* 518**,** 547-51.

GONZALEZ, R., GARITAONANDIA, I., ABRAMIHINA, T., WAMBUA, G. K., OSTROWSKA, A., BROCK, M., NOSKOV, A., BOSCOLO, F. S., CRAW, J. S., LAURENT, L. C., SNYDER, E. Y. & SEMECHKIN, R. A. 2013. Deriving dopaminergic neurons for clinical use. A practical approach. *Scientific Reports,* 3**,** 1463.

GORLOVOY, P., LARIONOV, S., PHAM, T. T. & NEUMANN, H. 2009. Accumulation of tau induced in neurites by microglial proinflammatory mediators. *Faseb j,* 23**,** 2502-13.

GOSSELIN, D., SKOLA, D., COUFAL, N. G., HOLTMAN, I. R., SCHLACHETZKI, J. C. M., SAJTI, E., JAEGER, B. N., O'CONNOR, C., FITZPATRICK, C., PASILLAS, M. P., PENA, M., ADAIR, A., GONDA, D. D., LEVY, M. L., RANSOHOFF, R. M., GAGE, F. H. & GLASS, C. K. 2017a. An environment-dependent transcriptional network specifies human microglia identity. *Science (New York, N.Y.),* 356**,** eaal3222.

GOSSELIN, D., SKOLA, D., COUFAL, N. G., HOLTMAN, I. R., SCHLACHETZKI, J. C. M., SAJTI, E., JAEGER, B. N., O'CONNOR, C., FITZPATRICK, C., PASILLAS, M. P., PENA, M., ADAIR, A., GONDA, D. D., LEVY, M. L., RANSOHOFF, R. M., GAGE, F. H. & GLASS, C. K. 2017b. An environment-dependent transcriptional network specifies human microglia identity. *Science,* 356.

GOTO, Y. & GRACE, A. A. 2005. Dopamine-dependent interactions between limbic and prefrontal cortical plasticity in the nucleus accumbens: disruption by cocaine sensitization. *Neuron,* 47**,** 255-66.

GRATUZE, M., LEYNS, C. E. G. & HOLTZMAN, D. M. 2018. New insights into the role of TREM2 in Alzheimer's disease. *Mol Neurodegener,* 13**,** 66.

GREGGIO, E., JAIN, S., KINGSBURY, A., BANDOPADHYAY, R., LEWIS, P., KAGANOVICH, A., VAN DER BRUG, M. P., BEILINA, A., BLACKINTON, J., THOMAS, K. J., AHMAD, R., MILLER, D. W., KESAVAPANY, S., SINGLETON, A., LEES, A., HARVEY, R. J., HARVEY, K. & COOKSON, M. R. 2006. Kinase activity is required for the toxic effects of mutant LRRK2/dardarin. *Neurobiol Dis,* 23**,** 329-41.

GRETEN-HARRISON, B., POLYDORO, M., MORIMOTO-TOMITA, M., DIAO, L., WILLIAMS, A. M., NIE, E. H., MAKANI, S., TIAN, N., CASTILLO, P. E., BUCHMAN, V. L. & CHANDRA, S. S. 2010. alphabetagamma-Synuclein triple knockout mice reveal age-dependent neuronal dysfunction. *Proc Natl Acad Sci U S A,* 107**,** 19573-8.

GRIFFIN, W. S., STANLEY, L. C., LING, C., WHITE, L., MACLEOD, V., PERROT, L. J., WHITE, C. L., 3RD & ARAOZ, C. 1989. Brain interleukin 1 and S-100 immunoreactivity are elevated in Down syndrome and Alzheimer disease. *Proc Natl Acad Sci U S A,* 86**,** 7611-5.

GRUBMAN, A., CHOO, X. Y., CHEW, G., OUYANG, J. F., SUN, G., CROFT, N. P., ROSSELLO, F. J., SIMMONS, R., BUCKBERRY, S., LANDIN, D. V., PFLUEGER, J., VANDEKOLK, T. H., ABAY, Z., ZHOU, Y., LIU, X., CHEN, J., LARCOMBE, M., HAYNES, J. M., MCLEAN, C., WILLIAMS, S., CHAI, S. Y., WILSON, T., LISTER, R., POUTON, C. W., PURCELL, A. W., RACKHAM, O. J. L., PETRETTO, E. & POLO, J. M. 2021. Transcriptional signature in microglia associated with A β plaque phagocytosis. *Nature Communications,* 12**,** 3015.

GUÉNIN, S., MAURIAT, M., PELLOUX, J., VAN WUYTSWINKEL, O., BELLINI, C. & GUTIERREZ, L. 2009. Normalization of qRT-PCR data: the necessity of adopting a systematic, experimental conditions-specific, validation of references. *J Exp Bot,* 60**,** 487-93.

GUERREIRO, R., WOJTAS, A., BRAS, J., CARRASQUILLO, M., ROGAEVA, E., MAJOUNIE, E., CRUCHAGA, C., SASSI, C., KAUWE, J. S., YOUNKIN, S., HAZRATI, L., COLLINGE, J., POCOCK, J., LASHLEY, T., WILLIAMS, J., LAMBERT, J. C., AMOUYEL, P., GOATE, A., RADEMAKERS, R., MORGAN, K., POWELL, J., ST GEORGE-HYSLOP, P., SINGLETON, A., HARDY, J. & ALZHEIMER GENETIC ANALYSIS, G. 2013. TREM2 variants in Alzheimer's disease. *N Engl J Med,* 368**,** 117-27.

GUILLOT-SESTIER, M. V., DOTY, K. R., GATE, D., RODRIGUEZ, J., JR., LEUNG, B. P., REZAI-ZADEH, K. & TOWN, T. 2015. Il10 deficiency rebalances innate immunity to mitigate Alzheimer-like pathology. *Neuron,* 85**,** 534-48.

GUO, J. L. & LEE, V. M. 2014. Cell-to-cell transmission of pathogenic proteins in neurodegenerative diseases. *Nat Med,* 20**,** 130-8.

GUO, M., WANG, J., ZHAO, Y., FENG, Y., HAN, S., DONG, Q., CUI, M. & TIEU, K. 2020. Microglial exosomes facilitate α -synuclein transmission in Parkinson's disease. *Brain,* 143**,** 1476-1497.

GUO, Y., WEI, X., YAN, H., QIN, Y., YAN, S., LIU, J., ZHAO, Y., JIANG, F. & LOU, H. 2019. TREM2 deficiency aggravates α -synuclein-induced neurodegeneration and neuroinflammation in Parkinson's disease models. *Faseb j,* 33**,** 12164-12174.

GUTTIKONDA, S. R., SIKKEMA, L., TCHIEU, J., SAURAT, N., WALSH, R. M., HARSCHNITZ, O., CICERI, G., SNEEBOER, M., MAZUTIS, L., SETTY, M., ZUMBO, P., BETEL, D., DE WITTE, L. D., PE'ER, D. & STUDER, L. 2021. Fully defined human pluripotent stem cell-derived microglia and tri-culture system model C3 production in Alzheimer's disease. *Nature Neuroscience,* 24**,** 343-354.

HAENSELER, W., SANSOM, S. N., BUCHRIESER, J., NEWEY, S. E., MOORE, C. S., NICHOLLS, F. J., CHINTAWAR, S., SCHNELL, C., ANTEL, J. P., ALLEN, N. D., CADER, M. Z., WADE-MARTINS, R., JAMES, W. S. & COWLEY, S. A. 2017a. A Highly Efficient Human

Pluripotent Stem Cell Microglia Model Displays a Neuronal-Co-culture-Specific Expression Profile and Inflammatory Response. *Stem Cell Reports,* 8**,** 1727-1742.

HAENSELER, W., ZAMBON, F., LEE, H., VOWLES, J., RINALDI, F., DUGGAL, G., HOULDEN, H., GWINN, K., WRAY, S., LUK, K. C., WADE-MARTINS, R., JAMES, W. S. & COWLEY, S. A. 2017b. Excess alpha-synuclein compromises phagocytosis in iPSC-derived macrophages. *Sci Rep,* 7**,** 9003.

HAENSELER, W., ZAMBON, F., LEE, H., VOWLES, J., RINALDI, F., DUGGAL, G., HOULDEN, H., GWINN, K., WRAY, S., LUK, K. C., WADE-MARTINS, R., JAMES, W. S. & COWLEY, S. A. 2017c. Excess α-synuclein compromises phagocytosis in iPSC-derived macrophages. *Scientific Reports,* 7**,** 9003.

HALL, S., JANELIDZE, S., SUROVA, Y., WIDNER, H., ZETTERBERG, H. & HANSSON, O. 2018. Cerebrospinal fluid concentrations of inflammatory markers in Parkinson's disease and atypical parkinsonian disorders. *Scientific Reports,* 8**,** 13276.

HALL, S., SUROVA, Y., ÖHRFELT, A., BLENNOW, K., ZETTERBERG, H. & HANSSON, O. 2016. Longitudinal Measurements of Cerebrospinal Fluid Biomarkers in Parkinson's Disease. *Mov Disord,* 31**,** 898-905.

HALL-ROBERTS, H., AGARWAL, D., OBST, J., SMITH, T. B., MONZÓN-SANDOVAL, J., DI DANIEL, E., WEBBER, C., JAMES, W. S., MEAD, E., DAVIS, J. B. & COWLEY, S. A. 2020. TREM2 Alzheimer's variant R47H causes similar transcriptional dysregulation to knockout, yet only subtle functional phenotypes in human iPSC-derived macrophages. *Alzheimer's Research & Therapy,* 12**,** 151.

HALLIDAY, G. M., HOLTON, J. L., REVESZ, T. & DICKSON, D. W. 2011. Neuropathology underlying clinical variability in patients with synucleinopathies. *Acta Neuropathol,* 122**,** 187-204.

HALLIDAY, G. M. & MCCANN, H. 2010. The progression of pathology in Parkinson's disease. *Ann N Y Acad Sci,* 1184**,** 188-95.

HALLIDAY, G. M. & STEVENS, C. H. 2011. Glia: initiators and progressors of pathology in Parkinson's disease. *Mov Disord,* 26**,** 6-17.

HANISCH, U. K. & KETTENMANN, H. 2007. Microglia: active sensor and versatile effector cells in the normal and pathologic brain. *Nat Neurosci,* 10**,** 1387-94.

HARTFIELD, E. M., YAMASAKI-MANN, M., RIBEIRO FERNANDES, H. J., VOWLES, J., JAMES, W. S., COWLEY, S. A. & WADE-MARTINS, R. 2014. Physiological characterisation of human iPS-derived dopaminergic neurons. *PLoS One,* 9**,** e87388.

HASSELMANN, J., COBURN, M. A., ENGLAND, W., FIGUEROA VELEZ, D. X., KIANI SHABESTARI, S., TU, C. H., MCQUADE, A., KOLAHDOUZAN, M., ECHEVERRIA, K., CLAES, C., NAKAYAMA, T., AZEVEDO, R., COUFAL, N. G., HAN, C. Z., CUMMINGS, B. J., DAVTYAN, H., GLASS, C. K., HEALY, L. M., GANDHI, S. P., SPITALE, R. C. & BLURTON-JONES, M. 2019. Development of a Chimeric Model to Study and Manipulate Human Microglia In Vivo. *Neuron,* 103**,** 1016-1033.e10.

HAYLEY, S., CROCKER, S. J., SMITH, P. D., SHREE, T., JACKSON-LEWIS, V., PRZEDBORSKI, S., MOUNT, M., SLACK, R., ANISMAN, H. & PARK, D. S. 2004. Regulation of dopaminergic loss by Fas in a 1-methyl-4-phenyl-1,2,3,6-tetrahydropyridine model of Parkinson's disease. *J Neurosci,* 24**,** 2045-53.

HAYNES, S. E., HOLLOPETER, G., YANG, G., KURPIUS, D., DAILEY, M. E., GAN, W. B. & JULIUS, D. 2006. The P2Y12 receptor regulates microglial activation by extracellular nucleotides. *Nat Neurosci,* 9**,** 1512-9.

HEINZ, S., BENNER, C., SPANN, N., BERTOLINO, E., LIN, Y. C., LASLO, P., CHENG, J. X., MURRE, C., SINGH, H. & GLASS, C. K. 2010. Simple combinations of lineage-determining transcription factors prime cis-regulatory elements required for macrophage and B cell identities. *Mol Cell,* 38**,** 576-89.

HELLWIG, K., KVARTSBERG, H., PORTELIUS, E., ANDREASSON, U., OBERSTEIN, T. J., LEWCZUK, P., BLENNOW, K., KORNHUBER, J., MALER, J. M., ZETTERBERG, H. & SPITZER, P. 2015. Neurogranin and YKL-40: independent markers of synaptic degeneration and neuroinflammation in Alzheimer's disease. *Alzheimers Res Ther,* 7**,** 74.

HELY, M. A., REID, W. G., ADENA, M. A., HALLIDAY, G. M. & MORRIS, J. G. 2008. The Sydney multicenter study of Parkinson's disease: the inevitability of dementia at 20 years. *Mov Disord,* 23**,** 837-44.

HEMAN-ACKAH, S. M., MANZANO, R., HOOZEMANS, J. J. M., SCHEPER, W., FLYNN, R., HAERTY, W., COWLEY, S. A., BASSETT, A. R. & WOOD, M. J. A. 2017. Alpha-synuclein induces the unfolded protein response in Parkinson's disease SNCA triplication iPSC-derived neurons. *Hum Mol Genet,* 26**,** 4441-4450.

HENDERSON, M. X., SENGUPTA, M., TROJANOWSKI, J. Q. & LEE, V. M. Y. 2019. Alzheimer's disease tau is a prominent pathology in LRRK2 Parkinson's disease. *Acta Neuropathol Commun,* 7**,** 183.

HENG, T. S., PAINTER, M. W. & IMMUNOLOGICAL GENOME PROJECT, C. 2008. The Immunological Genome Project: networks of gene expression in immune cells. *Nat Immunol,* 9**,** 1091-4.

HICKEY, W. F. & KIMURA, H. 1988. Perivascular microglial cells of the CNS are bone marrow-derived and present antigen in vivo. *Science,* 239**,** 290-2.

HICKEY, W. F., VASS, K. & LASSMANN, H. 1992. Bone marrow-derived elements in the central nervous system: an immunohistochemical and ultrastructural survey of rat chimeras. *J Neuropathol Exp Neurol,* 51**,** 246-56.

HICKMAN, S., IZZY, S., SEN, P., MORSETT, L. & EL KHOURY, J. 2018. Microglia in neurodegeneration. *Nature Neuroscience,* 21**,** 1359-1369.

HICKMAN, S. E., ALLISON, E. K. & EL KHOURY, J. 2008. Microglial dysfunction and defective beta-amyloid clearance pathways in aging Alzheimer's disease mice. *J Neurosci,* 28**,** 8354-60.

HICKMAN, S. E., KINGERY, N. D., OHSUMI, T. K., BOROWSKY, M. L., WANG, L. C., MEANS, T. K. & EL KHOURY, J. 2013. The microglial sensome revealed by direct RNA sequencing. *Nat Neurosci,* 16**,** 1896-905.

HODGE, R. D., BAKKEN, T. E., MILLER, J. A., SMITH, K. A., BARKAN, E. R., GRAYBUCK, L. T., CLOSE, J. L., LONG, B., JOHANSEN, N., PENN, O., YAO, Z., EGGERMONT, J., HÖLLT, T., LEVI, B. P., SHEHATA, S. I., AEVERMANN, B., BELLER, A., BERTAGNOLLI, D., BROUNER, K., CASPER, T., COBBS, C., DALLEY, R., DEE, N., DING, S.-L., ELLENBOGEN, R. G., FONG, O., GARREN, E., GOLDY, J., GWINN, R. P., HIRSCHSTEIN, D., KEENE, C. D., KESHK, M., KO, A. L., LATHIA, K., MAHFOUZ, A., MALTZER, Z., MCGRAW, M., NGUYEN, T. N., NYHUS, J., OJEMANN, J. G., OLDRE, A., PARRY, S., REYNOLDS, S., RIMORIN, C., SHAPOVALOVA, N. V., SOMASUNDARAM, S., SZAFER, A., THOMSEN, E. R., TIEU, M., QUON, G., SCHEUERMANN, R. H., YUSTE, R., SUNKIN, S. M., LELIEVELDT, B., FENG, D., NG, L., BERNARD, A., HAWRYLYCZ, M., PHILLIPS, J. W., TASIC, B., ZENG, H., JONES, A. R., KOCH, C. & LEIN, E. S. 2019. Conserved cell types with divergent features in human versus mouse cortex. *Nature,* 573**,** 61-68.

HOEFFEL, G., CHEN, J., LAVIN, Y., LOW, D., ALMEIDA, F. F., SEE, P., BEAUDIN, A. E., LUM, J., LOW, I., FORSBERG, E. C., POIDINGER, M., ZOLEZZI, F., LARBI, A., NG, L. G., CHAN, J. K., GRETER, M., BECHER, B., SAMOKHVALOV, I. M., MERAD, M. & GINHOUX, F. 2015. C-Myb(+) erythro-myeloid progenitor-derived fetal monocytes give rise to adult tissue-resident macrophages. *Immunity,* 42**,** 665-78.

HOEK, R. M., RUULS, S. R., MURPHY, C. A., WRIGHT, G. J., GODDARD, R., ZURAWSKI, S. M., BLOM, B., HOMOLA, M. E., STREIT, W. J., BROWN, M. H., BARCLAY, A. N. & SEDGWICK, J. D. 2000. Down-regulation of the macrophage lineage through interaction with OX2 (CD200). *Science,* 290**,** 1768-71.

HØJLUND, A., PETERSEN, M. V., SRIDHARAN, K. S. & ØSTERGAARD, K. 2017. Worsening of Verbal Fluency After Deep Brain Stimulation in Parkinson's Disease: A Focused Review. *Comput Struct Biotechnol J,* 15**,** 68-74.

HONG, S., BEJA-GLASSER, V. F., NFONOYIM, B. M., FROUIN, A., LI, S., RAMAKRISHNAN, S., MERRY, K. M., SHI, Q., ROSENTHAL, A., BARRES, B. A., LEMERE, C. A., SELKOE, D. J. & STEVENS, B. 2016. Complement and microglia mediate early synapse loss in Alzheimer mouse models. *Science,* 352**,** 712-716.

HOPP, S. C., LIN, Y., OAKLEY, D., ROE, A. D., DEVOS, S. L., HANLON, D. & HYMAN, B. T. 2018. The role of microglia in processing and spreading of bioactive tau seeds in Alzheimer's disease. *Journal of Neuroinflammation,* 15**,** 269.

HU, X., LEAK, R. K., SHI, Y., SUENAGA, J., GAO, Y., ZHENG, P. & CHEN, J. 2015. Microglial and macrophage polarization—new prospects for brain repair. *Nature Reviews Neurology,* 11**,** 56-64.

HUANG, E. J. & REICHARDT, L. F. 2001. Neurotrophins: roles in neuronal development and function. *Annu Rev Neurosci,* 24**,** 677-736.

HUH, C. J., ZHANG, B., VICTOR, M. B., DAHIYA, S., BATISTA, L. F., HORVATH, S. & YOO, A. S. 2016. Maintenance of age in human neurons generated by microRNA-based neuronal conversion of fibroblasts. *Elife,* 5.

HUME, D. A., PERRY, V. H. & GORDON, S. 1983. Immunohistochemical localization of a macrophage-specific antigen in developing mouse retina: phagocytosis of dying neurons and differentiation of microglial cells to form a regular array in the plexiform layers. *The Journal of cell biology,* 97**,** 253-257.

HUNG, J. J., ZENO, W. F., CHOWDHURY, A. A., DEAR, B. J., RAMACHANDRAN, K., NIETO, M. P., SHAY, T. Y., KAROUTA, C. A., HAYDEN, C. C., CHEUNG, J. K., TRUSKETT, T. M., STACHOWIAK, J. C. & JOHNSTON, K. P. 2019. Self-diffusion of a highly concentrated monoclonal antibody by fluorescence correlation spectroscopy: insight into protein–protein interactions and self-association. *Soft Matter,* 15**,** 6660-6676.

IBÁÑEZ, P., BONNET, A. M., DÉBARGES, B., LOHMANN, E., TISON, F., POLLAK, P., AGID, Y., DÜRR, A. & BRICE, A. 2004. Causal relation between alpha-synuclein gene duplication and familial Parkinson's disease. *Lancet,* 364**,** 1169-71.

ISHII, T., HAGA, S. & TOKUTAKE, S. 1979. Presence of neurofilament protein in Alzheimer's neurofibrillary tangles (ANT). An immunofluorescent study. *Acta Neuropathol,* 48**,** 105-12.

JAKES, R., SPILLANTINI, M. G. & GOEDERT, M. 1994. Identification of two distinct synucleins from human brain. *FEBS Lett,* 345**,** 27-32.

JANELIDZE, S., LINDQVIST, D., FRANCARDO, V., HALL, S., ZETTERBERG, H., BLENNOW, K., ADLER, C. H., BEACH, T. G., SERRANO, G. E., VAN WESTEN, D., LONDOS, E., CENCI, M.

A. & HANSSON, O. 2015. Increased CSF biomarkers of angiogenesis in Parkinson disease. *Neurology,* 85**,** 1834-1842.

JANEWAY, C. A., JR. 1989. Approaching the asymptote? Evolution and revolution in immunology. *Cold Spring Harb Symp Quant Biol,* 54 Pt 1**,** 1-13.

JAO, C. C., DER-SARKISSIAN, A., CHEN, J. & LANGEN, R. 2004. Structure of membrane-bound α-synuclein studied by site-directed spin labeling. *Proceedings of the National Academy of Sciences,* 101**,** 8331-8336.

JELLINGER, K. A. 2010. Synucleinopathies. *In:* KOMPOLITI, K. & METMAN, L. V. (eds.) *Encyclopedia of Movement Disorders.* Oxford: Academic Press.

JEONG, S. H., CHUNG, S. J., YOO, H. S., HONG, N., JUNG, J. H., BAIK, K., LEE, Y. H., SOHN, Y. H. & LEE, P. H. 2021. Beneficial effects of dipeptidyl peptidase-4 inhibitors in diabetic Parkinson's disease. *Brain,* 144**,** 1127-1137.

JOERS, V., TANSEY, M. G., MULAS, G. & CARTA, A. R. 2017. Microglial phenotypes in Parkinson's disease and animal models of the disease. *Progress in neurobiology,* 155**,** 57-75.

JOKINEN, P., BRÜCK, A., AALTO, S., FORSBACK, S., PARKKOLA, R. & RINNE, J. O. 2009. Impaired cognitive performance in Parkinson's disease is related to caudate dopaminergic hypofunction and hippocampal atrophy. *Parkinsonism Relat Disord,* 15**,** 88-93.

JONIKAS, M., MADILL, M., MATHY, A., ZEKOLL, T., ZOIS, C. E., WIGFIELD, S., KURZAWA-AKANBI, M., BROWNE, C., SIMS, D., CHINNERY, P. F., COWLEY, S. A. & TOFARIS, G. K. 2018. Stem cell modeling of mitochondrial parkinsonism reveals key functions of OPA1. *Ann Neurol,* 83**,** 915-925.

JUCKER, M. & WALKER, L. C. 2013. Self-propagation of pathogenic protein aggregates in neurodegenerative diseases. *Nature,* 501**,** 45-51.

JUCKER, M. & WALKER, L. C. 2018. Propagation and spread of pathogenic protein assemblies in neurodegenerative diseases. *Nat Neurosci,* 21**,** 1341-1349.

JURGA, A. M., PALECZNA, M. & KUTER, K. Z. 2020. Overview of General and Discriminating Markers of Differential Microglia Phenotypes. *Frontiers in Cellular Neuroscience,* 14.

KALIA, L. V., LANG, A. E., HAZRATI, L. N., FUJIOKA, S., WSZOLEK, Z. K., DICKSON, D. W., ROSS, O. A., VAN DEERLIN, V. M., TROJANOWSKI, J. Q., HURTIG, H. I., ALCALAY, R. N., MARDER, K. S., CLARK, L. N., GAIG, C., TOLOSA, E., RUIZ-MARTÍNEZ, J., MARTI-MASSO, J. F., FERRER, I., LÓPEZ DE MUNAIN, A., GOLDMAN, S. M., SCHÜLE, B., LANGSTON, J. W., AASLY, J. O., GIORDANA, M. T., BONIFATI, V., PUSCHMANN, A., CANESI, M., PEZZOLI, G., MAUES DE PAULA, A., HASEGAWA, K., DUYCKAERTS, C., BRICE, A., STOESSL, A. J. & MARRAS, C. 2015. Clinical correlations with Lewy body pathology in LRRK2-related Parkinson disease. *JAMA Neurol,* 72**,** 100-5.

KARLSSON, K. R., COWLEY, S., MARTINEZ, F. O., SHAW, M., MINGER, S. L. & JAMES, W. 2008. Homogeneous monocytes and macrophages from human embryonic stem cells following coculture-free differentiation in M-CSF and IL-3. *Exp Hematol,* 36**,** 1167-75.

KARPOWICZ, R. J., JR., TROJANOWSKI, J. Q. & LEE, V. M. Y. 2019. Transmission of α-synuclein seeds in neurodegenerative disease: recent developments. *Laboratory investigation; a journal of technical methods and pathology,* 99**,** 971-981.

KATSIKOUDI, A., FICULLE, E., CAVALLINI, A., SHARMAN, G., GUYOT, A., ZAGNONI, M., EASTWOOD, B. J., HUTTON, M. & BOSE, S. 2020. Quantitative propagation of assembled human Tau from Alzheimer's disease brain in microfluidic neuronal cultures. *J Biol Chem,* 295**,** 13079-13093.

KAVSAK, P., RASMUSSEN, R. K., CAUSING, C. G., BONNI, S., ZHU, H., THOMSEN, G. H. & WRANA, J. L. 2000. Smad7 binds to Smurf2 to form an E3 ubiquitin ligase that targets the TGF beta receptor for degradation. *Mol Cell,* 6**,** 1365-75.

KENNEDY, D. W. & ABKOWITZ, J. L. 1997. Kinetics of central nervous system microglial and macrophage engraftment: analysis using a transgenic bone marrow transplantation model. *Blood,* 90**,** 986-93.

KEREN-SHAUL, H., SPINRAD, A., WEINER, A., MATCOVITCH-NATAN, O., DVIR-SZTERNFELD, R., ULLAND, T. K., DAVID, E., BARUCH, K., LARA-ASTAISO, D., TOTH, B., ITZKOVITZ, S., COLONNA, M., SCHWARTZ, M. & AMIT, I. 2017. A Unique Microglia Type Associated with Restricting Development of Alzheimer's Disease. *Cell,* 169**,** 1276-1290.e17.

KERKHOFS, A., XAVIER, A. C., DA SILVA, B. S., CANAS, P. M., IDEMA, S., BAAYEN, J. C., FERREIRA, S. G., CUNHA, R. A. & MANSVELDER, H. D. 2018. Caffeine Controls Glutamatergic Synaptic Transmission and Pyramidal Neuron Excitability in Human Neocortex. *Frontiers in Pharmacology,* 8.

KIELY, A. P., ASI, Y. T., KARA, E., LIMOUSIN, P., LING, H., LEWIS, P., PROUKAKIS, C., QUINN, N., LEES, A. J., HARDY, J., REVESZ, T., HOULDEN, H. & HOLTON, J. L. 2013. α-Synucleinopathy associated with G51D SNCA mutation: a link between Parkinson's disease and multiple system atrophy? *Acta Neuropathol,* 125**,** 753-69.

KIERDORF, K., ERNY, D., GOLDMANN, T., SANDER, V., SCHULZ, C., PERDIGUERO, E. G., WIEGHOFER, P., HEINRICH, A., RIEMKE, P., HOLSCHER, C., MULLER, D. N., LUCKOW, B., BROCKER, T., DEBOWSKI, K., FRITZ, G., OPDENAKKER, G., DIEFENBACH, A., BIBER, K., HEIKENWALDER, M., GEISSMANN, F., ROSENBAUER, F. & PRINZ, M. 2013a. Microglia emerge from erythromyeloid precursors via Pu.1- and Irf8-dependent pathways. *Nat Neurosci,* 16**,** 273-80.

KIERDORF, K., ERNY, D., GOLDMANN, T., SANDER, V., SCHULZ, C., PERDIGUERO, E. G., WIEGHOFER, P., HEINRICH, A., RIEMKE, P., HÖLSCHER, C., MÜLLER, D. N., LUCKOW, B., BROCKER, T., DEBOWSKI, K., FRITZ, G., OPDENAKKER, G., DIEFENBACH, A., BIBER, K., HEIKENWALDER, M., GEISSMANN, F., ROSENBAUER, F. & PRINZ, M. 2013b. Microglia emerge from erythromyeloid precursors via Pu.1- and Irf8-dependent pathways. *Nat Neurosci,* 16**,** 273-80.

KIM, B. W., JEONG, K. H., KIM, J. H., JIN, M., KIM, J. H., LEE, M. G., CHOI, D. K., WON, S. Y., MCLEAN, C., JEON, M. T., LEE, H. W., KIM, S. R. & SUK, K. 2016. Pathogenic Upregulation of Glial Lipocalin-2 in the Parkinsonian Dopaminergic System. *J Neurosci,* 36**,** 5608-22.

KIM, C., HO, D.-H., SUK, J.-E., YOU, S., MICHAEL, S., KANG, J., JOONG LEE, S., MASLIAH, E., HWANG, D., LEE, H.-J. & LEE, S.-J. 2013. Neuron-released oligomeric α-synuclein is an endogenous agonist of TLR2 for paracrine activation of microglia. *Nature Communications,* 4**,** 1562.

KIM, W. G., MOHNEY, R. P., WILSON, B., JEOHN, G. H., LIU, B. & HONG, J. S. 2000. Regional difference in susceptibility to lipopolysaccharide-induced neurotoxicity in the rat brain: role of microglia. *J Neurosci,* 20**,** 6309-16.

KITADA, T., ASAKAWA, S., HATTORI, N., MATSUMINE, H., YAMAMURA, Y., MINOSHIMA, S., YOKOCHI, M., MIZUNO, Y. & SHIMIZU, N. 1998. Mutations in the parkin gene cause autosomal recessive juvenile parkinsonism. *Nature,* 392**,** 605-8.

KONISHI, H. & KIYAMA, H. 2018. Microglial TREM2/DAP12 Signaling: A Double-Edged Sword in Neural Diseases. *Frontiers in Cellular Neuroscience,* 12.

KONISHI, H. & KIYAMA, H. 2020. Non-pathological roles of microglial TREM2/DAP12: TREM2/DAP12 regulates the physiological functions of microglia from development to aging. *Neurochemistry International,* 141**,** 104878.

KRASEMANN, S., MADORE, C., CIALIC, R., BAUFELD, C., CALCAGNO, N., EL FATIMY, R., BECKERS, L., O'LOUGHLIN, E., XU, Y., FANEK, Z., GRECO, D. J., SMITH, S. T., TWEET, G., HUMULOCK, Z., ZRZAVY, T., CONDE-SANROMAN, P., GACIAS, M., WENG, Z., CHEN, H., TJON, E., MAZAHERI, F., HARTMANN, K., MADI, A., ULRICH, J. D., GLATZEL, M., WORTHMANN, A., HEEREN, J., BUDNIK, B., LEMERE, C., IKEZU, T., HEPPNER, F. L., LITVAK, V., HOLTZMAN, D. M., LASSMANN, H., WEINER, H. L., OCHANDO, J., HAASS, C. & BUTOVSKY, O. 2017a. The TREM2-APOE Pathway Drives the Transcriptional Phenotype of Dysfunctional Microglia in Neurodegenerative Diseases. *Immunity,* 47**,** 566-581.e9.

KRASEMANN, S., MADORE, C., CIALIC, R., BAUFELD, C., CALCAGNO, N., EL FATIMY, R., BECKERS, L., O'LOUGHLIN, E., XU, Y. & FANEK, Z. 2017b. The TREM2-APOE pathway drives the transcriptional phenotype of dysfunctional microglia in neurodegenerative diseases. *Immunity,* 47**,** 566-581. e9.

KRIKS, S., SHIM, J.-W., PIAO, J., GANAT, Y. M., WAKEMAN, D. R., XIE, Z., CARRILLO-REID, L., AUYEUNG, G., ANTONACCI, C., BUCH, A., YANG, L., BEAL, M. F., SURMEIER, D. J., KORDOWER, J. H., TABAR, V. & STUDER, L. 2011. Dopamine neurons derived from human ES cells efficiently engraft in animal models of Parkinson's disease. *Nature,* 480**,** 547-551.

KRÜGER, R., KUHN, W., MÜLLER, T., WOITALLA, D., GRAEBER, M., KÖSEL, S., PRZUNTEK, H., EPPLEN, J. T., SCHÖLS, L. & RIESS, O. 1998. Ala30Pro mutation in the gene encoding alpha-synuclein in Parkinson's disease. *Nat Genet,* 18**,** 106-8.

KRUMOVA, P., MEULMEESTER, E., GARRIDO, M., TIRARD, M., HSIAO, H. H., BOSSIS, G., URLAUB, H., ZWECKSTETTER, M., KÜGLER, S., MELCHIOR, F., BÄHR, M. & WEISHAUPT, J. H. 2011. Sumoylation inhibits alpha-synuclein aggregation and toxicity. *J Cell Biol,* 194**,** 49-60.

KUPSCH, A., OERTEL, W. H., EARL, C. D. & SAUTTER, J. 1995. Neuronal transplantation and neurotrophic factors in the treatment of Parkinson's disease--update February 1995. *J Neural Transm Suppl,* 46**,** 193-207.

KUUSISTO, E., PARKKINEN, L. & ALAFUZOFF, I. 2003. Morphogenesis of Lewy bodies: dissimilar incorporation of alpha-synuclein, ubiquitin, and p62. *J Neuropathol Exp Neurol,* 62**,** 1241-53.

LAGERKVIST, A. C., FÖLDES-PAPP, Z., PERSSON, M. A. & RIGLER, R. 2001. Fluorescence correlation spectroscopy as a method for assessment of interactions between phage displaying antibodies and soluble antigen. *Protein Sci,* 10**,** 1522-8.

LAMBERT, J. C., IBRAHIM-VERBAAS, C. A., HAROLD, D., NAJ, A. C., SIMS, R., BELLENGUEZ, C., DESTAFANO, A. L., BIS, J. C., BEECHAM, G. W., GRENIER-BOLEY, B., RUSSO, G., THORTON-WELLS, T. A., JONES, N., SMITH, A. V., CHOURAKI, V., THOMAS, C., IKRAM, M. A., ZELENIKA, D., VARDARAJAN, B. N., KAMATANI, Y., LIN, C. F., GERRISH, A., SCHMIDT, H., KUNKLE, B., DUNSTAN, M. L., RUIZ, A., BIHOREAU, M. T., CHOI, S. H., REITZ, C., PASQUIER, F., CRUCHAGA, C., CRAIG, D., AMIN, N., BERR, C., LOPEZ, O. L., DE JAGER, P. L., DERAMECOURT, V., JOHNSTON, J. A., EVANS, D., LOVESTONE, S., LETENNEUR, L., MORÓN, F. J., RUBINSZTEIN, D. C., EIRIKSDOTTIR, G., SLEEGERS, K., GOATE, A. M., FIÉVET, N., HUENTELMAN, M. W., GILL, M., BROWN, K., KAMBOH, M. I., KELLER, L., BARBERGER-GATEAU, P., MCGUINESS, B., LARSON, E. B., GREEN, R.,

MYERS, A. J., DUFOUIL, C., TODD, S., WALLON, D., LOVE, S., ROGAEVA, E., GALLACHER, J., ST GEORGE-HYSLOP, P., CLARIMON, J., LLEO, A., BAYER, A., TSUANG, D. W., YU, L., TSOLAKI, M., BOSSÙ, P., SPALLETTA, G., PROITSI, P., COLLINGE, J., SORBI, S., SANCHEZ-GARCIA, F., FOX, N. C., HARDY, J., DENIZ NARANJO, M. C., BOSCO, P., CLARKE, R., BRAYNE, C., GALIMBERTI, D., MANCUSO, M., MATTHEWS, F., MOEBUS, S., MECOCCI, P., DEL ZOMPO, M., MAIER, W., HAMPEL, H., PILOTTO, A., BULLIDO, M., PANZA, F., CAFFARRA, P., NACMIAS, B., GILBERT, J. R., MAYHAUS, M., LANNEFELT, L., HAKONARSON, H., PICHLER, S., et al. 2013. Meta-analysis of 74,046 individuals identifies 11 new susceptibility loci for Alzheimer's disease. *Nat Genet,* 45**,** 1452-8.

LANG, C., CAMPBELL, K. R., RYAN, B. J., CARLING, P., ATTAR, M., VOWLES, J., PERESTENKO, O. V., BOWDEN, R., BAIG, F., KASTEN, M., HU, M. T., COWLEY, S. A., WEBBER, C. & WADE-MARTINS, R. 2019. Single-Cell Sequencing of iPSC-Dopamine Neurons Reconstructs Disease Progression and Identifies HDAC4 as a Regulator of Parkinson Cell Phenotypes. *Cell Stem Cell,* 24**,** 93-106 e6.

LAUBER, K., BLUMENTHAL, S. G., WAIBEL, M. & WESSELBORG, S. 2004. Clearance of apoptotic cells: getting rid of the corpses. *Mol Cell,* 14**,** 277-87.

LAWSON, L. J., PERRY, V. H., DRI, P. & GORDON, S. 1990. Heterogeneity in the distribution and morphology of microglia in the normal adult mouse brain. *Neuroscience,* 39**,** 151-70.

LEE, G., TANAKA, M., PARK, K., LEE, S. S., KIM, Y. M., JUNN, E., LEE, S.-H. & MOURADIAN, M. M. 2004. Casein Kinase II-mediated Phosphorylation Regulates α-Synuclein/Synphilin-1 Interaction and Inclusion Body Formation*. *Journal of Biological Chemistry,* 279**,** 6834-6839.

LEE, H., FLYNN, R., SHARMA, I., HABERMAN, E., CARLING, P. J., NICHOLLS, F. J., STEGMANN, M., VOWLES, J., HAENSELER, W., WADE-MARTINS, R., JAMES, W. S. & COWLEY, S. A. 2020. LRRK2 Is Recruited to Phagosomes and Co-recruits RAB8 and RAB10 in Human Pluripotent Stem Cell-Derived Macrophages. *Stem cell reports,* 14**,** 940-955.

LEE, K. W., CHEN, W., JUNN, E., IM, J. Y., GROSSO, H., SONSALLA, P. K., FENG, X., RAY, N., FERNANDEZ, J. R., CHAO, Y., MASLIAH, E., VORONKOV, M., BRAITHWAITE, S. P., STOCK, J. B. & MOURADIAN, M. M. 2011a. Enhanced phosphatase activity attenuates α-synucleinopathy in a mouse model. *J Neurosci,* 31**,** 6963-71.

LEE, M. K., STIRLING, W., XU, Y., XU, X., QUI, D., MANDIR, A. S., DAWSON, T. M., COPELAND, N. G., JENKINS, N. A. & PRICE, D. L. 2002. Human alpha-synuclein-harboring familial Parkinson's disease-linked Ala-53 --> Thr mutation causes neurodegenerative disease with alpha-synuclein aggregation in transgenic mice. *Proc Natl Acad Sci U S A,* 99**,** 8968-73.

LEE, S., LEE, W. H., LEE, M. S., MORI, K. & SUK, K. 2012. Regulation by lipocalin-2 of neuronal cell death, migration, and morphology. *J Neurosci Res,* 90**,** 540-50.

LEE, Y. S., PARK, J. S., KIM, J. H., JUNG, S. M., LEE, J. Y., KIM, S.-J. & PARK, S. H. 2011b. Smad6-specific recruitment of Smurf E3 ligases mediates TGF-β1-induced degradation of MyD88 in TLR4 signalling. *Nature Communications,* 2**,** 460.

LEES, A. J., HARDY, J. & REVESZ, T. 2009. Parkinson's disease. *Lancet,* 373**,** 2055-66.

LEMKE, G. 2017. Phosphatidylserine Is the Signal for TAM Receptors and Their Ligands. *Trends Biochem Sci,* 42**,** 738-748.

LESAGE, S., ANHEIM, M., LETOURNEL, F., BOUSSET, L., HONORÉ, A., ROZAS, N., PIERI, L., MADIONA, K., DÜRR, A., MELKI, R., VERNY, C. & BRICE, A. 2013. G51D α-synuclein mutation causes a novel parkinsonian-pyramidal syndrome. *Ann Neurol,* 73**,** 459-71.

LESAGE, S. & BRICE, A. 2009. Parkinson's disease: from monogenic forms to genetic susceptibility factors. *Hum Mol Genet,* 18**,** R48-59.

LEYH, J., PAESCHKE, S., MAGES, B., MICHALSKI, D., NOWICKI, M., BECHMANN, I. & WINTER, K. 2021. Classification of Microglial Morphological Phenotypes Using Machine Learning. *Frontiers in Cellular Neuroscience,* 15.

LI, B., GE, P., MURRAY, K. A., SHETH, P., ZHANG, M., NAIR, G., SAWAYA, M. R., SHIN, W. S., BOYER, D. R., YE, S., EISENBERG, D. S., ZHOU, Z. H. & JIANG, L. 2018. Cryo-EM of full-length α-synuclein reveals fibril polymorphs with a common structural kernel. *Nature Communications,* 9**,** 3609.

LI, J.-Q., TAN, L. & YU, J.-T. 2014a. The role of the LRRK2 gene in Parkinsonism. *Molecular neurodegeneration,* 9**,** 47-47.

LI, J.-Y., ENGLUND, E., HOLTON, J. L., SOULET, D., HAGELL, P., LEES, A. J., LASHLEY, T., QUINN, N. P., REHNCRONA, S., BJÖRKLUND, A., WIDNER, H., REVESZ, T., LINDVALL, O. & BRUNDIN, P. 2008. Lewy bodies in grafted neurons in subjects with Parkinson's disease suggest host-to-graft disease propagation. *Nature Medicine,* 14**,** 501-503.

LI, J. Q., TAN, L. & YU, J. T. 2014b. The role of the LRRK2 gene in Parkinsonism. *Mol Neurodegener,* 9**,** 47.

LI, S., LU, K., WANG, J., AN, L., YANG, G., CHEN, H., CUI, Y., YIN, X., XIE, P., XING, G., HE, F. & ZHANG, L. 2010. Ubiquitin ligase Smurf1 targets TRAF family proteins for ubiquitination and degradation. *Mol Cell Biochem,* 338**,** 11-7.

LIAO, Y. F., WANG, B. J., CHENG, H. T., KUO, L. H. & WOLFE, M. S. 2004. Tumor necrosis factor-alpha, interleukin-1beta, and interferon-gamma stimulate gamma-secretase-mediated cleavage of amyloid precursor protein through a JNK-dependent MAPK pathway. *J Biol Chem,* 279**,** 49523-32.

LIN, S., LIN, Y., NERY, J. R., URICH, M. A., BRESCHI, A., DAVIS, C. A., DOBIN, A., ZALESKI, C., BEER, M. A., CHAPMAN, W. C., GINGERAS, T. R., ECKER, J. R. & SNYDER, M. P. 2014. Comparison of the transcriptional landscapes between human and mouse tissues. *Proc Natl Acad Sci U S A,* 111**,** 17224-9.

LINDESTAM ARLEHAMN, C. S., DHANWANI, R., PHAM, J., KUAN, R., FRAZIER, A., REZENDE DUTRA, J., PHILLIPS, E., MALLAL, S., ROEDERER, M., MARDER, K. S., AMARA, A. W., STANDAERT, D. G., GOLDMAN, J. G., LITVAN, I., PETERS, B., SULZER, D. & SETTE, A. 2020. α-Synuclein-specific T cell reactivity is associated with preclinical and early Parkinson's disease. *Nat Commun,* 11**,** 1875.

LINDQVIST, D., HALL, S., SUROVA, Y., NIELSEN, H. M., JANELIDZE, S., BRUNDIN, L. & HANSSON, O. 2013. Cerebrospinal fluid inflammatory markers in Parkinson's disease--associations with depression, fatigue, and cognitive impairment. *Brain Behav Immun,* 33**,** 183-9.

LISMAN, J. E. & GRACE, A. A. 2005. The hippocampal-VTA loop: controlling the entry of information into long-term memory. *Neuron,* 46**,** 703-13.

LIU, D., GUO, J.-J., SU, J.-H., SVANBERGSSON, A., YUAN, L., HAIKAL, C., LI, W., GOURAS, G. & LI, J.-Y. 2021. Differential seeding and propagating efficiency of α-synuclein strains generated in different conditions. *Translational Neurodegeneration,* 10**,** 20.

LOBO-SILVA, D., CARRICHE, G. M., CASTRO, A. G., ROQUE, S. & SARAIVA, M. 2017. Interferon-β regulates the production of IL-10 by toll-like receptor-activated microglia. *Glia,* 65**,** 1439-1451.

LOPES, K. D. P., SNIJDERS, G. J. L., HUMPHREY, J., ALLAN, A., SNEEBOER, M. A. M., NAVARRO, E., SCHILDER, B. M., VIALLE, R. A., PARKS, M., MISSALL, R., VAN ZUIDEN, W., GIGASE,

F. A. J., KÜBLER, R., VAN BERLEKOM, A. B., HICKS, E. M., BÖTTCHER, C., PRILLER, J., KAHN, R. S., DE WITTE, L. D. & RAJ, T. 2022. Genetic analysis of the human microglial transcriptome across brain regions, aging and disease pathologies. *Nature Genetics,* 54**,** 4-17.

LORENZL, S., CALINGASAN, N., YANG, L., ALBERS, D. S., SHUGAMA, S., GREGORIO, J., KRELL, H. W., CHIRICHIGNO, J., JOH, T. & BEAL, M. F. 2004. Matrix metalloproteinase-9 is elevated in 1-methyl-4-phenyl-1,2,3,6-tetrahydropyridine-induced parkinsonism in mice. *Neuromolecular Med,* 5**,** 119-32.

LOVE, M. I., HUBER, W. & ANDERS, S. 2014. Moderated estimation of fold change and dispersion for RNA-seq data with DESeq2. *Genome Biology,* 15**,** 550.

LOZANO, A. M. & SNYDER, B. J. 2008. Deep brain stimulation for parkinsonian gait disorders. *J Neurol,* 255 Suppl 4**,** 30-1.

LOZANO, A. M., SNYDER, B. J., HAMANI, C., HUTCHISON, W. D. & DOSTROVSKY, J. O. 2010. Basal ganglia physiology and deep brain stimulation. *Mov Disord,* 25 Suppl 1**,** S71-5.

LUK, K. C., KEHM, V., CARROLL, J., ZHANG, B., O'BRIEN, P., TROJANOWSKI, J. Q. & LEE, V. M. Y. 2012a. Pathological α-synuclein transmission initiates Parkinson-like neurodegeneration in nontransgenic mice. *Science (New York, N.Y.),* 338**,** 949-953.

LUK, K. C., KEHM, V. M., ZHANG, B., O'BRIEN, P., TROJANOWSKI, J. Q. & LEE, V. M. 2012b. Intracerebral inoculation of pathological alpha-synuclein initiates a rapidly progressive neurodegenerative alpha-synucleinopathy in mice. *J Exp Med,* 209**,** 975-86.

LUK, K. C., KEHM, V. M., ZHANG, B., O'BRIEN, P., TROJANOWSKI, J. Q. & LEE, V. M. 2012c. Intracerebral inoculation of pathological α-synuclein initiates a rapidly progressive neurodegenerative α-synucleinopathy in mice. *J Exp Med,* 209**,** 975-86.

LUK, K. C., SONG, C., O'BRIEN, P., STIEBER, A., BRANCH, J. R., BRUNDEN, K. R., TROJANOWSKI, J. Q. & LEE, V. M. 2009. Exogenous alpha-synuclein fibrils seed the formation of Lewy body-like intracellular inclusions in cultured cells. *Proc Natl Acad Sci U S A,* 106**,** 20051-6.

LUO, F., LUO, S., QIAN, W., ZHANG, L., CHEN, C., XU, M., WANG, G., WANG, Z., WANG, J. & WANG, W. 2020. Developmental deficits and early signs of neurodegeneration revealed by PD patient derived dopamine neurons. *Stem Cell Research,* 49**,** 102027.

MA, S. X., SEO, B. A., KIM, D., XIONG, Y., KWON, S. H., BRAHMACHARI, S., KIM, S., KAM, T. I., NIRUJOGI, R. S., KWON, S. H., DAWSON, V. L., DAWSON, T. M., PANDEY, A., NA, C. H. & KO, H. S. 2021. Complement and Coagulation Cascades are Potentially Involved in Dopaminergic Neurodegeneration in α-Synuclein-Based Mouse Models of Parkinson's Disease. *J Proteome Res,* 20**,** 3428-3443.

MACKANESS, G. B. 1962. Cellular resistance to infection. *J Exp Med,* 116**,** 381-406.

MANTOVANI, A., SICA, A., SOZZANI, S., ALLAVENA, P., VECCHI, A. & LOCATI, M. 2004. The chemokine system in diverse forms of macrophage activation and polarization. *Trends Immunol,* 25**,** 677-86.

MANZONI, C. 2017. The LRRK2-macroautophagy axis and its relevance to Parkinson's disease. *Biochem Soc Trans,* 45**,** 155-162.

MARKER, D. F., PUCCINI, J. M., MOCKUS, T. E., BARBIERI, J., LU, S. M. & GELBARD, H. A. 2012. LRRK2 kinase inhibition prevents pathological microglial phagocytosis in response to HIV-1 Tat protein. *J Neuroinflammation,* 9**,** 261.

MAROTEAUX, L., CAMPANELLI, J. T. & SCHELLER, R. H. 1988. Synuclein: a neuron-specific protein localized to the nucleus and presynaptic nerve terminal. *J Neurosci,* 8**,** 2804-15.

MARSH, S. E., KAMATH, T., WALKER, A. J., DISSING-OLESEN, L., HAMMOND, T. R., YOUNG, A. M. H., ABDULRAOUF, A., NADAF, N., DUFORT, C., MURPHY, S., KOZAREVA, V., VANDERBURG, C., HONG, S., BULSTRODE, H., HUTCHINSON, P. J., GAFFNEY, D. J., FRANKLIN, R. J. M., MACOSKO, E. Z. & STEVENS, B. 2020. Single Cell Sequencing Reveals Glial Specific Responses to Tissue Processing & Enzymatic Dissociation in Mice and Humans. *bioRxiv*, 2020.12.03.408542.

MARTINEZ, F. O., SICA, A., MANTOVANI, A. & LOCATI, M. 2008. Macrophage activation and polarization. *Front Biosci,* 13**,** 453-61.

MARTINEZ-MARTIN, P., RODRIGUEZ-BLAZQUEZ, C., KURTIS, M. M. & CHAUDHURI, K. R. 2011. The impact of non-motor symptoms on health-related quality of life of patients with Parkinson's disease. *Mov Disord,* 26**,** 399-406.

MASSENGALE, M., WAGERS, A. J., VOGEL, H. & WEISSMAN, I. L. 2005. Hematopoietic cells maintain hematopoietic fates upon entering the brain. *The Journal of experimental medicine,* 201**,** 1579-1589.

MASUDA-SUZUKAKE, M., NONAKA, T., HOSOKAWA, M., OIKAWA, T., ARAI, T., AKIYAMA, H., MANN, D. M. & HASEGAWA, M. 2013. Prion-like spreading of pathological α-synuclein in brain. *Brain,* 136**,** 1128-38.

MATCOVITCH-NATAN, O., WINTER, D. R., GILADI, A., VARGAS AGUILAR, S., SPINRAD, A., SARRAZIN, S., BEN-YEHUDA, H., DAVID, E., ZELADA GONZÁLEZ, F., PERRIN, P., KEREN-SHAUL, H., GURY, M., LARA-ASTAISO, D., THAISS, C. A., COHEN, M., BAHAR HALPERN, K., BARUCH, K., DECZKOWSKA, A., LORENZO-VIVAS, E., ITZKOVITZ, S., ELINAV, E., SIEWEKE, M. H., SCHWARTZ, M. & AMIT, I. 2016. Microglia development follows a stepwise program to regulate brain homeostasis. *Science,* 353**,** aad8670.

MATHYS, H., ADAIKKAN, C., GAO, F., YOUNG, J. Z., MANET, E., HEMBERG, M., DE JAGER, P. L., RANSOHOFF, R. M., REGEV, A. & TSAI, L. H. 2017. Temporal Tracking of Microglia Activation in Neurodegeneration at Single-Cell Resolution. *Cell Rep,* 21**,** 366-380.

MATSUOKA, Y., PICCIANO, M., MALESTER, B., LAFRANCOIS, J., ZEHR, C., DAESCHNER, J. M., OLSCHOWKA, J. A., FONSECA, M. I., O'BANION, M. K., TENNER, A. J., LEMERE, C. A. & DUFF, K. 2001. Inflammatory responses to amyloidosis in a transgenic mouse model of Alzheimer's disease. *Am J Pathol,* 158**,** 1345-54.

MATZINGER, P. 1994. Tolerance, danger, and the extended family. *Annu Rev Immunol,* 12**,** 991-1045.

MBEFO, M. K., PALEOLOGOU, K. E., BOUCHARABA, A., OUESLATI, A., SCHELL, H., FOURNIER, M., OLSCHEWSKI, D., YIN, G., ZWECKSTETTER, M., MASLIAH, E., KAHLE, P. J., HIRLING, H. & LASHUEL, H. A. 2010. Phosphorylation of synucleins by members of the Polo-like kinase family. *J Biol Chem,* 285**,** 2807-22.

MCCARTHY, J. M., VIRDEE, J., BROWN, J., URSU, D., AHMED, Z., CAVALLINI, A. & NUTHALL, H. N. 2021. Development of P301S tau seeded organotypic hippocampal slice cultures to study potential therapeutics. *Scientific Reports,* 11**,** 10309.

MCGEER, P. L. & MCGEER, E. G. 1998. Mechanisms of cell death in Alzheimer disease--immunopathology. *J Neural Transm Suppl,* 54**,** 159-66.

MCGEER, P. L. & MCGEER, E. G. 2008. Glial reactions in Parkinson's disease. *Mov Disord,* 23**,** 474-83.

MCGEER, P. L., SCHWAB, C., PARENT, A. & DOUDET, D. 2003. Presence of reactive microglia in monkey substantia nigra years after 1-methyl-4-phenyl-1,2,3,6-tetrahydropyridine administration. *Ann Neurol,* 54**,** 599-604.

MCKERCHER, S. R., TORBETT, B. E., ANDERSON, K. L., HENKEL, G. W., VESTAL, D. J., BARIBAULT, H., KLEMSZ, M., FEENEY, A. J., WU, G. E., PAIGE, C. J. & MAKI, R. A. 1996. Targeted disruption of the PU.1 gene results in multiple hematopoietic abnormalities. *Embo j,* 15**,** 5647-58.

MCKINNON, R. D., PIRAS, G., IDA, J. A., JR. & DUBOIS-DALCQ, M. 1993. A role for TGF-beta in oligodendrocyte differentiation. *J Cell Biol,* 121**,** 1397-407.

MILDNER, A., SCHMIDT, H., NITSCHE, M., MERKLER, D., HANISCH, U. K., MACK, M., HEIKENWALDER, M., BRÜCK, W., PRILLER, J. & PRINZ, M. 2007. Microglia in the adult brain arise from Ly-6ChiCCR2+ monocytes only under defined host conditions. *Nat Neurosci,* 10**,** 1544-53.

MILLER, F. D. & KAPLAN, D. R. 2001. Neurotrophin signalling pathways regulating neuronal apoptosis. *Cell Mol Life Sci,* 58**,** 1045-53.

MILLER, J. A., HORVATH, S. & GESCHWIND, D. H. 2010. Divergence of human and mouse brain transcriptome highlights Alzheimer disease pathways. *Proc Natl Acad Sci U S A,* 107**,** 12698-703.

MILLS, C. D., KINCAID, K., ALT, J. M., HEILMAN, M. J. & HILL, A. M. 2000. M-1/M-2 macrophages and the Th1/Th2 paradigm. *J Immunol,* 164**,** 6166-73.

MITTELBRONN, M., DIETZ, K., SCHLUESENER, H. J. & MEYERMANN, R. 2001. Local distribution of microglia in the normal adult human central nervous system differs by up to one order of magnitude. *Acta Neuropathol,* 101**,** 249-55.

MIZUNO, T., KAWANOKUCHI, J., NUMATA, K. & SUZUMURA, A. 2003. Production and neuroprotective functions of fractalkine in the central nervous system. *Brain Res,* 979**,** 65-70.

MOEHLE, M. S., WEBBER, P. J., TSE, T., SUKAR, N., STANDAERT, D. G., DESILVA, T. M., COWELL, R. M. & WEST, A. B. 2012. LRRK2 inhibition attenuates microglial inflammatory responses. *The Journal of neuroscience : the official journal of the Society for Neuroscience,* 32**,** 1602-1611.

MOGI, M., KONDO, T., MIZUNO, Y. & NAGATSU, T. 2007. p53 protein, interferon-gamma, and NF-kappaB levels are elevated in the parkinsonian brain. *Neurosci Lett,* 414**,** 94-7.

MONFRINI, E. & DI FONZO, A. 2017. Leucine-Rich Repeat Kinase (LRRK2) Genetics and Parkinson's Disease. *Adv Neurobiol,* 14**,** 3-30.

MONK, P. N., SCOLA, A. M., MADALA, P. & FAIRLIE, D. P. 2007. Function, structure and therapeutic potential of complement C5a receptors. *Br J Pharmacol,* 152**,** 429-48.

MOORE, A. R., ZHOU, W.-L., JAKOVCEVSKI, I., ZECEVIC, N. & ANTIC, S. D. 2011. Spontaneous Electrical Activity in the Human Fetal Cortex In Vitro. *The Journal of Neuroscience,* 31**,** 2391-2398.

MOORS, T. E., MAAT, C. A., NIEDIEKER, D., MONA, D., PETERSEN, D., TIMMERMANS-HUISMAN, E., KOLE, J., EL-MASHTOLY, S. F., ZAGO, W., BARBOUR, R., MUNDIGL, O., KALUZA, K., HUBER, S., HUG, M. N., KREMER, T., RITTER, M., DZIADEK, S., GEURTS, J. J. G., GERWERT, K., BRITSCHGI, M. & VAN DE BERG, W. D. J. 2018. Detailed structural orchestration of Lewy pathology in Parkinson's disease as revealed by 3D multicolor STED microscopy. *bioRxiv***,** 470476.

MOSHER, K. I. & WYSS-CORAY, T. 2014. Microglial dysfunction in brain aging and Alzheimer's disease. *Biochem Pharmacol,* 88**,** 594-604.

MOSSER, D. M. & EDWARDS, J. P. 2008. Exploring the full spectrum of macrophage activation. *Nature Reviews Immunology,* 8**,** 958-969.

MRDJEN, D., PAVLOVIC, A., HARTMANN, F. J., SCHREINER, B., UTZ, S. G., LEUNG, B. P., LELIOS, I., HEPPNER, F. L., KIPNIS, J., MERKLER, D., GRETER, M. & BECHER, B. 2018. High-Dimensional Single-Cell Mapping of Central Nervous System Immune Cells Reveals Distinct Myeloid Subsets in Health, Aging, and Disease. *Immunity,* 48**,** 380-395.e6.

MUFFAT, J., LI, Y., YUAN, B., MITALIPOVA, M., OMER, A., CORCORAN, S., BAKIASI, G., TSAI, L. H., AUBOURG, P., RANSOHOFF, R. M. & JAENISCH, R. 2016. Efficient derivation of microglia-like cells from human pluripotent stem cells. *Nat Med,* 22**,** 1358-1367.

MÜLLER, T., BLUM-DEGEN, D., PRZUNTEK, H. & KUHN, W. 1998. Interleukin-6 levels in cerebrospinal fluid inversely correlate to severity of Parkinson's disease. *Acta Neurol Scand,* 98**,** 142-4.

MULLIN, S., STOKHOLM, M. G., HUGHES, D., MEHTA, A., PARBO, P., HINZ, R., PAVESE, N., BROOKS, D. J. & SCHAPIRA, A. H. V. 2021. Brain Microglial Activation Increased in Glucocerebrosidase (GBA) Mutation Carriers without Parkinson's disease. *Mov Disord,* 36**,** 774-779.

MURABE, Y. & SANO, Y. 1982. Morphological studies on neuroglia. VI. Postnatal development of microglial cells. *Cell Tissue Res,* 225**,** 469-85.

MURABE, Y. & SANO, Y. 1983. Morphological studies on neuroglia. VII. Distribution of "brain macrophages" in brains of neonatal and adult rats, as determined by means of immunohistochemistry. *Cell Tissue Res,* 229**,** 85-95.

MURAKAMI, G., WATABE, T., TAKAOKA, K., MIYAZONO, K. & IMAMURA, T. 2003. Cooperative inhibition of bone morphogenetic protein signaling by Smurf1 and inhibitory Smads. *Molecular biology of the cell,* 14**,** 2809-2817.

NALLS, M. A., PANKRATZ, N., LILL, C. M., DO, C. B., HERNANDEZ, D. G., SAAD, M., DESTEFANO, A. L., KARA, E., BRAS, J., SHARMA, M., SCHULTE, C., KELLER, M. F., AREPALLI, S., LETSON, C., EDSALL, C., STEFANSSON, H., LIU, X., PLINER, H., LEE, J. H., CHENG, R., IKRAM, M. A., IOANNIDIS, J. P., HADJIGEORGIOU, G. M., BIS, J. C., MARTINEZ, M., PERLMUTTER, J. S., GOATE, A., MARDER, K., FISKE, B., SUTHERLAND, M., XIROMERISIOU, G., MYERS, R. H., CLARK, L. N., STEFANSSON, K., HARDY, J. A., HEUTINK, P., CHEN, H., WOOD, N. W., HOULDEN, H., PAYAMI, H., BRICE, A., SCOTT, W. K., GASSER, T., BERTRAM, L., ERIKSSON, N., FOROUD, T. & SINGLETON, A. B. 2014. Large-scale meta-analysis of genome-wide association data identifies six new risk loci for Parkinson's disease. *Nat Genet,* 46**,** 989-93.

NEUDORFER, O., GILADI, N., ELSTEIN, D., ABRAHAMOV, A., TUREZKITE, T., AGHAI, E., RECHES, A., BEMBI, B. & ZIMRAN, A. 1996. Occurrence of Parkinson's syndrome in type I Gaucher disease. *Qjm,* 89**,** 691-4.

NEUMANN, H., KOTTER, M. R. & FRANKLIN, R. J. 2009a. Debris clearance by microglia: an essential link between degeneration and regeneration. *Brain,* 132**,** 288-95.

NEUMANN, J., BRAS, J., DEAS, E., O'SULLIVAN, S. S., PARKKINEN, L., LACHMANN, R. H., LI, A., HOLTON, J., GUERREIRO, R., PAUDEL, R., SEGARANE, B., SINGLETON, A., LEES, A., HARDY, J., HOULDEN, H., REVESZ, T. & WOOD, N. W. 2009b. Glucocerebrosidase mutations in clinical and pathologically proven Parkinson's disease. *Brain,* 132**,** 1783-94.

NEWBERRY, R. W., LEONG, J. T., CHOW, E. D., KAMPMANN, M. & DEGRADO, W. F. 2020. Deep mutational scanning reveals the structural basis for α-synuclein activity. *Nature Chemical Biology,* 16**,** 653-659.

NGUYEN, M. & KRAINC, D. 2018. LRRK2 phosphorylation of auxilin mediates synaptic defects in dopaminergic neurons from patients with Parkinson's disease. *Proc Natl Acad Sci U S A,* 115**,** 5576-5581.

NIE, J., XIE, P., LIU, L., XING, G., CHANG, Z., YIN, Y., TIAN, C., HE, F. & ZHANG, L. 2010. Smad ubiquitylation regulatory factor 1/2 (Smurf1/2) promotes p53 degradation by stabilizing the E3 ligase MDM2. *J Biol Chem,* 285**,** 22818-30.

NIMMERJAHN, A., KIRCHHOFF, F. & HELMCHEN, F. 2005. Resting microglial cells are highly dynamic surveillants of brain parenchyma in vivo. *Science,* 308**,** 1314-8.

NUSSBAUM, R. L. & ELLIS, C. E. 2003. Alzheimer's disease and Parkinson's disease. *N Engl J Med,* 348**,** 1356-64.

O'REGAN, G., DESOUZA, R. M., BALESTRINO, R. & SCHAPIRA, A. H. 2017. Glucocerebrosidase Mutations in Parkinson Disease. *J Parkinsons Dis,* 7**,** 411-422.

OIKONOMIDI, A., TAUTVYDAITĖ, D., GHOLAMREZAEE, M. M., HENRY, H., BACHER, M. & POPP, J. 2017. Macrophage Migration Inhibitory Factor is Associated with Biomarkers of Alzheimer's Disease Pathology and Predicts Cognitive Decline in Mild Cognitive Impairment and Mild Dementia. *J Alzheimers Dis,* 60**,** 273-281.

OKAJIMA, T. & TSURUTA, F. 2018. Microglial dynamics during brain development. *Neural regeneration research,* 13**,** 222-223.

OKAZAWA, H., MOTEGI, S., OHYAMA, N., OHNISHI, H., TOMIZAWA, T., KANEKO, Y., OLDENBORG, P. A., ISHIKAWA, O. & MATOZAKI, T. 2005. Negative regulation of phagocytosis in macrophages by the CD47-SHPS-1 system. *J Immunol,* 174**,** 2004-11.

OLIVEIRA, L. M. A., FALOMIR-LOCKHART, L. J., BOTELHO, M. G., LIN, K. H., WALES, P., KOCH, J. C., GERHARDT, E., TASCHENBERGER, H., OUTEIRO, T. F., LINGOR, P., SCHÜLE, B., ARNDT-JOVIN, D. J. & JOVIN, T. M. 2015. Elevated α-synuclein caused by SNCA gene triplication impairs neuronal differentiation and maturation in Parkinson's patient-derived induced pluripotent stem cells. *Cell Death & Disease,* 6**,** e1994-e1994.

ONUSKA, K. M. 2020. The Dual Role of Microglia in the Progression of Alzheimer's Disease. *The Journal of Neuroscience,* 40**,** 1608-1610.

OPPENHEIM, R. W., PREVETTE, D., TYTELL, M. & HOMMA, S. 1990. Naturally occurring and induced neuronal death in the chick embryo in vivo requires protein and RNA synthesis: evidence for the role of cell death genes. *Dev Biol,* 138**,** 104-13.

OSTERGAARD, K., JONES, S. A., HYMAN, C. & ZIMMER, J. 1996. Effects of donor age and brain-derived neurotrophic factor on the survival of dopaminergic neurons and axonal growth in postnatal rat nigrostriatal cocultures. *Exp Neurol,* 142**,** 340-50.

PAISÁN-RUÍZ, C., JAIN, S., EVANS, E. W., GILKS, W. P., SIMÓN, J., VAN DER BRUG, M., LÓPEZ DE MUNAIN, A., APARICIO, S., GIL, A. M., KHAN, N., JOHNSON, J., MARTINEZ, J. R., NICHOLL, D., MARTÍ CARRERA, I., PENA, A. S., DE SILVA, R., LEES, A., MARTÍ-MASSÓ, J. F., PÉREZ-TUR, J., WOOD, N. W. & SINGLETON, A. B. 2004. Cloning of the gene containing mutations that cause PARK8-linked Parkinson's disease. *Neuron,* 44**,** 595-600.

PALIS, J., ROBERTSON, S., KENNEDY, M., WALL, C. & KELLER, G. 1999. Development of erythroid and myeloid progenitors in the yolk sac and embryo proper of the mouse. *Development,* 126**,** 5073-84.

PÅLSSON-MCDERMOTT, E. M. & O'NEILL, L. A. J. 2020. Targeting immunometabolism as an anti-inflammatory strategy. *Cell Res,* 30**,** 300-314.

PANAGIOTAKOPOULOU, V., IVANYUK, D., DE CICCO, S., HAQ, W., ARSIĆ, A., YU, C., MESSELODI, D., OLDRATI, M., SCHÖNDORF, D. C., PEREZ, M.-J., CASSATELLA, R. P.,

JAKOBI, M., SCHNEIDERHAN-MARRA, N., GASSER, T., NIKIĆ-SPIEGEL, I. & DELEIDI, M. 2020. Interferon-γ signaling synergizes with LRRK2 in neurons and microglia derived from human induced pluripotent stem cells. *Nature Communications,* 11**,** 5163.

PANDYA, H., SHEN, M. J., ICHIKAWA, D. M., SEDLOCK, A. B., CHOI, Y., JOHNSON, K. R., KIM, G., BROWN, M. A., ELKAHLOUN, A. G., MARIC, D., SWEENEY, C. L., GOSSA, S., MALECH, H. L., MCGAVERN, D. B. & PARK, J. K. 2017. Differentiation of human and murine induced pluripotent stem cells to microglia-like cells. *Nat Neurosci,* 20**,** 753-759.

PARHIZKAR, S., ARZBERGER, T., BRENDEL, M., KLEINBERGER, G., DEUSSING, M., FOCKE, C., NUSCHER, B., XIONG, M., GHASEMIGHARAGOZ, A., KATZMARSKI, N., KRASEMANN, S., LICHTENTHALER, S. F., MÜLLER, S. A., COLOMBO, A., MONASOR, L. S., TAHIROVIC, S., HERMS, J., WILLEM, M., PETTKUS, N., BUTOVSKY, O., BARTENSTEIN, P., EDBAUER, D., ROMINGER, A., ERTÜRK, A., GRATHWOHL, S. A., NEHER, J. J., HOLTZMAN, D. M., MEYER-LUEHMANN, M. & HAASS, C. 2019. Loss of TREM2 function increases amyloid seeding but reduces plaque-associated ApoE. *Nature Neuroscience,* 22**,** 191-204.

PARK, J., WETZEL, I., MARRIOTT, I., DRÉAU, D., D'AVANZO, C., KIM, D. Y., TANZI, R. E. & CHO, H. 2018. A 3D human triculture system modeling neurodegeneration and neuroinflammation in Alzheimer's disease. *Nature neuroscience,* 21**,** 941-951.

PARK, S. H. 2005. Fine tuning and cross-talking of TGF-beta signal by inhibitory Smads. *J Biochem Mol Biol,* 38**,** 9-16.

PASANEN, P., MYLLYKANGAS, L., SIITONEN, M., RAUNIO, A., KAAKKOLA, S., LYYTINEN, J., TIENARI, P. J., PÖYHÖNEN, M. & PAETAU, A. 2014. Novel α-synuclein mutation A53E associated with atypical multiple system atrophy and Parkinson's disease-type pathology. *Neurobiol Aging,* 35**,** 2180.e1-5.

PATIR, A., SHIH, B., MCCOLL, B. W. & FREEMAN, T. C. 2019. A core transcriptional signature of human microglia: Derivation and utility in describing region-dependent alterations associated with Alzheimer's disease. *Glia,* 67**,** 1240-1253.

PATTARINI, R., SMEYNE, R. J. & MORGAN, J. I. 2007. Temporal mRNA profiles of inflammatory mediators in the murine 1-methyl-4-phenyl-1,2,3,6-tetrahydropyrimidine model of Parkinson's disease. *Neuroscience,* 145**,** 654-668.

PENG, C., GATHAGAN, R. J., COVELL, D. J., MEDELLIN, C., STIEBER, A., ROBINSON, J. L., ZHANG, B., PITKIN, R. M., OLUFEMI, M. F., LUK, K. C., TROJANOWSKI, J. Q. & LEE, V. M. 2018. Cellular milieu imparts distinct pathological alpha-synuclein strains in alpha-synucleinopathies. *Nature,* 557**,** 558-563.

PENG, C., TROJANOWSKI, J. Q. & LEE, V. M. Y. 2020a. Protein transmission in neurodegenerative disease. *Nature Reviews Neurology,* 16**,** 199-212.

PENG, G., QIU, J., LIU, H., ZHOU, M., HUANG, S., GUO, W., LIN, Y., CHEN, X., LI, Z., LI, G., ZHANG, W., ZHANG, Y., LI, X., WU, Z., WEI, L., YANG, X., ZHU, X., MO, M. & XU, P. 2020b. Analysis of Cerebrospinal Fluid Soluble TREM2 and Polymorphisms in Sporadic Parkinson's Disease in a Chinese Population. *J Mol Neurosci,* 70**,** 294-301.

PENG, Q., MALHOTRA, S., TORCHIA, J. A., KERR, W. G., COGGESHALL, K. M. & HUMPHREY, M. B. 2010. TREM2- and DAP12-dependent activation of PI3K requires DAP10 and is inhibited by SHIP1. *Sci Signal,* 3**,** ra38.

PERRY, V. H., HUME, D. A. & GORDON, S. 1985. Immunohistochemical localization of macrophages and microglia in the adult and developing mouse brain. *Neuroscience,* 15**,** 313-26.

PERRY, V. H., NICOLL, J. A. R. & HOLMES, C. 2010. Microglia in neurodegenerative disease. *Nature Reviews Neurology,* 6**,** 193-201.

PICKRELL, A. M., HUANG, C. H., KENNEDY, S. R., ORDUREAU, A., SIDERIS, D. P., HOEKSTRA, J. G., HARPER, J. W. & YOULE, R. J. 2015. Endogenous Parkin Preserves Dopaminergic Substantia Nigral Neurons following Mitochondrial DNA Mutagenic Stress. *Neuron,* 87**,** 371-81.

PLENZ, D. & KITAI, S. T. 1998. Regulation of the nigrostriatal pathway by metabotropic glutamate receptors during development. *J Neurosci,* 18**,** 4133-44.

PLESCHER, M., SEIFERT, G., HANSEN, J. N., BEDNER, P., STEINHÄUSER, C. & HALLE, A. 2018. Plaque-dependent morphological and electrophysiological heterogeneity of microglia in an Alzheimer's disease mouse model. *Glia,* 66**,** 1464-1480.

PLUVINAGE, J. V., HANEY, M. S., SMITH, B. A. H., SUN, J., IRAM, T., BONANNO, L., LI, L., LEE, D. P., MORGENS, D. W., YANG, A. C., SHUKEN, S. R., GATE, D., SCOTT, M., KHATRI, P., LUO, J., BERTOZZI, C. R., BASSIK, M. C. & WYSS-CORAY, T. 2019. CD22 blockade restores homeostatic microglial phagocytosis in ageing brains. *Nature,* 568**,** 187-192.

POCOCK, J. M. & PIERS, T. M. 2018. Modelling microglial function with induced pluripotent stem cells: an update. *Nat Rev Neurosci,* 19**,** 445-452.

POEWE, W., SEPPI, K., TANNER, C. M., HALLIDAY, G. M., BRUNDIN, P., VOLKMANN, J., SCHRAG, A.-E. & LANG, A. E. 2017. Parkinson disease. *Nature Reviews Disease Primers,* 3**,** 17013.

POLYMEROPOULOS, M. H., LAVEDAN, C., LEROY, E., IDE, S. E., DEHEJIA, A., DUTRA, A., PIKE, B., ROOT, H., RUBENSTEIN, J., BOYER, R., STENROOS, E. S., CHANDRASEKHARAPPA, S., ATHANASSIADOU, A., PAPAPETROPOULOS, T., JOHNSON, W. G., LAZZARINI, A. M., DUVOISIN, R. C., DI IORIO, G., GOLBE, L. I. & NUSSBAUM, R. L. 1997. Mutation in the alpha-synuclein gene identified in families with Parkinson's disease. *Science,* 276**,** 2045-7.

POPOVA, G., SOLIMAN, S. S., KIM, C. N., KEEFE, M. G., HENNICK, K. M., JAIN, S., LI, T., TEJERA, D., SHIN, D., CHHUN, B. B., MCGINNIS, C. S., SPEIR, M., GARTNER, Z. J., MEHTA, S. B., HAEUSSLER, M., HENGEN, K. B., RANSOHOFF, R. R., PIAO, X. & NOWAKOWSKI, T. J. 2021. Human microglia states are conserved across experimental models and regulate neural stem cell responses in chimeric organoids. *Cell Stem Cell,* 28**,** 2153-2166.e6.

POSTUMA, R. B., AARSLAND, D., BARONE, P., BURN, D. J., HAWKES, C. H., OERTEL, W. & ZIEMSSEN, T. 2012. Identifying prodromal Parkinson's disease: pre-motor disorders in Parkinson's disease. *Mov Disord,* 27**,** 617-26.

POULIN, J.-F., CARONIA, G., HOFER, C., CUI, Q., HELM, B., RAMAKRISHNAN, C., CHAN, C. S., DOMBECK, D. A., DEISSEROTH, K. & AWATRAMANI, R. 2018. Mapping projections of molecularly defined dopamine neuron subtypes using intersectional genetic approaches. *Nature neuroscience,* 21**,** 1260-1271.

PRANKE, I. M., MORELLO, V., BIGAY, J., GIBSON, K., VERBAVATZ, J. M., ANTONNY, B. & JACKSON, C. L. 2011. α-Synuclein and ALPS motifs are membrane curvature sensors whose contrasting chemistry mediates selective vesicle binding. *J Cell Biol,* 194**,** 89-103.

PREISSLER, J., GROSCHE, A., LEDE, V., LE DUC, D., KRÜGEL, K., MATYASH, V., SZULZEWSKY, F., KALLENDRUSCH, S., IMMIG, K., KETTENMANN, H., BECHMANN, I., SCHÖNEBERG, T. & SCHULZ, A. 2015. Altered microglial phagocytosis in GPR34-deficient mice. *Glia,* 63**,** 206-15.

PRILLER, J., FLÜGEL, A., WEHNER, T., BOENTERT, M., HAAS, C. A., PRINZ, M., FERNÁNDEZ-KLETT, F., PRASS, K., BECHMANN, I., DE BOER, B. A., FROTSCHER, M., KREUTZBERG, G. W., PERSONS, D. A. & DIRNAGL, U. 2001. Targeting gene-modified hematopoietic cells

to the central nervous system: use of green fluorescent protein uncovers microglial engraftment. *Nat Med,* 7**,** 1356-61.

PRINGSHEIM, T., JETTE, N., FROLKIS, A. & STEEVES, T. D. 2014. The prevalence of Parkinson's disease: a systematic review and meta-analysis. *Mov Disord,* 29**,** 1583-90.

PRONIN, A. N., MORRIS, A. J., SURGUCHOV, A. & BENOVIC, J. L. 2000. Synucleins are a novel class of substrates for G protein-coupled receptor kinases. *J Biol Chem,* 275**,** 26515-22.

PROUKAKIS, C., DUDZIK, C. G., BRIER, T., MACKAY, D. S., COOPER, J. M., MILLHAUSER, G. L., HOULDEN, H. & SCHAPIRA, A. H. 2013. A novel α-synuclein missense mutation in Parkinson disease. *Neurology,* 80**,** 1062-4.

PRUSINER, S. B. 1982. Novel proteinaceous infectious particles cause scrapie. *Science,* 216**,** 136-44.

PRUSINER, S. B. 1987. Prions causing degenerative neurological diseases. *Annu Rev Med,* 38**,** 381-98.

PRUSINER, S. B. 2012. Cell biology. A unifying role for prions in neurodegenerative diseases. *Science,* 336**,** 1511-3.

PRUSINER, S. B. 2013. Biology and genetics of prions causing neurodegeneration. *Annu Rev Genet,* 47**,** 601-23.

PRUSINER, S. B., WOERMAN, A. L., MORDES, D. A., WATTS, J. C., RAMPERSAUD, R., BERRY, D. B., PATEL, S., OEHLER, A., LOWE, J. K., KRAVITZ, S. N., GESCHWIND, D. H., GLIDDEN, D. V., HALLIDAY, G. M., MIDDLETON, L. T., GENTLEMAN, S. M., GRINBERG, L. T. & GILES, K. 2015. Evidence for alpha-synuclein prions causing multiple system atrophy in humans with parkinsonism. *Proc Natl Acad Sci U S A,* 112**,** E5308-17.

PURVES, D. & LICHTMAN, J. W. 1980. Elimination of synapses in the developing nervous system. *Science,* 210**,** 153-7.

RANSOHOFF, R. M. 2016. A polarizing question: do M1 and M2 microglia exist? *Nature Neuroscience,* 19**,** 987-991.

RASMUSSEN, M. A., HOLST, B., TÜMER, Z., JOHNSEN, M. G., ZHOU, S., STUMMANN, T. C., HYTTEL, P. & CLAUSEN, C. 2014. Transient p53 suppression increases reprogramming of human fibroblasts without affecting apoptosis and DNA damage. *Stem cell reports,* 3**,** 404-413.

RECASENS, M., ALMOLDA, B., PÉREZ-CLAUSELL, J., CAMPBELL, I. L., GONZÁLEZ, B. & CASTELLANO, B. 2021. Chronic exposure to IL-6 induces a desensitized phenotype of the microglia. *Journal of Neuroinflammation,* 18**,** 31.

REN, M., GUO, Y., WEI, X., YAN, S., QIN, Y., ZHANG, X., JIANG, F. & LOU, H. 2018. TREM2 overexpression attenuates neuroinflammation and protects dopaminergic neurons in experimental models of Parkinson's disease. *Exp Neurol,* 302**,** 205-213.

REZAIE, P., DEAN, A., MALE, D. & ULFIG, N. 2005. Microglia in the cerebral wall of the human telencephalon at second trimester. *Cereb Cortex,* 15**,** 938-49.

REZAIE, P. & MALE, D. 2002. Mesoglia & microglia--a historical review of the concept of mononuclear phagocytes within the central nervous system. *J Hist Neurosci,* 11**,** 325-74.

RICHARME, G., MIHOUB, M., DAIROU, J., BUI, L. C., LEGER, T. & LAMOURI, A. 2015. Parkinsonism-associated protein DJ-1/Park7 is a major protein deglycase that repairs methylglyoxal- and glyoxal-glycated cysteine, arginine, and lysine residues. *The Journal of biological chemistry,* 290**,** 1885-1897.

RICHTER, M., VIDOVIC, N., BIBER, K., DOLGA, A., CULMSEE, C. & DODEL, R. 2020. The neuroprotective role of microglial cells against amyloid beta-mediated toxicity in organotypic hippocampal slice cultures. *Brain Pathol,* 30**,** 589-602.

RISSIN, D. M., KAN, C. W., CAMPBELL, T. G., HOWES, S. C., FOURNIER, D. R., SONG, L., PIECH, T., PATEL, P. P., CHANG, L., RIVNAK, A. J., FERRELL, E. P., RANDALL, J. D., PROVUNCHER, G. K., WALT, D. R. & DUFFY, D. C. 2010. Single-molecule enzyme-linked immunosorbent assay detects serum proteins at subfemtomolar concentrations. *Nat Biotechnol,* 28**,** 595-9.

RODRIGUES, R. J., TOMÉ, A. R. & CUNHA, R. A. 2015. ATP as a multi-target danger signal in the brain. *Front Neurosci,* 9**,** 148.

ROSTAMI, J., HOLMQVIST, S., LINDSTRÖM, V., SIGVARDSON, J., WESTERMARK, G. T., INGELSSON, M., BERGSTRÖM, J., ROYBON, L. & ERLANDSSON, A. 2017. Human Astrocytes Transfer Aggregated Alpha-Synuclein via Tunneling Nanotubes. *J Neurosci,* 37**,** 11835-11853.

ROUX, A., WANG, X., BECKER, K. & MA, J. 2020. Modeling alpha-Synucleinopathy in Organotypic Brain Slice Culture with Preformed alpha-Synuclein Amyloid Fibrils. *J Parkinsons Dis,* 10**,** 1397-1410.

ROY, S. & WOLMAN, L. 1969. Ultrastructural observations in Parkinsonism. *J Pathol,* 99**,** 39-44.

RUSSO, I., BUBACCO, L. & GREGGIO, E. 2014. LRRK2 and neuroinflammation: partners in crime in Parkinson's disease? *J Neuroinflammation,* 11**,** 52.

SAIJO, K. & GLASS, C. K. 2011. Microglial cell origin and phenotypes in health and disease. *Nature Reviews Immunology,* 11**,** 775-787.

SAITO, Y., KAWASHIMA, A., RUBERU, N. N., FUJIWARA, H., KOYAMA, S., SAWABE, M., ARAI, T., NAGURA, H., YAMANOUCHI, H., HASEGAWA, M., IWATSUBO, T. & MURAYAMA, S. 2003. Accumulation of Phosphorylated α -Synuclein in Aging Human Brain. *Journal of Neuropathology & Experimental Neurology,* 62**,** 644-654.

SALAT, D. & TOLOSA, E. 2013. Levodopa in the treatment of Parkinson's disease: current status and new developments. *J Parkinsons Dis,* 3**,** 255-69.

SÁNCHEZ-DANÉS, A., RICHAUD-PATIN, Y., CARBALLO-CARBAJAL, I., JIMÉNEZ-DELGADO, S., CAIG, C., MORA, S., DI GUGLIELMO, C., EZQUERRA, M., PATEL, B., GIRALT, A., CANALS, J. M., MEMO, M., ALBERCH, J., LÓPEZ-BARNEO, J., VILA, M., CUERVO, A. M., TOLOSA, E., CONSIGLIO, A. & RAYA, A. 2012a. Disease-specific phenotypes in dopamine neurons from human iPS-based models of genetic and sporadic Parkinson's disease. *EMBO Mol Med,* 4**,** 380-95.

SÁNCHEZ-DANÉS, A., RICHAUD-PATIN, Y., CARBALLO-CARBAJAL, I., JIMÉNEZ-DELGADO, S., CAIG, C., MORA, S., DI GUGLIELMO, C., EZQUERRA, M., PATEL, B., GIRALT, A., CANALS, J. M., MEMO, M., ALBERCH, J., LÓPEZ-BARNEO, J., VILA, M., CUERVO, A. M., TOLOSA, E., CONSIGLIO, A. & RAYA, A. 2012b. Disease-specific phenotypes in dopamine neurons from human iPS-based models of genetic and sporadic Parkinson's disease. *EMBO molecular medicine,* 4**,** 380-395.

SANCHEZ-GUAJARDO, V., FEBBRARO, F., KIRIK, D. & ROMERO-RAMOS, M. 2010. Microglia acquire distinct activation profiles depending on the degree of alpha-synuclein neuropathology in a rAAV based model of Parkinson's disease. *PLoS One,* 5**,** e8784.

SANDOR, C., ROBERTSON, P., LANG, C., HEGER, A., BOOTH, H., VOWLES, J., WITTY, L., BOWDEN, R., HU, M., COWLEY, S. A., WADE-MARTINS, R. & WEBBER, C. 2017. Transcriptomic profiling of purified patient-derived dopamine neurons identifies

convergent perturbations and therapeutics for Parkinson's disease. *Human Molecular Genetics,* 26**,** 552-566.

SANTOSTEFANO, K. E., HAMAZAKI, T., BIEL, N. M., JIN, S., UMEZAWA, A. & TERADA, N. 2015. A practical guide to induced pluripotent stem cell research using patient samples. *Laboratory Investigation,* 95**,** 4-13.

SATOH, J., ASAHINA, N., KITANO, S. & KINO, Y. 2014. A Comprehensive Profile of ChIP-Seq-Based PU.1/Spi1 Target Genes in Microglia. *Gene Regul Syst Bio,* 8**,** 127-39.

SCHEIBLICH, H., DANSOKHO, C., MERCAN, D., SCHMIDT, S. V., BOUSSET, L., WISCHHOF, L., EIKENS, F., ODAINIC, A., SPITZER, J., GRIEP, A., SCHWARTZ, S., BANO, D., LATZ, E., MELKI, R. & HENEKA, M. T. 2021. Microglia jointly degrade fibrillar alpha-synuclein cargo by distribution through tunneling nanotubes. *Cell,* 184**,** 5089-5106.e21.

SCHENCK, C. H., BUNDLIE, S. R., ETTINGER, M. G. & MAHOWALD, M. W. 1986. Chronic behavioral disorders of human REM sleep: a new category of parasomnia. *Sleep,* 9**,** 293-308.

SCHÖNDORF, D. C., AURELI, M., MCALLISTER, F. E., HINDLEY, C. J., MAYER, F., SCHMID, B., SARDI, S. P., VALSECCHI, M., HOFFMANN, S., SCHWARZ, L. K., HEDRICH, U., BERG, D., SHIHABUDDIN, L. S., HU, J., PRUSZAK, J., GYGI, S. P., SONNINO, S., GASSER, T. & DELEIDI, M. 2014. iPSC-derived neurons from GBA1-associated Parkinson's disease patients show autophagic defects and impaired calcium homeostasis. *Nature Communications,* 5**,** 4028.

SCHULZ, C., GOMEZ PERDIGUERO, E., CHORRO, L., SZABO-ROGERS, H., CAGNARD, N., KIERDORF, K., PRINZ, M., WU, B., JACOBSEN, S. E., POLLARD, J. W., FRAMPTON, J., LIU, K. J. & GEISSMANN, F. 2012. A lineage of myeloid cells independent of Myb and hematopoietic stem cells. *Science,* 336**,** 86-90.

SCHWARZ, N., HEDRICH, U. B. S., SCHWARZ, H., P.A, H., DAMMEIER, N., AUFFENBERG, E., BEDOGNI, F., HONEGGER, J. B., LERCHE, H., WUTTKE, T. V. & KOCH, H. 2017. Human Cerebrospinal fluid promotes long-term neuronal viability and network function in human neocortical organotypic brain slice cultures. *Scientific Reports,* 7**,** 12249.

SCHWARZ, N., UYSAL, B., WELZER, M., BAHR, J., LAYER, N., LÖFFLER, H., STANAITIS, K., PA, H., WEBER, Y., HEDRICH, U., HONEGGER, J., SKODRAS, A., BECKER, A., WUTTKE, T. & KOCH, H. 2019. Long-term adult human brain slice cultures as a model system to study human CNS circuitry and disease. *eLife,* 8.

SENGERS, B. G., MCGINTY, S., NOURI, F. Z., ARGUNGU, M., HAWKINS, E., HADJI, A., WEBER, A., TAYLOR, A. & SEPP, A. 2016. Modeling bispecific monoclonal antibody interaction with two cell membrane targets indicates the importance of surface diffusion. *MAbs,* 8**,** 905-15.

SEVENICH, L. 2018. Brain-Resident Microglia and Blood-Borne Macrophages Orchestrate Central Nervous System Inflammation in Neurodegenerative Disorders and Brain Cancer. *Frontiers in Immunology,* 9.

SHAHMORADIAN, S. H., LEWIS, A. J., GENOUD, C., HENCH, J., MOORS, T. E., NAVARRO, P. P., CASTANO-DIEZ, D., SCHWEIGHAUSER, G., GRAFF-MEYER, A., GOLDIE, K. N., SUTTERLIN, R., HUISMAN, E., INGRASSIA, A., GIER, Y., ROZEMULLER, A. J. M., WANG, J., PAEPE, A., ERNY, J., STAEMPFLI, A., HOERNSCHEMEYER, J., GROSSERUSCHKAMP, F., NIEDIEKER, D., EL-MASHTOLY, S. F., QUADRI, M., VAN, I. W. F. J., BONIFATI, V., GERWERT, K., BOHRMANN, B., FRANK, S., BRITSCHGI, M., STAHLBERG, H., VAN DE BERG, W. D. J. & LAUER, M. E. 2019. Lewy pathology in Parkinson's disease consists of crowded organelles and lipid membranes. *Nat Neurosci,* 22**,** 1099-1109.

SHARAF, A., KRIEGLSTEIN, K. & SPITTAU, B. 2013. Distribution of microglia in the postnatal murine nigrostriatal system. *Cell Tissue Res,* 351**,** 373-82.

SHI, M., BRADNER, J., HANCOCK, A. M., CHUNG, K. A., QUINN, J. F., PESKIND, E. R., GALASKO, D., JANKOVIC, J., ZABETIAN, C. P., KIM, H. M., LEVERENZ, J. B., MONTINE, T. J., GINGHINA, C., KANG, U. J., CAIN, K. C., WANG, Y., AASLY, J., GOLDSTEIN, D. & ZHANG, J. 2011. Cerebrospinal fluid biomarkers for Parkinson disease diagnosis and progression. *Ann Neurol,* 69**,** 570-80.

SHI, Y., ZHANG, W., YANG, Y., MURZIN, A. G., FALCON, B., KOTECHA, A., VAN BEERS, M., TARUTANI, A., KAMETANI, F., GARRINGER, H. J., VIDAL, R., HALLINAN, G. I., LASHLEY, T., SAITO, Y., MURAYAMA, S., YOSHIDA, M., TANAKA, H., KAKITA, A., IKEUCHI, T., ROBINSON, A. C., MANN, D. M. A., KOVACS, G. G., REVESZ, T., GHETTI, B., HASEGAWA, M., GOEDERT, M. & SCHERES, S. H. W. 2021. Structure-based classification of tauopathies. *Nature,* 598**,** 359-363.

SHIBASAKI, Y., BAILLIE, D. A., ST CLAIR, D. & BROOKES, A. J. 1995. High-resolution mapping of SNCA encoding alpha-synuclein, the non-A beta component of Alzheimer's disease amyloid precursor, to human chromosome 4q21.3-->q22 by fluorescence in situ hybridization. *Cytogenet Cell Genet,* 71**,** 54-5.

SHIN, D. I., BANNING, U., KIM, Y. M., VERHEYEN, J., HANNEN, M., BÖNIG, H. & KÖRHOLZ, D. 1999. Interleukin 10 inhibits TNF-alpha production in human monocytes independently of interleukin 12 and interleukin 1 beta. *Immunol Invest,* 28**,** 165-75.

SHRIVASTAVA, A. N., BOUSSET, L., RENNER, M., REDEKER, V., SAVISTCHENKO, J., TRILLER, A. & MELKI, R. 2020. Differential Membrane Binding and Seeding of Distinct α -Synuclein Fibrillar Polymorphs. *Biophysical Journal,* 118**,** 1301-1320.

SIGURDSSON, E. M., WISNIEWSKI, T. & FRANGIONE, B. 2002. Infectivity of amyloid diseases. *Trends in Molecular Medicine,* 8**,** 411-413.

SIMARD, A. R. & RIVEST, S. 2004. Bone marrow stem cells have the ability to populate the entire central nervous system into fully differentiated parenchymal microglia. *Faseb j,* 18**,** 998-1000.

SIMARD, A. R., SOULET, D., GOWING, G., JULIEN, J. P. & RIVEST, S. 2006. Bone marrow-derived microglia play a critical role in restricting senile plaque formation in Alzheimer's disease. *Neuron,* 49**,** 489-502.

SIMMNACHER, K., LANFER, J., RIZO, T., KAINDL, J. & WINNER, B. 2020. Modeling Cell-Cell Interactions in Parkinson's Disease Using Human Stem Cell-Based Models. *Frontiers in Cellular Neuroscience,* 13.

SINGLETON, A. B., FARRER, M., JOHNSON, J., SINGLETON, A., HAGUE, S., KACHERGUS, J., HULIHAN, M., PEURALINNA, T., DUTRA, A., NUSSBAUM, R., LINCOLN, S., CRAWLEY, A., HANSON, M., MARAGANORE, D., ADLER, C., COOKSON, M. R., MUENTER, M., BAPTISTA, M., MILLER, D., BLANCATO, J., HARDY, J. & GWINN-HARDY, K. 2003. alpha-Synuclein locus triplication causes Parkinson's disease. *Science,* 302**,** 841.

SLANZI, A., IANNOTO, G., ROSSI, B., ZENARO, E. & CONSTANTIN, G. 2020. In vitro Models of Neurodegenerative Diseases. *Frontiers in cell and developmental biology,* 8**,** 328-328.

SMITH, A. M. & DRAGUNOW, M. 2014. The human side of microglia. *Trends Neurosci,* 37**,** 125-35.

SOLDNER, F., HOCKEMEYER, D., BEARD, C., GAO, Q., BELL, G. W., COOK, E. G., HARGUS, G., BLAK, A., COOPER, O., MITALIPOVA, M., ISACSON, O. & JAENISCH, R. 2009. Parkinson's disease patient-derived induced pluripotent stem cells free of viral reprogramming factors. *Cell,* 136**,** 964-977.

SONG, W., HOOLI, B., MULLIN, K., JIN, S. C., CELLA, M., ULLAND, T. K., WANG, Y., TANZI, R. E. & COLONNA, M. 2017. Alzheimer's disease-associated TREM2 variants exhibit either decreased or increased ligand-dependent activation. *Alzheimers Dement,* 13**,** 381-387.

SONG, W. M. & COLONNA, M. 2018. The identity and function of microglia in neurodegeneration. *Nature Immunology,* 19**,** 1048-1058.

SPEICHER, A. M., WIENDL, H., MEUTH, S. G. & PAWLOWSKI, M. 2019. Generating microglia from human pluripotent stem cells: novel in vitro models for the study of neurodegeneration. *Molecular Neurodegeneration,* 14**,** 46.

SPILLANTINI, M. G., CROWTHER, R. A., JAKES, R., HASEGAWA, M. & GOEDERT, M. 1998. alpha-Synuclein in filamentous inclusions of Lewy bodies from Parkinson's disease and dementia with lewy bodies. *Proc Natl Acad Sci U S A,* 95**,** 6469-73.

SPILLANTINI, M. G. & GOEDERT, M. 2018. Neurodegeneration and the ordered assembly of α-synuclein. *Cell Tissue Res,* 373**,** 137-148.

SPILLANTINI, M. G., SCHMIDT, M. L., LEE, V. M. Y., TROJANOWSKI, J. Q., JAKES, R. & GOEDERT, M. 1997. α-Synuclein in Lewy bodies. *Nature,* 388**,** 839-840.

SPITZ, M., PEREIRA, J. S., NICARETA, D. H., ABREU GDE, M., BASTOS, E. F., SEIXAS, T. L. & PIMENTEL, M. M. 2015. Association of LRRK2 and GBA mutations in a Brazilian family with Parkinson's disease. *Parkinsonism Relat Disord,* 21**,** 825-6.

SRIRAM, K., MATHESON, J. M., BENKOVIC, S. A., MILLER, D. B., LUSTER, M. I. & O'CALLAGHAN, J. P. 2002. Mice deficient in TNF receptors are protected against dopaminergic neurotoxicity: implications for Parkinson's disease. *Faseb j,* 16**,** 1474-6.

STEFANIS, L. 2012. α-Synuclein in Parkinson's disease. *Cold Spring Harbor perspectives in medicine,* 2**,** a009399-a009399.

STEVENS, B., ALLEN, N. J., VAZQUEZ, L. E., HOWELL, G. R., CHRISTOPHERSON, K. S., NOURI, N., MICHEVA, K. D., MEHALOW, A. K., HUBERMAN, A. D., STAFFORD, B., SHER, A., LITKE, A. M., LAMBRIS, J. D., SMITH, S. J., JOHN, S. W. & BARRES, B. A. 2007. The classical complement cascade mediates CNS synapse elimination. *Cell,* 131**,** 1164-78.

STOKER, T. B., BLAIR, N. F. & BARKER, R. A. 2017. Neural grafting for Parkinson's disease: challenges and prospects. *Neural Regen Res,* 12**,** 389-392.

STOPPINI, L., BUCHS, P. A. & MULLER, D. 1991. A simple method for organotypic cultures of nervous tissue. *J Neurosci Methods,* 37**,** 173-82.

STREIT, W. J. 2006. Microglial senescence: does the brain's immune system have an expiration date? *Trends Neurosci,* 29**,** 506-10.

STROHÄKER, T., JUNG, B. C., LIOU, S.-H., FERNANDEZ, C. O., RIEDEL, D., BECKER, S., HALLIDAY, G. M., BENNATI, M., KIM, W. S., LEE, S.-J. & ZWECKSTETTER, M. 2019. Structural heterogeneity of α-synuclein fibrils amplified from patient brain extracts. *Nature Communications,* 10**,** 5535.

STUDER, L., VERA, E. & CORNACCHIA, D. 2015. Programming and Reprogramming Cellular Age in the Era of Induced Pluripotency. *Cell Stem Cell,* 16**,** 591-600.

SU, H., NA, N., ZHANG, X. & ZHAO, Y. 2017. The biological function and significance of CD74 in immune diseases. *Inflamm Res,* 66**,** 209-216.

SULZER, D. & EDWARDS, R. H. 2019. The physiological role of alpha-synuclein and its relationship to Parkinson's Disease. *J Neurochem,* 150**,** 475-486.

SVAHN, A. J., DON, E. K., BADROCK, A. P., COLE, N. J., GRAEBER, M. B., YERBURY, J. J., CHUNG, R. & MORSCH, M. 2018. Nucleo-cytoplasmic transport of TDP-43 studied in real time: impaired microglia function leads to axonal spreading of TDP-43 in degenerating motor neurons. *Acta Neuropathol,* 136**,** 445-459.

SZEPESI, Z., MANOUCHEHRIAN, O., BACHILLER, S. & DEIERBORG, T. 2018. Bidirectional Microglia-Neuron Communication in Health and Disease. *Frontiers in cellular neuroscience,* 12**,** 323-323.

TAKAHASHI, K. & YAMANAKA, S. 2006. Induction of pluripotent stem cells from mouse embryonic and adult fibroblast cultures by defined factors. *Cell,* 126**,** 663-76.

TAKATA, K., KOZAKI, T., LEE, C. Z. W., THION, M. S., OTSUKA, M., LIM, S., UTAMI, K. H., FIDAN, K., PARK, D. S., MALLERET, B., CHAKAROV, S., SEE, P., LOW, D., LOW, G., GARCIA-MIRALLES, M., ZENG, R., ZHANG, J., GOH, C. C., GUL, A., HUBERT, S., LEE, B., CHEN, J., LOW, I., SHADAN, N. B., LUM, J., WEI, T. S., MOK, E., KAWANISHI, S., KITAMURA, Y., LARBI, A., POIDINGER, M., RENIA, L., NG, L. G., WOLF, Y., JUNG, S., ÖNDER, T., NEWELL, E., HUBER, T., ASHIHARA, E., GAREL, S., POULADI, M. A. & GINHOUX, F. 2017. Induced-Pluripotent-Stem-Cell-Derived Primitive Macrophages Provide a Platform for Modeling Tissue-Resident Macrophage Differentiation and Function. *Immunity,* 47**,** 183-198.e6.

TAMGÜNEY, G. & KORCZYN, A. D. 2018. A critical review of the prion hypothesis of human synucleinopathies. *Cell Tissue Res,* 373**,** 213-220.

TAN, A. K. 2001. Current and emerging treatments in Parkinson's disease. *Ann Acad Med Singap,* 30**,** 128-33.

TAN, J., TOWN, T. & MULLAN, M. 2000. CD45 inhibits CD40L-induced microglial activation via negative regulation of the Src/p44/42 MAPK pathway. *J Biol Chem,* 275**,** 37224-31.

TAN, Y.-L., YUAN, Y. & TIAN, L. 2020. Microglial regional heterogeneity and its role in the brain. *Molecular Psychiatry,* 25**,** 351-367.

TANAKA, A., TO, J., O'BRIEN, B., DONNELLY, S. & LUND, M. 2017. Selection of reliable reference genes for the normalisation of gene expression levels following time course LPS stimulation of murine bone marrow derived macrophages. *BMC immunology,* 18**,** 43-43.

TANJI, K., MORI, F., IMAIZUMI, T., YOSHIDA, H., MATSUMIYA, T., TAMO, W., YOSHIMOTO, M., ODAGIRI, H., SASAKI, M., TAKAHASHI, H., SATOH, K. & WAKABAYASHI, K. 2002. Upregulation of alpha-synuclein by lipopolysaccharide and interleukin-1 in human macrophages. *Pathol Int,* 52**,** 572-7.

TANSEY, M. G., WALLINGS, R. L., HOUSER, M. C., HERRICK, M. K., KEATING, C. E. & JOERS, V. 2022. Inflammation and immune dysfunction in Parkinson disease. *Nature Reviews Immunology*.

TANUDJOJO, B., SHAIKH, S. S., FENYI, A., BOUSSET, L., AGARWAL, D., MARSH, J., ZOIS, C., HEMAN-ACKAH, S., FISCHER, R., SIMS, D., MELKI, R. & TOFARIS, G. K. 2021. Phenotypic manifestation of α-synuclein strains derived from Parkinson's disease and multiple system atrophy in human dopaminergic neurons. *Nature Communications,* 12**,** 3817.

TARUTANI, A., ARAI, T., MURAYAMA, S., HISANAGA, S. I. & HASEGAWA, M. 2018. Potent prion-like behaviors of pathogenic α-synuclein and evaluation of inactivation methods. *Acta Neuropathol Commun,* 6**,** 29.

TASIC, B., MENON, V., NGUYEN, T. N., KIM, T. K., JARSKY, T., YAO, Z., LEVI, B., GRAY, L. T., SORENSEN, S. A., DOLBEARE, T., BERTAGNOLLI, D., GOLDY, J., SHAPOVALOVA, N., PARRY, S., LEE, C., SMITH, K., BERNARD, A., MADISEN, L., SUNKIN, S. M., HAWRYLYCZ, M., KOCH, C. & ZENG, H. 2016. Adult mouse cortical cell taxonomy revealed by single cell transcriptomics. *Nature Neuroscience,* 19**,** 335-346.

TAVIAN, M. & PÉAULT, B. 2005. Embryonic development of the human hematopoietic system. *Int J Dev Biol,* 49**,** 243-50.

TAY, T. L., MAI, D., DAUTZENBERG, J., FERNÁNDEZ-KLETT, F., LIN, G., SAGAR, DATTA, M., DROUGARD, A., STEMPFL, T., ARDURA-FABREGAT, A., STASZEWSKI, O., MARGINEANU, A., SPORBERT, A., STEINMETZ, L. M., POSPISILIK, J. A., JUNG, S., PRILLER, J., GRÜN, D., RONNEBERGER, O. & PRINZ, M. 2017. A new fate mapping system reveals context-dependent random or clonal expansion of microglia. *Nat Neurosci,* 20**,** 793-803.

TEJERA, D. & HENEKA, M. T. 2016. Microglia in Alzheimer's disease: the good, the bad and the ugly. *Curr Alzheimer Res,* 13**,** 370-80.

THÉVENET, J., PESCINI GOBERT, R., HOOFT VAN HUIJSDUIJNEN, R., WIESSNER, C. & SAGOT, Y. J. 2011. Regulation of LRRK2 expression points to a functional role in human monocyte maturation. *PLoS One,* 6**,** e21519.

TIMMERMAN, R., BURM, S. M. & BAJRAMOVIC, J. J. 2018. An Overview of in vitro Methods to Study Microglia. *Frontiers in Cellular Neuroscience,* 12.

TOFARIS, G. K., KIM, H. T., HOUREZ, R., JUNG, J. W., KIM, K. P. & GOLDBERG, A. L. 2011. Ubiquitin ligase Nedd4 promotes alpha-synuclein degradation by the endosomal-lysosomal pathway. *Proc Natl Acad Sci U S A,* 108**,** 17004-9.

TOFARIS, G. K., RAZZAQ, A., GHETTI, B., LILLEY, K. S. & SPILLANTINI, M. G. 2003. Ubiquitination of alpha-synuclein in Lewy bodies is a pathological event not associated with impairment of proteasome function. *J Biol Chem,* 278**,** 44405-11.

TOLOSA, E., VILA, M., KLEIN, C. & RASCOL, O. 2020. LRRK2 in Parkinson disease: challenges of clinical trials. *Nature Reviews Neurology,* 16**,** 97-107.

TONNESEN, J., PARISH, C. L., SORENSEN, A. T., ANDERSSON, A., LUNDBERG, C., DEISSEROTH, K., ARENAS, E., LINDVALL, O. & KOKAIA, M. 2011. Functional integration of grafted neural stem cell-derived dopaminergic neurons monitored by optogenetics in an in vitro Parkinson model. *PLoS One,* 6**,** e17560.

TRAN, J., ANASTACIO, H. & BARDY, C. 2020. Genetic predispositions of Parkinson's disease revealed in patient-derived brain cells. *npj Parkinson's Disease,* 6**,** 8.

TREMBLAY, M., STEVENS, B., SIERRA, A., WAKE, H., BESSIS, A. & NIMMERJAHN, A. 2011. The role of microglia in the healthy brain. *J Neurosci,* 31**,** 16064-9.

TREXLER, A. J. & RHOADES, E. 2009. Alpha-synuclein binds large unilamellar vesicles as an extended helix. *Biochemistry,* 48**,** 2304-6.

UCAR, B., KAJTEZ, J., FOIDL, B. M., EIGEL, D., WERNER, C., LONG, K. R., EMNÉUS, J., BIZEAU, J., LOMORA, M., PANDIT, A., NEWLAND, B. & HUMPEL, C. 2021. Biomaterial based strategies to reconstruct the nigrostriatal pathway in organotypic slice co-cultures. *Acta Biomaterialia,* 121**,** 250-262.

UEDA, Y., GULLIPALLI, D. & SONG, W. C. 2016. Modeling complement-driven diseases in transgenic mice: Values and limitations. *Immunobiology,* 221**,** 1080-90.

UENO, M., FUJITA, Y., TANAKA, T., NAKAMURA, Y., KIKUTA, J., ISHII, M. & YAMASHITA, T. 2013. Layer V cortical neurons require microglial support for survival during postnatal development. *Nat Neurosci,* 16**,** 543-51.

ULLAND, T. K. & COLONNA, M. 2018. TREM2 — a key player in microglial biology and Alzheimer disease. *Nature Reviews Neurology,* 14**,** 667-675.

ULLAND, T. K., SONG, W. M., HUANG, S. C., ULRICH, J. D., SERGUSHICHEV, A., BEATTY, W. L., LOBODA, A. A., ZHOU, Y., CAIRNS, N. J., KAMBAL, A., LOGINICHEVA, E., GILFILLAN, S., CELLA, M., VIRGIN, H. W., UNANUE, E. R., WANG, Y., ARTYOMOV, M. N., HOLTZMAN, D. M. & COLONNA, M. 2017. TREM2 Maintains Microglial Metabolic Fitness in Alzheimer's Disease. *Cell,* 170**,** 649-663.e13.

ULLOA, L., DOODY, J. & MASSAGUÉ, J. 1999. Inhibition of transforming growth factor-beta/SMAD signalling by the interferon-gamma/STAT pathway. *Nature,* 397**,** 710-3.

ULMER, T. S., BAX, A., COLE, N. B. & NUSSBAUM, R. L. 2005. Structure and dynamics of micelle-bound human alpha-synuclein. *J Biol Chem,* 280**,** 9595-603.

UVERSKY, V. N. 2003. A protein-chameleon: conformational plasticity of alpha-synuclein, a disordered protein involved in neurodegenerative disorders. *J Biomol Struct Dyn,* 21**,** 211-34.

VALENTE, E. M., ABOU-SLEIMAN, P. M., CAPUTO, V., MUQIT, M. M., HARVEY, K., GISPERT, S., ALI, Z., DEL TURCO, D., BENTIVOGLIO, A. R., HEALY, D. G., ALBANESE, A., NUSSBAUM, R., GONZÁLEZ-MALDONADO, R., DELLER, T., SALVI, S., CORTELLI, P., GILKS, W. P., LATCHMAN, D. S., HARVEY, R. J., DALLAPICCOLA, B., AUBURGER, G. & WOOD, N. W. 2004. Hereditary early-onset Parkinson's disease caused by mutations in PINK1. *Science,* 304**,** 1158-60.

VAMVACA, K., VOLLES, M. J. & LANSBURY, P. T., JR. 2009. The first N-terminal amino acids of alpha-synuclein are essential for alpha-helical structure formation in vitro and membrane binding in yeast. *J Mol Biol,* 389**,** 413-24.

VAN DER POLL, T., JANSEN, J., LEVI, M., TEN CATE, H., TEN CATE, J. W. & VAN DEVENTER, S. J. 1994. Regulation of interleukin 10 release by tumor necrosis factor in humans and chimpanzees. *J Exp Med,* 180**,** 1985-8.

VAN WILGENBURG, B., BROWNE, C., VOWLES, J. & COWLEY, S. A. 2013. Efficient, long term production of monocyte-derived macrophages from human pluripotent stem cells under partly-defined and fully-defined conditions. *PLoS One,* 8**,** e71098.

VARGAS, K. J., MAKANI, S., DAVIS, T., WESTPHAL, C. H., CASTILLO, P. E. & CHANDRA, S. S. 2014. Synucleins regulate the kinetics of synaptic vesicle endocytosis. *J Neurosci,* 34**,** 9364-76.

VASSAR, P. S. & CULLING, C. F. 1959. Fluorescent stains, with special reference to amyloid and connective tissues. *Arch Pathol,* 68**,** 487-98.

VAWTER, M. P., DILLON-CARTER, O., TOURTELLOTTE, W. W., CARVEY, P. & FREED, W. J. 1996. TGFbeta1 and TGFbeta2 concentrations are elevated in Parkinson's disease in ventricular cerebrospinal fluid. *Exp Neurol,* 142**,** 313-22.

VERA, E., BOSCO, N. & STUDER, L. 2016. Generating Late-Onset Human iPSC-Based Disease Models by Inducing Neuronal Age-Related Phenotypes through Telomerase Manipulation. *Cell Rep,* 17**,** 1184-1192.

VERHOOG, M. B., GORIOUNOVA, N. A., OBERMAYER, J., STROEDER, J., HJORTH, J. J. J., TESTA-SILVA, G., BAAYEN, J. C., DE KOCK, C. P. J., MEREDITH, R. M. & MANSVELDER, H. D. 2013. Mechanisms Underlying the Rules for Associative Plasticity at Adult Human Neocortical Synapses. *The Journal of Neuroscience,* 33**,** 17197.

VIERBUCHEN, T., OSTERMEIER, A., PANG, Z. P., KOKUBU, Y., SÜDHOF, T. C. & WERNIG, M. 2010. Direct conversion of fibroblasts to functional neurons by defined factors. *Nature,* 463**,** 1035-41.

VILCHEZ, D., SAEZ, I. & DILLIN, A. 2014. The role of protein clearance mechanisms in organismal ageing and age-related diseases. *Nat Commun,* 5**,** 5659.

VILLAR-PIQUÉ, A., LOPES DA FONSECA, T. & OUTEIRO, T. F. 2016. Structure, function and toxicity of alpha-synuclein: the Bermuda triangle in synucleinopathies. *J Neurochem,* 139 Suppl 1**,** 240-255.

VOGIATZI, T., XILOURI, M., VEKRELLIS, K. & STEFANIS, L. 2008. Wild type alpha-synuclein is degraded by chaperone-mediated autophagy and macroautophagy in neuronal cells. *J Biol Chem,* 283**,** 23542-56.

VOLPICELLI-DALEY, L. A., LUK, K. C. & LEE, V. M. Y. 2014. Addition of exogenous α -synuclein preformed fibrils to primary neuronal cultures to seed recruitment of endogenous α -synuclein to Lewy body and Lewy neurite-like aggregates. *Nature protocols,* 9**,** 2135-2146.

VOLPICELLI-DALEY, L. A., LUK, K. C., PATEL, T. P., TANIK, S. A., RIDDLE, D. M., STIEBER, A., MEANEY, D. F., TROJANOWSKI, J. Q. & LEE, V. M. 2011. Exogenous α -synuclein fibrils induce Lewy body pathology leading to synaptic dysfunction and neuron death. *Neuron,* 72**,** 57-71.

VON BARTHELD, C. S., BAHNEY, J. & HERCULANO-HOUZEL, S. 2016. The search for true numbers of neurons and glial cells in the human brain: A review of 150 years of cell counting. *The Journal of comparative neurology,* 524**,** 3865-3895.

WANG, L., DAS, U., SCOTT, D. A., TANG, Y., MCLEAN, P. J. & ROY, S. 2014. α -synuclein multimers cluster synaptic vesicles and attenuate recycling. *Current biology : CB,* 24**,** 2319-2326.

WANG, P., WU, P., SIEGEL, M. I., EGAN, R. W. & BILLAH, M. M. 1994. IL-10 inhibits transcription of cytokine genes in human peripheral blood mononuclear cells. *The Journal of Immunology,* 153**,** 811-816.

WANG, S., MUSTAFA, M., YUEDE, C. M., SALAZAR, S. V., KONG, P., LONG, H., WARD, M., SIDDIQUI, O., PAUL, R., GILFILLAN, S., IBRAHIM, A., RHINN, H., TASSI, I., ROSENTHAL, A., SCHWABE, T. & COLONNA, M. 2020. Anti-human TREM2 induces microglia proliferation and reduces pathology in an Alzheimer's disease model. *J Exp Med,* 217.

WANG, W.-Y., TAN, M.-S., YU, J.-T. & TAN, L. 2015a. Role of pro-inflammatory cytokines released from microglia in Alzheimer's disease. *Annals of translational medicine,* 3**,** 136-136.

WANG, X., PARK, J., SUSZTAK, K., ZHANG, N. R. & LI, M. 2019. Bulk tissue cell type deconvolution with multi-subject single-cell expression reference. *Nat Commun,* 10**,** 380.

WANG, Y., CELLA, M., MALLINSON, K., ULRICH, J. D., YOUNG, K. L., ROBINETTE, M. L., GILFILLAN, S., KRISHNAN, G. M., SUDHAKAR, S., ZINSELMEYER, B. H., HOLTZMAN, D. M., CIRRITO, J. R. & COLONNA, M. 2015b. TREM2 lipid sensing sustains the microglial response in an Alzheimer's disease model. *Cell,* 160**,** 1061-71.

WANG, Y., ULLAND, T. K., ULRICH, J. D., SONG, W., TZAFERIS, J. A., HOLE, J. T., YUAN, P., MAHAN, T. E., SHI, Y., GILFILLAN, S., CELLA, M., GRUTZENDLER, J., DEMATTOS, R. B., CIRRITO, J. R., HOLTZMAN, D. M. & COLONNA, M. 2016. TREM2-mediated early microglial response limits diffusion and toxicity of amyloid plaques. *J Exp Med,* 213**,** 667-75.

WEBB, J. L., RAVIKUMAR, B., ATKINS, J., SKEPPER, J. N. & RUBINSZTEIN, D. C. 2003. Alpha-Synuclein is degraded by both autophagy and the proteasome. *J Biol Chem,* 278**,** 25009-13.

WELCH, J. D., KOZAREVA, V., FERREIRA, A., VANDERBURG, C., MARTIN, C. & MACOSKO, E. Z. 2019. Single-Cell Multi-omic Integration Compares and Contrasts Features of Brain Cell Identity. *Cell,* 177**,** 1873-1887.e17.

WEST, A. B., MOORE, D. J., BISKUP, S., BUGAYENKO, A., SMITH, W. W., ROSS, C. A., DAWSON, V. L. & DAWSON, T. M. 2005. Parkinson's disease-associated mutations in leucine-rich repeat kinase 2 augment kinase activity. *Proc Natl Acad Sci U S A,* 102**,** 16842-7.

WESTON, L. L., JIANG, S., CHISHOLM, D., JANTZIE, L. L. & BHASKAR, K. 2021. Interleukin-10 deficiency exacerbates inflammation-induced tau pathology. *Journal of Neuroinflammation,* 18**,** 161.

WILSON, D. H., RISSIN, D. M., KAN, C. W., FOURNIER, D. R., PIECH, T., CAMPBELL, T. G., MEYER, R. E., FISHBURN, M. W., CABRERA, C., PATEL, P. P., FREW, E., CHEN, Y., CHANG, L., FERRELL, E. P., VON EINEM, V., MCGUIGAN, W., REINHARDT, M., SAYER, H., VIELSACK, C. & DUFFY, D. C. 2016. The Simoa HD-1 Analyzer: A Novel Fully Automated Digital Immunoassay Analyzer with Single-Molecule Sensitivity and Multiplexing. *J Lab Autom,* 21**,** 533-47.

WITHERS, G. S., GEORGE, J. M., BANKER, G. A. & CLAYTON, D. F. 1997. Delayed localization of synelfin (synuclein, NACP) to presynaptic terminals in cultured rat hippocampal neurons. *Brain Res Dev Brain Res,* 99**,** 87-94.

WRIGHT, G. J., JONES, M., PUKLAVEC, M. J., BROWN, M. H. & BARCLAY, A. N. 2001. The unusual distribution of the neuronal/lymphoid cell surface CD200 (OX2) glycoprotein is conserved in humans. *Immunology,* 102**,** 173-9.

WRIGHT, G. J., PUKLAVEC, M. J., WILLIS, A. C., HOEK, R. M., SEDGWICK, J. D., BROWN, M. H. & BARCLAY, A. N. 2000. Lymphoid/neuronal cell surface OX2 glycoprotein recognizes a novel receptor on macrophages implicated in the control of their function. *Immunity,* 13**,** 233-42.

XIAO, L., GONG, L. L., YUAN, D., DENG, M., ZENG, X. M., CHEN, L. L., ZHANG, L., YAN, Q., LIU, J. P., HU, X. H., SUN, S. M., LIU, J., MA, H. L., ZHENG, C. B., FU, H., CHEN, P. C., ZHAO, J. Q., XIE, S. S., ZOU, L. J., XIAO, Y. M., LIU, W. B., ZHANG, J., LIU, Y. & LI, D. W. C. 2010. Protein phosphatase-1 regulates Akt1 signal transduction pathway to control gene expression, cell survival and differentiation. *Cell Death & Differentiation,* 17**,** 1448-1462.

XIE, M., LIU, Y. U., ZHAO, S., ZHANG, L., BOSCO, D. B., PANG, Y.-P., ZHONG, J., SHETH, U., MARTENS, Y. A., ZHAO, N., LIU, C.-C., ZHUANG, Y., WANG, L., DICKSON, D. W., MATTSON, M. P., BU, G. & WU, L.-J. 2022. TREM2 interacts with TDP-43 and mediates microglial neuroprotection against TDP-43-related neurodegeneration. *Nature Neuroscience,* 25**,** 26-38.

XIONG, M., QIAN, Q., LIANG, X. & WEI, Y. D. 2022. Serum levels of lipocalin-2 in patients with Parkinson's disease. *Neurol Sci,* 43**,** 1755-1759.

XU, E., BODDU, R., ABDELMOTILIB, H. A., SOKRATIAN, A., KELLY, K., LIU, Z., BRYANT, N., CHANDRA, S., CARLISLE, S. M., LEFKOWITZ, E. J., HARMS, A. S., BENVENISTE, E. N., YACOUBIAN, T. A., VOLPICELLI-DALEY, L. A., STANDAERT, D. G. & WEST, A. B. 2022. Pathological α-synuclein recruits LRRK2 expressing pro-inflammatory monocytes to the brain. *Molecular Neurodegeneration,* 17**,** 7.

YAMASAKI, R., LU, H., BUTOVSKY, O., OHNO, N., RIETSCH, A. M., CIALIC, R., WU, P. M., DOYKAN, C. E., LIN, J., COTLEUR, A. C., KIDD, G., ZORLU, M. M., SUN, N., HU, W., LIU, L., LEE, J. C., TAYLOR, S. E., UEHLEIN, L., DIXON, D., GU, J., FLORUTA, C. M., ZHU, M., CHARO, I. F., WEINER, H. L. & RANSOHOFF, R. M. 2014. Differential roles of microglia and monocytes in the inflamed central nervous system. *J Exp Med,* 211**,** 1533-49.

YANG, W., HAMILTON, J. L., KOPIL, C., BECK, J. C., TANNER, C. M., ALBIN, R. L., RAY DORSEY, E., DAHODWALA, N., CINTINA, I., HOGAN, P. & THOMPSON, T. 2020. Current and

projected future economic burden of Parkinson's disease in the U.S. *npj Parkinson's Disease,* 6**,** 15.

YANG, Y., BOZA-SERRANO, A., DUNNING, C. J. R., CLAUSEN, B. H., LAMBERTSEN, K. L. & DEIERBORG, T. 2018. Inflammation leads to distinct populations of extracellular vesicles from microglia. *Journal of Neuroinflammation,* 15**,** 168.

YANG, Y., SHI, Y., SCHWEIGHAUSER, M., ZHANG, X., KOTECHA, A., MURZIN, A. G., GARRINGER, H. J., CULLINANE, P. W., SAITO, Y., FOROUD, T., WARNER, T. T., HASEGAWA, K., VIDAL, R., MURAYAMA, S., REVESZ, T., GHETTI, B., HASEGAWA, M., LASHLEY, T., SCHERES, S. H. W. & GOEDERT, M. 2022. Cryo-EM structures of α-synuclein filaments from Parkinson's disease and dementia with Lewy bodies. *bioRxiv***,** 2022.07.12.499706.

YAO, J., HARVATH, L., GILBERT, D. L. & COLTON, C. A. 1990. Chemotaxis by a CNS macrophage, the microglia. *J Neurosci Res,* 27**,** 36-42.

YE, X., ZHU, M., CHE, X., WANG, H., LIANG, X.-J., WU, C., XUE, X. & YANG, J. 2020. Lipopolysaccharide induces neuroinflammation in microglia by activating the MTOR pathway and downregulating Vps34 to inhibit autophagosome formation. *Journal of Neuroinflammation,* 17**,** 18.

YOUNG, A. M. H., KUMASAKA, N., CALVERT, F., HAMMOND, T. R., KNIGHTS, A., PANOUSIS, N., PARK, J. S., SCHWARTZENTRUBER, J., LIU, J., KUNDU, K., SEGEL, M., MURPHY, N. A., MCMURRAN, C. E., BULSTRODE, H., CORREIA, J., BUDOHOSKI, K. P., JOANNIDES, A., GUILFOYLE, M. R., TRIVEDI, R., KIROLLOS, R., MORRIS, R., GARNETT, M. R., TIMOFEEV, I., JALLOH, I., HOLLAND, K., MANNION, R., MAIR, R., WATTS, C., PRICE, S. J., KIRKPATRICK, P. J., SANTARIUS, T., MOUNTJOY, E., GHOUSSAINI, M., SORANZO, N., BAYRAKTAR, O. A., STEVENS, B., HUTCHINSON, P. J., FRANKLIN, R. J. M. & GAFFNEY, D. J. 2021. A map of transcriptional heterogeneity and regulatory variation in human microglia. *Nature Genetics,* 53**,** 861-868.

ZARRANZ, J. J., ALEGRE, J., GÓMEZ-ESTEBAN, J. C., LEZCANO, E., ROS, R., AMPUERO, I., VIDAL, L., HOENICKA, J., RODRIGUEZ, O., ATARÉS, B., LLORENS, V., GOMEZ TORTOSA, E., DEL SER, T., MUÑOZ, D. G. & DE YEBENES, J. G. 2004. The new mutation, E46K, of alpha-synuclein causes Parkinson and Lewy body dementia. *Ann Neurol,* 55**,** 164-73.

ZEISEL, A., MUÑOZ-MANCHADO, A. B., CODELUPPI, S., LÖNNERBERG, P., LA MANNO, G., JURÉUS, A., MARQUES, S., MUNGUBA, H., HE, L., BETSHOLTZ, C., ROLNY, C., CASTELO-BRANCO, G., HJERLING-LEFFLER, J. & LINNARSSON, S. 2015. Brain structure. Cell types in the mouse cortex and hippocampus revealed by single-cell RNA-seq. *Science,* 347**,** 1138-42.

ZEISS, C. J. 2017. From Reproducibility to Translation in Neurodegenerative Disease. *ILAR Journal,* 58**,** 106-114.

ZHANG, B., GAITERI, C., BODEA, L. G., WANG, Z., MCELWEE, J., PODTELEZHNIKOV, A. A., ZHANG, C., XIE, T., TRAN, L., DOBRIN, R., FLUDER, E., CLURMAN, B., MELQUIST, S., NARAYANAN, M., SUVER, C., SHAH, H., MAHAJAN, M., GILLIS, T., MYSORE, J., MACDONALD, M. E., LAMB, J. R., BENNETT, D. A., MOLONY, C., STONE, D. J., GUDNASON, V., MYERS, A. J., SCHADT, E. E., NEUMANN, H., ZHU, J. & EMILSSON, V. 2013. Integrated systems approach identifies genetic nodes and networks in late-onset Alzheimer's disease. *Cell,* 153**,** 707-20.

ZHANG, L., ZHANG, C., ZHU, Y., CAI, Q., CHAN, P., UÉDA, K., YU, S. & YANG, H. 2008. Semi-quantitative analysis of alpha-synuclein in subcellular pools of rat brain neurons: an immunogold electron microscopic study using a C-terminal specific monoclonal antibody. *Brain Res,* 1244**,** 40-52.

ZHANG, X., ZHANG, L., CHENG, X., GUO, Y., SUN, X., CHEN, G., LI, H., LI, P., LU, X., TIAN, M., QIN, J., ZHOU, H. & JIN, G. 2014. IGF-1 promotes Brn-4 expression and neuronal differentiation of neural stem cells via the PI3K/Akt pathway. *PLoS One,* 9**,** e113801.

ZHOU, H., LI, X. M., MEINKOTH, J. & PITTMAN, R. N. 2000. Akt regulates cell survival and apoptosis at a postmitochondrial level. *J Cell Biol,* 151**,** 483-94.

ZHOU, Y., SONG, W. M., ANDHEY, P. S., SWAIN, A., LEVY, T., MILLER, K. R., POLIANI, P. L., COMINELLI, M., GROVER, S., GILFILLAN, S., CELLA, M., ULLAND, T. K., ZAITSEV, K., MIYASHITA, A., IKEUCHI, T., SAINOUCHI, M., KAKITA, A., BENNETT, D. A., SCHNEIDER, J. A., NICHOLS, M. R., BEAUSOLEIL, S. A., ULRICH, J. D., HOLTZMAN, D. M., ARTYOMOV, M. N. & COLONNA, M. 2020. Human and mouse single-nucleus transcriptomics reveal TREM2-dependent and TREM2-independent cellular responses in Alzheimer's disease. *Nat Med,* 26**,** 131-142.

ZIMPRICH, A., BISKUP, S., LEITNER, P., LICHTNER, P., FARRER, M., LINCOLN, S., KACHERGUS, J., HULIHAN, M., UITTI, R. J., CALNE, D. B., STOESSL, A. J., PFEIFFER, R. F., PATENGE, N., CARBAJAL, I. C., VIEREGGE, P., ASMUS, F., MÜLLER-MYHSOK, B., DICKSON, D. W., MEITINGER, T., STROM, T. M., WSZOLEK, Z. K. & GASSER, T. 2004. Mutations in LRRK2 cause autosomal-dominant parkinsonism with pleomorphic pathology. *Neuron,* 44**,** 601-7.

ZÖLLER, T., SCHNEIDER, A., KLEIMEYER, C., MASUDA, T., POTRU, P. S., PFEIFER, D., BLANK, T., PRINZ, M. & SPITTAU, B. 2018. Silencing of TGFβ signalling in microglia results in impaired homeostasis. *Nature Communications,* 9**,** 4011.

ZUJOVIC, V., BENAVIDES, J., VIGÉ, X., CARTER, C. & TAUPIN, V. 2000. Fractalkine modulates TNF-alpha secretion and neurotoxicity induced by microglial activation. *Glia,* 29**,** 305-15.